

**RISK DETECTION FOR THE PREVENTION OF FALLS ON
STAIRS IN OLDER PEOPLE**

Malarvizhi Ram

A thesis submitted in partial fulfilment of the requirements of Liverpool
John Moores University for the degree of Doctor of Philosophy

February 2022

Abstract

One of the most hazardous and demanding tasks for older people is stair negotiation, often resulting in falls. These falls lead to significant loss of mobility and independence. In addition, after stair falls, quality of life is affected, often leading to serious complications. This stair falls cost National Health Service (NHS) approximately £2.3bn per year.

A laboratory-based motion capture system and force plates are currently used to investigate older people's fall risk factors while on the stairs to prevent falls whilst ascending or descending stairs. However, these procedures are costly, needs a dedicated motion laboratory, and use expensive and cumbersome equipment.

Laboratory-based measurements help identify key fall risk factors that affect people in a controlled environment. However, implementing effective prevention measures requires regular monitoring of these factors over a long period in the user's environment (home), where a fall is likely to occur. Therefore, there is an urgent need for low-cost devices to measure these risk parameters in a home environment and provide accurate and repeatable results to detect people who are all at risk.

This work aimed to detect the stair fall risk factors using wearable sensors incorporated in shoes and machine learning algorithms to detect risk factors to improve the ability of older adults to negotiate different staircase environments safely. This aim had been achieved through four studies:

In the first study, wearable sensors were incorporated into a standard shoe to detect stair-fall risk parameters. These parameters were identified as stair fall risk parameters in a controlled laboratory environment. The fall risk parameters were foot clearance and foot

contact length ratio. A sensor insole was designed to detect foot contact length ratio (foot overhang) using force-sensitive resistors. Two distance sensors (VL6180X) were attached to the shoe to detect foot clearance for ascending and descending. In addition, BNO055 IMU was fitted in the shoe to measure foot motion kinematics such as velocity and acceleration.

In the second study, the developed wearable sensor shoe was tested in the laboratory for validation against the current motion system's standard biomechanical risk factors during stair negotiation. Foot clearance was validated with an accuracy of 0.05mm, and the precision was between 4.79mm to -4.67mm. Foot contact length ratio was validated with an accuracy of -2%, and the precision was between 10% to -13.91%.

The developed sensor shoe was tested in the third study at different exemplar houses staircases to measure stair fall risk factors. In addition, a comparison was made between lab and houses to measure stair-negotiation behaviour changes. The results showed a significant difference in selected stair fall biomechanical factors among the three exemplar houses and laboratory stairs.

In the fourth study, the supervised machine learning algorithm was trained to classify fall risk using collected sensor data along with self-reported falls. The support vector machine algorithm was trained to classify stair fall risk with a precision of 90.4%, a sensitivity of 88.9%, and an F-measure of 90%. So, this trained algorithm can be used in the future to predict stair fall risk at home environments based on data collected from the developed sensors and instrumented shoes.

Future research should include more stair fall risk factors and more people in real-life stair negotiation conditions (houses) to improve future stair fall risk prediction.

Acknowledgements

I want to thank my supervisors, Prof. Bill Baltzopoulos and Prof. Andy Shaw, for offering me a PhD scholarship to begin my research career at Liverpool John Moores University (LJMU) and inspiring and supporting me during the PhD. In addition, I would like to thank Prof. Bill Baltzopoulos support and advice that helped me to face the challenges more successfully.

I want to thank my supervisory team Prof. Maganaris CN, Dr. Cullen J, Dr. O'Brien, and the members of the RISCS (Research to Improve Stair Climbing Safety) group of Liverpool John Moores University for their valuable feedback and continuous support throughout my PhD journey.

Furthermore, I wish to acknowledge all the older adults who voluntarily visited the lab and stayed in touch with me for six months.

I also would like to thank all my fellow students (especially the climbing group) in the university's biomechanics and engineering departments.

Finally, I would like to thank my family and friends for their continuous support. Special thanks go to my husband, Dr Ram, and son Sidharth, who supported me all these years.

Contents

Abstract	ii
Acknowledgements	iv
Publications	ix
List of Figures	x
List of Tables	xx
List of Abbreviations	xxiii
CHAPTER 1: General Introduction	1
1.1 Stairs fall Introduction	2
1.2 Thesis statement	3
1.3 Motivation	3
1.4 Aim and Objectives (Project Description).....	4
1.5 Summary of contribution.....	7
CHAPTER 2: Literature Review	8
2.1 Stair Fall Background	9
2.1.1. Staircase Terminology	9
2.1.2. What is stair falling?	9
2.1.3. Why do older people fall on stairs?	10
2.1.4. Stair gait analysis	10
2.1.5. What are the hazards associated with stair negotiation?.....	11
2.1.6. UK Stair fall history	13
2.1.7. Causes and Risk factors of stair falls	13
2.2 Current Solutions to acquire stair fall risk factors.....	18
2.2.1. Laboratory-based approach.....	18
2.2.2. Motion capture analysis for stair fall risk detection.....	18
2.3 Wearable sensors to detect stair fall risk parameters.....	20
2.3.1. The available sensor solution for stair falls parameters	20
2.4 Wearable Sensor Shoe Solution	22
CHAPTER 3: Sensor Shoe Development	24
3.1 Introduction	25
3.2 Sensor selection	25
3.2.1. Foot clearance	25
3.2.2. Foot contact length, stance time, swing time and cadence	26
3.2.3. Linear acceleration, Velocity, Angular velocity, and Foot angle (Pitch)...	26
3.3 Methods	33
3.3.1. Instrumented sensor shoe physical implementation.....	33

3.3.2.	Insole design	36
3.3.3.	LabVIEW user interface for data collection	38
3.4	Results	40
3.4.1.	Bandwidth requirements	40
3.4.2.	Distance sensor specification	40
3.4.3.	Force Sensitive Resistor (FSR) sensor specification	49
3.4.4.	Foot contact length	59
3.4.5.	BNO055 IMU	61
3.5	Discussion.....	69
3.6	Conclusion	71
CHAPTER 4: Sensor Shoe’s stair fall risk parameters validation		72
4.1	Introduction	73
4.2	Methods	73
4.2.1.	Participants.....	73
4.2.2.	Laboratory staircase structure	73
4.2.3.	Data collection procedure	74
4.2.4.	Data collection for sensor shoe and VICON system:	75
4.2.5.	VICON data analysis.....	76
4.2.6.	Sensor shoe data analysis	79
4.3	Results	81
4.3.1.	Foot Clearance results between Sensor and Vicon	82
4.3.2.	Foot Contact length ratio results between Sensor and Vicon	87
4.3.3.	Cycle time (Cadence) results between Sensor and Vicon.....	91
4.4	Discussion.....	94
4.5	Conclusion	96
CHAPTER 5: Stair fall-risk parameters comparison between a controlled environment and uncontrolled environment.....		97
5.1	Abstract.....	98
5.2	Introduction	98
5.3	Hypothesis 1	100
5.4	Hypothesis 2	100
5.5	Hypothesis 3	100
5.6	Methods	100
5.6.1.	Participants.....	100
5.6.2.	Staircase configuration.....	100
5.6.3.	Procedures	104
5.6.4.	Data analysis	105

5.6.5.	Statistics	106
5.7	Results	107
5.7.1.	Differences between three houses' staircase during stair ascent	107
5.7.2.	Differences between Laboratory and Houses during stairs ascent.....	112
5.7.3.	Difference between fallers and non-fallers during stairs ascent	114
5.7.4.	Differences between three houses during stair descent.....	118
5.7.5.	Differences between laboratory and houses during stairs descent.....	119
5.7.6.	Differences between fallers and non-fallers during stair descent	121
5.8	Discussion.....	123
5.8.1.	First Hypothesis	124
5.8.2.	Second Hypothesis	125
5.8.3.	Third Hypothesis.....	126
5.8.4.	Other fall risk parameters.....	128
5.9	Conclusion	129
CHAPTER 6: Identify Fall Risk using Novel sensor and Machine learning algorithm		131
6.1	Abstract.....	132
6.2	Introduction	132
6.3	Methods	135
6.3.1.	Sensor Shoe Design	135
6.3.2.	Participants.....	135
6.3.3.	Data collection location.....	135
6.3.4.	Data collection procedure	135
6.4	Data Analysis and features extraction	137
6.4.1.	Pre-processing	137
6.4.2.	Features extraction	138
6.5	Features Selection.....	146
6.5.1.	Feature selection using F-test.....	146
6.5.2.	Feature selection using rank features (chi-square test)	148
6.6	Training Classification Algorithms	150
6.6.1.	Classification Evaluation Metrics	150
6.6.2.	Classification Algorithms	152
6.6.3.	Validation Methods.....	155
6.7	Results	155
6.7.1.	Full Feature set results	156
6.7.2.	Chi-square Feature set results	158
6.7.3.	F-Test Feature set results	160

6.8 Discussion.....	162
6.8.1. The prediction of stair fall risk in future	164
6.9 Conclusion.....	166
CHAPTER 7: General Discussion.....	167
7.1 Purpose	168
7.2 Summary of experimental findings	168
7.3 Stair falls.....	174
7.4 Limitations.....	175
7.5 Future recommendations	176
7.6 Implications of this project.....	177
7.7 Conclusion.....	177
A. Appendices.....	179
References.....	219

Publications

Peer-reviewed paper

- Selvaraj, Malarvizhi, et al. "Stair fall risk detection using wearable sensors." *2018 11th International Conference on Developments in eSystems Engineering (DeSE)*. IEEE, 2018.

Conference papers

- Selvaraj M, Baltzopoulos V, Shaw A, Maganaris CN, Cullen J, O'Brien T. Stair Fall Risk Detection in Older People Based on Foot Clearance. Poster presented at the Faculty of Science Postgraduate Research Day, Liverpool John Moores University, Liverpool, UK, 2017.
- Selvaraj M, Baltzopoulos V, Shaw A, Maganaris CN, Cullen J, O'Brien T. Stair fall Risk detection using wearable sensors. Paper presented at the Faculty of Science Postgraduate Research Day, Liverpool John Moores University, Liverpool, UK, 2018.
- Selvaraj M, Baltzopoulos V, Shaw A, Maganaris CN, Cullen J, O'Brien T, Kot P. Stair fall risk detection using wearable sensors. Paper presented at 11th International Conference on Developments in eSystems Engineering (DeSE), Cambridge, UK, 2018.

List of Figures

<i>Figure 2.1 Staircase Structure</i>	<i>9</i>
<i>Figure 3.1 Instrumented shoe with PCB Module, and Insole fitted.....</i>	<i>34</i>
<i>Figure 3.2 Back of the instrumented insole, two distance sensors and one IMU sensor fitted</i>	<i>35</i>
<i>Figure 3.3 Case for IMU and Distance sensor</i>	<i>36</i>
<i>Figure 3.4 Instrumented insole designed in eagle software</i>	<i>37</i>
<i>Figure 3.5 Instrumented flexible Insole printed and fitted with ten FSRs</i>	<i>37</i>
<i>Figure 3.6 Instrumented data collection user interface, COM port3 to connect with Arduino for synchronisation, COM port to connect with left sensor shoe and COM port2 to connect with right sensor shoe. Use Vicon button used for lab data collection, start, and stop buttons were used for houses data collection.....</i>	<i>39</i>
<i>Figure 3.7 Time of Flight concept(STMicroelectronics 2010)</i>	<i>42</i>
<i>Figure 3.8 Distance sensor under different material, it was $28\text{mm}\pm 3\text{mm}$.....</i>	<i>44</i>
<i>Figure 3.9 Distance sensor calibration curve, sensor angle set for zero degrees to 60 degrees by increasing it in 10o (0o, 10o,20o, 30o,40o,50o, 60o), and measured for 10mm,15mm,20mm,25mm,30mm,35mm and 40mm. Linear correlation $r^2 = 0.9226$</i>	<i>46</i>

<i>Figure 3.10 Descending vertical foot clearance measurement calculation, while the foot crossing the step edge foot clearance was calculated as a distance between the back distance sensor and step edge.....</i>	<i>48</i>
<i>Figure 3.11 Graphical representation of minimum foot clearance calculation while descending.....</i>	<i>48</i>
<i>Figure 3.12 FSR made of these three layers (Electronics 2010).....</i>	<i>50</i>
<i>Figure 3.13 Voltage divider circuit for a force-sensitive resistor (FSR) with 10kohm resistor</i>	<i>51</i>
<i>Figure 3.14 Voltage Vs Forces, 5voltage steadily drops up to 30n, after that voltage drops was very minimal, which was hard to measure.....</i>	<i>52</i>
<i>Figure 3.15 To overcome minimum voltage drop and measure forces up to 100N, a voltage divider circuit was created with two Operational amplifiers (Op-amp).....</i>	<i>53</i>
<i>Figure 3.16 Voltage Vs Higher Forces graphical representation shows that the voltage would not change until 29N; once the force reaches 30N, the voltage drops.</i>	<i>55</i>
<i>Figure 3.17 Voltage Vs less force graphical representation, the voltage would not change after 30N heavily, it only measures 1N to 30N, after(>30N) that the voltage change would be minimal.....</i>	<i>56</i>
<i>Figure 3.18 Calibration Curve for higher force (A) to measure 30N to 100N and lower force (B) to measures 1N to 30N. After designing circuit with Op-Amp, the FSR was calibrated with material testing machine.....</i>	<i>58</i>
<i>Figure 3.19 Printed flexible Insole fitted with ten FSR sensors with the Sensor number</i>	<i>59</i>

<i>Figure 3.20 FSR results for higher force (>30N to 100N)</i>	60
<i>Figure 3.21 Accelerometer and Gyroscope Specification (Townsend 2018)</i>	63
<i>Figure 3.22 Accelerometer sensor bias test result</i>	64
<i>Figure 3.23 Gyroscope Sensor Bias result, the offset is ± 20</i>	65
<i>Figure 3.24 Coordinate System for BNO055 IMU (Townsend 2018)</i>	66
<i>Figure 3.25 Linear Acceleration</i>	67
<i>Figure 3.26 Angular Velocity</i>	68
<i>Figure 3.27 Velocity results for going up</i>	68
<i>Figure 3.28 Calculated Pitch (foot angle) for going up</i>	69
<i>Figure 3.29 Lower limb circuit board, IMU sensors fitted with thigh, shank, and sacrum to calculate range of motion and centre of mass control</i>	70
<i>Figure 4.1 Laboratory custom-built instrumented seven-step staircase structure image, first four steps fitted with a force plate, twenty-four infrared cameras were around the staircase</i>	74
<i>Figure 4.2 Lab data collection setup, left side image was sensor shoe with computer connected with Bluetooth in one side of the computer, the other side of the computer connected with VICON system, right side image was participant with markers and sensor shoe</i>	75
<i>Figure 4.3 Sensor and Vicon System Synchronisation. A computer connected with a Vicon system. Vicon synchronization port was connected with Arduino; then this Arduino</i>	

connected with a laptop, which contains a user interface to collect data from the sensor shoe. Finally, two Bluetooth dongles were connected to the computer to signal the sensor shoe to start and stop data collection. 76

Figure 4.4 Vicon foot clearance calculation of the right foot using the above foot model. A two- dimensional outline of the shoe (A) was digitized and linked to three markers (first metatarsophalangeal joint: RMP1, fifth metatarsophalangeal joint: RMP5 and calcaneus lateralis: RLCL) of the static measurement. The virtual outline of the shoe was then projected in the movement trials. Foot clearance was calculated as the minimal distance between the virtual shoe and the step edge, within the orange colour area between 1 and 2 shown in (B). 78

Figure 4.5 VICON Foot contact length ratio calculation, the Foot contact length ratio was calculated at touch-down using the rigid virtual shoe (blue line) as: Foot placement ratio = $(x / (x + y)) * 100\%$ 79

Figure 4.6 Foot clearance calculation for sensors, for ascending front distance sensor measures vertical distance while crossing the stair edge, back distance sensor measures vertical distance while crossing the stair edge 79

Figure 4.7 Foot Contact length ratio calculation, (A) shows the flexible sensor insole with nine sensors, the distance between each sensor was 2.9cm, (B) sample table shows how foot contact length was calculated, (C) shows the schematic representation of foot contact length calculation..... 80

Figure 4.8 Foot clearance correlation coefficient (r^2) results between sensors and VICON (Laboratory System) (a) Step one foot clearance correlation, (b) Step two-foot clearance correlation, (c) Step three-foot clearance correlation, (d) Step four-foot clearance

correlation, (e) Step five clearance correlation, (f) Step six-foot clearance correlation, (g) Step seven-foot clearance correlation, (h) All seven steps combined foot clearance correlation. Step one, step seven, and all seven steps combined foot clearance correlation showed a high positive linear correlation between data from the sensors and the VICON system.83

Figure 4.9 Bland-Altman plot of foot clearance between the sensor method and the VICON method in the Laboratory. The X-axis represents the average of the sensor and vicon foot clearance; Y-axis represents the difference between sensor and vicon foot clearance. The indigo horizontal line denotes the mean difference between sensor and VICON method which was 0.1mm, while the top red horizontal line represents the upper limits of agreement ($\text{Mean difference} + 1.96 \times \text{SD of difference}$) which was 4.8mm, the bottom red line represents the lower limits of agreement ($\text{Mean difference} - 1.96 \times \text{SD of difference}$) which was -4.7mm. Purple lines shows the confidence limit for the upper and lower limits of agreement. The Orange small circles are data points, and when shown out of the confidence limits these are called outliers; four outliers in total (4 out of 175 datapoints). The orange horizontal line shows the line of equality, and it is possible to determine if bias is significant or not. This equality line was within the confidence interval of the mean difference, so the bias was not significant (0.1 mm).85

Figure 4.10 Foot contact length ratio correlation results between the sensor and VICON (Laboratory System). (a) step one- Foot contact length ratio correlation results, (b) step two- Foot contact length ratio correlation results, (c) step three- Foot contact length ratio correlation results, (d) step four- Foot contact length ratio correlation results. Among the four steps, step two showed a higher positive linear correlation between data from the sensors and the VICON system compared to the other three steps.87

Figure 4.11 Four steps combined foot contact length ratio correlation between sensors and VICON (Laboratory system) with high positive linear correlation88

Figure 4.12 Bland-Altman plot of foot contact length ratio agreement between the sensor method and the VICON method in the Laboratory. The X-axis represents the average of the sensor and vicon foot contact length ratio; Y-axis represents the difference between sensor and vicon foot contact length ratio. The indigo horizontal line denotes the mean difference between sensor and VICON method which was -2%, while upper red line represents the upper limits of agreement (Mean difference+1.96 ×SD of difference) which was 10%, the lower red line represents the lower limits of agreement (Mean difference-1.96× SD of difference) which was -13.9%. Purple lines shows the confidence limits for the upper and lower limits of agreement. The Orange small circle are data points, when shown out of the confidence limits are called outliers, four outliers in total (4 out of 100 datapoints). The Orange horizontal line shows the line of equality, it is possible to determine if bias is significant or not. This equality line was not within the confidence interval of the mean difference, so the bias is significant (-2%).....90

Figure 4.13 Cycle time correlation results between instrumented sensor shoe and Vicon, moderate positive linear correlation.....91

Figure 4.14 Bland-Altman plot of cycle time between the sensor method and the VICON method in the Laboratory. The X-axis represents the average of the sensor and vicon cycle time; Y-axis represents the difference between sensor and vicon cycle time. The indigo horizontal line denotes the mean difference between the sensor and VICON method, which was 0.22s, while upper red lines represent the upper limits of agreement (Mean difference+1.96 ×SD of difference) which was 0.58s, the lower red line represents the lower limits of agreement (Mean difference-1.96× SD of difference) which was -0.15s.

Purple lines show the confidence limits for the upper and lower limits of agreement. There are no outliers in the cycle time because no data point has gone out of the confidence limit. The Orange horizontal line shows the line of equality, and it is possible to determine if bias is significant or not. This equality line was not within the confidence interval of the mean difference, so the bias is significant (0.22s). 93

Figure 5.1 LJMU's Exemplar House, which contains three houses 101

Figure 5.2 1920's and 1970's staircase design 102

Figure 5.3 2010's staircase design..... 103

Figure 5.4 Laboratory custom built instrumented seven-step staircase structure..... 104

Figure 5.5 Interval plot for difference of mean in Cadence for three houses, it displays that older people were cautious using 2010's staircase and confident in using straight staircase (1920 and 1970's house) so they spent less time to climb stairs. 107

Figure 5.6 Confidence interval (CI) for the three different houses' cadence, the confidence intervals for the (2010-1970, 2010-1920) these house pairs of means range does not include zero, which indicates that the difference is statistically significant. 108

Figure 5.7 Interval plot for the difference of means in step7 foot clearance for three houses, it displays that in step7 older people have more clearance in 1970s house compared to other houses foot clearance 109

Figure 5.8 Confidence interval (CI) for the three different houses' foot clearance, the confidence intervals for the (1970-1920) house pairs of means range does not include zero, which indicates that the difference is statistically significant. 109

<i>Figure 5.9 Interval plot for the difference of mean in foot contact length ratio for three houses, it displays that in step3 older people have more foot contact length ratio in 1970s and 1920s house compared to other houses foot contact length ratio.....</i>	<i>111</i>
<i>Figure 5.10 Confidence interval (CI) for the three different houses' foot contact length. The confidence intervals for all three house pairs of means range do not include zero, which indicates that the difference is statistically significant for all three houses.....</i>	<i>111</i>
<i>Figure 6.1 Acceleration up data for time domain to frequency domain conversion, x is frequency and y is amplitude.....</i>	<i>140</i>
<i>Figure 6.2 Stance time Swing time graphical representation, stance time was calculated as the duration of the foot contact on the step, swing time was calculated as the duration of the foot off the step.....</i>	<i>142</i>
<i>Figure 6.3 Features selection using a Filter method (F-Test), CDF means Cumulative distribution function, p values smaller than 0.05 has more discrimination features between fallers and non-fallers, so those features were selected to create a machine learning algorithm.....</i>	<i>147</i>
<i>Figure 6.4 Feature selection using the Chi-square test, the features selected by predictor rank has more discrimination features between fallers and non-fallers, so those features were selected to create a machine learning algorithm</i>	<i>149</i>
<i>Figure 6.5 Example for k-NN (Wikipedia).....</i>	<i>154</i>
<i>Figure 6.6 Selected three feature set for classification training.....</i>	<i>155</i>

<i>Figure 6.7 Area Under the Curve (AUC) results for best two classifiers using Full feature set, cubic SVM algorithm produced 87% AUC and the Fine KNN produced 80% AUC</i>	157
<i>Figure 6.8 Confusion matrix for SVM</i>	158
<i>Figure 6.9 Area Under the Curve (AUC) results for best two classifiers using chi-square feature set, cubic SVM algorithm produced 93% AUC and the Boosted trees produced 95% AUC</i>	160
<i>Figure 6.10 Area Under the Curve (AUC) results for best two classifiers using F-Test feature set, cubic SVM algorithm produced 94% AUC and the Ensemble Ada Boost produced 94% AUC</i>	161
<i>Figure 6.11 (A)Training (B)Validation (C)Trained algorithm for future testing</i>	165
<i>Figure A.1 Right Shoe's PCB schematic design Eagle software</i>	179
<i>Figure A.2 Right Shoe's PCB board design from Eagle software</i>	179
<i>Figure A.3 Left Shoe's PCB board design from Eagle software</i>	180
<i>Figure A.4 Left Shoe's PCB board design from Eagle software</i>	180
<i>Figure A.5 Insole's design from Eagle software</i>	181
<i>Figure A.6 User Interface designed using LABVIEW software</i>	181
<i>Figure A.7 COM ports and Trigger process</i>	182
<i>Figure A.8 Trigger to start data collection from Vicon</i>	182

<i>Figure A.9 After receiving start trigger, start signal send to shoes PCB board.....</i>	<i>183</i>
<i>Figure A.10 Trigger to stop data collection from Vicon.....</i>	<i>183</i>
<i>Figure A.11 After receiving stop trigger, start stop send to shoes PCB board</i>	<i>184</i>
<i>Figure A.12 Writing data in the SD (Secure Digital) card.....</i>	<i>184</i>
<i>Figure A.13 Error message generation</i>	<i>185</i>
<i>Figure A.14 FSR testing with Material Testing Machine</i>	<i>185</i>
<i>Figure A.15 Sensors used to develop sensor shoe</i>	<i>187</i>
<i>Figure A.16 Berg Balance Scale.....</i>	<i>188</i>

List of Tables

Table 2.1 Standard stair dimensions for private and public building	14
Table 3.1 Stair fall risk parameter with the chosen sensor	28
Table 3.2 Distance Sensor Specification.....	42
Table 3.3 Detailed offset calculation for the distance sensor.....	45
Table 3.4 Distance sensor offset and accuracy testing results	46
Table 3.5 Relevant parameters of the interlink FSR-402.....	50
Table 3.6 Higher force calculation(vout1) used to measure forces from 30N to 100N...54	
Table 3.7 Low force Vout2 calculation used to measure forces from 1N to 30N	56
Table 3.8 Foot contact length calculation for Ascending	59
Table 3.9 Foot contact length calculation for Descending.....	59
Table 4.1 Foot clearance correlation results between sensors and VICON.....	83
Table 4.2 Foot clearance Pearson correlation result between sensors and VICON.....	84
Table 4.3 Foot contact length ratio's correlation between sensors and VICON.....	88
Table 4.4 Foot contact length ratio Pearson correlation	89
Table 4.5 Cycle time's Pearson correlation results between sensors and VICON method	92

Table 5.1 Foot clearance Mean for all three houses (ascending).....	110
Table 5.2 Post hoc result for foot contact length (FCL) ratio for each step in all three houses (ascending)	112
Table 5.3 Difference between Laboratory and House ascend ANOVA results.....	114
Table 5.4 difference between fallers and non-fallers in ascent.....	115
Table 5.5 Difference between fallers and non-fallers in different environments during ascent.....	116
Table 5.6 Post hoc result for foot contact length ratio for each step in all three houses (descending)	119
Table 5.7 Difference between Laboratory and House descend ANOVA results.....	120
Table 5.8 Difference between fallers and non-fallers in descending	122
Table 5.9 Difference between fallers and non-fallers in different environments in descending.....	122
Table 6.1 Data collection location and trial details.....	136
Table 6.2 Extracted Features details	138
Table 6.3 Biomechanical features for fallers and non-fallers (Mean \pm SD)	143
Table 6.4 Personal Features for fallers and non-fallers(Mean \pm SD)	144
Table 6.5 Berg Balance results.....	144
Table 6.6 Fear of Falling results	145

Table 6.7 Follow-up fall risk results	145
Table 6.8 P-value for selected Features	147
Table 6.9 Confusion matrix with advanced classification metrics (Matrix 2019).....	151
Table 6.10 Full Feature set classification results	156
Table 6.11 Classification results for the chi-square feature set	159
Table 6.12 Classification results for F-Test feature set.....	161
Table 6.13 Chi-square and F-Test classification results in comparison, green colour indicates that the first-best results for that evaluation metrics, the red colour shows the second-best results for that evaluation metrics	163
Table A.1 Six months follow up fall information	188

List of Abbreviations

BBS	Berg balance scale
NHS	National Health Service
ROM	Range of motion
IMU	Inertia Measurement Unit
PCB	Printed Circuit Board
I2c	Inter-Integrated Circuit
SD	Secure Digital
FSR	Force Sensitive Resistor
Vout	Voltage output
AoI	Angle of Incidence
MAE	Mean Absolute Error
RMSE	Root Mean Squared Error
UK	United Kingdom
FC	Foot Clearance
FCL	Foot Contact Length
M	Mean
SD	Standard Deviation
LJMU	Liverpool John Moores University
BRE	Building Research Establishment
KNN	K-Nearest Neighbors algorithm
SVM	Support Vector Machine
ROC	Receiver Operating Characteristic curve'
AUC	Area under the receiver operator characteristic curve

TP	True positive
FP	False Positive
TN	True Negative
FN	False Negative
TPR	True positive Rate
FPR	False Positive Rate
CDF	Cumulative Distribution Function
FFT	Fast Fourier Transform

CHAPTER 1: General Introduction

1.1 Stair fall Introduction

Falls can happen to anyone, but the most vulnerable are old age people. Even though falls are common, they can lead to injuries and death if serious. Approximately 1 in 3 older people aged 65 and over and lives in the home environment experience at least one fall a year (Lord, Ward et al. 1993). Not all falls cause serious injuries. However, some falls could lead to bone fractures that reduce confidence. When older people lose their confidence, they become withdrawn and dependent, which has several serious consequences (Cumming, Salkeld et al. 2000).

The most hazardous and demanding tasks for older people are stair negotiation, often resulting in falls, with 7-35% of these falls occurring on stairs (Jacobs 2016). Compared to level walking, fewer falls occur on stairs; however, these stair falls are the second leading cause of accidental death (Startzell, Owens et al. 2000). Also, stair falls cost National Health Service (NHS) approximately £2.3bn per year (Age 2010).

Laboratory-based motion capture and force plates are currently used to investigate older people's fall risk factors while on the stairs to prevent a fall. These motion capture systems analyse all body segments using highly accurate computer-based optical tracking systems. These motion capture systems produce accurately quantified results for body movements examined within the laboratory. However, this procedure is costly, needs dedicated motion laboratory space, and uses cumbersome equipment that might interfere with the movement.

So, there is a need for low-cost devices to measure fall risk factors in the home environment and provide accurate and repeatable results to detect people who are all at risk. Long-term monitoring of stair gait is also needed to analyse stair fall risk factors.

This thesis discusses instrumented sensor shoe system development for uninterrupted monitoring of factors related to stair falls. This system includes an instrumented insole and an instrumented shoe, containing two distance sensors and an IMU sensor. The data are sent wirelessly via Bluetooth and provide information about the participants' fall risk factors such as acceleration, velocity, foot clearance and foot contact length ratio whilst negotiating stairs.

There were 25 subjects tested using the instrumented sensor shoe. The results from the sensor shoe compared to the motion analysis system (VICON) in a laboratory setting. In addition, the sensor shoe was also tested in an actual simulated home environment on three different exemplar houses staircases to check the instrumented sensor shoe's usability.

1.2 Thesis statement

The aim is to design, develop, calibrate, and use a wireless sensor instrumented shoe system capable of determining parameters linked to stair fall risk. The sensor system was designed to collect data unobtrusively and in any staircase over long periods. Moreover, it was designed not to interfere with gait. First, the sensor shoe was calibrated and used to collect data, and then these data were analysed to obtain information about the user's gait. These results were then validated against the optical tracking system (motion analysis system available at the biomechanics laboratory). Finally, the analysed data were used to classify high and low fall risks using standard pattern recognition techniques.

1.3 Motivation

Falls are widespread and challenging for older adults; one-third of older people aged 65 and above experience at least one fall every year. These falls lead to significant loss of mobility and independence. This stair falls severely affect the quality of life, resulting in early death or secondary complications during hospitalization, usually the following surgery to repair a fracture. Even though older people stair fall has detrimental effects, a system that can be used to timely identify people at high risk is currently lacking.

Stair fall-risk assessment is currently achieved using laboratory-based equipment. Unfortunately, several environmental differences make it practically impossible to accurately simulate an individual scenario in the laboratory. These include ecological differences between houses, such as the shape of the staircase, dimensions of steps, position and shape of handrails, and the material used to cover the steps and lighting.

Therefore, it is not feasible to systematically study and document what has caused the fall. Laboratory-based measurements help identify key fall risk factors (stair fall parameters) that affect people in a controlled environment. Implementing effective

prevention measures requires regular monitoring of these factors over a long period in the user's environment, where a fall is likely to occur.

Therefore, there is an urgent need to test these risk parameters in a home environment. A simple wearable system is needed to test stair fall in a home environment. The recent advances in wearable sensor technology enable us to pursue research with small and inexpensive sensors. Therefore, in this research project, a simple wearable sensor instrumented shoe system (sensors incorporated in an actual shoe) was developed to investigate stair fall risk parameters in different home environments. This sensor shoe allows the collection of a vast quantity of data in the different domestic staircases that are difficult to get through the current laboratory motion systems.

1.4 Aim and Objectives (Project Description)

The overall aim was to detect fall risk using sensors and machine learning algorithms to improve older adults' ability to negotiate different staircase environments safely. This aim had been achieved through four objectives:

1. Developing a wearable sensor shoe to detect stair-fall risk parameters that had been identified as stair fall risk parameters in the controlled laboratory environment using current motion analysis systems (VICON).
2. Testing the developed instrumented sensors shoe in the laboratory for validation against the current motion system's (VICON) standard biomechanical measurements during stair negotiation.
3. Testing at different domestic houses' staircases using the wearable sensor shoe to collect large sets of biomechanical, behavioural, and environmental data as older individuals navigate different staircases in a natural home environment
4. Developing a machine learning system to detect fall risk using collected sensor data along with self-reported falls.

These objectives of the project have been realised by conducting four corresponding studies that are explained below.

1.4.1 Study 1: Sensor Development

The wearable sensor shoe system for stair-fall risk prediction had been developed especially for detecting relevant biomechanical parameters that previous laboratory-based research had shown to be risk factors for falling. The parameters include:

1. Foot clearance
2. Foot contact length ratio (foot overhang)
3. Temporal characteristics
 - Gait cadence
 - Gait velocity
 - Gait Acceleration

The slip and trip are the two most common fall mechanisms. In ascending, the risk of tripping is generally related to the distance between the forefoot and the step edge (Kesler, Horn et al. 2016), which is called foot clearance. The risk of tripping increases when the vertical distance of the foot to the edge of the step is reduced (Kesler et al., 2016). In addition, as the variability in foot clearance increases, the risk of tripping increases, as this may indicate that a person cannot maintain a safe foot trajectory (Hamel, Okita et al. 2005). The risk of slipping increases if the proportion of the foot in contact length with the step is reduced. In addition, as the variability of the foot in contact length with the step increases, the risk for slip increases, as this may indicate an inability to position the foot consistently and securely on the step.

In descending, similar to stair ascent, the risk for a trip is associated with foot clearance. However, during descent, this is usually the horizontal clearance of the foot's heel with the edge of the step. According to (Hamel, Okita et al. 2005) this research, the risk of falling from a staircase increases when foot clearance is decreased, and the variability of the foot clearance is increased. Similar to stair ascent, the risk of slipping increases during descending, when the proportion of foot in contact with the step is reduced (Roys and Wright 2005).

Cadence during stair ascent ranges between 90 steps/ min (Livingston et al., 1991) and 104 steps/min and stair descent range between 96 steps and 110 steps/min. Thus,

increased cadence indicates a riskier strategy that could increase the chance for a trip and slip (Zietz, Johannsen et al. 2011).

According to this research, gait velocity is another crucial risk factor (Di Giulio, Reeves et al. 2020). Older adults with increased fall risk tend to walk slowly. (Hemmatpour, Ferrero et al. 2019). CoM angular acceleration is another crucial risk factor. Sudden changes like a more significant peak and variance in CoM angular acceleration cause the risk of losing CoM while stepping down and leading to falling (Templer 1995). A fall event can be predicted by processing acceleration data (Hemmatpour, Ferrero et al. 2019). Even though CoM acceleration causes the fall, gait acceleration and velocity was calculated due to sensor constraints. We decided not to use many sensors all over the body because older people might not wear them longer. So we decided to use the sensor only with shoes and tried to gather information from the sensor shoe data and predict the future fall risk.

There was no literature available to combine all the above parameters to predict the risks of stairs in older adults using sensors. Therefore, three sensors were incorporated in the shoe to calculate all the above parameters: an IMU sensor, two distance sensors, and force sensors. The IMU sensor was used for motion analyses, fitted under the shoe's middle part because it was very small. The two distance sensors were used to find foot clearance for ascending and descending gaits. Finally, a force-sensitive resistor was used to create a sensor insole to find foot contact length ratio (foot overhang), and this insole was fitted inside the shoe.

1.4.2 Study2: Sensor Validation against a motion analysis system

Initially, the instrumented shoe was tested on a custom-made staircase located in the biomechanics laboratory. Collected sensor shoe data were filtered and processed in Matlab. In addition, laboratory-based motion data (VICON) was collected simultaneously; this data was filtered and processed in Visual3D. For comparison and validation, stair fall risk parameters such as foot clearance, foot contact length ratio, acceleration, cadence, and velocity were derived from VICON and sensor data.

1.4.3 Study3: Testing stair negotiation at three different exemplar houses

In this study, large sets of biomechanical, behavioural, and environmental data were collected in a realistic living environment of 25 older individuals in the LJMU's (Liverpool John Moores University) exemplar house's staircases using our developed instrumented shoe to assess whether our developed sensor system could predict all biomechanical fall risk parameters. Three different types of exemplar houses had been built at LJMU. Each house's staircase was different as each exemplar house resembles different eras' architectures, which were 1920's, 1970's and 2000's.

Factors such as foot clearance, degree of foot overhang on the step, speed of movement and use of handrails have been collected in the university's houses using the unobtrusive instrumented shoe. Environmental parameters, such as step dimensions, position, and shape of handrails, were also recorded. Finally, fear of falling from previous experience was also noted. This study could reveal the biomechanical response of older people to different home stair negotiations.

1.4.4. Study4: Developing a Machine learning algorithm to classify fallers

The follow up started after data collection at the LJMU's experimental houses, incidences of stair fall by the participants and the conditions under which they have experienced fall details were self-reported for six months. The self-reported information (who had fallen on stairs) and stair negotiation parameters (features) collected from three different houses were used to create a supervised machine learning algorithm to classify high fall risk people from those with low fall risk. The classification information can reduce the stair fall risk in the future.

1.5 Summary of contribution

The instrumented shoe with wearable sensors was used in a series of experiments to detect the risk parameters for stair fall and bridge the existing gap between laboratory-based research and the end-users environment. There were no previous studies on wearable sensors shoes to detect all the major biomechanical parameters to predict stair fall risk in older people using different real house staircases.

CHAPTER 2: Literature Review

2.1 Stair Fall Background

2.1.1. Staircase Terminology

The below staircase structure (Figure 2.1) describes the staircase terminologies.

- Tread: The horizontal surface of the stair is called Tread.
- Riser: The vertical surface of the stair is called Riser.
- Nosing: The portion of the tread that overhangs the front of the riser is called Nosing.
- Rise: The vertical dimension from tread to tread is called Rise.
- Going: The horizontal dimension from the riser to the riser is called Going.

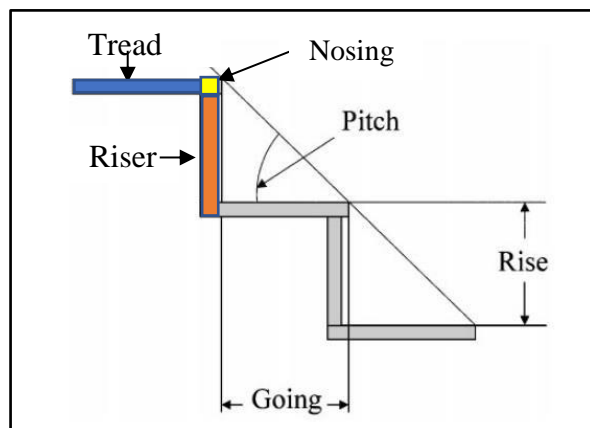


Figure 2.1 Staircase Structure

2.1.2. What is stair falling?

A fall is defined as "an unexpected event in which the person comes to rest on the ground, floor, or lower-level " (Lamb, Jørstad-Stein et al. 2005). The slip and trip are the two most common fall mechanisms. A trip is a sudden arrest in the swinging leg while the body continues its initial motion trajectory when the body's centre of gravity moves outside the base of support, causing a fall. A slip happens when there is not enough friction between the person's foot and the walking surface, which causes the foot to slide, resulting in a loss of balance and a subsequent fall.

There are more chances of a fall occurring during stair negotiation while the foot is on the swing phase. During this swing phase, the rear foot must pass two nosings, at this point, where the risk of tripping is higher. The subsequent risk occurs on stair ascent when the rear foot pushes off the lower tread. At this point, if the slip resistance of the tread is too small, then there may be a risk of slipping (Roys 2001).

2.1.3. Why do older people fall on the stairs?

Older people can fall due to the combination of the following reasons, interruption to their normal gait, losing balance, and inability to correct their balance. Their centre of gravity moves out of their base of support provided by their feet.

Because of the very different gait is used on stairs, is the reason for accidents differ significantly from that of accidents resulting from falls on the level. While walking, people continuously change their posture between unstable then retrieving it back to stable and the centre of gravity moving ahead. However, people get an even less stable gait on stairs than walking on the level. People balance themselves on one flexed leg as the other leg swings forward and to one side to take the next step. By comparison to walking on the level, this is slow-motion activity. The exaggerated gait, coupled with the increased precision demanded, makes stairs such a tricky balancing act on a course with many potential obstacles represented by the steps.

2.1.4. Stair gait analysis

Stair gait analysis involves studying lower limb movement patterns, identifying events during stair gait, measuring kinetic, kinematic, and temporal parameters. The gait consists of the stance and swing phase, and the stance phase involves weight acceptance, leg-pull up and forwards continuation. The swing phase involves foot clearance and foot contact length. Stair gait analysis is very useful for assessing and improving stair negotiation safety. During stair negotiation, gait analysis can identify older people with a stair fall risk and help improve balance and reduce stair injuries.

Individuals walking up and downstairs are summarised in the following, which is different from walking on a level surface. When they ascend stairs, the leading foot is placed approximately horizontal on the approaching step. The heel usually would be

placed onto the tread, while the ball of the foot is placed further ahead on the tread. Next is the stance phase, in which the rear foot commences its ascent, rising onto the tiptoe to aid in elevating the entire body upwards and forwards. The rear foot generates a strong force that allows the opposite leg muscles to flatten and straighten out, effortlessly elevating the body further upwards. Following this is the swing phase. The rearmost leg moves past the leading foot over two nosings' (two-step edges) onto the above step, and the cycle repeats.

Accidents tend to be more severe while in descent, where, during the swing phase, the leading foot travels over the two nosings (of the tread that the rear foot is currently on and the tread that the leading foot was on) halts above the tread below. Next is the stance phase, where the rear foot's metatarsal heads brace the entire bodyweight's entirety as the heel of the rear foot starts to rise. Simultaneously, the rear leg bends at the hip and knee, meaning that the individual using the stairs has now transferred their weight to the forward foot and commences a controlled fall forward and downwards. To absorb the impact of the fall, the toes of the foot are pointed down towards the lower tread, with the angle of the same foot increasing towards a vertical position as the escalation increases. Next, the shock of the impact is softened by the ball of the foot and, lastly, the heel when the foot is lowered onto the tread. The swing phase then begins with the leading foot, which was the rear foot, after the weight is transferred onto the forward foot, and the cycle repeats.

The most significant differences between the manner walking on the stair and walking on a level surface are that the transfer of weight vertically requires a controlled fall in descent or extra effort for ascending; and that individual step taken on stairs initiates on the toes and ball of the foot, rather than the heel.

2.1.5. What are the hazards associated with stair negotiation?

Accidents tend to be less severe when ascending (Templer 1995) because the older adult's centre of gravity is slightly forward. As a result, most falls are relatively insignificant and are towards the higher steps. When considering the gait, the most substantial risks are during the swing phase, as there is an increased risk of tripping when the rear foot travels over two nosings; this risk is predominantly heightened if there is a sizable variation in

the user's height along with the flight of stairs (Roys 2001). There is an additional hazard situation during ascent when the user pushes off the lower tread with the rear foot. There is a risk of the foot slipping at this point if the slip resistance of the tread is low. There is also a possibility that the user will completely miscalculate the next tread's position and will under-step, completely missing or sliding off the top edge of the step.

In contrast to this, accidents tend to result in more severe injuries when descending, given that a fall in this position could end in the older adults hitting any number of stairs en-route, descending the full flight by falling or tumbling down, potentially resulting in fatal injuries. Consequently, head injuries and broken bones are widespread in accidents concerning the descending steps compared to ascending them. There is no major problem with the descent if the treads' going (area of space for foot contact length on step) is greater in size than the older adults' shod foot. However, the problems are exaggerated as the goings decrease in size since this means that one of two possible outcomes have the opportunity to occur. Older adults will either allow the toes of their feet to hang over the edge of the tread or begin to turn their feet outwards; so that each foot is placed at an acute angle to the walking line (the direction of travel). Older adults may be at risk of catching their heel on the nosing or the riser of the step above if they do not initiate one of these compensatory measures as they may not be able to place their foot flat and securely on the tread. As a result, older adults may fall forward down the stairs due to either of these situations.

There is a high risk of sliding off the step if older adults allow their toes to hang off of the edge, bearing the angle of their foot in mind as it hits the lower tread and the fact that they are in a controlled fall. As a result, older adults will either fall forwards or backwards, depending on the relation between their front foot and the older adults' centre of gravity position, and whether any reactionary-saving measures, such as grabbing the handrail, are made. Although they may be very painful, there is a relatively low risk of causing severe injuries when slipping down a flight of stairs or falling backwards (in descent). However, as mentioned above, more severe injuries are likely to result from falling forwards (in descent).

2.1.6. UK Stair fall history

There are approximately 6000 deaths annually as an outcome of a home accident, showing that falls represent a significant health problem in the United Kingdom. In addition, these deaths are often associated with perturbation during everyday activities such as ambulation, stair ascent, or stair descent (NHS 2018).

Falls can happen to anyone, but the most vulnerable are older people, even though falls are common when overlooked, which causes injuries. Approximately 1 in 3 older people aged 65 and over, lives in the home environment will experience at least one fall a year (NHS 2018). Not all falls cause serious injuries. But some of the falls could lead to broken bones, which will reduce the person's confidence. When older people lose their confidence, they will become withdrawn and dependent (NHS 2018).

'Royal Society for the prevention of accidents' refer to fall as the most typical accident, more common in women than men. It is also reported that more people over 65 years die at home because of the accident than outside (Applebey 2016).

In 2015, about 787 deaths were reported due to falling from stairs in England and Wales. This figure had increased by 20.5% from 2012 (Applebey 2016). The most common accident in old age is falling from stairs and steps. This fall accounts for approximately 60% of the geriatric population's deaths. The most typical death mode amongst these is falling from steps and stairs (Applebey 2016). There are five times greater stair fall accidents in 75 years and older populations, and about 100 thousand elderly are treated for stairs-related falls each year (Applebey 2016).

Besides, little research has investigated the contributing factors to imbalance during stair negotiation, which leads to stair falls. This project aims to identify older adults who are most vulnerable to falling but have not yet experienced a fall. Identifying fall risk is vital since tailored exercise programs or activities and changes in the living environment may help prevent falls on stairs if applied when a person at risk is identified.

2.1.7. Causes and Risk factors of stair falls

Often, 'multifactorial' causes are reported as contributing factors to a stair fall event. We can divide the risk factors into the following categories.

- Environmental factors
- Personal factors
- Behavioural factors

Environmental factors:

In daily life situations, people will encounter a wide range of staircases with various dimensions, which will have a different influence on the risk of falling. Dimensions of the steps of the stairs can amplify the risk of falling. The stair dimension is described using three terms: rise, going, and pitch (Figure 2.1).

The staircase dimensions are essential factors in the stair fall event (Scott, Menz et al. 2007). The stairway going is also very important. Tread risers are also a vital part. If the risers are huge, older people may fatigue immediately and are more likely to trip. When risers are very small or shallow, older adults may be tempted to take more than one step at a time, which leads to more chances of misstepping. The steepness or pitch of a stair may influence the likelihood of a fall. Tread risers are also an important aspect.

Building regulations permit a private staircase to be made up of individual steps with each rise between 100-220 mm and a going length between 225-350 mm and a maximum incline of 41.5°. Similarly, the public staircase (Scott, Menz et al. 2007) to be made up of individual steps with each rise between 100-190 mm and a going length between 250-350 mm and a maximum incline of 38°. These ranges permit a considerable variation in staircase design (Table 2.1).

Table 2.1 Standard stair dimensions for private and public building

Stair category	Rise(mm)		Going(mm)	
	Min	Max	Min	Max
Private	100	220	225	350
Public	100	190	250	350

When the rise is less than 100mm, it is associated with more trips. Also, 220mm is the maximum chance for people to negotiate their steps (Institution 1985) safely.

The staircase structure can magnify the demands placed on the individual. For example, steep staircases create larger loading forces at foot contact and cause a more significant redistribution of forces at the joints than less steep staircases. It is also known that transition steps from the level onto the stairs or from the stairs onto the level are more demanding than the continuous steps in-between (Roys 2001).

More precisely, staircases with an inadequate step tread to safely place the foot can restrict movement and threaten safety. Additionally, a stair with a higher riser is more challenging for older adults who, for example, have higher muscle weakness. It has been found that older adults can safely negotiate stairs with a lower step riser (Bertuccio and Cesari 2009) compared to younger adults. Even for standard step risers, older subjects operate closer to their maximum capacities of joint range of motion (Reeves, Spanjaard et al. 2008, Samuel, Rowe et al. 2011), thus increasing their risk for a fall. Risky techniques employed by older people during stair negotiation can also increase the risk of falling. Older people might change their techniques over time because of their functional impairments or fear of falling (Zietz, Johannsen et al. 2011). For example, older people may have a large foot overhang on landing when stair walking and higher variability in foot clearance (Hamel, Okita et al. 2005), both of which increase the risk for a slip or trip on the stairs.

Navigating through the stairs with caution is crucial for a fall, particularly the top and bottom three steps on a flight. Studies have demonstrated many stairway accidents occur on these top or bottom stairs (Templer, Archea et al. 1985). At these locations, the older adult may be looking around for the next part of the journey or the route to be taken; that's why older adults attention may not be entirely focussed on the stairway (Templer 1995). Carpets or flooring with dazzling patterns may also disguise the edge of stair treads and cause a misplaced foot.

The steepness or pitch of a stair may influence the likelihood of a fall. British Standards control the angle of steepness. However, in private buildings, the pitch may often exceed the maximum of 41.5 degrees. This increased pitch contributes to an increased possibility of accidents. Accidents are nearly twice as likely on stairs consisting of straight steps with no immediate landings, and the stairs' pitch is more than 42° (Applebey 2016). In addition,

the Colchester council reported that the lack of any handrail doubles the likelihood of a fall.

Stairway type is another factor that contributes to falls. This research (Templer 1995) found that straight flights of stairs without landings accounted for 52% of all accidents. This straight might be the case because the path of straight flights is often clear and uninterrupted, so older adults are reassured into a false sense of security and reduced attention. However, straight flights may also result in more severe injuries because there is no place where the fall may be broken on the stairway.

Personal Factors

Stair users' characteristics may often contribute to stairway falls. The next important factor of stairway fall is age; older people are more prone to stairway fall. Vision impairment and balance problems associated with ageing are the main reasons for the high prevalence of stair-fall injuries in old age. The decreasing visual and balance perception from feet and joints makes it difficult for older adults to judge the stairs' edges well. In addition, the above mentioned age-related personal decline challenges the older adults to make their judgments towards the swinging limb's foot clearance (Cavanagh, Mulfinger et al. 1997). To potentially make matters worse, bone density also diminishes with age, so the injuries sustained may be more serious.

With increasing age, both the health and agility of the human body deteriorates, resulting in an increased risk of falling among older people. With ageing, an adult experiences a loss in muscle mass, strength, and power, accompanied by a reduced range of motion in the lower limb joints. Reduced muscle mass and slower nerve conduction velocity lead to inadequate and delayed muscle contraction and force production within a reduced range of motion. These changes adversely affect an individual's ability to recover from a threat to balance when quick reactive and appropriate muscle activation is necessary. In addition to muscle strength, an appropriate range of motion in the lower leg joints are essential for safe walking and stair negotiation.

This study (Pauls 1985) reported that approximately 85% of deaths resulting from stair accidents occur in people over 65. With the increasing number of older people in the population, stair accidents are also likely to increase. Another study on falls in homes

(Applebey 2016) showed that individuals over 75 are thirteen times more likely to get injured than children aged 0-9. According to the US National Safety Council statistics, 84% of the people who died after a fall are over 65 (Roys 2001). Mainly, stairway injuries among the elderly (in this case, over 65) are more likely to result in hospitalization.

Familiarity with the house and stairs is often helpful; however, this can become an issue in some circumstances. For example, when poor housekeeping is maintained or transient changes to the house environment, the individual can face unexpected changes to their familiarity; these changes could make the older people a fall sufferer. Other important characteristics can be dizziness and fainting or muscle strength weaknesses in the knee and ankle joint muscles, increasing stair-fall incidents (Nagata 1991).

Behavioural factors

Certain behaviours may influence the likelihood of experiencing a stairway fall. Carrying items are commonly linked with falls on the stairs. According to (Nagata 1991), carrying objects on stairs leads to 24% of stairway falls. It also decreases the chance of recovering from a loss of balance since the hands are not free to grab onto a handrail. Stairway users' whole-body balance may alter while carrying objects on stairs; this balance alteration leads to a fall.

Fear of falling

Fear of falling is one of the crucial factors associated with falls in particularly older individuals. It varies from 22% (Wijlhuizen, de Jong et al. 2007) to 63% (Dias, Freire et al. 2011) by reviewing the literature. The fear of falling limits people's outdoor activities (Wijlhuizen, de Jong et al. 2007, Dias, Freire et al. 2011). It creates a vicious problem as they do not go outdoor; reduced physical activity may result in reduced muscle strength, which increases the chance of actual fall and fear (Wijlhuizen, de Jong et al. 2007). This fear of falling may also change their walking pattern in some older adults. Also, the older adult with a fear of falling may use devices like handrails to increase their balance, this is more common if they had a fall already (Murphy and Isaacs 1982).

2.2 Current Solutions to acquire stair fall risk factors

The motion capture system (photoelectronic systems for Motion Analysis) and force plate are used to analyse older people's gait while on the stairs to prevent stair falls.

2.2.1. Laboratory-based approach

Motion capture system uses infrared cameras (Mikhailchuk 2017) to record people's movements in three dimensions. In addition, motion capture systems use a marker or optical systems. Markers are commonly small ball-like attachments the size of a marble or reflective circle. These markers are placed on the body with specific guidelines for better quality data. Anatomical landmarks are selected for their reliability in determining joint motion.

The most common motion capture systems are Vicon, Motion Analysis, OptoTrack, NDI, DARI Motion, Phoenix Technologies, Inc., and Xsens. The most used motion capture systems in biomechanics are VICON and OptoTrack. Both VICON and OptoTrack systems are optical tracking systems that track three-dimensional movement trajectories of reflective markers with up to 1mm accuracy. Force platforms represent the gold standard method for determining gait events. The force platform appears as one of the most common tools to provide information on three orthogonal forces and moments exerted by the human body.

Motion capture helps connect other data sets like force platforms, which helps understand joint angle and body motions from different perspectives. However, capturing full-body motion requires a controlled laboratory to allow robust data collection.

Although the Motion capture system is considered a “gold standard system”, it requires cumbersome equipment and tight clothes for marker placement which may cause participants to alter their gait. In addition, the cost of most motion capture systems is not cheap, and it requires a fully equipped laboratory on average.

2.2.2. Motion capture analysis for stair fall risk detection

Motion capture systems are used for many stairs-related projects; each research focuses on different stair falls factors mentioned above. For example, these studies (Tinetti,

Doucette et al. 1995, Hamel and Cavanagh 2004) compared stair gait between younger and older adults, showing that older adults do slower ascend and descend with stairs. Older people also show greater stance, double the support times, and reduced vertical forces when accepting their weight and push-off. In addition, the fear of falling factor has been examined in this research (Tiedemann, Sherrington et al. 2007). Their findings show that older adults who have a fear of falling take cautious strategies such as velocity decreases, toe clearance increases, stable centre of mass or centre of pressure displacements. The previous evidence shows that older adults are at greater risk for falls on stairs because of their less stability when negotiating stairs.

Furthermore, Slip and trip are the two most important mechanisms for a stair fall. The possibility of a trip is associated with foot clearance, which has been widely studied (Tinetti, Doucette et al. 1995, Arens, Freudenthaler et al. 1999) using motion capture systems. Their findings show that older people have a range of highly inconstant or variable minimum foot clearance (Tinetti, Doucette et al. 1995, Arens, Freudenthaler et al. 1999) and low foot clearance (Zietz and Hollands 2009). The minimum vertical foot clearance was calculated as the minimum overall distance between the stair edge and the toe(ascending) or heel(descending) during the swing phase (Simoneau, Cavanagh et al. 1991). Also, the possibility of the trip increases when the foot clearance variability increases, showing a person's inability to maintain a safe foot trajectory on the stairs (Roys 2001).

The distance between the stair edge and the toe cap describes the foot overhang, indicating whether only a part of or the whole foot is placed on the stairs. The possibility of a slip is associated with the frictional forces between the percentage of foot contact length and the step (Roys and Wright 2005). High frictional forces increase the chance for a slip of the step-in ascent during push-off and descent during the loading phase. Also, the risk of slip increases when the foot contact length is reduced; for example, a large part of the foot overhangs over the step edge. Moreover, the risk for a slip is increased when the variability in the foot contact length and required frictional forces increases, indicating an inability to place the foot safely on the step consistently.

2.3 Wearable sensors to detect stair fall risk parameters

The motion capture systems require the maintenance of a high technology motion laboratory, and cumbersome equipment needs to be attached to the participant that needs to visit the laboratory. However, this high-cost method produces quantified and accurate results when testing in the laboratory. Motion capture systems have been used in many stair fall studies and found stair fall risk parameters and causes: foot clearance, foot contact length, foot clearance variability, foot contact length variability, acceleration, and velocity. However, motion capture results on their own are not a good solution, so we need to test at the home environment and more often and longitudinally.

So, there is a need for a low-cost device that detects falls, which can provide quantitative and repeatable results over extended periods in an older adult's home environment. Also, there is a need for monitoring participants' stair gait over long periods. Therefore, more research focuses on sensor technology with high demand for inexpensive fall risk detection. Many sensor technologies are available for motion analysis, namely accelerometers, gyroscopes, footswitches, load cells, and force-sensing resistors, facilitating the general gait parameters' accurate acquisition.

However, no stair gait analysis system already exists using wearable sensors. Therefore, this project's motivation is to design and develop a low-cost, reliable, and portable instrumented sensor shoe capable of predicting stair fall risk parameters. Instrumented shoe system helps perform the stair gait analysis in a less expensive and non-traditional motion laboratory environment. In addition, it also helps to collect a vast quantity of long-term data from various environments, and some are not possibly obtained in a conventional gait analysis laboratory system.

2.3.1. The available sensor solution for stair falls parameters

Foot clearance parameters

The shoe-integrated direct foot clearance measurement system is the most unexplored topic in stair gait analysis and biomechanics research. An accelerometer sensor has been used to calculate foot clearance in level walking. However, accelerometer data gives unreliable results because of drifts and errors (Aminian and Najafi 2004, Lai, Begg et al.

2008). Sensing minimum foot clearance (MFC) using only accelerometer measurement on uneven, bumpy surfaces or during stair descent or ascent is problematic. It does not directly measure foot clearance but instead calculates it using acceleration data, so it is unreliable.

MIT Media Laboratory has developed an electric field sensing technique and proves that this technique can calculate foot clearance on level walking (Lamb, Jørstad-Stein et al. 2005). The drawback of this system is that it can only measure up to 5cm (Wahab 2009). An ultrasonic sensor has been used to calculate foot clearance (Hamel and Cavanagh 2004); this system's problem is that the ultrasonic sensor is too big to fit in the shoe, which might affect participants' walking. The studies mentioned above focus on level walking foot clearance, so we need to find a simple, low-cost sensor to detect foot clearance on the stairs.

Foot overhang parameters

There is no sensor shoe available to calculate foot overhanging on the stairs; some force sensors-based insoles exits are used to calculate foot distribution while level walking. Force distribution measurements allow examining force changes under localized regions and extracting the foot's orientation and position [Yip and Prieto, 1996].

The in-shoe devices display more advantages when compared with the force platform or floor-mounted systems. Participants can wear the in-shoe device while walking in their normal gait. The in-shoe device can monitor multiple steps while the force platform cannot. Because of wireless communication development, in-shoe devices can also be used in laboratory, clinic, and outdoor environments. This in-shoe also extends the usable locations for older people or patients at risk. Up-to-date research to obtain the acceleration and orientation velocity of joints using gyroscopes and accelerometers has been carried out. The commercially available in-shoe measurement systems are F-Scan systems and Pedar systems, but they are application-oriented devices, and these systems are costly. One example instrumented system was developed by (Grandez, Bustamante et al. 2009) and his colleagues based on tiny electronic circuits that collect and transmit data from force-sensing resistors. A separate sensor and load cells have been used to measure and sense force and torque. This is not only low-cost but also appropriately designed to obtain

forces accurately and reliably. Unfortunately, the load cell problem is too heavy and can hardly fit in the shoes.

A multimodal approach was used in the insole motion measurement system. This instrumented insole system consists of an array of force-sensing resistors (FSRs), a dual-axis gyroscope, and a tri-axis accelerometer. This combination of sensors allows for the plantar pressure measurement and detects the necessary motion patterns for further analysis in the fields of fall risk detection and physical activity measurement (Jagos, Oberzaucher et al. 2010).

Also, many other instrumented insole designs were created with several sensors to measure different kinematics and kinetics forces based on their research or study requirements. For example, wireless gait analysis system by digital textile sensors (Yang, Chou et al. 2009), wireless modular sensor architecture and its application in on-shoe gait analysis (Benbasat, Morris et al. 2003), compact modular wireless sensor platform (Benbasat and Paradiso 2005), and the list goes on.

However, all these customs made or instrumented sensors did not focus on stair fall risk parameters like foot contact length (foot overhang) and other parameters. This project aims to create a custom-made insole that can find foot overhanging and other parameters to identify stair fall risk in a typical living environment.

2.4 Wearable Sensor Shoe Solution

Stair falls are the main reason for the injury, and the loss of independence for older people and stair fall increases the NHS's demands. Stair fall risk parameters have been identified using extensive study on stairs in the laboratory. However, laboratory-based fall risk parameters require expensive, cumbersome material. Also, using laboratory-based equipment is not able to test at real houses. Therefore, there is a need to identify stair fall risk parameters using a simple wearable solution to fill the gap between the laboratory and real-time houses. Wearable sensor solutions have been studied extensively for different purposes. Still, none of the wearable solutions has attempted to detect stair fall risk parameters in older people at different real house staircases. Besides, the older adults who tested in the staircases must be followed up for an extended period to find older adults at risk of falling at stairs. The follow-up for a period helps to document falls on

stairs that occur after testing in the laboratory. However, no prospective study focused on stair falls using wearable sensors. After testing, obtaining future fall information would help identify the biomechanical stair fall risk factors that separate stair fallers from non-fallers. Machine learning algorithms help to improve the classification accuracy of stair fallers from non-fallers. However, there is no machine learning study available for older adults' stair fall risk data collected in different real houses and follow-ups.

So, this project's motivation was to design and develop a low cost, reliable, and portable instrumented sensor shoe system to detect stair fall risk factors in a typical living environment. After testing, older adults needed to be followed up for a period to document fall history, which occurs post-testing. We need to develop a machine-learning algorithm to predict stair fall risk in the future. The instrumented sensor shoe was developed to achieve our aim, described in chapter 3. The designed sensor shoe was tested in the laboratory, and stair fall risk parameters were validated against the Vicon system described in chapter4. Developed instrumented sensor shoe was tested at different houses staircase, and the results were compared in chapter5. A machine-learning algorithm was used to classify fallers and non-fallers in chapter6. Chapter7 explains the summary of findings and future recommendations to improve stair safety.

CHAPTER 3: Sensor Shoe Development

3.1 Introduction

This chapter focused on designing an instrumented sensor shoe with an insole to measure stair fall risk parameters. Several main aspects are needed to develop an instrumented insole to obtain the most practical design. The main aspects were sensor selection, sensor positions, power supply, signal conditioning, data logging, data transmission, data storage, and data analysis. To cover all those aspects, this chapter is divided into four sections, which are sensor selection, instrumented sensor shoe implementation methods, discussion about sensors specifications and results.

3.2 Sensor selection

The first step in designing instrumented sensor shoes was selecting the appropriate sensors to create an instrumented sensor shoe system capable of sensing stair fall risk parameters. Chapter 2 Literature review identified some of the significant stair fall risk parameters through other stair fall studies and research articles. Those parameters were foot clearance, foot contact length, cadence, stance time, swing time, linear gait acceleration, gait velocity, angular velocity, and foot angle (pitch).

3.2.1. Foot clearance

Currently, foot clearance measurements are being done using the electric field sensing technique (Morris 2004, Bamberg, Benbasat et al. 2008) in level walking. However, it can only measure up to 5cm, and it requires a minimum of 5 layers of electrodes and insulators, which increases the total thickness of the insole. The other method is based on the ultrasonic sensor technique (Bakar, Wahab et al. 2013), which is also widely used in level walking; this sensor system is larger in size, so it is not ideal for stair climbing research.

The VL6180X distance sensor was selected to measure foot clearance; this sensor was chosen due to its size, measurement range, and accuracy. This VL6180X sensor contains a distance sensor and a light sensor. Two distance sensors were implemented to measure foot clearance. Two distance sensors were placed at the back (underneath the shoe's sole), under the toes and the heel. The front sensor was used to calculate ascending vertical foot clearance, and the rear sensor was used for descending vertical foot clearance.

3.2.2. Foot contact length, stance time, swing time and cadence

Force Sensitive Resistors (FSR) were selected and placed underneath the foot to measure foot contact length. An FSR is a sensor whose electrical resistance decreases as the applied load increases. Up to ten FSRs were placed underneath the foot from the heel to toe to calculate foot contact length during foot landing in stair climbing. Further analysis of the FSR sensor results helps determine foot stance time, swing time, and cadence.

Other force sensors or pressure sensors like fine-grain printed arrays of FSRs, Tekscan's F-Scan system were considered, providing extensive information about the pressure distribution underneath the foot. However, the higher market price of Tekscan's proprietary system is not a cost-effective choice for this research.

3.2.3. Linear acceleration, Velocity, Angular velocity, and Foot angle (Pitch)

An Inertial Measurement Unit (IMU) sensor was chosen for this purpose and was placed at the back of the shoe in the middle. IMU sensor contains three orthogonal gyroscopes and three orthogonal accelerometers, which can measure angular velocity and linear acceleration in a three-dimensional space. An IMU sensor is placed in a typical configuration to cover three different spatial axes. Like any sensor, accelerometers and gyroscopes are also prone to measurement errors. The data measured by an accelerometer is often obscured by noise, and a gyroscope must cope with drift over time. However, since both sensors capture an object's movement data, these errors are compensated by combining accelerometer and gyroscope data. By doing this way, the relative heading and speed of an object can be estimated in a process called sensor fusion. In addition, some IMUs are equipped with a magnetometer, which can compensate for the drift error in the accelerometer.

On the other hand, the magnetometer can provide a constant reference (magnetic north), allowing the relative heading to be transformed into an absolute orientation (Chabikuli, Fast et al. 2017). The Velocity and the position can be obtained from single and double integration to the acceleration component's time corresponding to the foot's forward motion in all three directions. The gyroscope provides information about the foot's rotation, which can be integrated with time to give the angle.

There are many readymade IMU solutions available. These products incorporate all the needed hardware, software and output 3D orientation data in Euler angles or quaternions. The IMU systems manufactured by Xsens, MicroStrain, VectorNav, Intersens, PNI and Crossbow are well known for this purpose. The downsides of these readymade IMU solutions are expensive; some models need manual calibration and are too sensitive to magnetic distortions.

Although many inexpensive IMUs available, far fewer products output 3D orientation data. Following are the essential elements of an IMU sensor for this research purpose,

- Output 3D orientation data in quaternion or Euler angle format, using the onboard computational device (microcontroller)
- Small physical size
- Good accuracy
- no angular drifting in time
- Low price (range of £20 - £50)

We chose BNO055 IMU based on these criteria for this project, and it has a 32bit microcontroller (high-speed Cortex-M0 based processor) running the BSX3.0 FusionLib software. The on-board fusion algorithm fuses the triaxial 14bit BMA055 accelerometer, a triaxial 16bit BMI055 gyroscope, and a triaxial BMM055 geomagnetic sensor into a single composite sensor.

Table 3.1 shows the stair fall risk parameter with the selected sensors that were used for this project.

Table 3.1 Stair fall risk parameter with the chosen sensor

Parameter	Sensor	Accuracy
Foot contact length ratio	Force Sensitive Resister	$\pm 5\%$ to $\pm 25\%$ of established nominal resistance (FSR user manual), Curve fitting calibration method was used to improve accuracy, $R^2 = 0.97$ lower forces, $R^2 = 0.99$ higher forces
Foot clearance	Range sensor VL6180X	± 3 mm
Orientation, stride velocity, displacement	IMU BNO055	Acc: 1 LSB/mg Gyro: 0.05 IMU (sensor fusion): $\pm 1\%$
Stance time, swing time	FSR, Range sensor	± 3 mm

3.2.4 Other Components

Apart from choosing the suitable sensors for this research, there are more essential components needed to build instrumented sensor shoes (Appendix D show the images of all the sensors used to develop sensor shoe) as the followings,

1. Bluno Nano Microcontroller
2. Arduino
3. I2c Multiplexer
4. Analog to digital multiplexer
5. SD card
6. Amplifier
7. Voltage regulator
8. Battery power supply

All these components technical details, working principles and implementation details are further explained in this chapter.

3.2.4.1 Bluno Nano microcontroller

The Atmega 328 microcontroller chip was used in the Bluno Nano board. Bluno Nano integrates a TI CC2540 BT 4.0 chip with the Arduino UNO development board (DFROBOT 2015). It allows wireless programming via Bluetooth Low Energy (BLE) and supports the AT command to configure the BLE. The Bluno Nano board contains an integrated Bluetooth module that directly transmits any data written over a 'Bluetooth Low Energy (BLE)' connection to its serial port. In this module, the firmware can be upgraded easily. This microcontroller is the perfect choice for BLE projects with limited space or weight. BLE is a low power version of Bluetooth 4.0, which runs with power sources for an extended period. Transmission range was confirmed through testing to be reliable up to 20 metres for indoor and 60m for outdoors, with the non-existence of any large physical barrier.

Bluno Nano contains two types of pins: analog pins (A), which can read a range of values and digital pins (D), which can read and write data. Two distance sensors and one IMU sensor are needed to connect with the Bluno Nano microcontroller through a serial communication protocol (inter-integrated communication, I2c). For this, the Bluno Nano microcontroller needs three sets of I2c pins; each set comprises one A4 analog pin (serial data) and one A5 analog pin (serial clock). However, in a standard Bluno Nano microcontroller, only one set of I2c connections is possible. An I2c multiplexer was used to connect the required three sets of I2c pins to the microcontroller. All three sensors (two distance sensors and one IMU sensor) were connected to this I2c multiplexer, which finally connects to the Bluno Nano microcontroller.

In this project, up to 10 'Force-sensitive resistors (FSR)' were selected; to connect these FSRs with the microcontroller needed more analog pins than available. Analog to digital multiplexer was used to overcome this issue, and this multiplexer was connected to the microcontroller to make these FSRs work; 13 resistors and two amplifiers were needed for each shoe. A Printed circuit board(PCB) was created to connect all these resistors, amplifiers, sensors, power supply and microcontroller, and a 7v battery-powered power supply was used. Technical details of this multiplexer and other components are explained below.

3.2.4.2 Arduino

Arduino software was used to write coding to Bluno Nano microcontroller. The Arduino Software is user friendly with an open-source electronics platform, which allows users to write program code and upload them on a microcontroller board. C/C++ language has been used to write coding in Arduino. The Arduino software included all the necessary sensor libraries to make instrumented sensor shoes work. After adding all the libraries, coding was written to get the desired output (Appendix G).

3.2.4.3 I2C Multiplexer

The IMU and two distance sensors that use I2c communication share the same hardware ID. This same hardware ID prohibits using a common I2c bus as the sensors are indistinguishable from one another. Our design provides an independent I2c channel for each sensor using I2c multiplexer to overcome this issue,

The TCA9548A I2c multiplexer was used to collect data across all the three sensors that were concurrently operating I2c channels. Its technical specifications are as follows ((Instruments 2015):

- Selectable I2C address 0x70-0x77
- Operating Voltage: 1.65-5.5V
- Weight: 1.8g
- Product Dimensions: 30.6mm x 17.6mm x 2.7mm / 1.2” x 0.7” x 0.1”

The use of an eight-channel I2c multiplexer (Instruments, 2015) allows our design to support up to eight independent sensors and presents a layer of expandability to our system.

It comprises two distance sensors, a BNO055 IMU sensor that collects various forms of motion data. These sensors communicate via the I2c protocol and are wired through a TCA9548A I2c multiplexer to the Bluno Nano microcontroller. The Bluno Nano microcontroller functions as a master, facilitating data collection, formatting, and transmission over Bluetooth 4.0 to our SD card.

3.2.4.4 Analog to Digital multiplexer:

Spark Fun's Analog to Digital Multiplexer CD74HC4067 breakout board was used to multiplex FSR sensors. It has a 16 Channel Analog Multiplexer. This chip is like a rotary switch; it internally routes the common pin (SIG on the board) to one of 16 channel pins (C1 to C16 in the board). It works with both digital and analog signals, and the connections function in either direction (Sparkfun 2005).

To make this work, four digital outputs from the Bluno Nano microcontroller connected with analog multiplexer's pins S0-S3. This analog multiplexer gives provision to connect 16 FSR sensors if we need to increase the FSR sensor or need to include other sensors in the future.

3.2.4.4 Operational Amplifiers (LM358)

The operational amplifier is an amplifier where the output voltage is proportional to the negative of its input voltage. The LM358 is a low power quad operational amplifier (Sparkfun 2005), consisting of four independent, high gain, internal frequency compensated operational amplifiers. LM358 operational amplifiers were used in a voltage divider configuration of the design to achieve a switch-like response where a certain amount of force is required to break the sensor's resistance to allow a proportional voltage to leak/go through it. The resistance value of the pull-down resistor is inversely proportional to the force sensitivity range of the FSR, which limits the current.

It is explicitly designed to operate from a single power supply over a wide range of voltages. The low power supply current drain is independent of the magnitude of the power supply voltage. The LM358 connection details are explained in the FSR sensor implementation part.

3.2.4.5 Battery power Supply

Without a power supply, the whole instrumented system cannot function. Therefore, providing enough electrical power to make the instrumented sensor shoe's measurements work was crucial in operating the entire system. Meanwhile, attention should be paid to selecting the voltage source, which would supply the correct range of required voltages

for the system's electrical and electronic circuitry. Hence, electronic components such as voltage regulators were implemented to ensure no extra voltage would cause overflow or damage to circuitry.

The 7.4 V Rechargeable batteries (Sparkfun 2005) were used to provide the required voltage to the whole design for smooth operation. Voltage regulators were used in this design to regulate and maintain the input voltage at a constant level. The difference between the actual output voltages with the internal fixed reference voltage was amplified and used to control the regulation element to correct the voltage error.

3.1.4.6 Voltage Regulator (LM7805)

A 7.4 V battery has been used to supply power to the electronic components in this design. Typically, most electronic components' operating power ranges from 2.0 V to 5.0 V, where too high input voltage may cause damage. Therefore, an LM7805 5.0 V (STMicroelectronics 2018) voltage regulator was used to lower the input voltage before the voltage was supplied to the whole circuit. The LM7805 5.0 V voltage regulator consists of three-terminal pins: input, ground, and output pins.

3.1.4.7 Data Storage

Data storage is a sub-system used by the instrumented sensor shoe to store the collected data for further analysis. An individual micro-SD card for each shoe was used in this model to record the real-time data and to store the collected data. The data was stored as CSV files by using LabVIEW software.

Adafruit provides a micro-SD breakout board that was connected to a Bluno Nano micro-controller. Arduino has been used to create a file in the micro-SD cards (Electronics 2010), which contains all the necessary data logging methods. 5v power supply was used. To make the SD breakout board work, CLK pin from micro-SD board connected to D13 (digital 13) pin in Bluno Nano micro-controller. Similarly, these pins were connected D0 to D12 pin, D1 to D11pin and CS to D10pin.

Adafruit Micro-SD breakout board was implemented into the instrumented sensor shoe system. SanDisk Extreme 4GB microSD cards were used for this project. All the collected data were logged into the micro-SD cards with its built-in capability (writing speeds up to 90 MB/S) by the Arduino. An Arduino programme was created with a for loop. This programme creates CSV files from digits 00 up to 999, based on whether the file already exists or not. A string was created to write the structure of the data file.

3.3 Methods

3.3.1. Instrumented sensor shoe physical implementation

Some of the functional requirements were considered to design this instrumented sensor shoe as follows,

1. Should not affect the stair climbing gait
2. To collect data for both the feet
3. Wireless
4. It is available in different sizes of insoles and instrumented shoes, so anyone can use them.

One of the sensor shoe's essential requirements is that it should not affect the participants' gait while climbing stairs and the hardware had to be small, compact, and lightweight. There are published research evidence (Hausdorff, Zeman et al. 1999) that have shown that even when the lower extremities are loaded with different weights, this can result in subtle effects on the stair gaits. So, instrumented insole final prototype was made under 300gm.

Both shoes were instrumented to get both feet motion data at the same time. Figure 3.1 shows the instrumented sensor shoe. The instrumented sensor shoe comprised one PCB (Printed circuit board) module and instrumented insole. PCB module was mounted to the shoe's lateral side using a robust Velcro strap. The Instrumented insole was placed inside the shoe. We used shoe sizes 6 to 10 to accommodate women and men participants in our research. The Instrumented insole can have 6 to 10 'Force-sensitive resistors' to collect the pressure data depending on the shoe size.

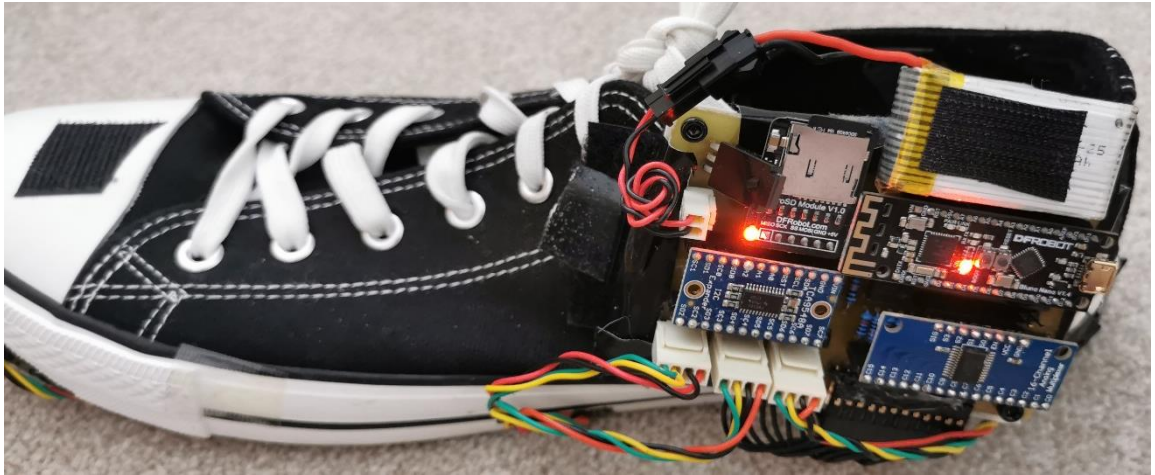


Figure 3.1 Instrumented shoe with PCB Module, and Insole fitted

A Printed Circuit Board (PCB) is vital in holding the entire instrumented sensor shoe's hardware together. PCB connects various electronic components on a shared physical platform. PCB was created using EAGLE software (EAGLE is an acronym for Easily Applicable Graphical Layout Editors).

The PCB module contained the Bluno Nano microcontroller with Bluetooth (BLE). This Bluetooth made instrumented shoe into a wireless system. PCB module contains additional components, which are IC2 multiplexers for IMU and range sensor, an analogue multiplexer, resistors, an amplifier for the insole, voltage controller and connection for the inputs from the power supply. After designing the PCB, two separate PCBs were printed for both left and right feet.

IMU sensor was fitted at the back of the shoe's middle part to measure the foot motion directly on the stairs. In this way, foot angle output is zero when the foot is flat. When the foot starts to move, the IMU sensor helps to measure the foot angle. This foot angle information is vital because if the participant has a larger foot angle with less foot contact length, this can cause a fall.

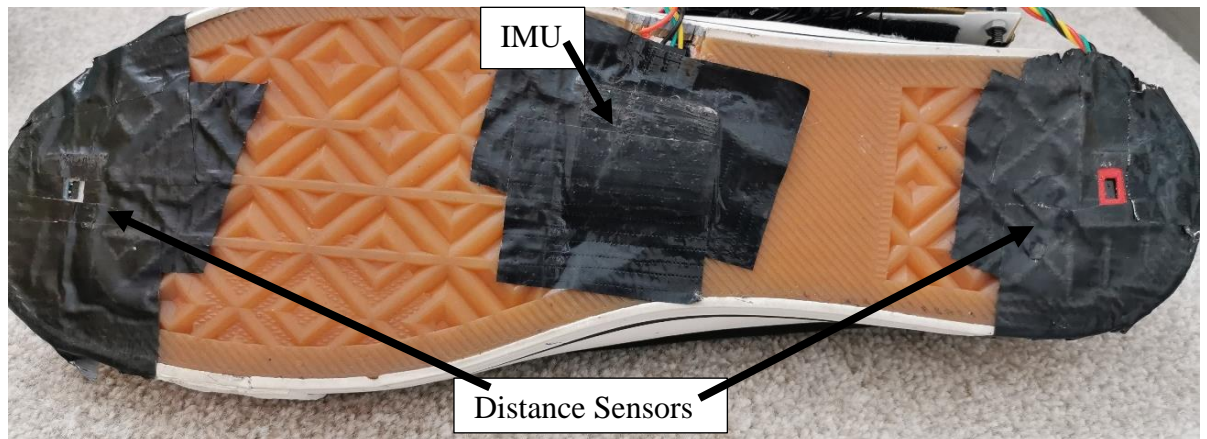


Figure 3.2 Back of the instrumented insole, two distance sensors and one IMU sensor fitted

We fitted two distance sensors at the back of the shoe. The front distance sensor was fitted just beneath and parallel to the toes, and the rear one was fitted right beneath the heel (Figure 3.2).

The reasons for fitting the sensors at the back of the shoe are as follows,

- Distance sensor can directly measure the distance between shoe and stair edge
- To calculate vertical foot clearance in ascending, we need to know precisely when the toe crosses the stair edge. Placing the sensor closer to the toe is essential to find out this information. So 'front distance sensor' was placed at the back of the shoe, parallel to the toes.
- To calculate vertical foot clearance in descending, we need to know precisely when the heel crosses the stair edge. To find out this information, placing a sensor right at the back of the heel is essential.

The Inertial Measurement Unit (IMU) and distance sensors can get damaged while walking. Two separate cases (boxes) were used to protect the Inertial Measurement Unit (IMU) and the distance sensors from damage. These cases were designed using ‘solid works’ software. Box type case was designed for the IMU sensor, while the distance sensor’s case was designed differently. Because the distance sensor’s sensing module needs to see the object to measure the distance, the case was designed with a small *rectangular opening*. Figure 3.3 shows the IMU sensor case and distance sensor case. IMU and distance sensor cases were printed using nylon material. Nylon filament is a reliable, durable, and versatile 3D printing material. Also, it is thin and flexible, with very high inter-layer adhesion.

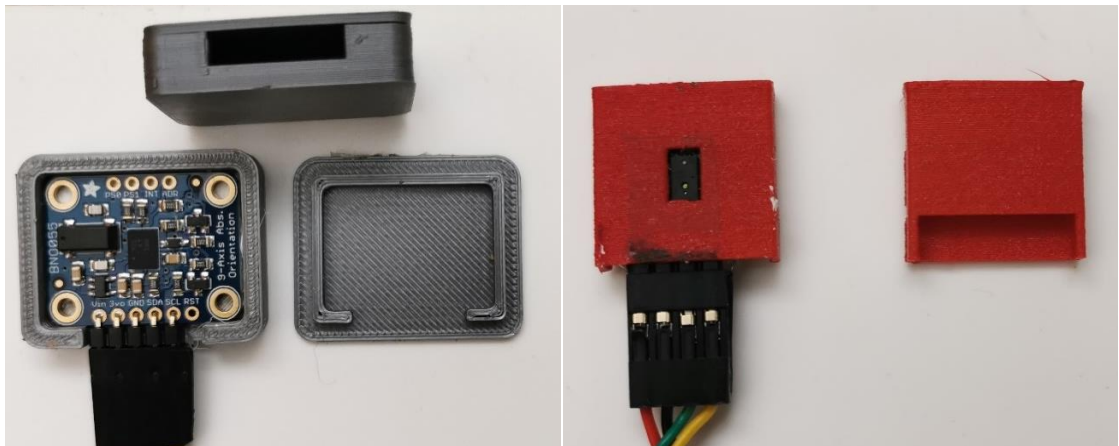


Figure 3.3 Case for IMU and Distance sensor

A Lab view program was created as a user interface (explained later in this chapter) to send start and stop signals to the shoe’s microcontroller. Next, the microcontroller sends data to each shoe’s SD card (Each shoe has a separate SD card), where the data gets stored and transmitted to the computer for further analysis.

3.3.2. Insole design

Eagle software was used to design instrumented insole, and flexible PCB lamination material was used to print the insole design. Figure 3.4 shows the insole design. Flexible PCB (Flex FR4) was just 0.127mm thick, double-sided, 1/2oz copper material, and it is ideal for making flexible circuits. This Flex FR4 PCB is semi-rigid, and a high-quality laminate allows the creation of flexible PCB and solder components directly onto the copper tracks using standard soldering techniques and temperatures.

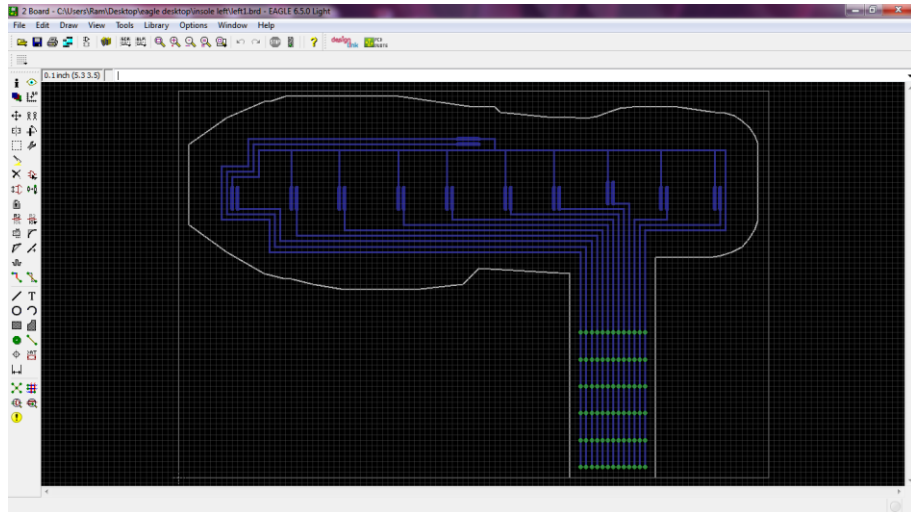


Figure 3.4 Instrumented insole designed in eagle software

After printing a flexible insole, FSRs were soldered onto it. Figure 3.5 shows the Instrumented insole. The instrumented insole accommodates several FSR sensors connected to the PCB module via a connector pin.

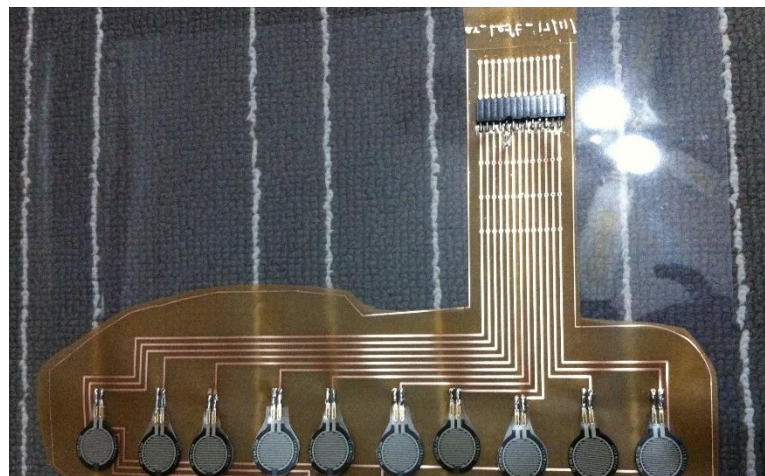


Figure 3.5 Instrumented flexible Insole printed and fitted with ten FSRs

The insole contained from 6 to 10 FSRs in line. The insole provided a straightforward method to position the sensors in order beneath the foot. The reason for placing the sensors in the line was to calculate the foot contact length directly. Therefore, we will get the force readings only when the foot touches the stairs during the stance phase. When

the foot is not touching the stairs, we will not get any force reading. Also, when the foot is in the swing phase, we will not get any force readings.

The FSR sensors were purposefully facing downwards for sensor safety. They were placed in the middle of the shoes, with the sensors and wires coming off from the shoes' lateral (outside) aspect. An additional layer of insole hid these for protection. The distance between each sensor was 26mm to 29mm, and these were noted down for future calculation.

3.3.3. LabVIEW user interface for data collection

The user interface for data collection was developed using LabVIEW software (Laboratory Virtual Instrument Engineering Workbench), a system-design platform and development environment for a visual programming language from National Instruments [NI]. LabVIEW is commonly used for data acquisition, instrument control, and industrial automation.

LabVIEW has built-in functions that can read serial data sent by Arduino to LabVIEW's VI (Virtual Instrument). A way to do so is to use 'VISA resource' to get data serially.

VISA serial was used to get settings from Arduino. The data has a baud rate of 115200 and was transferred in 8 bits. Baud rate refers to the number of signal or symbol changes that occur per second (Frenzel 2012). A 'while loop' was created to read data from the 'COM port' whenever serial communication occurred. There were three 'COM ports' created. Left shoe 'COM port', right shoe 'COM port', and triggering 'COM port'.

Data collection was done in two different settings (laboratory and three different house settings). In Laboratory, data was collected via the 'VICON system'. To synchronise VICON with the shoes, 'Vicon's sync out port' was connected to an 'Arduino microcontroller analog pin'.

When the 'Vicon system' starts collecting data, Vicon's synchronise port will send a 'high voltage signal' to Arduino. Arduino continuously checks these voltages; when the voltage reaches 'greater than 3v', this will send an 'H' signal to LabVIEW. As soon as the 'Vicon system' stops collecting data, the 'Vicon's synchronise port' will send a low voltage

signal to Arduino. On receiving this low voltage signal of ‘less than 3v’, the Arduino will send an ‘L’ signal to the LabVIEW.

LabVIEW continuously checks the ‘Arduino trigger port’; when LabVIEW receives an ‘H’ signal, LabVIEW sends a ‘start signal’ to both the shoes via a dedicated Bluetooth system to start data collection from the shoes. When LabVIEW receives an ‘L’ signal, LabVIEW sends a ‘stop signal’ in the above manner to stop data collection by the shoes.

Once the data collection is started, LabVIEW reads the data sent by the shoes and writes them into an ‘SD storage card’ with a ‘Unique/itemised file name’ for each data. This Unique file will be closed when the LabVIEW receives the ‘L’ signal by sending a ‘stop signal’ to the shoes.

In houses, data collection was done without Vicon triggering (Appendix B). LabVIEW sent a signal directly to shoes to start and stop data collection. Figure 3.6 shows the LabVIEW user interface, which we created to collect data from instrumented shoes.

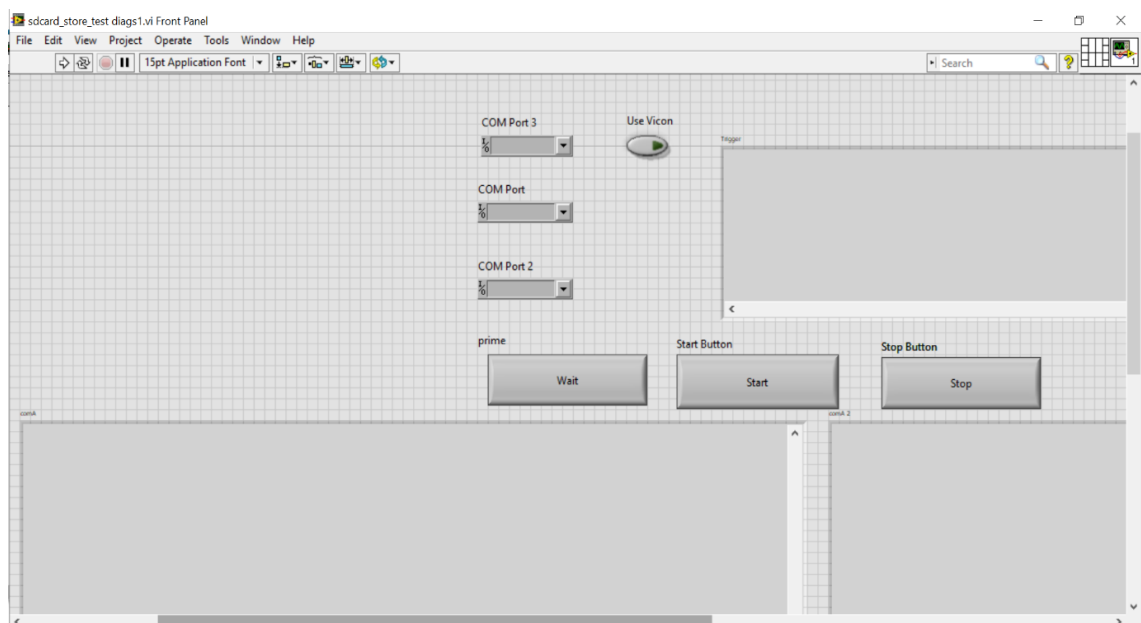


Figure 3.6 Instrumented data collection user interface, COM port3 to connect with Arduino for synchronisation, COM port to connect with left sensor shoe and COM port2 to connect with right sensor shoe. Use Vicon button used for lab data collection, start, and stop buttons were used for houses data collection.

3.4 Results

This section discusses each sensor, including an overview of the sensor's working principle and the signal conditioning and implementation used in the instrumented sensor shoe system. A table summarizing relevant parameters of each sensor (as provided by manufacturers) is included.

3.4.1. Bandwidth requirements

The average step rate of adults is just under 120 steps per minute, which corresponds to a stride frequency of 2Hz. Each sensor worked well with a high sampling rate on its own. For example, the IMU sensor gave 50hz data when tested on its own. The distance sensor also gave 50hz data. In this project, there were between seven to ten force-sensitive resistors used. Each Force-sensitive resistor provided two outputs, so a total of twenty sets of output at a time. Instrumented sensor shoe circuit output contains twenty FSR sets of data, two distance sensor data, three-axis accelerometer, three-axis gyroscope, roll, pitch, yaw, and time data, which was more than 30 sets of data. Due to the large quantity of data, bandwidth was reduced to 20hz. The comparison was made between the 20hz data in the circuit and 50hz data to avoid missing any crucial information. The result showed that 20hz data did not miss any crucial data. So 20hz bandwidth is used for data collection.

3.4.2. Distance sensor specification

The VL6180X product is based on ST's patented 'Flight Sense™ technology'. This ground-breaking technology allows absolute distance to be measured independent of target reflectance (STMicroelectronics 2010). Instead of estimating the distance by measuring the amount of light reflected from the object (which is significantly influenced by colour and surface), the VL6180X precisely measures the time the light takes to travel to the nearest object and reflect the sensor (Time-of-Flight) (STMicroelectronics 2010).

Combining an IR emitter, a range sensor and an ambient light sensor in a three-in-one, ready-to-use package, the VL6180X is easy to integrate.

The main advantages offered by this technology are:

- (i) transmitter and receiver integrated into the same module
- (ii) small sensor dimensions
- (iii) accuracy independent from experimental factors (e.g., the intensity of the ambient light)
- (iv) low power consumption ($\sim 2\text{--}5$ mA).

Thus, VL6180x distance sensors are suitable to use for human movement applications. The module is designed for low power operation. Ranging and light intensity measurements can perform at user-defined intervals. Multiple thresholds and interrupt schemes are supported to minimize host operations. Host control and result reading used I2c serial communication.

3.4.2.1 Working Principle

The VL6180X uses ST's 'Flight Sense technology' to measure how long it takes for emitted pulses of infrared laser light to be reflected to a detector from an object, making it essentially a short-range LIDAR (Light Detection and Ranging) sensor. This 'time-of-flight (TOF)' measurement enables it to accurately determine the absolute distance to a target with 1mm resolution, without the object's reflectance influencing the measurement (STMicroelectronics 2010). It can measure distances up to 250mm. The microcontroller embedded in the ST devices handles all calculations and noise reduction. The reasons for choosing this sensor are low cost, small size, and accuracy. Figure 3.7 shows the TOF concept, multiplying the time frame and the speed of light in the air gives the distance.

$$\text{Speed of light}(c)= 299,792,458 \text{ meters/second}$$

$$\text{Time}(t)= ((\text{To object}+\text{Return}))/2$$

$$\text{Distance}=c*t$$

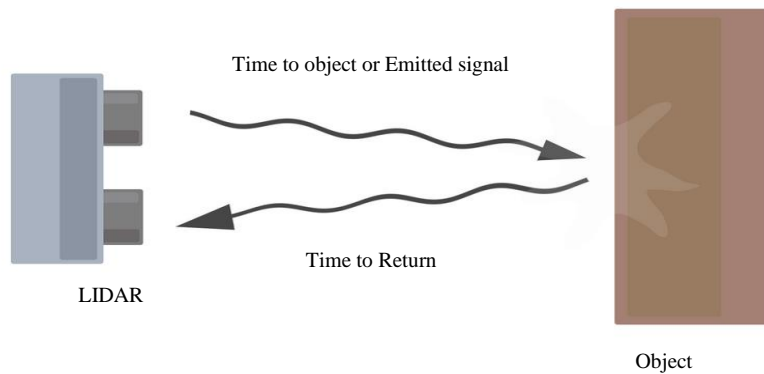


Figure 3.7 Time of Flight concept (STMicroelectronics 2010)

Table 3.2 shows the specification of the selected distance for foot clearance (STMicroelectronics 2010).

Table 3.2 Distance Sensor Specification

Feature	Details
Size	0.5" × 0.7" × 0.085" (13 mm × 18 mm × 2 mm)
Mass	0.5 g (0.02 oz)
Operating voltage	2.7 V to 5.5 V
Output format (I ² C)	8-bit distance reading
Distance measuring range	0 mm to 250 mm
Resolution	1 mm
Temperature-dependent drift	15mm
Accuracy	± 3mm
Noise	2.0mm maximum
Frequency	30 Hz
Laser-Infrared Emitter	850 nm
Manufacturer	Pololu

3.4.2.2 Calibration and Accuracy testing

An initial study found that ‘IR-ToF sensors’ (VL6180X, STMicroelectronics, Geneva, Switzerland) can provide better accuracy than alternative technologies (Bertuletti, Cereatti et al. 2016). Furthermore, the sensor manufacturers (e.g., ST Microelectronics) only report the sensor performance under very specific and controlled conditions in the datasheet. Therefore, it is crucial to evaluate the system performance under working conditions simulating the real scenarios.

For this specific study, the IR-ToF proximity sensor sampling rate was set to 20 Hz, and since the minimum foot clearance is generally less than 250 mm, the measurement range was set to 0–250 mm.

We analysed the following factors, which could potentially affect the accuracy associated with distance estimation:

- (i) Colours of the target surface (grey carpet, white carpet, and wood)
- (ii) Distance (from 0 to 250 mm)
- (iii) Angle of incidence (0,10,20,30, 40,50,60)

All three influence factors were tested both in static and dynamic conditions. These factors were chosen to cover the range of possible configurations occurring during stair walking. In static acquisitions, the target (carpet) was kept stationary in front of the ‘VL6180x distance sensor’ (fitted in the shoe). While during dynamic acquisitions, the sensor shoe was moved to the desired position.

The first distance experiment was done with white carpets, grey carpets, and wood material. Next, distance sensors were fitted with shoes, and it was kept at 28mm from the wood, grey and white carpet. Similar results were found for all the materials tested. According to the VL6180X distance sensor’s datasheet, accuracy is $\pm 3\text{mm}$; this is clear from this experiment as well (Figure 3.8).

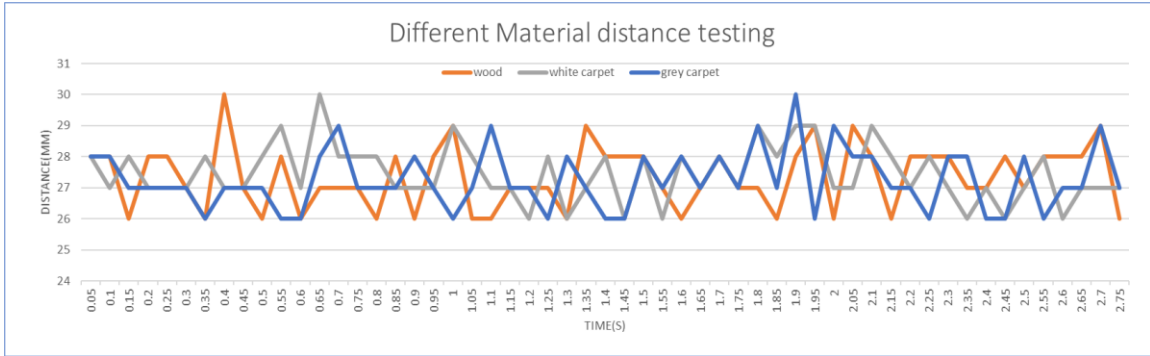


Figure 3.8 Distance sensor under different material, it was $28\text{mm} \pm 3\text{mm}$

Based on the results provided by the initial investigation on the influence of the target's colour, we decided to use the white carpet for the subsequent experimental acquisitions. The second experiment was to check the accuracy of Angle of Incidence (AoI) and Distance measurement. The distance measurement was done whilst the AoI was kept from zero degrees to 60 degrees by increasing it in 10-degree ($0^\circ, 10^\circ, 20^\circ, 30^\circ, 40^\circ, 50^\circ, 60^\circ$). For each testing, the ‘mean value’ of the distance provided by the sensor and actual distance (manually measured by the ruler) were computed, and the absolute difference of these two was derived.

The overall ‘Mean error (BIAS)’, ‘Mean absolute error (MAE)’ and ‘Mean absolute percentage error (MAE%)’ were computed by averaging differences over a few trials. The ‘Root Mean Squared Error (RMSE)’ was calculated. The calculations were done using the following formula,

The error has been calculated using the below formula (3.1) as the sensor value (S_t) minus the actual (A_t)

$$e_t = A_t - S_t \dots\dots\dots (3.1)$$

The **bias** is the average error, and n is the number of historical periods. Bias was calculated using formula (3.2).

$$bias = \frac{1}{n} \sum_n e_t \dots\dots\dots (3.2)$$

The **Mean Absolute Percentage Error (MAPE)** measures forecast accuracy. MAPE is the sum of the individual absolute errors divided by the actual value (each period separately). It is the average of the percentage errors. MAPE was calculated using the formula (3.3).

$$MAPE = \frac{1}{n} \sum \frac{|e_t|}{d_t} \dots\dots\dots(3.3)$$

The **Mean Absolute Error (MAE)** was calculated using the formula (3.4).

$$MAE = \frac{1}{n} \sum |e_t| \dots\dots\dots(3.4)$$

The **Root Mean Squared Error (RMSE)** is defined as the average squared error's square root. RMSE was calculated using formula (3.5).

$$RMSE = \sqrt{\frac{1}{n} \sum e_t^2} \dots\dots\dots(3.5)$$

Table 3.3 Detailed offset calculation for the distance sensor

Period t	Degrees D	Actual(mm) A _t	Measured(mm) S _t	Error E _t =A _t -S _t	Absolute Value of Error E _t = A _t -S _t	Square of Error (A _t -S _t) ^2	Absolute value of error divided by actual value (A _t -S _t) /A _t
1	0	10	12	-2	2	4	0.2
2	10	15	14	1	1	1	0.0666667
3	20	20	18	2	2	4	0.1
4	30	25	27	-2	2	4	0.08
5	40	30	34	-4	4	16	0.1333333
6	50	35	34	1	1	1	0.0285714
7	60	40	35	5	5	25	0.125
Mean		25	24.85714286	0.1428571	2.42857143	7.857142857	0.815

Table 3.3 shows the detailed calculation for distance sensor offset and accuracy testing for a different angle of incidence (AoI). Offsets and accuracy were calculated using the above formulas. Our results showed that low BIAS rate (0.1) for this sensor, and the absolute error for the sensor was 2.4mm, which was less than the maximum given by the company's sensor specifications. Also, the RMSE was only 7.85mm; these results are shown in Table 3.4.

Table 3.4 Distance sensor offset and accuracy testing results

N	7
Bias	1mm
MAE	2.4 mm
RMSE	7.85mm
MAPE	8.1%

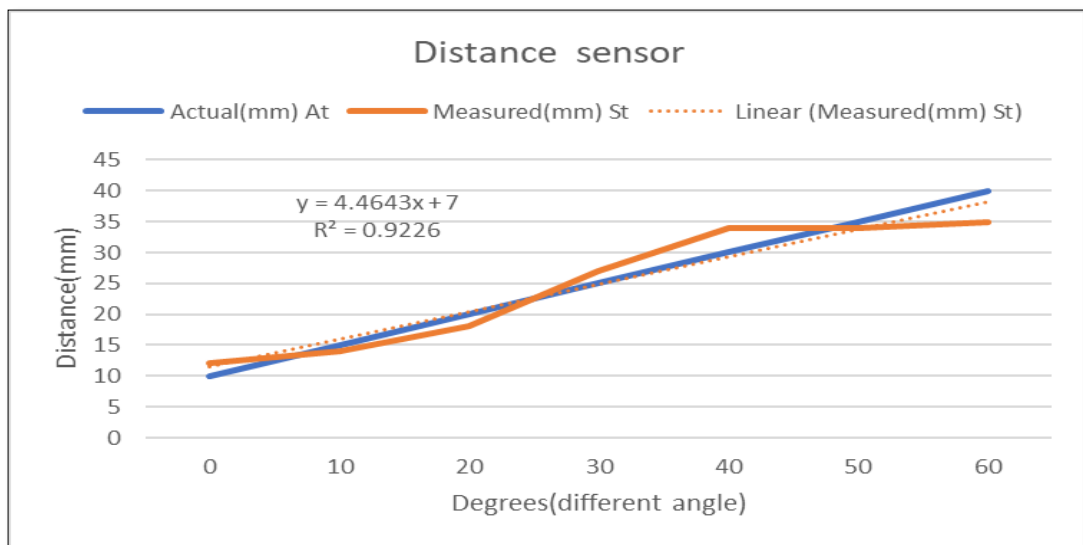


Figure 3.9 Distance sensor calibration curve, sensor angle set for zero degrees to 60 degrees by increasing it in 10 (00, 10, 20, 30, 40, 50, 60), and measured for 10mm, 15mm, 20mm, 25mm, 30mm, 35mm and 40mm. Linear correlation $r^2 = 0.9226$

Based on the above result, the graph was plotted. Figure 3.9 shows the calibration curve. The x-axis was degrees; the y-axis was distance. The plot between actual and distance sensor values formed a linear correlation in this experiment. This Linear correlation was calculated with the formula ' $y= 4.4643x+7$ ' to calibrate the range sensors and our 'R square value' was 0.9226, which confirmed a significant correlation between these two measurement values.

3.4.2.2.3 Foot clearance calculation

Distance sensors were fitted at the front and back of the sensor. Foot clearance measurement was taken between the front(ascending), back (descending) distance sensor and to the edge of the landing stair whilst both ascending (when the toe crosses the edge) and descending (when the heel crosses the edge).

It was a vertical foot clearance measurement, which could be picked up easily whilst plotting the measurements over the graph, where the point abrupt measurement change happens. Figure 3.10 shows how measurements were picked up easily. For example, while going down the stairs, a subject starts swinging their left foot from the stance phase; minimum foot clearance was calculated while crossing the stair edge. After crossing the stair edge during this swing phase, the foot reaches the first maximum value; then, this value slowly goes down.

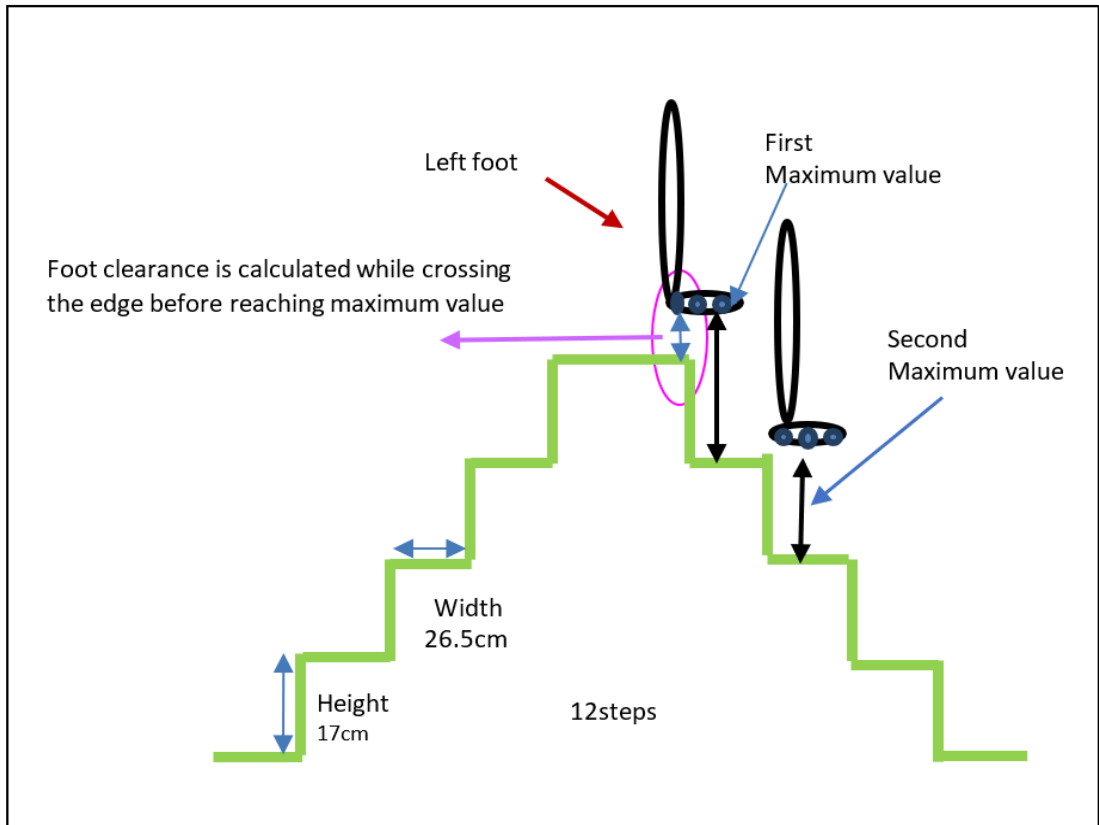


Figure 3.10 Descending vertical foot clearance measurement calculation, while the foot crossing the step edge foot clearance was calculated as a distance between the back distance sensor and step edge

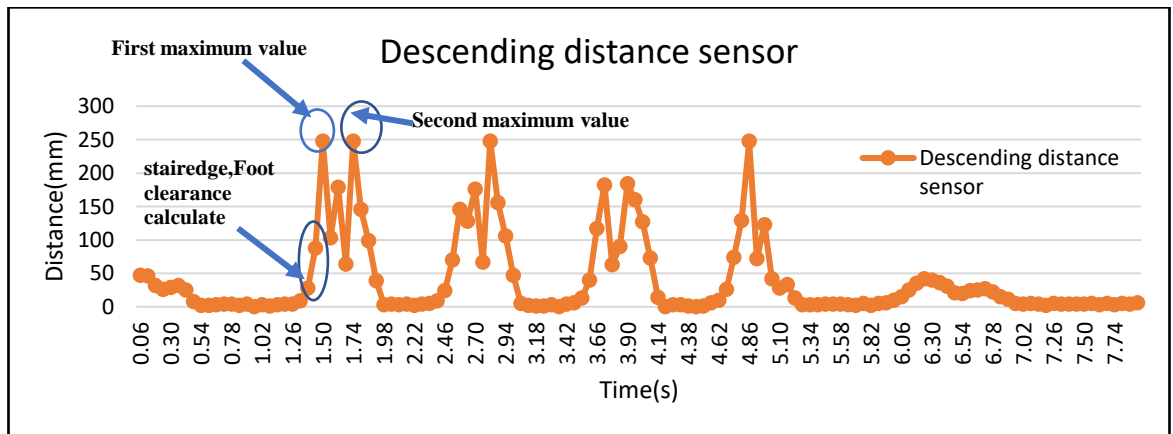


Figure 3.11 Graphical representation of minimum foot clearance calculation while descending

Figure 3.11 shows the foot clearance calculation graph for descending. While descending, the foot must cross two stair edges. While crossing the first step edge, minimum foot clearance was calculated. After crossing the first edge, the sensor reaches the first maximum and goes down, and after crossing the second stair edge, the sensor reaches the

second maximum value and goes down. Matlab was used to calculate foot clearance using the above information.

3.4.3. Force Sensitive Resistor (FSR) sensor specification

'Force-sensitive resistor (FSR)' is a type of resistive sensor that experiences a decrease in electrical resistance when force is applied orthogonally to the sensor's active area. Though less accurate than a load cell, FSRs are generally inexpensive, and when manufactured from polymers, the typical thickness is on the order of 0.25mm.

We used the force-sensitive resistors (FSR) manufactured by Interlink Electronics (FSR-402 short), which has a circular sensing area with a diameter of 13mm (Electronics 2010). In our custom built-instrumented shoes, we placed 6 to 10 of these FSR sensors underneath the foot, from toe to heel, in a line depending upon the shoe size.

3.4.3.1 FSR working principle

The FSR-402s are polymer-based sensors and consist of three layers. The lowest layer is a flexible substrate coated with a printable semiconductor material. The middle layer is a spacer adhesive, with material only along the outline of the part, providing an open region at the device's active area. The top layer is a flexible substrate, printed with interdigitating electrodes and two printed leads connected to solder tabs. The active area of the sensor is the area containing the electrodes. FSR-402 uses a 0.13mm layer of polyetherimide for the top and bottom layers, with a 0.15mm layer of acrylic for the spacer. The transparent polyether sulfone has excellent temperature resistance, moderate chemical resistance, and good flexibility. On the other hand, polyetherimide is a semi-transparent substrate with excellent temperature resistance, excellent chemical resistance, and limited flexibility (Figure 3.12).

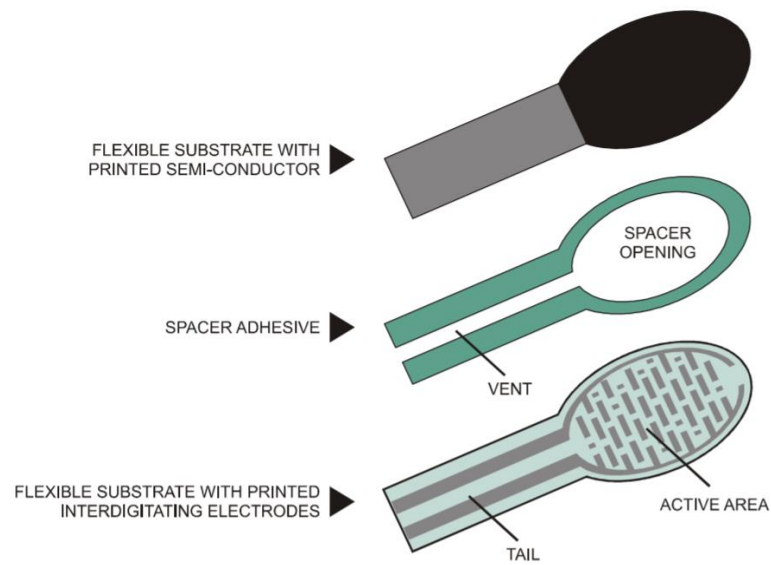


Figure 3.12 FSR made of these three layers (Electronics 2010)

The semiconductor material on the lowest layer of the FSR provides an electrical connection between the sets of interdigitating electrodes. The adhesive provides an air gap between the semiconductor and the electrodes when there is no force applied; this keeps the high sensor resistance. When force is applied across the active area, the electrodes are pressed into the semiconductor, reducing the resistance across the sensor. Table 3.5 shows the FSR parameters and specifications (Electronics 2010).

Table 3.5 Relevant parameters of the interlink FSR-402

Parameter	Value
Force sensitivity range	<100g to >10kg depending on mechanics
Pressure sensitivity range	< 0.1 kg/cm ² to > 10 kg/cm ²
part-to-part repeatability	±15% to 25% of established nominal resistance
Single part repeatability	±2% to 5% of established nominal resistance
Current consumption	1mA/cm ² of applied force
Resolution	0.5% full scale
Temperature Range	-30°C to +70°C
Sensitivity to Noise/ Vibration	Not significantly affected
Devices rise time	1.2 msec
Lifetime	>10 million actuations
Hysteresis	+10% average

3.4.3.2 FSR Implementation

We used a voltage divider circuit to measure changes in resistance of the FSRs; a simple voltage divider circuit explained this as below in Figure 3.13.

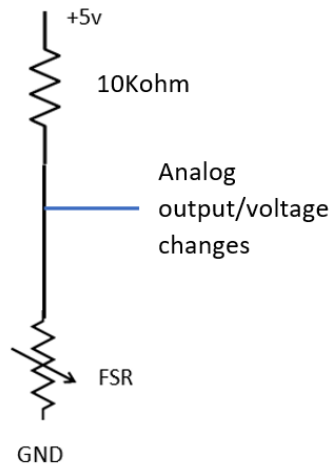


Figure 3.13 Voltage divider circuit for a force-sensitive resistor (FSR) with 10kohm resistor

The output can be explained by the following equation 3.6 (Ohm's law).

$$v_{out} = v * \left(\frac{FSR}{R+FSR} \right) \dots\dots\dots (3.6)$$

In this configuration, the output voltage decreases with increasing force. This circuit produced an output voltage inversely proportional to FSR resistance, which is inversely proportional to the applied force. The result was an inverse proportionality between force and voltage.

We used a 10Kohm fixed resistor (R) to maximize the desired force sensitivity range and to limit the current. A 5voltage power supply was preferred in this circuit. The graph Figure 3.14 shows the results of implemented 'voltage divider circuit' producing a non-linear output, which could measure forces up to 30N accurately. There was a challenge when this force reached more than 30N; the voltage change was very minimal, making it hard to measure the force.

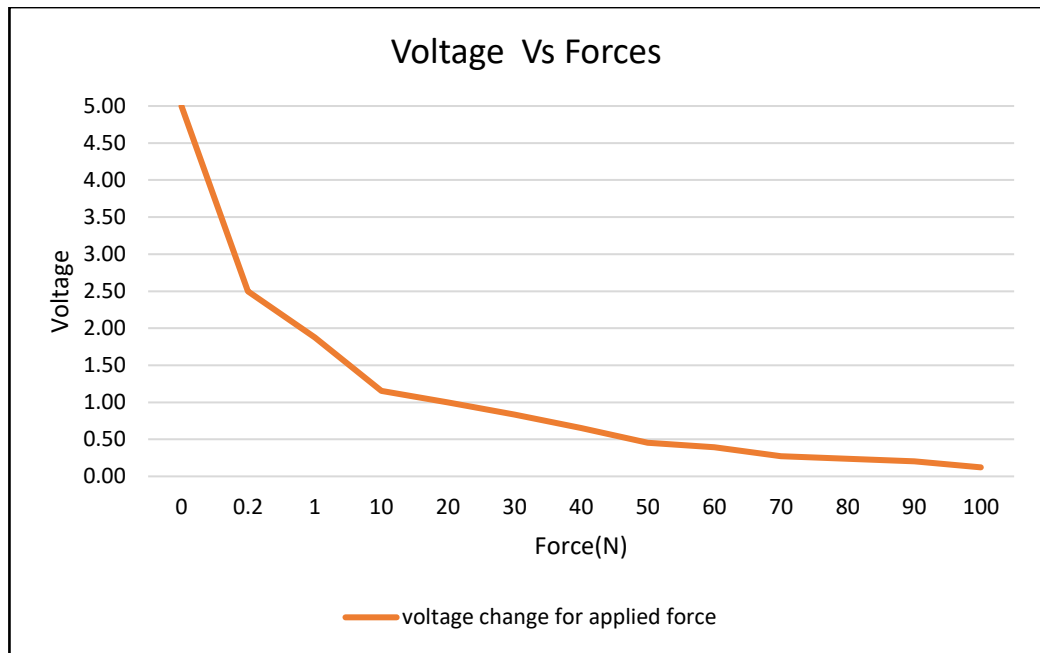


Figure 3.14 Voltage Vs Forces, 5voltage steadily drops up to 30n, after that voltage drops was very minimal, which was hard to measure

To overcome this challenge, we implemented an additional FSR divider with a unity gain amplifier using ‘Op-amp LM-358’ shown in Figure 3.15. This offset compensated ‘Op-amp LM-358’ offers high input impedance that has been recommended for use by Interlink Electronics (FSR integration guide).

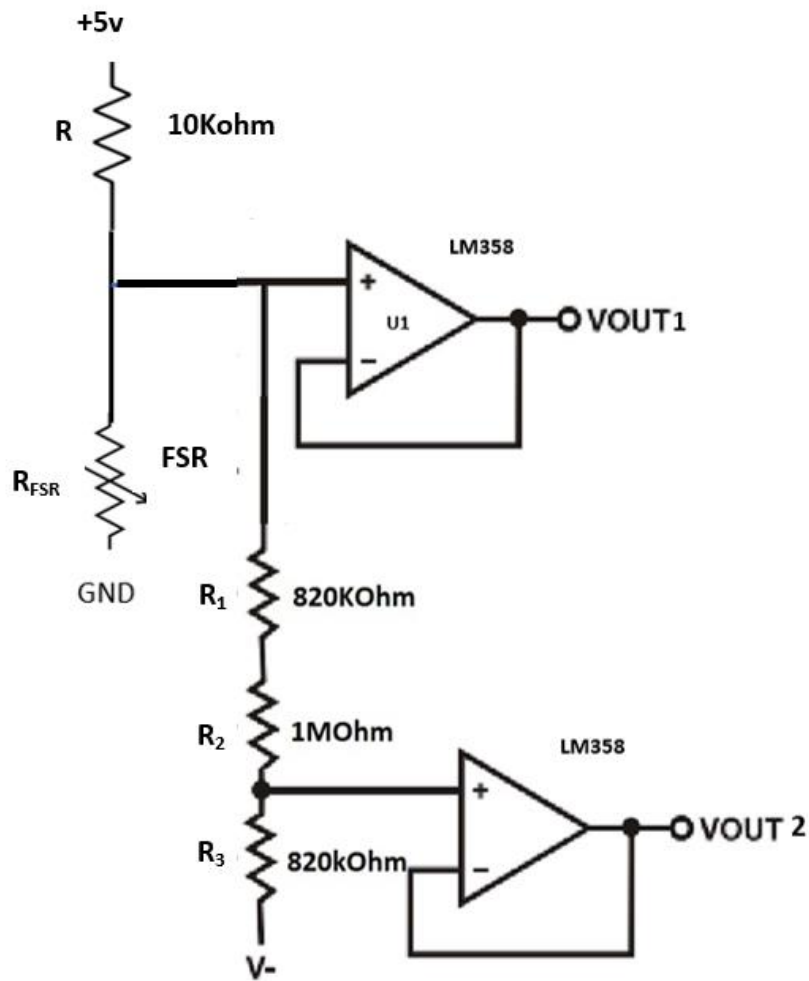


Figure 3.15 To overcome minimum voltage drop and measure forces up to 100N, a voltage divider circuit was created with two Operational amplifiers (Op-amp)

Two identical amplifiers were incorporated on a single board, which does the parallel processing. The comparator can compare two voltages (reference voltage and sensing voltage). The reference voltage is a set force threshold voltage (1.1v) used to compare against the sensing voltage, which comes from the voltage divider. When the sensing voltage exceeds the reference voltage, the Op-amp turns ON. The circuit output was divided into two parallel vout-1 to work with 2/3-threshold force and vout-2 to work with 1/3 threshold force. For example, this helps the FSR measure a force up to 100N; when vout-2 measured 30N from 0N, vout-1 can measure up to 100N from 30N.

All the resistors share a 5v common current, and the value of the resistor decides the circuit current and there-by ratio between vout-1 and vout-2, which was calculated using the ohm's law equation (3.7).

$$v_{out} = v * \left(\frac{R_{FSR}}{R + R_{FSR}} \right) \dots\dots\dots (3.7)$$

The low bias currents of these op-amps reduce the error due to the voltage divider's source impedance. Vout1 compares the threshold voltage with sensing voltage when the sensing voltage =>1.1v, then op-amp turns on (Table 3.6). When the weight reaches 30N, it starts sensing forces in this table.

Table 3.6 Higher force calculation(vout1) used to measure forces from 30N to 100N

N	Kg	fsr(resistance)	R(10kohm)	Ratio=FSR/FSR+R	sensing voltage=5*Ratio	mv	vr1.1(Analog result)	threshold voltage (1.1v)
0	0.00	1000000000000000000.00	10000.00	1.00	5.00	5000	1023	1.10
0.2	0.02	10000.00	10000.00	0.50	2.50	2500	1023	1.10
1	0.10	6000.00	10000.00	0.38	1.88	1875	1023	1.10
10	1.02	4000.00	10000.00	0.29	1.43	1429	1023	1.10
20	2.02	3000.00	10000.00	0.23	1.15	1154	1023	1.10
30	3.04	2000.00	10000.00	0.17	0.83	833	775	0.83
40	4.06	1500.00	10000.00	0.13	0.65	652	607	0.65
50	5.08	990.00	10000.00	0.09	0.45	450	419	0.45
60	6.08	850.00	10000.00	0.08	0.39	392	364	0.39
70	7.08	575.00	10000.00	0.05	0.27	272	253	0.27
80	8.08	500.00	10000.00	0.05	0.24	238	221	0.24
90	9.08	425.00	10000.00	0.04	0.20	204	190	0.20
100	10.08	250.00	10000.00	0.02	0.12	122	113	0.12

The plotted results showed improved response with the improved parallel circuit with non-linearity in the higher range shown in Figure 3.16. The higher force measurement was done up to 100N from 30N.

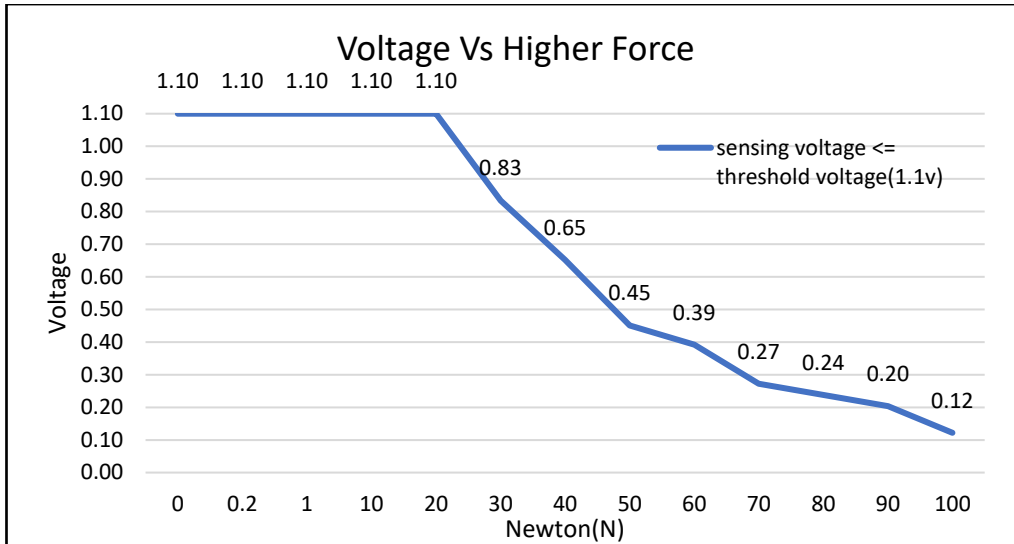


Figure 3.16 Voltage Vs Higher Forces graphical representation shows that the voltage would not change until 29N; once the force reaches 30N, the voltage drops.

The parallel circuit optimised the desired low force sensitivity range and limited the current through the FSR. Three resistors R1, R2 and R3 were created high impedance that let the low current for vout2, and the ratio was calculated using ohm’s law equation 3.8 and 3.9, as below,

$$V_{out2} = V * \frac{(\text{ratio} * R_3)}{R_{tot}} \dots \dots \dots (3.8)$$

$$\text{ratio} = \frac{R_{FSR}}{R_{FSR} + R} \dots \dots \dots (3.9)$$

Here, $R_{tot} = R1 + R2 + R3$ and $V=5V(5000mv)$

The results are calculated in Table 3.7. Vout2 measures tiny changes in the force.

Table 3.7 Low force Vout2 calculation used to measure forces from 1N to 30N

N	Serial result(ratio1) R/R+FSR	820kohm+ 820kohm+ 1mohm	Ratio2(parallel result)	V=5*ratio2	mV	vr1.1	vr1.1/no of resistors	Voltage
0	1.00	2640000.00	0.31	1.55	1553.03	1023	409.20	0.44
0	0.50	2640000.00	0.16	0.78	776.52	722	288.86	0.31
1	0.38	2640000.00	0.12	0.58	582.39	542	216.65	0.23
10	0.29	2640000.00	0.09	0.44	443.72	413	165.06	0.18
20	0.23	2640000.00	0.07	0.36	358.39	333	133.32	0.14
30	0.17	2640000.00	0.05	0.26	258.84	241	96.29	0.10
40	0.13	2640000.00	0.04	0.20	202.57	188	75.36	0.08
50	0.09	2640000.00	0.03	0.14	139.90	130	52.04	0.06
60	0.08	2640000.00	0.02	0.12	121.67	113	45.26	0.05
70	0.05	2640000.00	0.02	0.08	84.44	79	31.41	0.03
80	0.05	2640000.00	0.01	0.07	73.95	69	27.51	0.03
90	0.04	2640000.00	0.01	0.06	63.31	59	23.55	0.03
100	0.02	2640000.00	0.01	0.04	37.88	35	14.09	0.03

Results are plotted, as shown in Figure 3.17. Moreover, it was observed that the graph exhibits improved response with nonlinearity in the lower range. This low force measurement is used to measure forces up to 30N accurately.

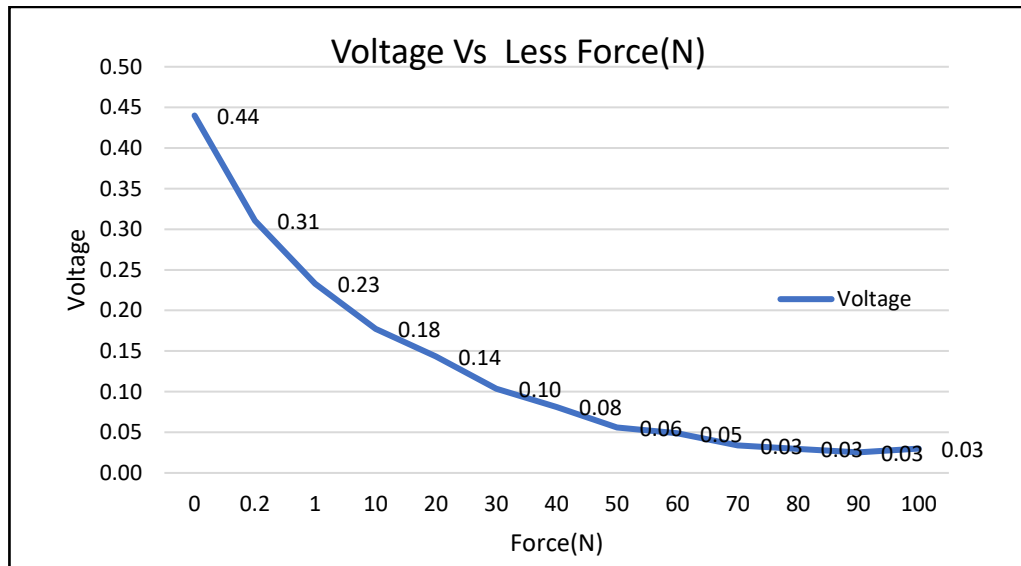


Figure 3.17 Voltage Vs less force graphical representation, the voltage would not change after 30N heavily, it only measures 1N to 30N, after(>30N) that the voltage change would be minimal

After the above FSR implementation, sensitivity and calibration were carried out in the laboratory to verify the desired results.

3.4.3.3 Sensitivity

The output of the FSR can be based on the applied force and the method of the application. Therefore, FSRs can be biased if it is bent. The FSRs can be bent by two mechanisms, by simple folding motion, depending on the shoe and the FSR placement location beneath the foot. FSRs are placed in the middle of the insole from toe to heel in a line to overcome this. We expect there will not be any typical bending underneath the middle foot, and the area of the foot is much larger than the FSR sensing area where the bending due to indentation is less possible. The FSRs also have temperature and humidity sensors, affecting their performance within the shoe environment.

3.4.3.4 Calibration

The zero offset was not required. Hence the FSRs are loaded under the foot inside a shoe with a snugly tied lace. Therefore, the load on FSRs when the foot is in the air is not expected to be 0kg. So long as the sensitivity is determined at small values close to 0 kilograms, zero offsets are not required. These FSR outputs are non-linear, and their single part repeatability is from $\pm 2\%$ to $\pm 5\%$ of the nominal resistance. Sometimes we may face challenges like adhesive layer breakage can lead to an increased non-linearity.

The FSR was calibrated of their output to the units of applied force in kg. Each FSR was tested in the material testing machine (Appendix C). The ‘Tinius Olsen material testing machine’ was used to apply successive forces from 0.25kg to 10kg, continually recording the actual applied force and the corresponding outputs of the FSRs simultaneously.

The graph Figure 3.18 shows the calibration results, FSR higher and lower forces voltage vs material testing machine forces, with a second x-axis showing the equivalent applied force unit from the testing machine. FSR worked the way it was implemented; FSR’s more force(vout1) output worked after reaching 30N machine force. FSR’s less force(vout2) result worked up to 30N from 0N.

A single curve fit the calibration data for multiple FSRs rather than fitting individual curves for each FSR. Few of the FSRs were tested, and the output of all the FSRs grouped. The results were correlated.

To capture the non-linear relationship between the FSR higher force output and applied force, ‘fourth-order Polynomial curve fitting’ was used for calibration. Formula 3.10 was used for this curve fitting, and the R squared value for this curve fitting was 0.9984. This result showed the excellent reliability of the sensors.

$$y = 3E-05x^4 - 0.0023x^3 + 0.0706x^2 - 0.2793x + 32.803 \dots \dots \dots (3.10)$$

From Figure 3.18, to capture the non-linear relationship between the FSR lower force output and applied force, ‘third-order Polynomial curve fitting’ was used for calibration. The formula 3.11 was used for this curve fitting, and the R squared value for this curve fitting was $R^2 = 0.9766$. This result showed the excellent reliability of the sensors.

$$y = 6E-06x^3 - 0.0019x^2 + 0.1923x - 3.6929 \dots \dots \dots (3.11)$$

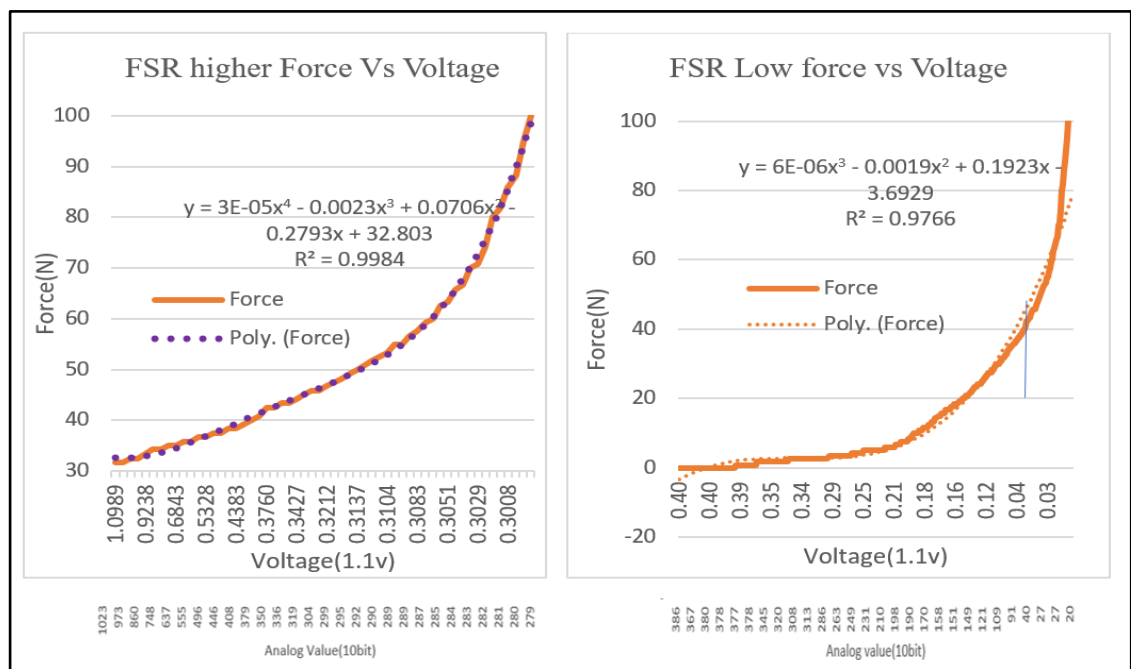


Figure 3.18 Calibration Curve for higher force (A) to measure 30N to 100N and lower force (B) to measures 1N to 30N. After designing circuit with Op-Amp, the FSR was calibrated with material testing machine

3.4.4. Foot contact length

Table 3.8 Foot contact length calculation for Ascending

Foot contact length % Ascending										
shoe size	10th sensor	9th sensor	8th sensor	7th sensor	6th sensor	5th sensor	4th sensor	3rd sensor	2nd sensor	1st sensor
6	n/a	n/a	n/a	n/a	100	83	66	49	32	15
7	n/a	n/a	n/a	100	86	72	57	43	29	15
8	n/a	n/a	100	88	75	63	50	38	25	13
9	n/a	100	89	78	67	56	45	34	23	12
10	100	90	80	70	60	50	40	30	20	10

Table 3.9 Foot contact length calculation for Descending

Foot contact length % Descending										
shoe size	1 st sensor	2 nd sensor	3 rd sensor	4 th sensor	5 th sensor	6 th sensor	7 th sensor	8 th sensor	9 th sensor	10 th sensor
6	100	83	66	49	32	15	n/a	n/a	n/a	n/a
7	100	86	72	57	43	29	15	n/a	n/a	n/a
8	100	88	75	63	50	38	25	13	n/a	n/a
9	100	89	78	67	56	45	34	23	12	n/a
10	100	90	80	70	60	50	40	30	20	10

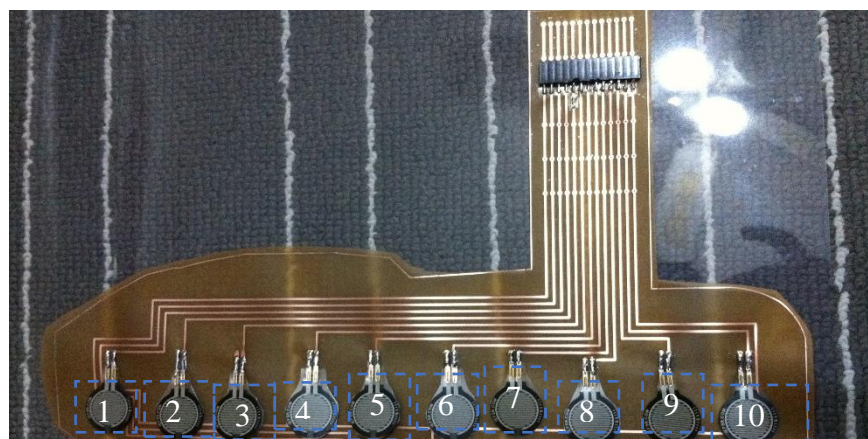


Figure 3.19 Printed flexible Insole fitted with ten FSR sensors with the Sensor number

We used Figure 3.19, Table 3.8, and Table 3.9 to find out which sensor has force or not. The foot contact length ratio was calculated as below; for example, the above sensor insole has ten sensors; its total length was 32cm. The distance between sensors was 3.2cm which was 10% of the whole insole length. When calculating the ascending foot contact length ratio, one needs to check the heel sensor forces. If all the sensor has the forces, 100% of the foot is placed on the stairs. If only the last sensor does not have any force ($100\% - 10\% = 90\%$), 90% of the foot is placed on the stairs. Suppose the last two sensors do not have forces, which means ($100\% - 20\% = 80\%$) 80% of the foot placed on the stairs. Similarly, remaining sensor forces were checked to measure the foot contact length ratio. For descending foot contact length ratio, check front sensor's forces; based on the forces and length of insole, the foot contact length ratio was calculated.

As we have already explained, we have created the instrumented sensor shoes, with a variable number of sensors based on the shoe sizes (Table 3.8 and Table 3.9) with a measured distance between each sensor. By doing this, we calculated the exact 'foot contact length distance' in percentage. We used this percentage of foot contact length distance data for further analysis.

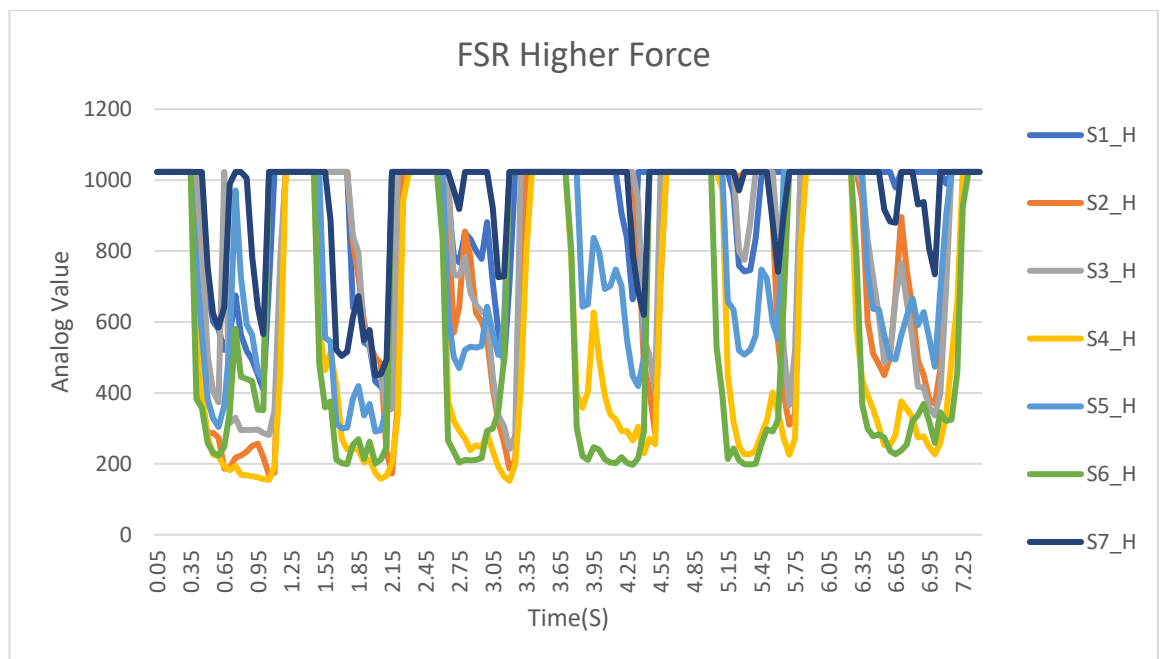


Figure 3.20 FSR results for higher force (>30N to 100N)

The insole was tested in the stairs for going up trial. There was seven FSR sensor in the insole. In Figure 3.20 high force graph shows the forces applied from all the sensors. According to this graph, S7's sensor force was applied on step 1 and 2 while no force was applied on step 3, 4, 5 and 6. S6's sensor force was applied on all the steps. 86% of the foot placed on all the steps, 14% of foot overhanging. The foot contact length was calculated using Tables 3.8 and 3.9.

3.4.3.5 Stance time

Stance time is when the foot is in contact with the floor. Stance time was calculated from the first contact with the step and ended with the same foot's last contact on the same step.

3.4.3.6 Swing time

It is when the foot is not in contact with the floor. To be precise, 'the time is taken for the leg to swing through while the body is in single support on the other leg'. During swing time, instrumented insole produces no force changes because the foot is in the air.

3.4.3.7 Cadence (cycle time)

The average duration of two gait cycles (one of the left limbs and one of the right limbs) was taken as a cadence for stair ascent and stair descent.

3.4.5. BNO055 IMU

IMU BNO055 from Bosch company was used in this project. It has a 32bit microcontroller (high-speed Cortex-M0 based processor) running the BSX3.0 Fusion Lib software. The on-board fusion algorithm fuses the triaxial 14bit BMA055 accelerometer, a triaxial 16bit BMI055 gyroscope and a triaxial BMM055 geomagnetic sensor into a 'single composite sensor'. The sensor fusion used an extended Kalman filter algorithm, inbuilt low and high pass filtering and autocalibration and temperature compensation (GmbH 2020). These features were used to fuse the three sensors' data into a quaternion representation of absolute orientation and provide linear acceleration, gravity, and Euler angle outputs (adafruit, BNO055). The results were directly read via I2c (inter-integrated circuit) serial communication protocol from internal registers. IMU sensor size was significantly small (3.8mm x 5.2mm x 1.1 mm). The BO055 IMU sensor used a low

power, micro-electro-mechanical system (MEMS) accelerometer, gyroscope, and magnetometer.

3.3.4.1 Capacitive MEMS Accelerometer

A capacitive accelerometer sensor was used to build the BNO055 IMU sensor. The capacitive MEMS accelerometer has high sensitivity and accuracy at high temperatures. In addition, the device depends only on the capacitive value that occurs due to the change in distance between the plates, and it does not change the values depending on the base materials used.

A simple MEMS accelerometer mainly consists of a movable microstructure or a proof mass connected to a mechanical suspension system. The movable plates and the fixed outer plates act as capacitor plates. When acceleration is applied, the proof mass moves accordingly, which produces a capacitance between the movable and the fixed outer plates. MEMS accelerometer measures both static acceleration (resulting from gravity) and dynamic acceleration resulting from shock, vibration, linear motion, or other types of motion.

3.3.4.2 MEMS Gyroscope

BNO055 IMU used MEMS gyroscope, which provides low-noise angular rate (gyroscopic) measurement at low power consumption (Woodman 2007). MEMS gyroscope uses Coriolis effect and vibrating element to measure angular velocity. MEMS gyroscope uses vibrating masses that vibrates along a drive axis primarily, and a secondary vibration is induced along the perpendicular sense axis, which displaces the mass from its original path when the gyroscope is rotated (Woodman 2007). The working principles of a gyroscope where the rotation around respective axes is introduced. The gyroscope introduces capacitance changes to detect this displacement. Based on this, the angular velocity of the IMU can be measured and by integrating the signal, we can obtain orientation.

Bosch BNO055		
	Gyroscope	Accelerometer
Range	programmable, 125 – 2000°/s	programmable, ±2 - ±16g
AD convertor	16bit	14bit
Sensitivity	16LSB/°/s	1LSB/mg
- tolerance	±1 (max ±3) %	±1 (max ±4) %
- temperature drift	±0.03 (max ±0.07) %/K	±0.03 %/K
Nonlinearity	±0.05 (max ±0.2) %FS	±0.5 (max 2) %FS
Zero rate/g offset	±1 (max ±3)°/s	±80 (max ±150) mg
- temperature drift	±0.015 (max ±0.03) °/s per K	±1 (max ±3.5) mg/K
- voltage drift	0.1 °/s/V	±1.5 (max ±2.5) mg/K
Bandwidth	programmable, 12 – 523 Hz	programmable, 8 – 1000Hz
Output noise density	0.014°/s/√Hz (at 47Hz)	150 (max 190) µg/√Hz
Cross Axis Sensitivity	±1 (max ±3) %	±1 (max ±2) %

Figure 3.21 Accelerometer and Gyroscope Specification (Townsend 2018)

Figure 3.21 shows the specification of the accelerometer and gyroscope. Default ±4g for accelerometer and 2000dps for gyroscope was used in fusion mode.

3.4.4.3 Calibration

Three types of information about the accelerometer were required: the zero offset (to centre the output around zero), the sensitivity (to convert the output to units of m/s²), and the orientation of the accelerometers relative to the foot to interpret the sensor output accurately.

3.4.4.4 Zero offsets and sensitivity

Determining the sensitivity of the accelerometers was straightforward by using gravity. Naturally, the gravitational acceleration vector, g, is stable, accurate, and readily available.

The sensor fusion software runs the calibration algorithm of all the three sensors (accelerometer, gyroscope, and magnetometer) in the background to remove the offsets. The following procedure was done to calibrate the IMU. The gyroscope was kept standing still in one position to calibrate the gyroscope. Moreover, to calibrate the magnetometer,

'figure 8' motions were made in 3 dimensions, but with current devices, fast magnetic compensation occurs with enough normal device movement. The BNO055 was placed in 6 standing positions for +X, -X, +Y, +Y, -Y, +Z and -Z to calibrate the accelerometer. The BNO055 also provides information about the current calibration status. Four statuses can be read from the IMU's registers: SYS (system), GYR (gyroscope), ACC (accelerometer), MAG (magnetometer). These statuses hold a value from 0 (uncalibrated) to 3 (fully calibrated). The SYS status depends on the status of all three sensors.

If the calibration status is '0' in sensor fusion mode, the sensor could not find the north pole. Therefore, if the data is collected during this time, the sensor provides relative orientation values instead of absolute orientation values. However, once calibration status > 0 means that the BNO055 sensor has found the north pole, it can give the absolute orientation values (Townsend 2018).

Every sensor has a specific bias based on its physical properties and manufacturing. Individual BNO055 sensor static testing confirmed sensor data usability and bias. The sensor has a minimal bias seen in the average signal output, even when no movement is present.

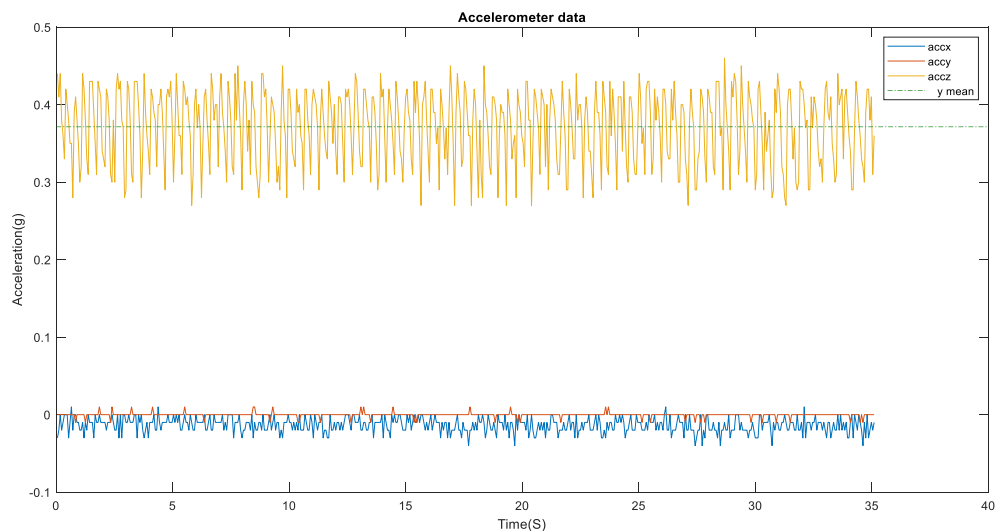


Figure 3.22 Accelerometer sensor bias test result

For this testing, BNO055 was idle for a period. The accelerometer sensor data bias is shown in Figure 3.22. The x (accx) and y(accy) acceleration have an average value around

zero. The z (accz) acceleration is $\pm 1g$ due to gravity. By estimating the bias for each axis, these values can be repositioned around zero.

To measure sensor bias in the gyroscope, BNO055 was kept static over a period. Static bias results for Gyroscope's angular velocities (gx, gy, gz) are shown in Figure 3.23. Results showed that gyroscope offset is $\pm 2^0$.

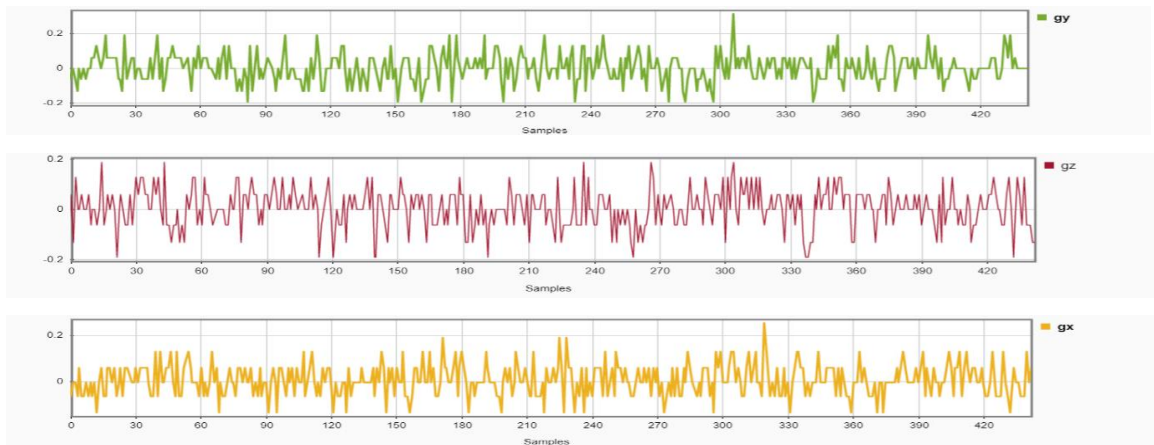


Figure 3.23 Gyroscope Sensor Bias result, the offset is $\pm 2^0$

The sensor data has been verified and has minimal standstill drift over a period, and this reinforces our selection of the BNO055 IMU and further supports the reliability of the received data.

3.4.4.5 Orientation

Understanding the default orientation of the sensor is very important to understand the acquired data. Figure 3.24 shows the default coordinate system of the BNO055 sensor (Townsend 2018). This coordinate system was used for the rest of the experiment and data analysis. Rotation in the x-axis is called roll (ψ), rotation in the y-axis is called pitch (θ), and rotation in the z-axis is called Yaw (ϕ).

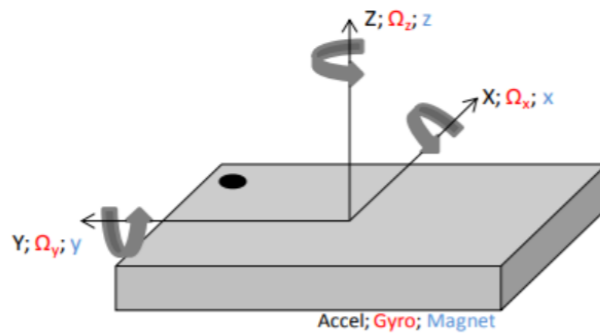


Figure 3.24 Coordinate System for BNO055 IMU (Townsend 2018)

We can access IMU output in either fusion mode or non-fusion mode; Fusion mode gives processed data while non-fusion mode gives raw data. In this project, fusion mode was used for data collection. In the fusion mode orientation, outputs are accessed by either Euler angles or quaternion. Euler angles are relatively easy to understand, but it has a singularity problem when the yaw angle is 90°, called gimbal lock. It is impossible to reorient when a gimbal lock occurs without an external reference. Euler angle orientation is not fully defined, meaning that roll and pitch are not stable values when yaw is approaching 90 degrees. So Euler angles were not used to calculate the foot motion in this project.

Quaternions orientation was used to measure foot motion. Quaternions provide a measurement technique that does not suffer from gimbal lock but are more complex than Euler angles. A quaternion consists of four numbers: one scalar and a three-component vector.

$$q = (w, xi, yj, zk)$$

Where w , x , y , and z are real numbers and i , j , and k are quaternion units. Typically, w , x , y , and z are kept in the range between -1 and 1, and

$$\sqrt{w^2 + x^2 + y^2 + z^2} = 1$$

All these w,x,y and z numbers reorient vectors in a single rotation with or without changes in length.

The sensor fusion modes also provide linear accelerations(for example, the acceleration applied due to movement) and angular velocity and quaternion orientation data.

3.4.4.6 Linear acceleration, velocity, Angular velocity, and Foot angle (Pitch)

Individual BNO055 sensor was tested for dynamic movements like walking stairs up and down to confirm sensor data usability. The participant was wearing instrumented sensor shoes and then walked up and down the stairs.

Figures 3.25 and 3.26 show the processed BNO055 output of linear acceleration and angular velocity for going up data. Again, when the foot is placed on the floor, the acceleration value goes zero.

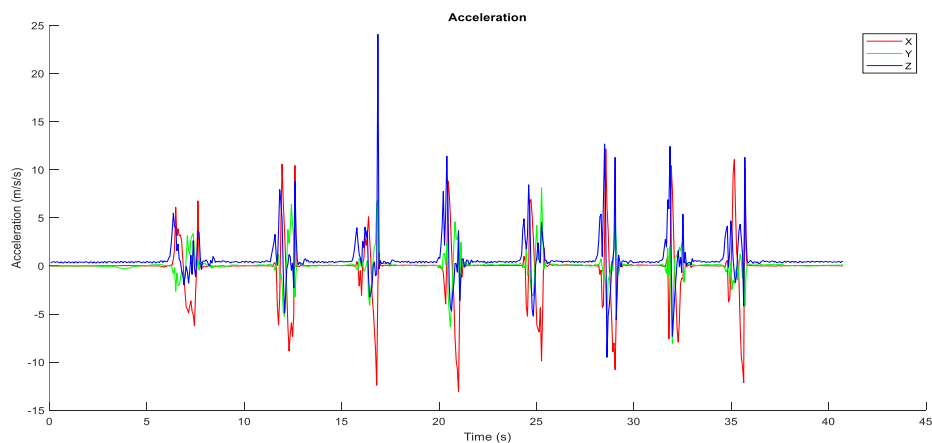


Figure 3.25 Linear Acceleration

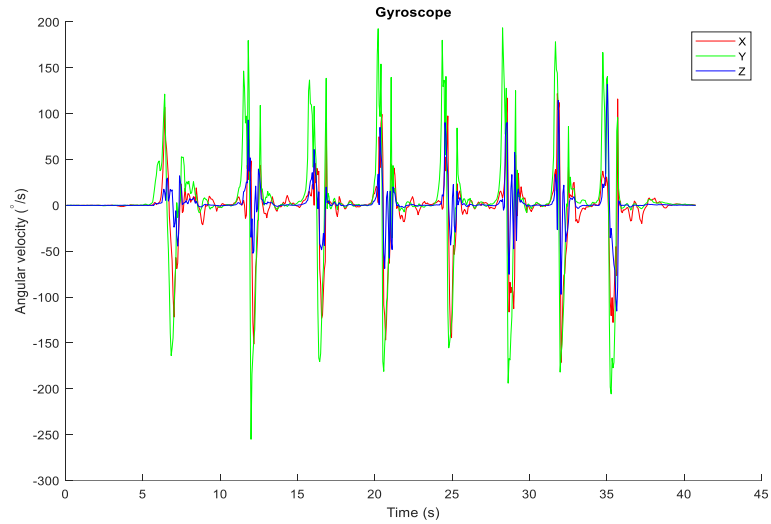


Figure 3.26 Angular Velocity

This linear acceleration data was further processed in Matlab to calculate the velocity on the stairs. The velocity was obtained from single integration to the acceleration component's time corresponding to the foot's forward motion in all three directions. The below Figure 3.27 shows the results of the calculated velocity for going up data. For steps 1 and 4 have higher velocity than the other steps. The velocity range for this going up is between 1.25m/s to 2m/s.

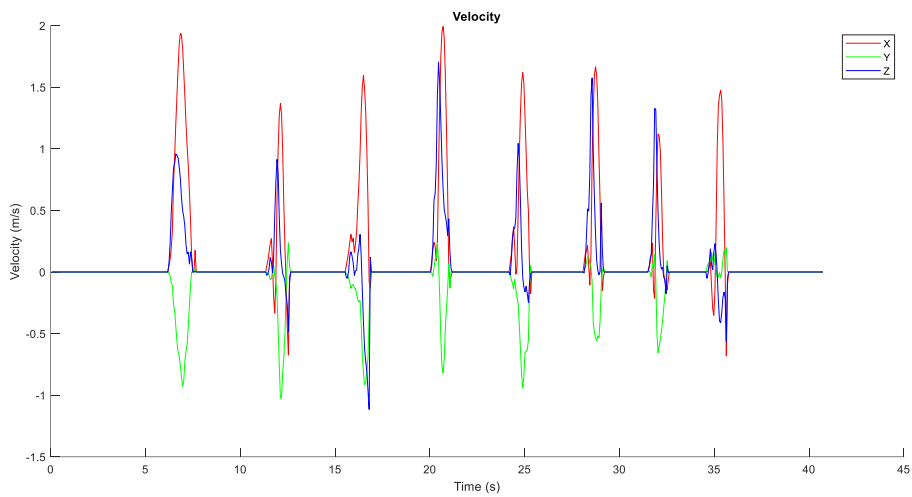


Figure 3.27 Velocity results for going up

The quaternion data provides information about the rotation of the foot. The below formula was used to calculate the foot angle from quaternion,

$$\text{double pitch} = \text{asin}(2 * \text{quat.w}() * \text{quat.y}() - \text{quat.x}() * \text{quat.z}());$$

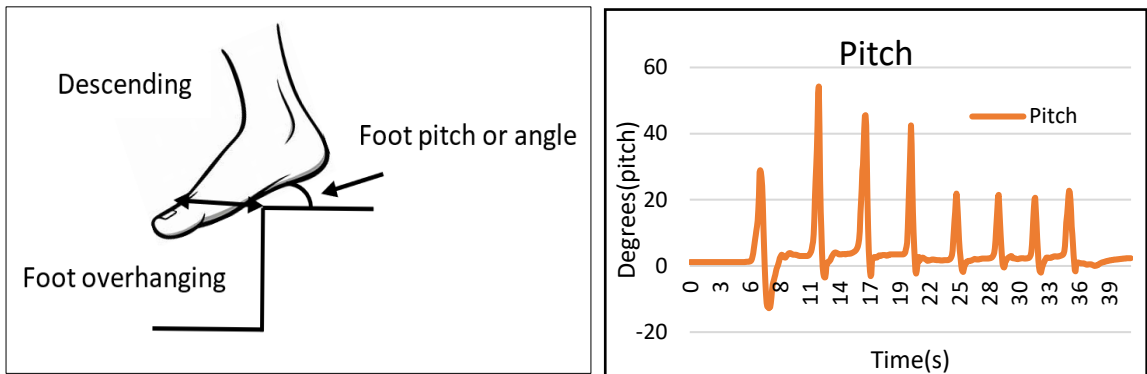


Figure 3.28 Calculated Pitch (foot angle) for going up

Figure 3.28 shows the calculated pitch for going up. According to this figure, the participant's foot lifted between 20° to 55° . when the heel lifted (plantarflexion), the foot angle went up (positive). When the toe was raised (dorsiflexion), the foot angle value went down (Negative).

3.5 Discussion

An instrumented shoe was developed to detect stair fall risk parameters at the community level and not only in the laboratory. Three low-cost sensors were used to create the instrumented shoe: a vl6180x distance sensor, a BNO055 IMU and an FSR force sensor; each sensor shoe cost £200 to develop, so a total cost of £400 for both instrumented shoes.

The current instrumented setup could only measure vertical clearance, not horizontal clearance. However, horizontal clearance is also necessary while descending stairs to find risk for slip. Therefore, this project's printed circuit board can add a few more distance sensors. With this ability, we can fit the distance sensor at the shoe's back (heel counter) to find horizontal foot clearance while descending stairs. We tried to include the distance sensor at the back (heel counter) of the shoe, but the data collection frequency went down and also, it was hard to fit it back (heel counter) of the shoe. In addition, when the shoe's

outer layer was thinner, the sensor went inside and was uncomfortable, so we didn't use this sensor for data collection.

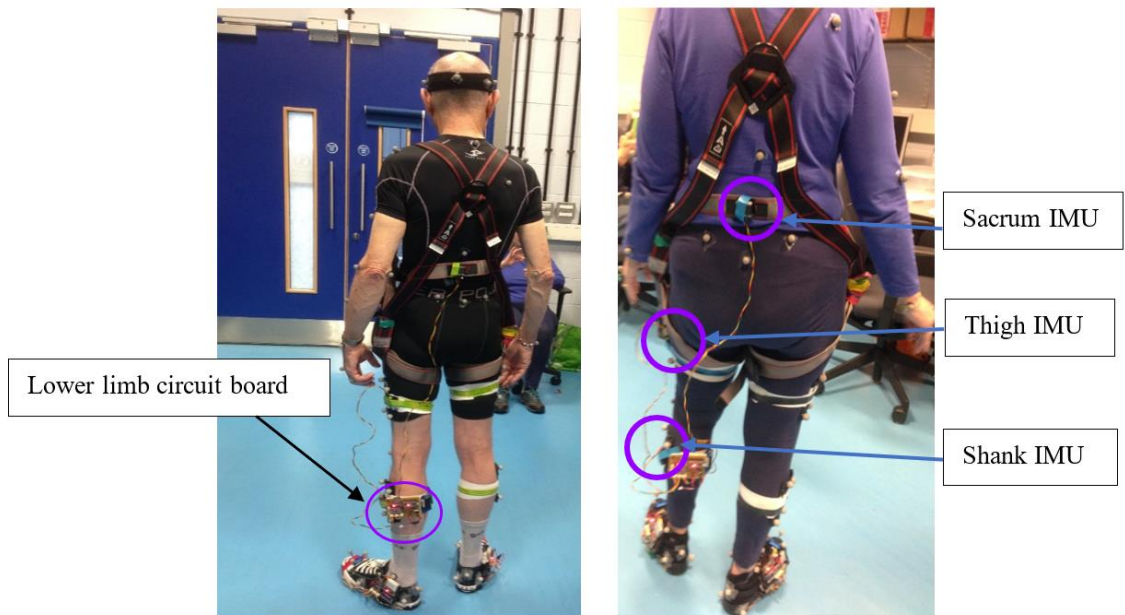


Figure 3.29 Lower limb circuit board, IMU sensors fitted with thigh, shank, and sacrum to calculate range of motion and centre of mass control

The other stair fall risk parameters are a range of motion and centre of mass control. It has been shown that accelerometers can determine a range of spatiotemporal gait parameters and give insight into the control of the CoM, which is an indicator for the risk of a loss of CoM control during stair descent. To measure the range of motion and centre of mass, we designed a lower limb circuit board containing three IMU sensors with one microcontroller, storage card and power supply. Figure 3.29 shows that one IMU was fitted at the Thigh, the second one was fitted at the Shank, and the third was fitted at the Sacrum. Thus, three IMU sensors can measure the range of motion at the hip, knee, and ankle and the centre of mass control.

The problem with this circuit was the wired circuit. A lower limb circuit board was created with long wires for each IMU sensor to fit this circuit to all older people. Unfortunately, this long wire became a problem, and the reduced wire could not fit with others. This wired circuit affected older peoples' gait, and also, the sensor itself moved, didn't get the correct data, so didn't use that sensor for further data collection.

Fitting many sensors all over the body might affect a participant's daily activity, whereas if the sensors are incorporated in the shoe, many people will happily wear them at home to collect data for longer; that was the reason for focusing on only instrumented shoes. Even though few risk parameters were implemented, we can predict the fall risk in the future using this powerful parameter. The sensor shoe has the potential to add more sensors in future. Older people can use this sensor shoe at home without any assistance (just pressing the button in the shoe). Data will be stored in the storage (SD) card. Those data will be processed later to predict stair fall risk. This system won't affect their gait, is less expensive, and can collect data for longer.

3.6 Conclusion

This project's motivation was to design and develop a low cost, reliable, and portable instrumented sensor shoe system to detect stair fall risk factors in a typical living environment. An instrumented shoe system was investigated and designed, which contains a custom-made insole that can find foot contact length ratio. And distance sensors are fitted in the shoe to calculate foot clearance, inertia measurement unit (IMU) sensor to find motion parameters. Instrumented sensor shoes and insole were developed for different sizes. The designed instrumented sensor shoe was calibrated using different methods. Also, these sensor shoes were tested on the stairs for static and dynamic motions to measure accuracy and repeatability. Selected sensors were achieved good accuracy. Developed sensor shoe system enabled the stair gait analysis in a less expensive and non-traditional motion laboratory environment. Instrumented sensor shoe was tested on the staircase, and risk parameters were extracted from the stair testing. These results are validated against VICON systems in the next chapter.

CHAPTER 4: Sensor Shoe's stair fall risk parameters validation

4.1 Introduction

We have developed sensor shoes to fill the gap between laboratory and real-world environments. The first step was to test and validate the sensor shoe's stair fall risk parameters against the VICON system, which was considered a golden standard to predict fall parameters. The main factors of stair fall are foot clearance and foot contact length ratio (foot overhang). So, it is essential to validate these two parameters against the vicon system.

4.2 Methods

4.2.1. Participants

Twenty-five older adults participated in this study. (Age: $70.72 \pm 4.0Y$; bodymass: $70.18 \pm 10.0\text{kg}$; body height: $1.62 \pm 0.06\text{m}$; female:20; male:5). All the participants were recruited from the local community of Wirral and Liverpool, UK. All these participants lived independently, able to climb stairs without help. The study was approved by the Liverpool John Moores University ethics committee in the UK (REF: 18/SPS/024). After the explained procedure, informed written consent was obtained from all participants.

4.2.2. Laboratory staircase structure

Custom made instrumented staircase was used to take measurements in the laboratory settings. This staircase was made up of seven steps in total, and force platforms (1080Hz, 9260AA, Kistler AG, CH) were embedded in the lower four steps from 1 to 4 to obtain kinetic data. The staircase configuration followed building regulations and guidelines in the UK (British-Standards-Institute, 1984). Custom made staircase configuration has matched the design of a private home, with the set rise at 19.5cm (the vertical distance from one step to the next) and the flat run at 23.5cm. Handrails were placed on both sides of the staircase.



Figure 4.1 Laboratory custom-built instrumented seven-step staircase structure image, first four steps fitted with a force plate, twenty-four infrared cameras were around the staircase

Figure 4.1 shows the 7-step custom made staircase structure. The staircase steps and the top landing and walkway steps were independent structures, once it was placed in the desired position, the top landing was fixed, and the walkway was secured on the floor. The structure did not separate or roll away from each other by connecting the metal frameworks of each step using bolts; then staircase was connected to the top landing on one side and the walkway on the other side. Twenty-four infrared camera system (120Hz, Vicon, Oxford Metrics, UK) was used to obtain kinematic data.

4.2.3. Data collection procedure

The participants ascended and descended the instrumented staircase at their own preferred pace in a step-by-step manner (for example, alternative limb lead on each step) with handrails if needed. The participants dressed in tight-fitting Lycra shorts and shirts during stair negotiation and wore our instrumented sensor shoes. A five-point safety harness was fitted with all participants, and this safety harness was attached to the overhead belay safety system to ensure safety. A trained member of the research team supported each participant's overhead belay safety system by holding the safety rope system attached to the floor. Participants performed a few familiarisation trials. After familiarisation, participants performed five trials; the final three trials were selected for further analysis among these trials.

4.2.4. Data collection for sensor shoe and VICON system:

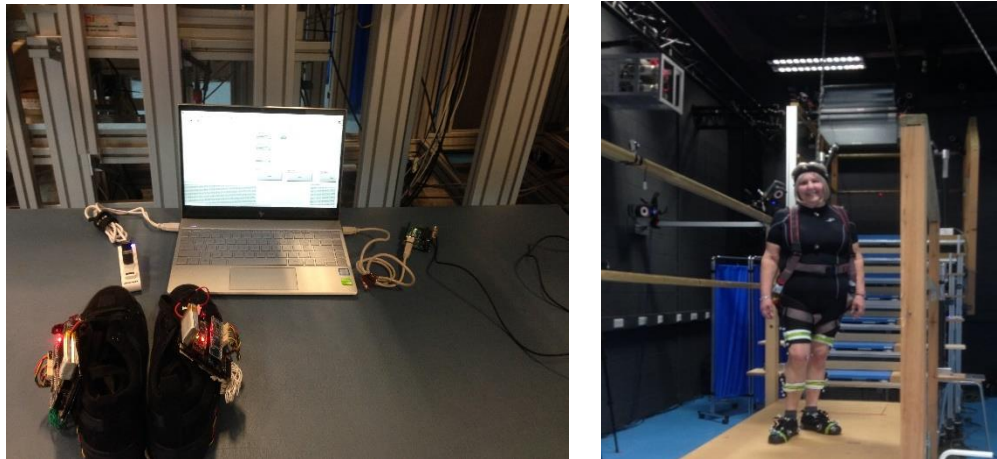


Figure 4.2 Lab data collection setup, left side image was sensor shoe with computer connected with Bluetooth in one side of the computer, the other side of the computer connected with VICON system, right side image was participant with markers and sensor shoe

In the laboratory, sensor shoe data was collected with VICON Synchronously. To synchronise VICON data with the shoes, first, 'Vicon's sync out port' was connected to an 'Arduino microcontroller analog pin'. Then this Arduino microcontroller is connected to a laptop computer (Figure 4.2). Next, two Bluetooth (BLE-Bluetooth Low Energy) USPs (Universal Serial Port) connected with a laptop, and a LabVIEW user interface was created in that laptop computer. Bluetooth1 sends the signal to the left shoe, and Bluetooth2 sends the signal to the right shoe (Figure 4.3).

When the vicon system collects data, Vicon's synchronise port sends a 'high voltage signal' to Arduino. Arduino continuously checks these voltages; when the voltage reaches 'greater than 3v', this sends an 'H' signal to LabVIEW. As soon as the 'Vicon system' stops collecting data, the 'Vicon's synchronise port' sends a low voltage signal to Arduino. On receiving this low voltage signal of 'less than 3v', the Arduino sends an 'L' signal to the LabVIEW.

Data collection with VICON

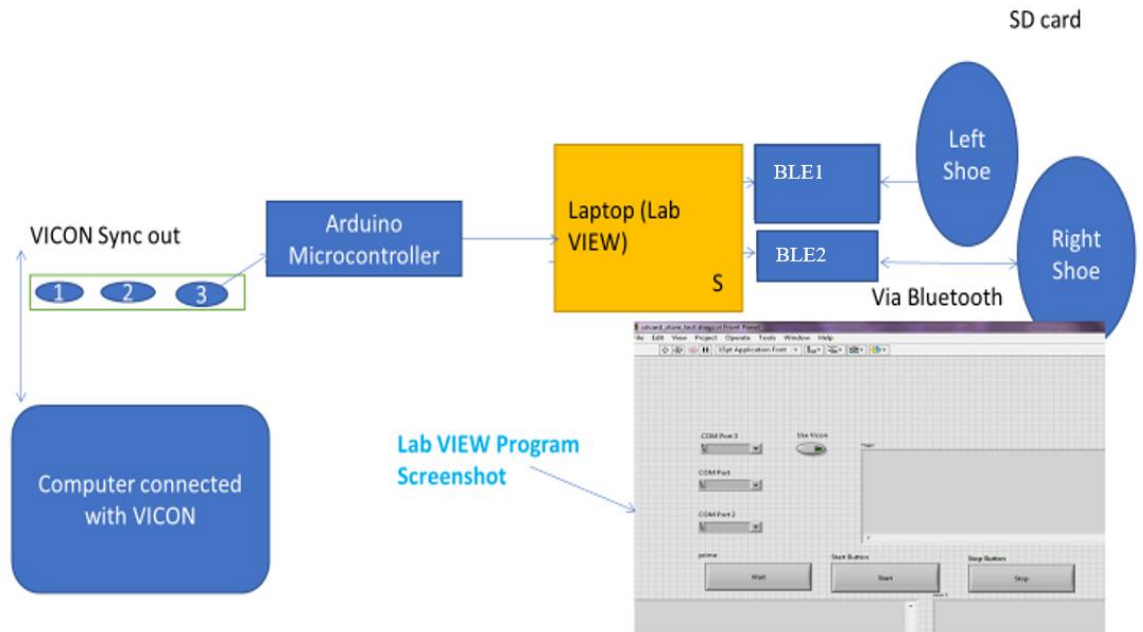


Figure 4.3 Sensor and Vicon System Synchronisation. A computer connected with a Vicon system. Vicon synchronization port was connected with Arduino; then this Arduino connected with a laptop, which contains a user interface to collect data from the sensor shoe. Finally, two Bluetooth dongles were connected to the computer to signal the sensor shoe to start and stop data collection.

LabVIEW continuously checks the ‘Arduino trigger port’; when LabVIEW receives an ‘H’ signal, LabVIEW sends a ‘start signal’ to both the shoes via a dedicated Bluetooth system to start data collection from the shoes. When LabVIEW receives an ‘L’ signal, LabVIEW sends a ‘stop signal’ in the above manner to stop data collection by the shoes.

Once the data collection is started, LabVIEW reads the data sent by the shoes and writes them into an ‘SD storage card’ with a ‘Unique/itemised file name’ for each data. This Unique file is closed when the LabVIEW receives the ‘L’ signal by sending a ‘stop signal’ to the shoes. After finishing the trials, all the files were transferred to the computer from an SD card for further analysis.

4.2.5. VICON data analysis

Full-body kinematics was obtained using a 15 segment (head, thorax, pelvis, upper arms, lower arms, hands, thighs, shanks, feet) full-body six-degrees of freedom. The kinematic model was defined using 76 reflective markers (diameter 14 mm). The segmental data

were defined in visual3D based on Dempster's regression equations (Dempster 1955) and used geometrical volumes to represent each segment (Hanavan Jr 1964). After data collection, all kinetic and kinematic data were filtered using a low-pass fourth-order Butterworth filter with a cut-off frequency of 6 Hz. Force plates were used to obtain gait events.

Kinematic data were obtained using a 24 infrared camera system (120Hz, Vicon, Oxford Metrics, UK). Kinetic data were synchronously recorded from four force platforms. Foot clearance, foot contact length ratio and foot motion data were obtained using a 24 infrared camera system (120Hz, Vicon, Oxford Metrics, UK). The participant's sensor shoes were digitalised manually. The participant's sensor shoe's two-dimensional outline was obtained by taking a picture of the sensor shoe outline drawn on an A4 paper (Figure 4.4) and imported using ImageJ (National Institutes of Health, Bethesda, USA). The coordinates of up to 600 virtual markers representing the individual shoe sole outline were calculated in Matlab. The position of three markers fixed on the shoe (first metatarsophalangeal joint (*RMP1*), fifth metatarsophalangeal joint (*RMP5*) and calcaneus lateral (*RLCL*)). And these markers were digitised in the two-dimensional drawing using the static measurement. These static measurements included the above three markers position in a 3D (three dimensions) space, which helps determine the position of the shoe's virtual outline relative to the markers. The virtual outline of the shoe was then projected in movement trials, again relative to the three markers.

The foot clearance (Figure 4.4) was obtained during the swing phase when the virtual shoe outline of the leading limb passed the vertical position (1) of the step edge up until the outline passed the horizontal position of the step edge (2). The minimal clearance of the virtual shoe was determined within this time frame. The minimal foot clearance was determined for steps 1-7 in all three trials. The mean value across the three trials was considered for further analysis.

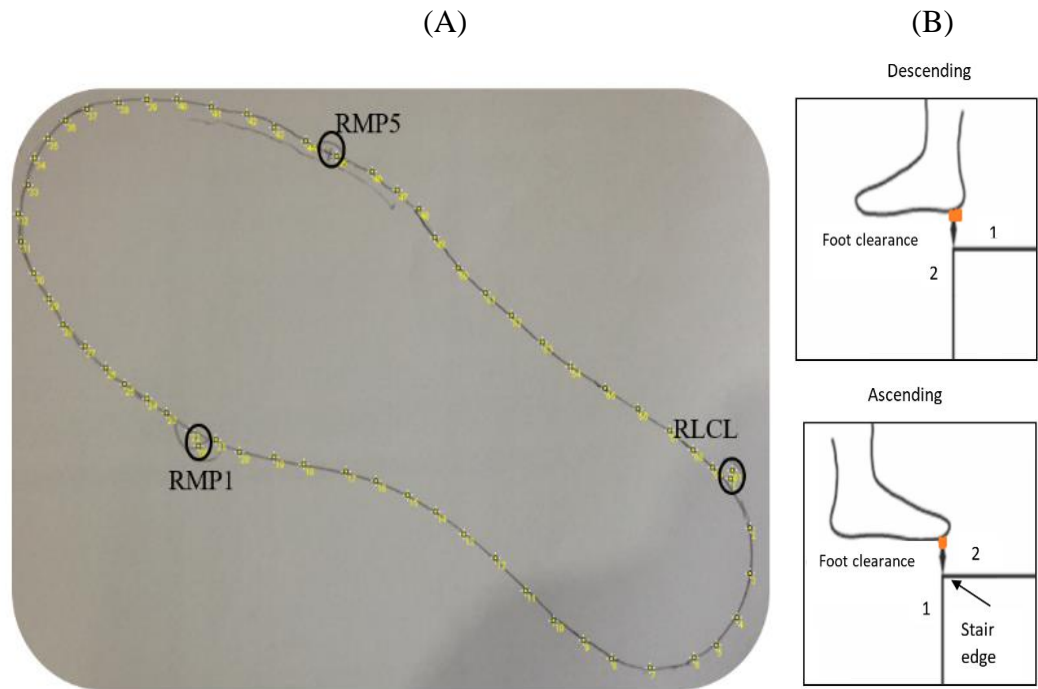


Figure 4.4 Vicon foot clearance calculation of the right foot using the above foot model. A two-dimensional outline of the shoe (A) was digitized and linked to three markers (first metatarsophalangeal joint: RMP1, fifth metatarsophalangeal joint: RMP5 and calcaneus lateralis: RLCL) of the static measurement. The virtual outline of the shoe was then projected in the movement trials. Foot clearance was calculated as the minimal distance between the virtual shoe and the step edge, within the orange colour area between 1 and 2 shown in (B).

We calculated the foot contact length ratio using the foot touchdown over the ‘force plate’, placed on steps 1 to 4. Distance X was measured, the distance between the step edge and the posterior foot end of the virtual shoe line, and distance Y is the distance between the step edge and the most anterior foot end of the virtual shoe outline (Figure 4.5).

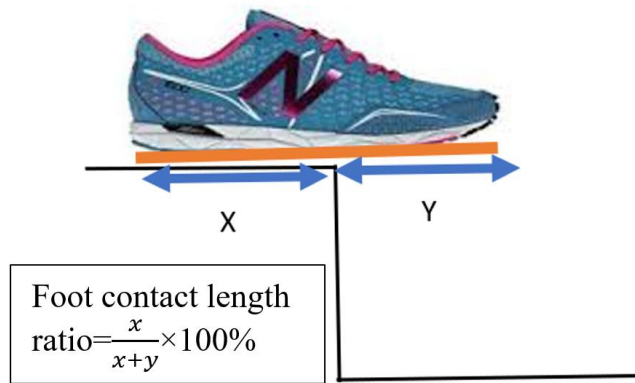


Figure 4.5 VICON Foot contact length ratio calculation, the Foot contact length ratio was calculated at touch-down using the rigid virtual shoe (blue line) as: Foot placement ratio = $(x / (x + y)) * 100\%$.

Foot contact length ratio was calculated using the formula $\frac{x}{(x+y)} \times 100\%$. The mean value across three trials was calculated and used for further analysis.

4.2.6. Sensor shoe data analysis

Sensor shoe development was explained in chapter3. So, the only summary of the foot clearance and foot contact length ratio is presented in this chapter.

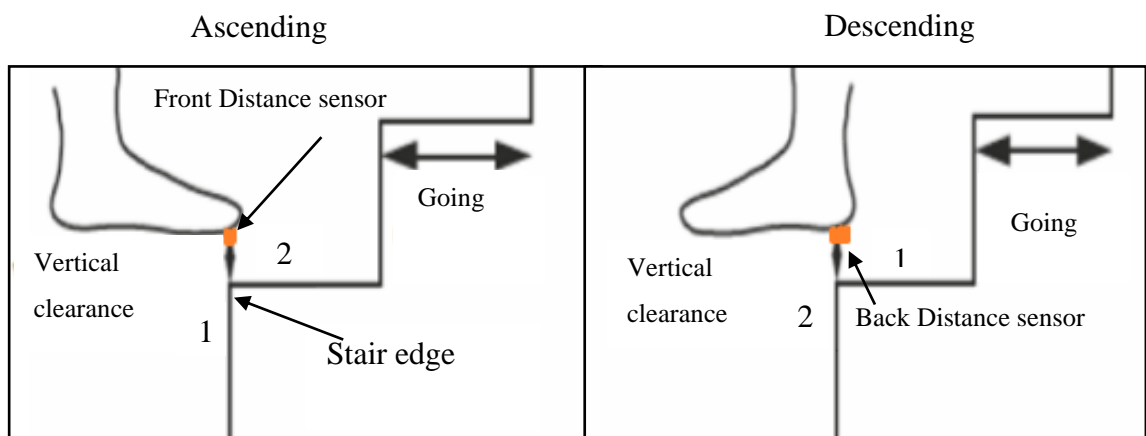


Figure 4.6 Foot clearance calculation for sensors, for ascending front distance sensor measures vertical distance while crossing the stair edge, back distance sensor measures vertical distance while crossing the stair edge

For descending, foot clearance was calculated during the swing phase when the sensor shoe's back distance sensor of the leading limb (Figure 4.6) passed the step edge's vertical position (1). For ascending, during the swing phase, when the sensor shoe's front distance sensor of the leading limb passed the second step edge (2) before placing the foot on the stairs.

Different sizes of sensor insole were created to fit various shoe sizes from 6 to 11. Each sensor insole had a different number of sensors. The number was given for each sensor from the toe as one to heel as number nine (last number). The foot contact length ratio was calculated as below; for example, the below sensor insole has nine sensors; the insole's total length was 26cm. The distance between sensors was 2.9cm which was 11% of the whole insole length. All the force sensors' force was checked to calculate ascending foot contact length ratio.

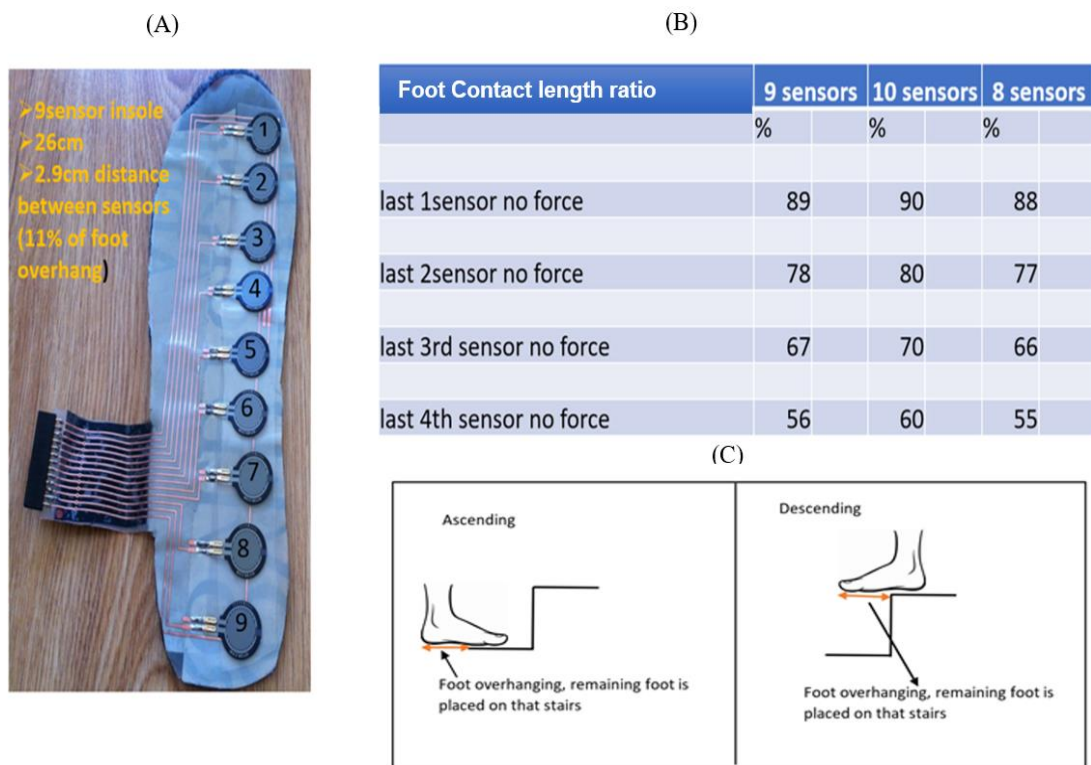


Figure 4.7 Foot Contact length ratio calculation, (A) shows the flexible sensor insole with nine sensors, the distance between each sensor was 2.9cm, (B) sample table shows how foot contact length was calculated, (C) shows the schematic representation of foot contact length calculation.

Figure 4.7 shows the foot contact length ratio calculation. For example, if all the sensors have the forces, 100% of the foot is placed on the stairs. If only the last sensor does not have any force ($100\% - 11\% = 89\%$), 89% of the foot is placed on the stairs. Suppose the last two sensors do not have forces, which means ($100\% - 22\% = 78\%$) 78% of the foot placed on the stairs. Similarly, the remaining sensor forces are checked to measure the foot contact length ratio. For descending foot contact length ratio, check front sensors' forces; based on the forces and length of insole, the foot contact length ratio was calculated.

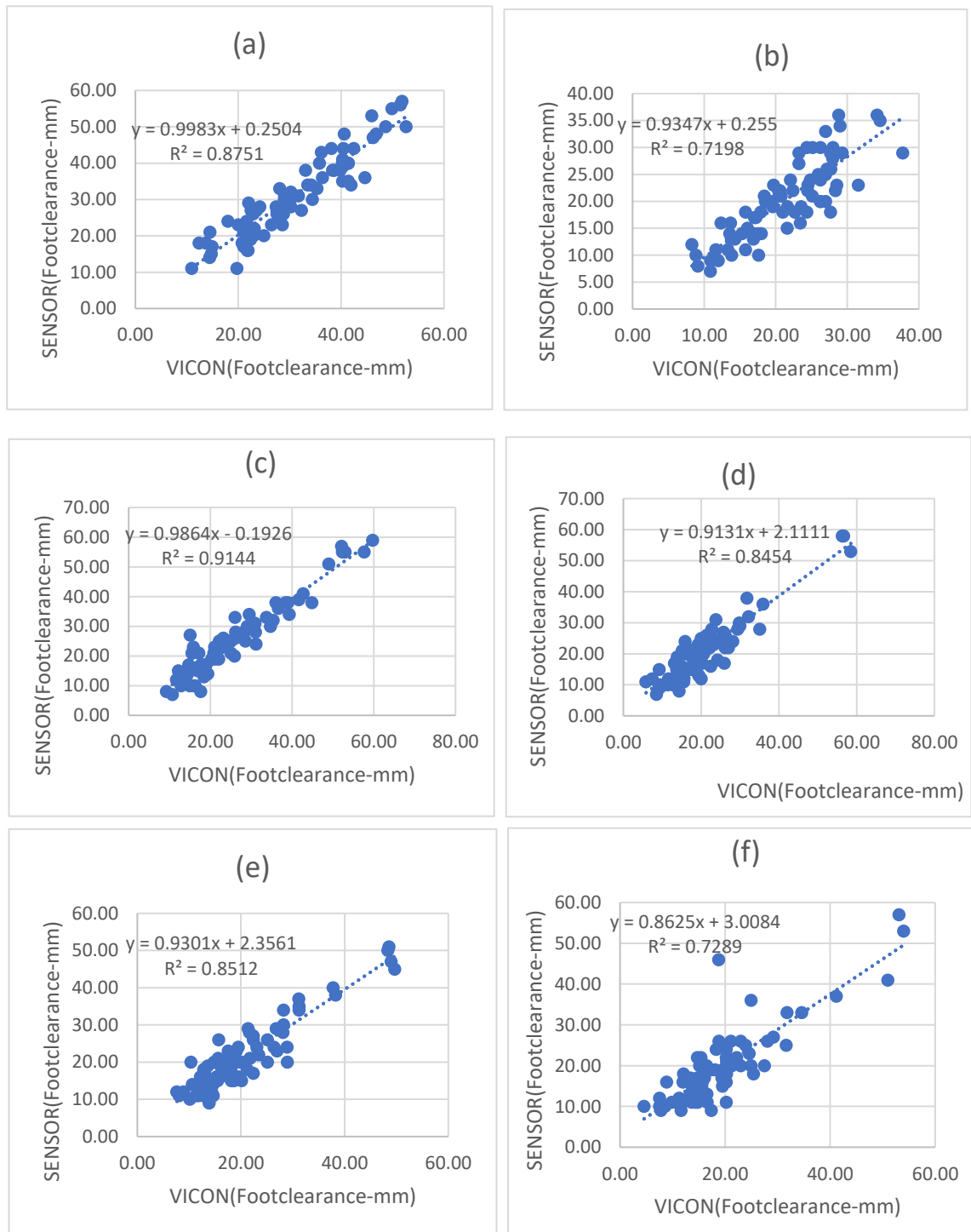
4.3 Results

Sensor-based stair fall risk parameters were validated with (well-established laboratory method) VICON based stair fall risk parameters. Three steps were used for validation,

- Step1: Correlation coefficients (r and r^2) were calculated to measure the sensor and vicon parameters relationship.
- Step2: Regression was calculated to find the best fit line.
- Step3: Bland-Altman plot was created to check the agreement between the sensor and vicon parameters.

Correlation checks the relationship between two variables, showing how strongly they are related. The most common correlation techniques are Pearson and product-moment correlation (correlation coefficient(r)). It is calculated as the covariance ratio between the variables to the product of their standard deviations. The correlation coefficient(r) ranges from +1 to -1. This value helps get an idea of the relationship strength; the correlation coefficient(r) value closer to +1 shows the strong positive linear relationship, close to -1 shows the strong negative linear relationship. R square is the square of the correlation coefficient and indicates the percentage of variation explained by the regression line out of the total variation.

4.3.1. Foot Clearance results between Sensor and Vicon



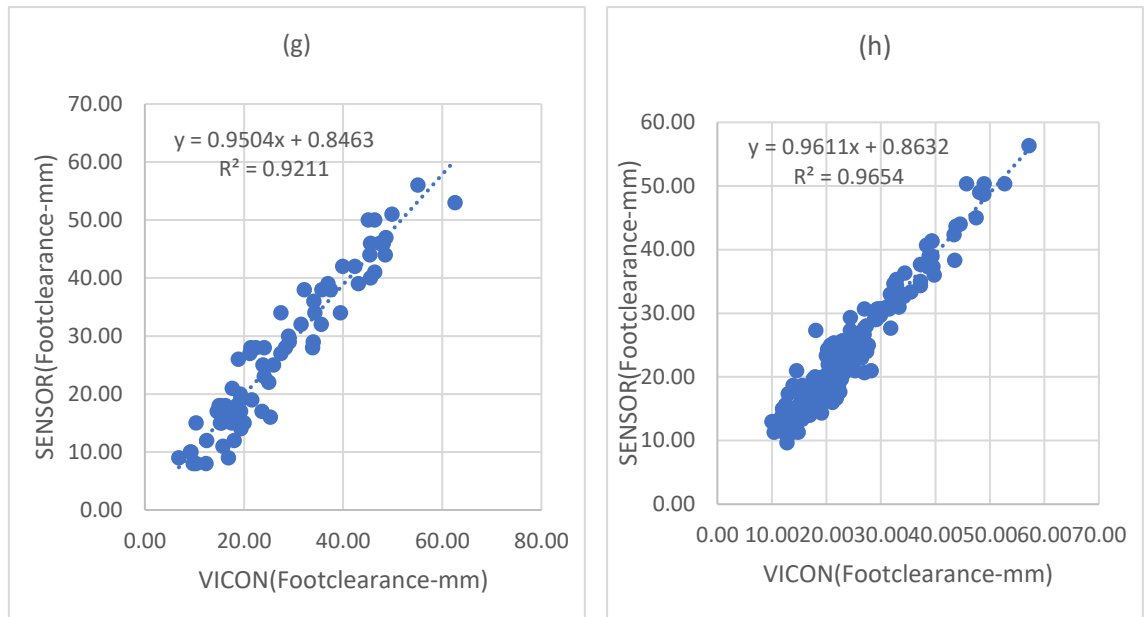


Figure 4.8 Foot clearance correlation coefficient (r^2) results between sensors and VICON (Laboratory System) (a) Step one foot clearance correlation, (b) Step two-foot clearance correlation, (c) Step three-foot clearance correlation, (d) Step four-foot clearance correlation, (e) Step five clearance correlation, (f) Step six-foot clearance correlation, (g) Step seven-foot clearance correlation, (h) All seven steps combined foot clearance correlation. Step one, step seven, and all seven steps combined foot clearance correlation showed a high positive linear correlation between data from the sensors and the VICON system.

This study used the Pearson correlation to check the relationship between sensor foot clearance and VICON foot clearance. The correlation coefficient was calculated for each step, a total of 7 steps with 3 trials ($N=75$, $3\text{trials} \times 25$ participants) (Figure 4.8).

Table 4.1 Foot clearance correlation results between sensors and VICON

Foot clearance calculation	Correlation coefficient (r^2)	Linear Regression
Step1	0.8751	$y = 0.9983x + 0.2504$
Step2	0.7198	$y = 0.9347x + 0.255$
Step3	0.9144	$y = 0.9864x - 0.1926$
Step4	0.8454	$y = 0.9131x + 2.1111$
Step5	0.8512	$y = 0.9301x + 2.3561$
Step6	0.7289	$y = 0.8625x + 3.0084$
Step7	0.9211	$y = 0.9504x + 0.8463$
Mean of all 7steps	0.9654	$Y = 0.9611x + 0.8632$

In total, there were 25 participants; each participant's three trials of foot clearance were used to calculate each step's correlation coefficients ($25 \times 3 = 75$ data). The mean value of three trials' foot clearance was used to calculate the overall correlation coefficient ($25 \text{ participants} \times 7 \text{ steps} = 175$ data points). The overall (Table 4.1) correlation coefficient was $r^2 = 0.96$ and $r = 0.967$, which was closer to +1, showed a strong positive linear correlation between sensor foot clearance and vicon foot clearance. Step3 and step7 had a high positive linear correlation (0.9144, 0.9211), step2 and 6 had slightly less positive correlation (0.7198, 0.7289). step1,4 and 5 (0.8751, 0.8454, 0.8512) had better correlation than the step2,6 and less correction than step3,7.

Table 4.2 Foot clearance Pearson correlation result between sensors and VICON

Pearson Correlations(r)			
		FC_VICON	FC_SENSOR
FC_VICON	Pearson Correlation	1	.967**
	Sig. (2-tailed)		.000
	N	175	175
FC_SENSOR	Pearson Correlation	.967**	1
	Sig. (2-tailed)	.000	
	N	175	175

** . Correlation is significant at the 0.01 level (2-tailed).

A Table 4.2 shows, Pearson correlation results for overall foot clearance between sensor and vicon $r = 0.967$ ($p < 0.000$). Because the p-value was less than 0.05 ($p < .05$), the null hypothesis (no significant relationship) was rejected, and the alternative hypothesis was accepted (there is a statistically significant relationship between sensor and vicon foot clearance). Linear regression was calculated to find the best line that predicts sensor foot clearance from the vicon foot clearance. The calculated linear regression results are in table 4.1.

The correlation coefficient describes the relationship between two variables (sensor and vicon foot clearance), but it does not describe their agreement (Bland and Altman 1986). Therefore, a high correlation does not mean a good agreement between two variables. So, the Bland-Altman plot was used to measure the agreement between two variables by constructing limits of agreement. These limits of agreement were calculated using the

mean and standard deviations of the difference between the sensor and vicon foot clearance measurements (Bland and Altman 1986).

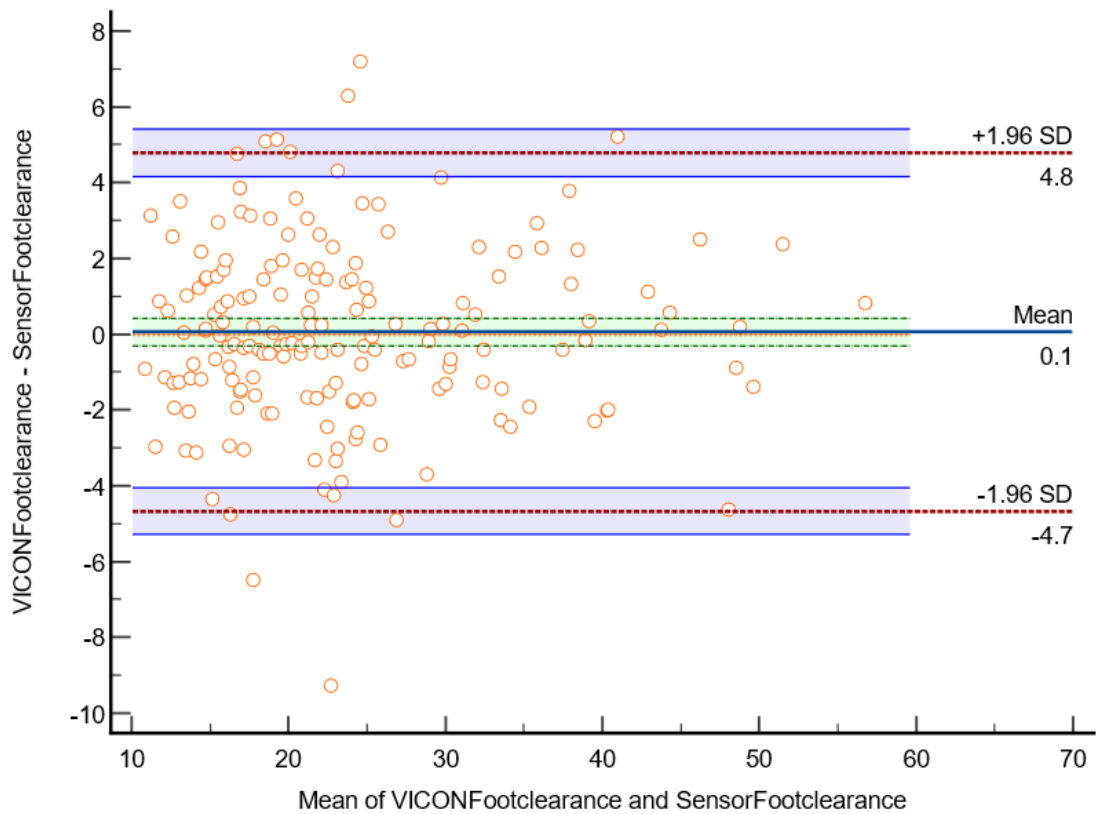


Figure 4.9 Bland-Altman plot of foot clearance between the sensor method and the VICON method in the Laboratory. The X-axis represents the average of the sensor and vicon foot clearance; Y-axis represents the difference between sensor and vicon foot clearance. The indigo horizontal line denotes the mean difference between sensor and VICON method which was 0.1mm, while the top red horizontal line represents the upper limits of agreement (Mean difference+1.96 ×SD of difference) which was 4.8mm, the bottom red line represents the lower limits of agreement (Mean difference-1.96× SD of difference) which was -4.7mm. Purple lines shows the confidence limit for the upper and lower limits of agreement. The Orange small circles are data points, and when shown out of the confidence limits these are called outliers; four outliers in total (4 out of 175 datapoints). The orange horizontal line shows the line of equality, and it is possible to determine if bias is significant or not. This equality line was within the confidence interval of the mean difference, so the bias was not significant (0.1 mm).

The scatter plot shows Bland-Altman’s agreement results for sensor and vicon foot clearance. The X-axis represents the average of the sensor and vicon foot clearance; Y-axis represents the difference between sensor and vicon foot clearances. Plotting

difference against mean value helps find a possible relationship between measurement error and the actual value (Giavarina 2015). For example, from Figure 4.9, the average of the differences was 0.05mm(bias). This mean difference was not zero, which means that, on average, the second method (sensor shoe) measures 0.0566mm more foot clearance than the first method (VICON).

Repeatability is the degree to which the same method produces the same results on repeated measurements. The standard deviation (SD) of all the individual differences was calculated to measure repeatability, 2.41mm. Approximately 5% (10 of 175 data points) of data points were outliers and exceeded the upper and lower limit of agreement. The Shapiro-Wilk method was used to check the normality of the data point in differences (vicon foot clearance data-sensor foot clearance data). The results ($p=.210$) showed that differences were normally distributed. The limit of agreement was calculated; 95% of the limits of agreement was between the upper limit (4.8mm) and lower limit (-4.7mm). Precision is the degree (confidence limit) to which values cluster around the mean distribution of values, which was the 95% confidence limit of upper (4.1mm to 5.4mm) and lower (-5.2mm to -4.0mm). The results measured by the VICON system may be 4.8mm above or 4.7mm below in sensor measurement of foot clearance. This confidence limit was small enough to be confident that the new method (sensor shoe) could be used to calculate foot clearance in place of the VICON.

4.3.2. Foot Contact length ratio results between Sensor and Vicon

Sensor-based foot contact length ratio was validated with (well-established laboratory method) VICON based foot contact length ratio.

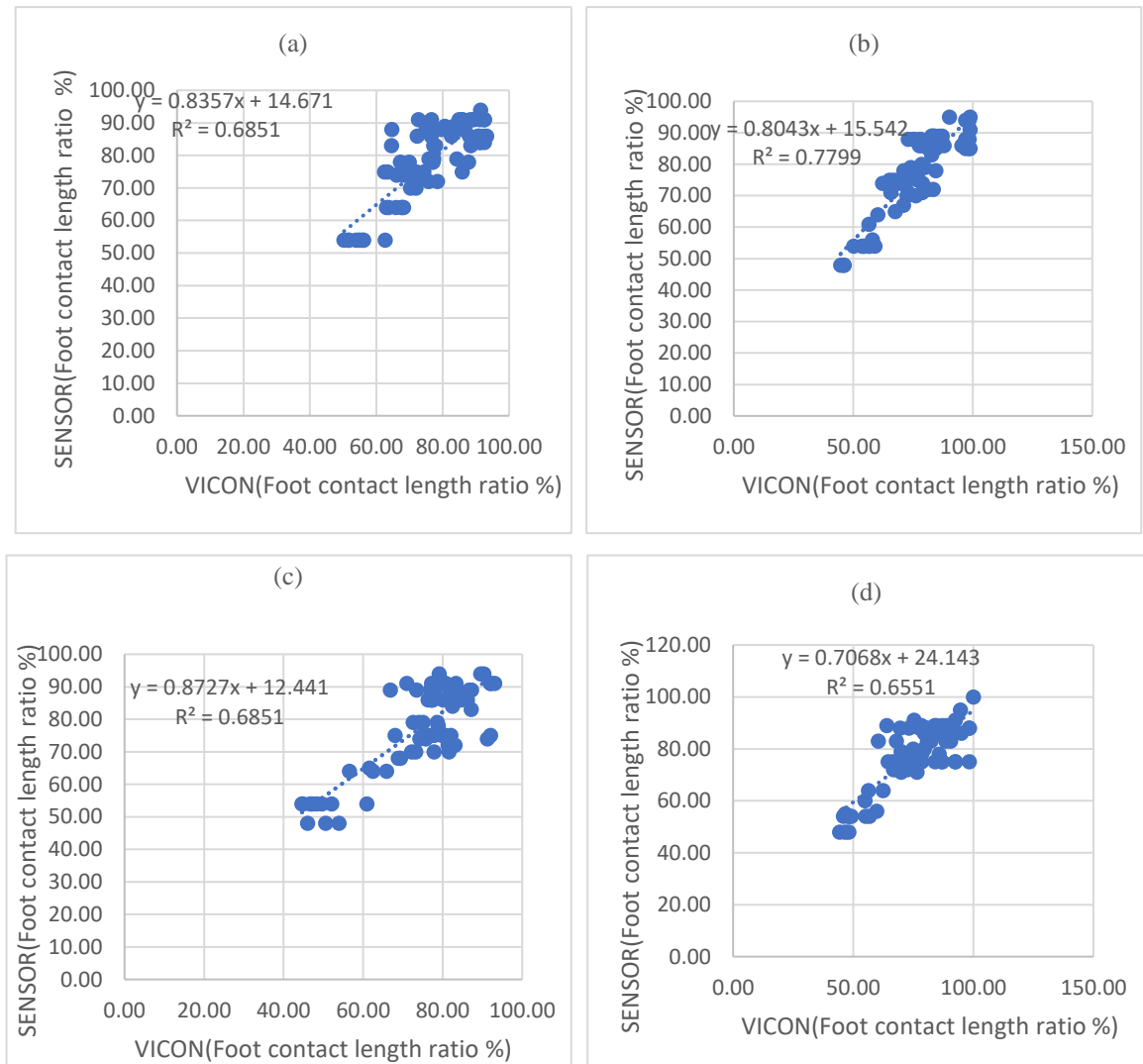


Figure 4.10 Foot contact length ratio correlation results between the sensor and VICON (Laboratory System). (a) step one- Foot contact length ratio correlation results, (b) step two- Foot contact length ratio correlation results, (c) step three- Foot contact length ratio correlation results, (d) step four- Foot contact length ratio correlation results. Among the four steps, step two showed a higher positive linear correlation between data from the sensors and the VICON system compared to the other three steps.

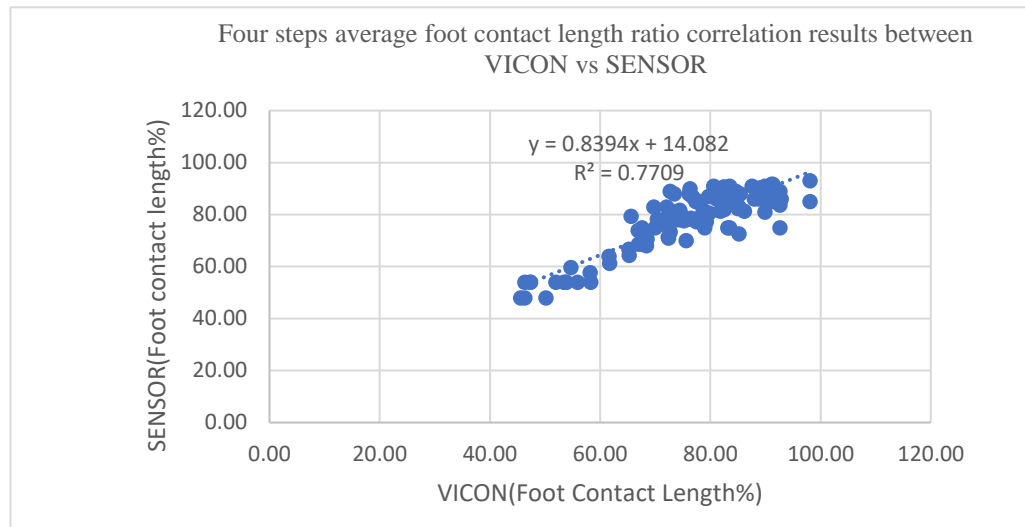


Figure 4.11 Four steps combined foot contact length ratio correlation between sensors and VICON (Laboratory system) with high positive linear correlation

Pearson correlation was used to check the relationship between the sensor’s foot contact length ratio and VICON’s foot contact length ratio. The correlation coefficient (Figure 4.10 and Figure 4.11) was calculated for all four force plates (N=75, 3trials×25 participants). In total, there were 25 participants; each participant’s three trials of foot contact length ratio were used to calculate all four force plates correlation coefficients (25×3=75 data). The mean value of three trials’ foot contact length ratio was used to calculate the overall correlation coefficient (25participants×4steps=100 data points).

Table 4.3 Foot contact length ratio’s correlation between sensors and VICON

Foot contact length ratio	Correlation coefficient (r^2)	Regression
Force plate1(FP1)	0.6851	$y = 0.8357x + 14.671$
Force plate2(FP2)	0.7799	$y = 0.8043x + 15.542$
Force plate3(FP3)	0.6851	$y = 0.8727x + 12.441$
Force plate4(FP4)	0.6551	$y = 0.7068x + 24.143$
Combined Foot contact length ratio	0.7709	$y = 0.8394x + 14.082$

The overall correlation coefficient (Table 4.3) was $r^2 = 0.77$ and $r = 0.878$, closer to +1, showed a high positive linear correlation between sensor foot contact length and vicon contact length ratios. Force plate1,3 and 4 had a moderate positive linear correlation ($r^2 = 0.6851, 0.6851, 0.6551$) and ForcePlate2(FP2) had high positive linear correlation (0.7799). Linear regression was calculated to find the best line that predicts sensor contact length ratio from the VICON contact length ratio. The calculated linear regression results are in table 4.3.

Table 4.4 Foot contact length ratio Pearson correlation

Pearson Correlations			
		FO_VICON	FO_SENSOR
FO_VICON	Pearson Correlation	1	.878**
	Sig. (2-tailed)		.000
	N	100	100
FO_SENSOR	Pearson Correlation	.878**	1
	Sig. (2-tailed)	.000	
	N	100	100
**. Correlation is significant at the 0.01 level (2-tailed).			

A Table 4.4 shows, Pearson correlation results for overall foot contact length ratio between sensor and vicon $r = 0.878$ ($p < 0.000$). Because the p-value was less than 0.000 ($p < .000$), the null hypothesis (no significant relationship) was rejected, and the alternative hypothesis was accepted (there is a statistically significant relationship between sensor and vicon contact length ratio).

The correlation coefficient describes the relationship between two variables (sensor and vicon contact length ratio (Table 4.4), but it does not describe their agreement. A high correlation does not mean a good agreement between two variables. So, the Bland-Altman plot was used to measure the agreement between two variables by constructing limits of agreement. These limits of agreement were calculated using the mean and standard deviations of the difference between sensor and vicon foot clearance measurements.

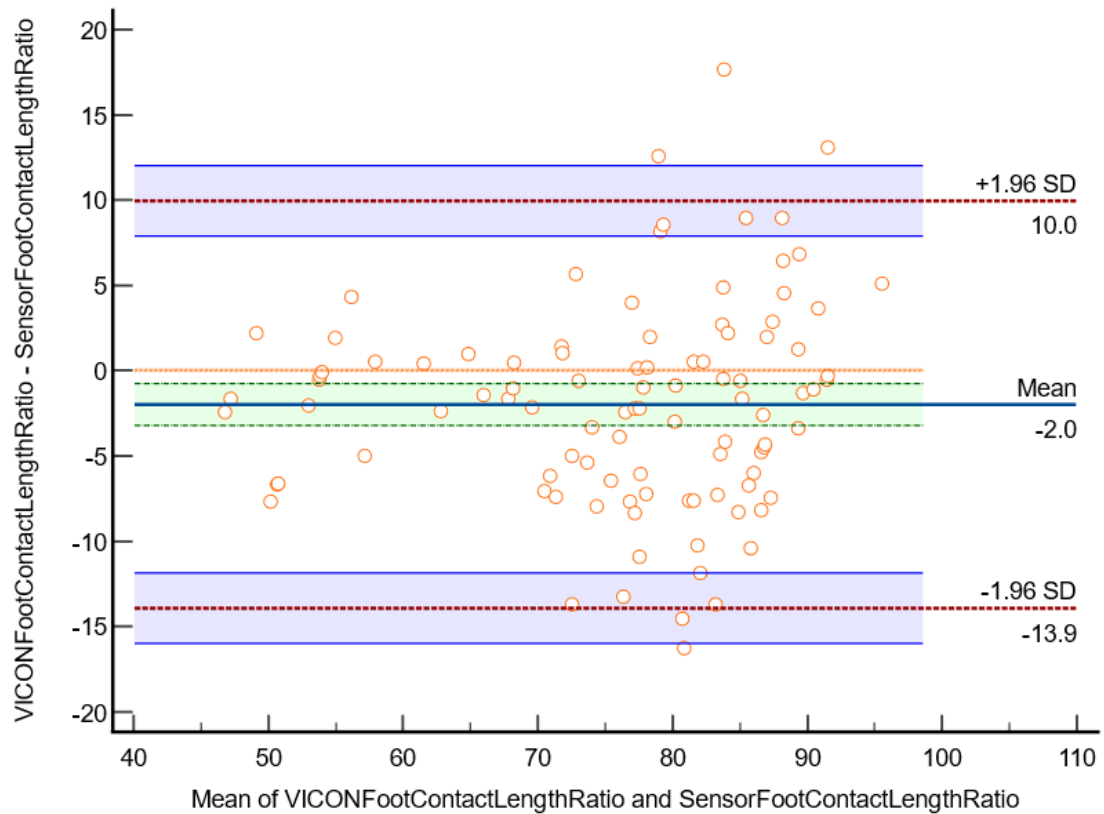


Figure 4.12 Bland-Altman plot of foot contact length ratio agreement between the sensor method and the VICON method in the Laboratory. The X-axis represents the average of the sensor and vicon foot contact length ratio; Y-axis represents the difference between sensor and vicon foot contact length ratio. The indigo horizontal line denotes the mean difference between sensor and VICON method which was -2%, while upper red line represents the upper limits of agreement (Mean difference + 1.96 × SD of difference) which was 10%, the lower red line represents the lower limits of agreement (Mean difference - 1.96 × SD of difference) which was -13.9%. Purple lines show the confidence limits for the upper and lower limits of agreement. The Orange small circles are data points, when shown out of the confidence limits are called outliers, four outliers in total (4 out of 100 datapoints). The Orange horizontal line shows the line of equality, it is possible to determine if bias is significant or not. This equality line was not within the confidence interval of the mean difference, so the bias is significant (-2%).

The scatter plot shows Bland-Altman's agreement results for sensor and vicon foot contact length ratio. The X-axis represents the average of the sensor and vicon foot contact length ratio; Y-axis represents the difference between the sensor and vicon foot contact length ratio. Plotting the difference against the mean value helps to find a possible relationship between measurement error and actual value. From Figure 4.12, the average of the differences was -2% (bias). This mean difference was not zero, which means that, on average, the second method (sensor shoe) measures -2% more-foot contact length ratio

than the first method (VICON). Repeatability is the degree to which the same method produces the same results on repeated measurements. The standard deviation (SD) of all the individual differences was calculated to measure repeatability, 6.08%. Approximately 4% (4 of 100 data points) of data points were outliers and exceeded the upper and lower limit of agreement. Shapiro-Wilk method was used to check the normality of the data point in differences (vicon foot contact length ratio -sensor foot contact length ratio), and the results ($p=.266$) showed that differences were normally distributed. Limits of the agreement were calculated; 95% of the limits of agreement were between 10% (upper limit) and -13.91% (lower limit). Precision is the degree (confidence limit) to which values cluster around the mean distribution of values, which was the 95% confidence limit for upper (7.8% to 12%) and 95% confidence limit for lower limits of agreement (-15.97% to -11%). Therefore, the foot contact length ratio results measured by the VICON system is -13.91 % less or 10% more than sensor-based measurements. This confidence limit was small enough to ensure that the new method (sensor shoe) could calculate the foot contact length ratio in place of the VICON method.

4.3.3. Cycle time (Cadence) results between Sensor and Vicon

Sensor-based cycle time was validated with (well-established laboratory method) VICON based cycle time.

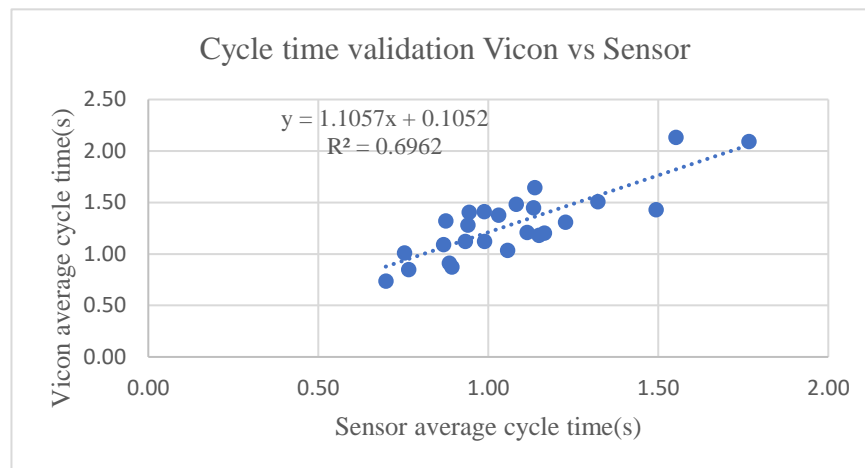


Figure 4.13 Cycle time correlation results between instrumented sensor shoe and Vicon, moderate positive linear correlation

Pearson correlation was used to check the relationship between the instrumented sensor shoe's cycle time and VICON's cycle time. The correlation coefficient (Figure 4.13) was calculated as an average cycle time for each participant (N=25, 3trials×25 participants). There were 25 participants; each participant's three trials of cycle time were averaged to calculate correlation coefficients. The overall cycle time correlation coefficient (Figure 4.13) was $r^2 = 0.69$, closer to +1, which showed a positive linear correlation between the sensor shoe's cycle time and vicon cycle time.

Table 4.5 Cycle time's Pearson correlation results between sensors and VICON method

Correlations			
		sensor	vicon
sensor	Pearson Correlation	1	.835**
	Sig. (2-tailed)		.000
	N	25	25
vicon	Pearson Correlation	.835**	1
	Sig. (2-tailed)	.000	
	N	25	25
**. Correlation is significant at the 0.01 level (2-tailed).			

A Table 4.5 shows, Pearson correlation results for overall cycle time between sensor and vicon $r = 0.835$ ($p < 0.000$). Because the p-value was less than 0.000 ($p < .000$), the null hypothesis (there is no significant relationship between sensor and vicon cycle time) was rejected. And the alternative hypothesis was accepted (there is a statistically significant relationship between sensor and vicon cycle time). Linear regression was calculated to find the best line that predicts sensor cycle time from the vicon cycle time. The calculated linear regression (Figure 4.13) results $y = 1.1057x + 0.1052$.

The correlation coefficient describes the relationship between two variables (sensor and vicon cycle time (Table 4.4), but it does not describe their agreement. A high correlation does not mean a good agreement between two variables. So, the Bland-Altman plot was used to measure the agreement between two variables by constructing limits of agreement. These limits of agreement were calculated using mean and standard deviations of the difference between sensor and vicon cycle time measurements.

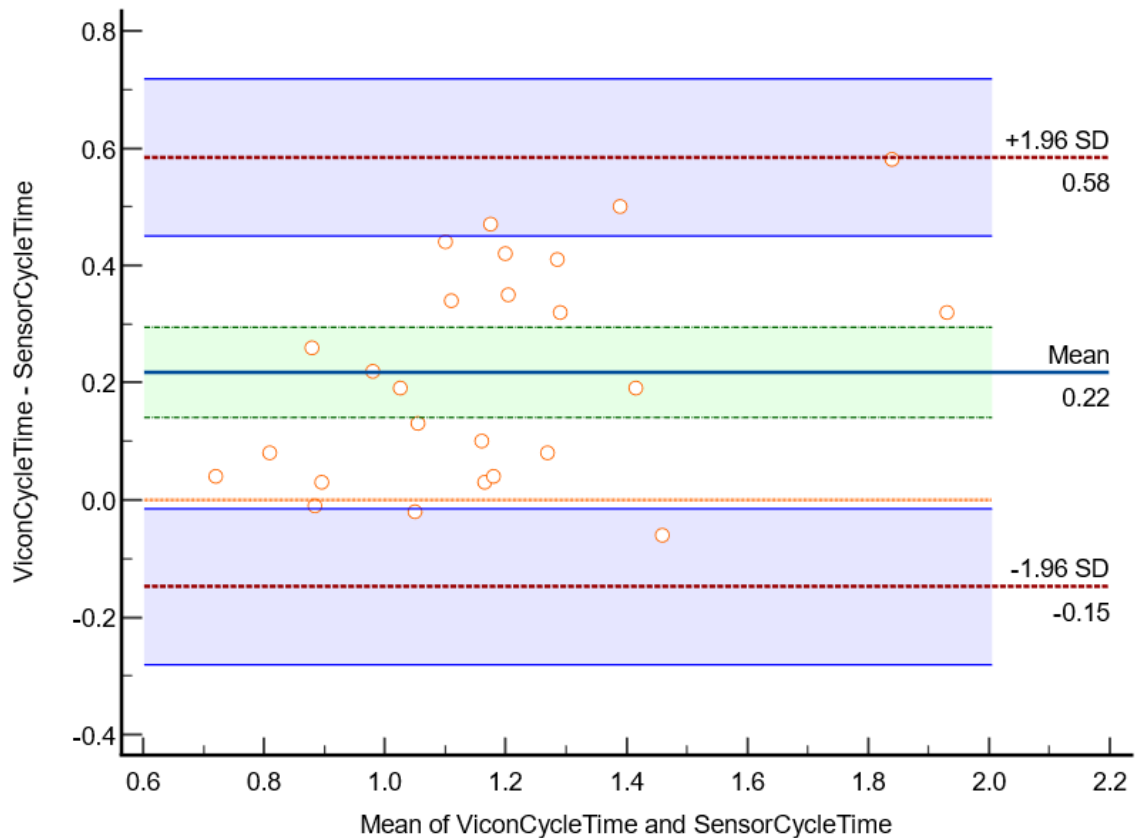


Figure 4.14 Bland-Altman plot of cycle time between the sensor method and the VICON method in the Laboratory. The X-axis represents the average of the sensor and vicon cycle time; Y-axis represents the difference between sensor and vicon cycle time. The indigo horizontal line denotes the mean difference between the sensor and VICON method, which was 0.22s, while upper red lines represent the upper limits of agreement ($\text{Mean difference} + 1.96 \times \text{SD of difference}$) which was 0.58s, the lower red line represents the lower limits of agreement ($\text{Mean difference} - 1.96 \times \text{SD of difference}$) which was -0.15s. Purple lines show the confidence limits for the upper and lower limits of agreement. There are no outliers in the cycle time because no data point has gone out of the confidence limit. The Orange horizontal line shows the line of equality, and it is possible to determine if bias is significant or not. This equality line was not within the confidence interval of the mean difference, so the bias is significant (0.22s).

The scatter plot shows Bland-Altman's agreement results for sensor and vicon cycle time. The X-axis represents the average sensor and vicon cycle time; the Y-axis represents the difference between sensor and vicon cycle time. Plotting the difference against the mean value helps to find a possible relationship between measurement error and real value. From Figure 4.14, the average of the differences was .22s(bias). This mean difference was not zero, which means that, on average, the second method (sensor shoe) measures

.22s less cycle time than the first method (VICON). Repeatability is the degree to which the same method produces the same results on repeated measurements. The standard deviation (SD) of all the individual differences was calculated to measure repeatability, which was .1867seconds. Shapiro-Wilk method was used to check the normality of the data point in differences (vicon cycle time -sensor cycle time), and the results ($p=.186$) showed that differences were normally distributed. Finally, limits of the agreement were calculated; 95% of the limits of agreement were between 0.58s (upper limit) and -0.15s (lower limit). Precision is the degree (confidence limit) to which values cluster around the mean distribution of values, which was the 95% confidence limit of upper limits of agreement (0.45s to 0.71s) and the 95% confidence limit of lower limits of agreement (-0.28s to -0.01s). The results measured by the VICON system may be 0.1seconds above or 0.57seconds below in sensor measurement of cycle time. This confidence limit was small enough to ensure that the new method (sensor shoe) could calculate cycle time in place of the VICON method.

4.4 Discussion

There are different approaches available to track human motion, with the main ones being Optical motion systems (such as Vicon or Optotrak) and commercial IMU sensors such as MTw(Xsens). However, the most widely used and accepted system to track stair climbing motion is optical motion systems because they have high accuracy when operating in controlled environments. This Vicon optical motion system was used in our lab, so this was chosen to compare against the sensor-based results.

Instrumented shoe derived fall risk parameters such as foot clearance, foot contact length and cycle time were validated against the Vicon system. There were two different methods used for this purpose based on correlations and the Bland Altman plots (B&A). The correlation coefficient describes the relationship between two methods (sensor and vicon); sensor shoe's foot clearance, foot contact length ratio and cycle time had a high positive linear correlation with parameters measured with the Vicon system. But this correlation does not describe their agreement (Bland and Altman 1986). A high correlation does not mean a good agreement between two variables. So, the Bland-Altman plot was used to measure the agreement between the two methods by constructing limits of agreement.

The B&A plot system does not express if the agreement is sufficient or suitable to use a method or the other indifferently. It simply quantifies the bias and a range of agreement, within which 95% of the differences between the two measurements are included. Therefore, we need to define the maximum acceptable difference (limits of agreement expected) between the two methods. For example, if 5 mm is set as an acceptable difference for foot clearance between the sensor and Vicon means that if the sensor measurement is 5 mm more or less than the Vicon system measurement of the same parameter, it is then accepted. Next, we need to compare the bias and limits of agreement results with prior acceptable differences. If both bias and limits of agreement (LoA) fall within the acceptable difference, the new method(sensor) may be used interchangeably with the established method (Vicon). On the other hand, if the bias and limits of the agreement exceed the acceptable difference, the new method(sensor) would be considered unacceptable in practice.

This research set 5mm as the maximum acceptable difference for foot clearance. The B&A plot results showed that the sensor shoe's foot clearance measurements were 0.05mm(bias), and the limits of agreements results were from 4.7mm to -4.6mm. This range falls within the maximum acceptable difference, so this method of calculating foot clearance can be used in the future.

The maximum acceptable difference for foot contact length was set at 15% for this research. The B&A plot results showed that the sensor shoe's foot contact length measurements were -2%(bias), and the limits of agreements results were from 10% to -13.9%. This limit falls within the acceptable difference, so this method of calculating foot contact length can be used in the future.

The maximum acceptable difference for cycle time for this research was set 0.5seconds. The B&A plot results showed that the sensor shoe's cycle time measurements were 0.2 seconds(bias), and the limits of agreements results were from 0.5 seconds to -0.14 seconds. This limit comes within the acceptable difference, so this method of calculating cycle time can be used in the future.

This 95% limit of agreement was small enough to be confident that the new method (sensor shoe) can be used to calculate foot clearance, foot contact length ratio and cycle time in place of the VICON method.

4.5 Conclusion

In this chapter, the sensor shoe's fall risk parameters were validated against the vicon system using correlation and the Bland Altman plot method. Sensor shoe's fall risk parameter had a high positive linear correlation with the vicon system. Sensor shoe's fall risk parameters results for Bland Altman plot was within the acceptable difference. So, this sensor shoe can be used in the future to calculate foot clearance, foot contact length ratio and cycle time. In the future need to extract more fall risk parameters using sensor shoes, and those parameters should be validated against the vicon system.

**CHAPTER 5: Stair fall-risk parameters
comparison between a controlled environment
and uncontrolled environment**

5.1 Abstract

One of the significant health problems for older people is falling on the stairs. Identifying stair fall risk factors are mostly limited to a controlled environment, with a given set of stair dimensions. These identified stair fall risk parameters are useful. However, it remains unknown whether the conclusions drawn would still apply to the testing that takes place in other domestic staircases with different dimensions. The purpose of this study was to investigate whether selected biomechanical stepping behaviour such as foot clearance, percentage of the foot placed on the stairs (foot contact length ratio), and cadence are maintained when the staircase dimensions are different. Twenty-five older adults (>65 years) walked in a custom made seven-step laboratory staircase (rise 19.5 cm, and a going 23.5 cm) and three different LJMU's Exemplar houses. The modern Exemplar houses' staircases contain one winder staircase and two straight staircases. Three important biomechanical factors of stair fall risk were measured using instrumented sensor shoes. Matlab was used to extract fall risk parameters from the collected data. In SPSS, one-way ANOVA was used to compare fall risk parameters for each step in different houses' staircases. In addition, laboratory-based fall risk parameters were compared with house results. The first ANOVA results suggested significant differences in the houses' selected stair fall biomechanical factors. And the second ANOVA results indicated significant differences between laboratory and house for the selected stair fall biomechanical factors. Finally, the third ANOVA results suggested significant differences between the Fallers and non-Fallers groups within the laboratory and houses for the selected stair fall biomechanical factors.

5.2 Introduction

In daily life situations, people encounter a wide range of staircases with various dimensions, and all have a different influence on the risk of falling. Staircase dimensions are essential to avoid stair falls, and the dimensions of the steps in stairs can amplify the risk of falling (Scott 2005). The staircase going is vital in determining the percentage of foot length placed on a stair tread. The staircase risers are also very important. If the risers are huge, older people may fatigue quickly and become vulnerable to the trip. When risers are very small or shallow, older adults may be tempted to take more than one step at a time, which leads to more chances of misstepping. The steepness or pitch of a stair may also influence the likelihood of a fall.

The UK Building regulations permit a private staircase to be made up of individual steps with each rise between 100-220 mm and a going length between 225-350 mm and a maximum incline of 41.5°. Similarly, the public staircase (Scott 2005) to be made up of individual steps with each rise between 100-190 mm and a going length between 250-350 mm and a maximum incline of 38°. These ranges permit a considerable variation in staircase design.

The staircase structure can magnify the demands placed on the individual. For example, steep staircases create larger loading forces at foot contact and cause a more significant redistribution of forces at the joints than less steep staircases. It is also known that the transition steps from the level onto the stairs or from the stairs onto the level are more demanding than the continuous steps in-between (Roys 2001).

More importantly, staircases with inadequate step tread to safely place the foot can restrict movements and threaten safety. Additionally, a stair with a higher riser is more challenging for older adults with higher muscle weakness. It has been found that older adults can safely negotiate stairs with a lower step riser (Bertucco and Cesari 2009) compared to younger adults. It is also evidenced that even for standard step risers, older adults operate closer to their maximum capacities of joint range of motion (Samuel, Rowe et al. 2011), thus increasing their risk for a fall. Risky techniques employed by older people during stair negotiation can also increase the risk of falling. Older people might change their techniques over time because of their functional impairments or fear of falling (Zietz, Johannsen et al. 2011). For example, older adults may have a large foot overhang on landing when stair walking and higher variability in foot clearance (Hamel, Okita et al. 2005), both of which increase the risk for a slip or trip on the stairs.

Identifying stair fall risk factors are mostly limited to a controlled environment, with a given set of stair dimensions. However, it remains unclear whether the conclusions drawn would still apply if the testing occurs in a different domestic staircase with different dimensions. So, this study aims to examine older adults fall risk in a controlled environment(laboratory) as well as real-time houses (LJMU's Exemplar houses). The purpose was to investigate whether selected biomechanical stepping behaviour such as foot clearance, foot contact length ratio and cadence was maintained when the staircase dimensions were different.

5.3 Hypothesis 1

Selected biomechanical stepping behaviour such as foot clearance, foot contact length ratio and cadence was not maintained when the older participants negotiated three LJMU's Exemplar houses' staircase.

5.4 Hypothesis 2

Selected biomechanical stepping behaviour such as foot clearance, foot contact length ratio and cadence was not maintained when the older participants negotiated staircases in the controlled environment(laboratory) and uncontrolled (real-time houses staircase) environment.

5.5 Hypothesis 3

Selected biomechanical stepping behaviour such as foot clearance, foot contact length ratio and cadence was not maintained between the high-risk group and low-risk group when they negotiated staircases within the controlled environment(laboratory) and uncontrolled (real houses staircase) environment.

5.6 Methods

5.6.1. Participants

Twenty-five older adults participated in this study (female:20; male:5; age:70.72±4.0Y; bodymass:70.18±10.0kg; body height:1.62±0.06m; mean and standard deviation). All the participants were recruited from the local community of Wirral and Liverpool, UK. All these participants lived independently, able to climb stairs without help. The study was approved by the Liverpool John Moores University ethics committee in the UK (REF: 18/SPS/024). After the explained procedure, informed written consent was obtained from all participants.

5.6.2. Staircase configuration

The measurements were conducted in the LJMU's Exemplar houses and custom-built seven-step staircase in the laboratory. Liverpool John Moores University (LJMU) has a branch of the BRE (Building Research Establishment) Innovation Park on the LJMU's Campus, opened in September 2016. The Innovation Park consists of three Exemplar

houses (Figure 5.1) that LJMU and BRE use to provide test facilities. These three houses have been constructed using staircase designs from the 1920s, 1970s and 2010s.



Figure 5.1 LJMU's Exemplar House, which contains three houses

The Exemplar houses have three different staircases (Figure 5.1). Space (area) was considered an essential factor in choosing different staircases for each Exemplar's house. 1920's house staircase was a straight staircase, which runs straight from the ground floor landing to the top floor landing with 12 steps and a handrail. The standard staircase going (width) was between 22cm to 30cm, and the standard rise (height) was 15cm to 22cm. The 1920's house staircase used 23cm going and 21cm rise (min going and nearly maximum rise). The 1970's house staircase was like the 1920s, except for the staircase location (the 1970's staircase was set next to the entrance door, and the 1920's staircase was placed in the middle of the house between two rooms). The staircase comprises a single linear flight that does not change direction. (Figure 5.2 for 1920 and 1970's house staircase)

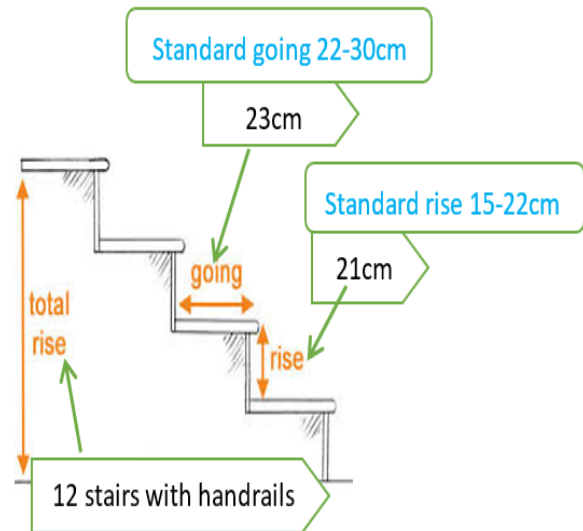


Figure 5.2 1920's and 1970's staircase design

The 2010's exemplar house has a winder staircase, with 11-steps and no handrail. The winder stairs were like L-shaped stairs, but instead of a straight landing, these stairs incorporate a 90-degree turning at the start and the end of the stairs (Figure 5.3). The winder stairs created exciting features with a seamless transition and saved more space without landing. However, these stairs were more challenging to navigate than other stairs. It is also true that negotiating winder stairs require more centre support.

Winder staircase was narrower on one side than the other. A series of winder stairs form a half circular-shaped stairway. Three steps were used to turn a 90degree; the intermediate step was called a kite winder as it looks similar to a kite-shaped quadrilateral. Figure 5.3 shows the 2010s house's staircase.

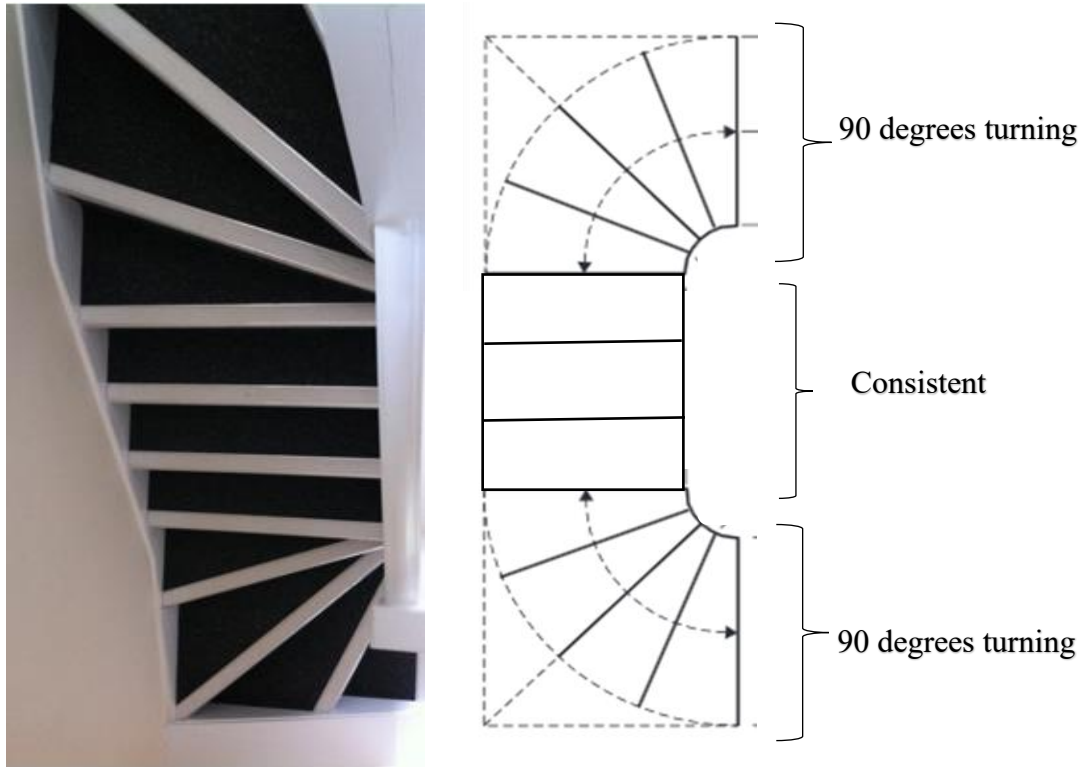


Figure 5.3 2010's staircase design

The measurements were conducted on a custom-made instrumented seven-step staircase with handrails on each side in the laboratory. The stairs had a top and bottom landing of sufficient length to complete an entry and exit phase. Each step had a riser height of 19.5 cm and a going length of 23.5 cm, within the current UK building regulations for commercial and private properties (Regulations 2000). Each of the bottom four steps contained a force-platform (FP; Kistler) sampling at 1080 Hz. During this study, whilst on the staircase, our participants wore a passive overhead safety harness operated by a trained belayer (Figure 5.4).



Figure 5.4 Laboratory custom built instrumented seven-step staircase structure

5.6.3. Procedures

Data collection took place with two sections lasting approximately 2 hours with a short break between the sections. Instrumented sensor shoe was used for data collection; this sensor shoe design and fall risk parameters calculation was explained in chapter 3 and 4. The first section was in the laboratory, and the participants completed the Berg Balance assessments, previous fall history and fear of falling questions. All participants were familiarised with the custom build laboratory staircase before data collection. Participants wore tight-fitting clothes and instrumented sensor shoes based on their shoe size and markers during familiarisation. And then, participants were fitted into the 5-point safety harness connected to an overhead safety rail via rope, controlled by a trained member of the research team who was also secured via rope to the floor. The participants navigated the stairs step-over-step and were permitted to use the handrails if they wished. They could ascend and descend as many times as they wanted until they were comfortable (usually two of each). After familiarisation, participants performed five more trials with the final three trials used for data analysis.

After the break, the second section was at the LJMU's Exemplar houses. All participants were familiarised with all three exemplar houses' staircase before the data collection. Participants wore comfortable clothes with sensor shoes; no markers and cameras were used in the houses. Sensor shoes and a computer were used to collect data in the houses. Sensor shoe's data collection procedure was explained in chapter 3.

All participants performed three ascending and descending trials for each house (3 houses \times 3 ascending \times 3 descending) in a total of eighteen trials. The participants navigated the stairs step-over-step and were permitted to use the handrails if they wished.

5.6.4. Data analysis

The percentage of foot contact length indicates the slip-induced fall risk due to foot positioning relative to the step edge. A reduced percentage of foot contact length is associated with greater fall risk. Foot clearance indicates trip-induced fall risk, where a smaller foot clearance is associated with greater fall risk. So, in this study, these parameters were analysed to measure the fall risk.

For the laboratory data, the foot clearance and percentage foot contact length, the foot's 3D motion were captured using 24 infrared Vicon cameras, covering the whole stairs, landing, and walkway (120 Hz, Vicon, Oxford Metrics, UK). Kinetic data were synchronously recorded from four different force platforms (1080 Hz, 9260AA, Kistler AG, CH), embedded in the stairs' lower four steps (Step1-4, see Figure 5.4). Foot markers were placed on the lateral and medial malleolus (ankle), first and fifth meta-phalange joints (base of big and little toe) and on the posterior calcaneus (heel). Additional markers were placed on the lateral and medial calcaneus, and a rigid cluster of three markers was placed over the toes. A rigid 2D surface model of the shoe sole outline was created by tracing the shoes' outline onto paper. The outline was digitised, and the position of each digitised point was referenced from the centre of the lateral calcaneus origin to the first and fifth meta-phalange markers. These markers were tracked throughout the movement trials. The digitised shoe sole boundary was used for foot clearance to determine the linear distance to the step edge (during the swing). For percentage foot contact length, the linear distance between the furthest forward (ascent) or backward (descent) point of the outline to the step edge was calculated and converted to a percentage of the total length. To calculate foot clearance and percentage of foot contact length, kinematic and kinetic data imported into Matlab (R2017b, The MathWorks, Natick, USA) along with step-edge locations (defined by custom-made clusters of known dimensions), the participant static calibration, and the digitised shoe sole outlines (ImageJ: National Institutes of Health, Bethesda, USA).

The sensor shoe synchronised with the VICON system in the laboratory, so both sensor and VICON data were collected simultaneously. In addition, sensor shoes' foot clearance was calculated from the distance sensor, percentage of foot contact length was calculated from the FSR sensor insole. For detailed information, refer to chapter3(Sensor shoe development).

Descending stairs fast may result in a fall, as an increased speed could negatively modify the foot clearance and foot contact length. Therefore, the average duration of two gait cycles (one of the left limbs and one of the right limbs) was taken as a cadence for stair ascent and stair descent. In addition to foot clearance, foot contact length and cadence, the trial-to-trial variability of these parameters were also calculated as the average of the variability across the three trials for each of the analysed steps. Variability is a risk factor for falls, as more variability can indicate a person's inability to maintain a steady/safe movement pattern (Hausdorff, Zemaný et al. 1999).

5.6.5. Statistics

Older adults were followed up for 6months after testing; based on the occurrence of a fall in the 6months, older adults were classified into fallers and non-fallers. A fall was self-reported and defined as an event that inadvertently resulted in a person coming to rest on the ground or floor or other lower level.

Three ANOVA comparison tests were conducted; the first ANOVA test compared the difference in fall risk parameters between individuals in different houses (independent of fall history). One-way ANOVA and post-hoc tests were conducted, with alpha level 0.05. Post-hoc analyses were Tukey's HSD tests to account for multiple comparisons. Raw data from three trials for each house (18 trials for each participant, 9trials for ascending and 9trials for descending), a total of 25 participants ($18 \times 25 = 450$ total trial data), and each step treated separately, i.e., individual analyses performed for each of the eleven steps to compare between the house.

The second ANOVA test was conducted to compare the difference between laboratory and houses (independent of follow up fall details). There were seven steps in the laboratory; foot clearance was calculated for all seven steps in the laboratory. To compare this seven-step foot clearance with house data, only first, fourth, fifth, sixth, seventh,

eighth, and last steps foot clearance were considered for houses. The foot contact length ratio was calculated for four steps where force plates were placed in the laboratory. Only the first four steps' foot contact lengths were considered to compare this four-step foot contact length with a house.

The third ANOVA test investigated differences in fall risk parameter measures within each condition (laboratory versus exemplar houses' stairs) and between the two fall risk groups (fallers versus non-fallers). A mixed ANOVA (Analysis of Variance) test was conducted for ascent and descent. In the case of significant interactions, posthoc tests were performed where appropriate. Post-hoc analyses were Tukey's HSD tests to account for multiple comparisons. Alpha level was set at 0.05. For this test, the data were averaged for all three trials; only start, end, and middle stairs averaged data were used to compare laboratory and houses.

5.7 Results

5.7.1. Differences between three houses' staircase during stair ascent

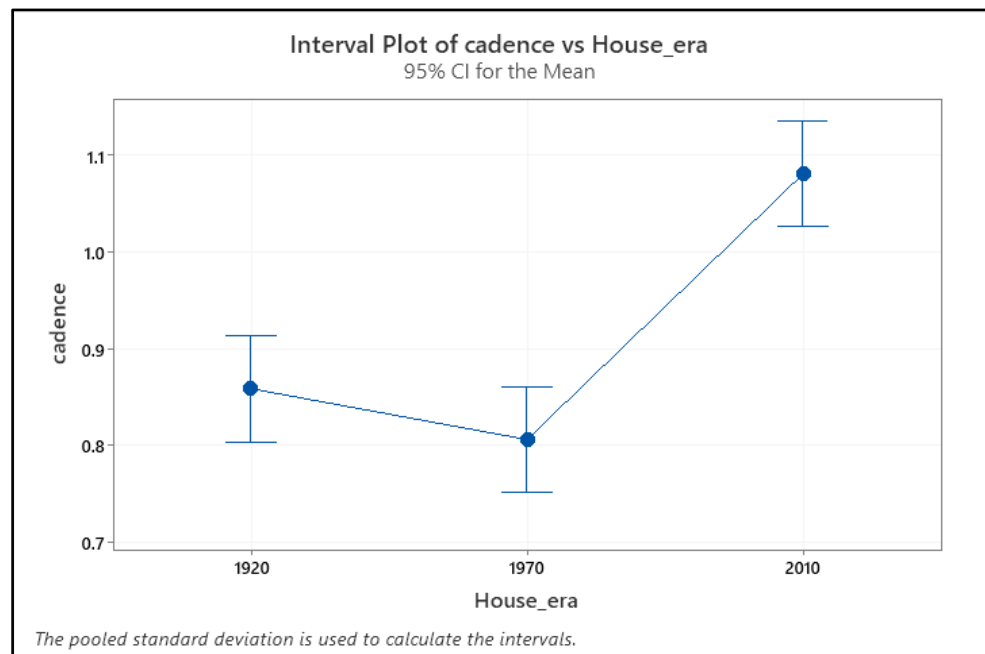


Figure 5.5 Interval plot for difference of mean in Cadence for three houses, it displays that older people were cautious using 2010's staircase and confident in using straight staircase (1920 and 1970's house) so they spent less time to climb stairs.

There was a significant difference (Figure 5.5 and Figure 5.6) in cadence between different house stairs ($F(2,224) = 25.52, p = .00$). Similar cadence was used in the 1920s and 1970s house stairs ($M=0.850s, M=0.800s$). In contrast, older adults took more time to climb 2010s stairs due to winder stairs ($M=1.08s$). These results showed that older adults were more cautious while using difficult (winder) stairs.

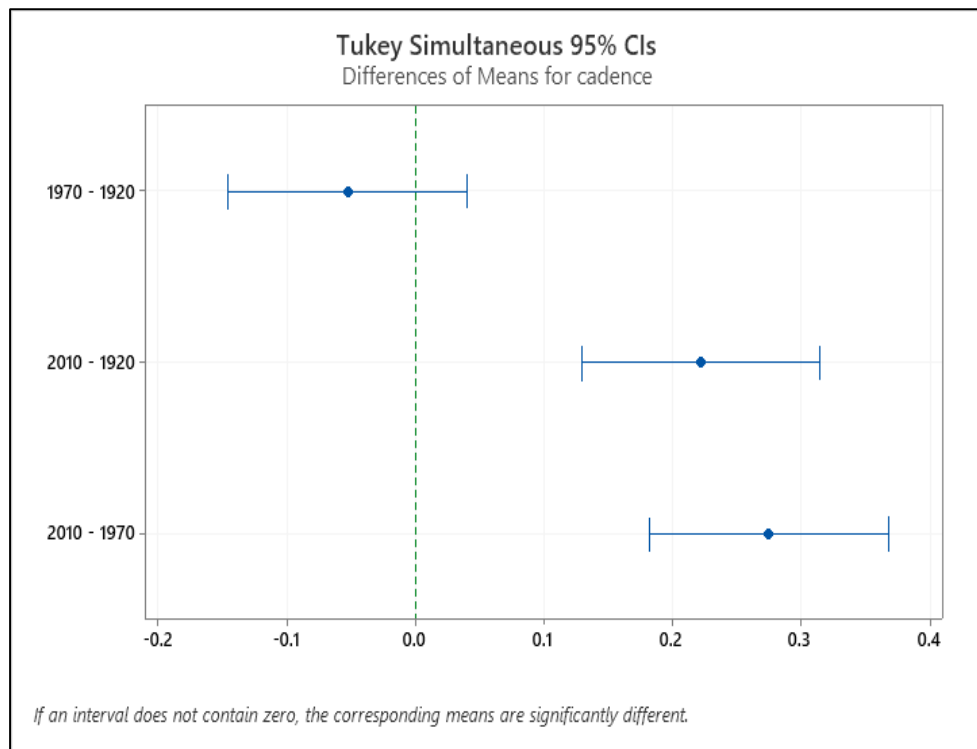


Figure 5.6 Confidence interval (CI) for the three different houses' cadence, the confidence intervals for the (2010-1970, 2010-1920) these house pairs of means range does not include zero, which indicates that the difference is statistically significant.

Older adults' foot clearance increased in the 1970's staircase (Figure 5.7). For example, there was a main effect of different staircase dimension on foot clearance over step7 ($F(2,224) = 3.39, p = .0036$). Post-hoc comparisons (Figure 5.8) revealed that increased foot clearance in the 1970s ($M=30.23mm$) compared to 1920's and 2010's ($M=25.01mm, M=26.12mm$) staircase. These 1920's and 2010's reduced foot clearance might lead to an increase in the chances of falling. There were no changes in foot clearance during the entry and exit steps in different houses' staircases.

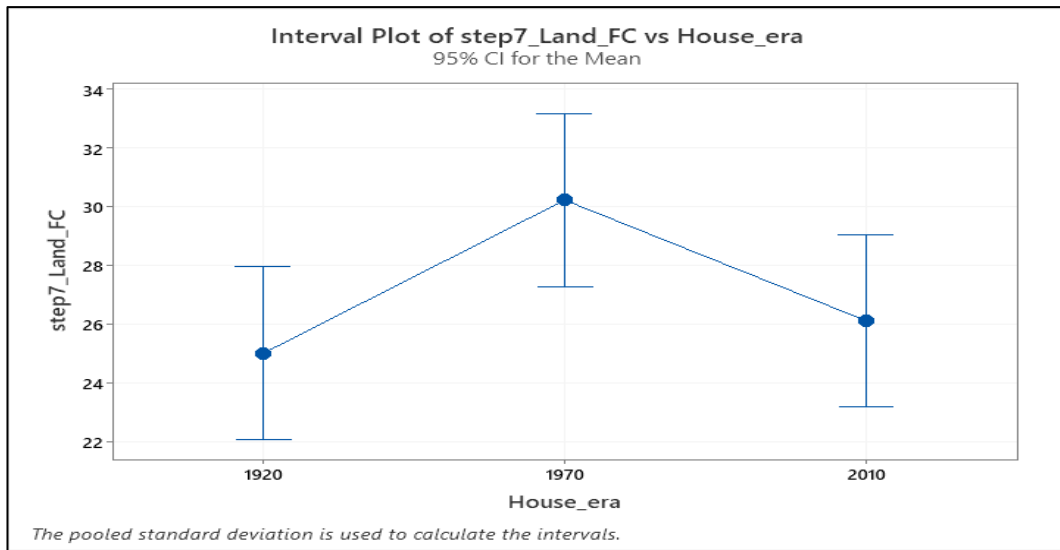


Figure 5.7 Interval plot for the difference of means in step7 foot clearance for three houses, it displays that in step7 older people have more clearance in 1970s house compared to other houses foot clearance

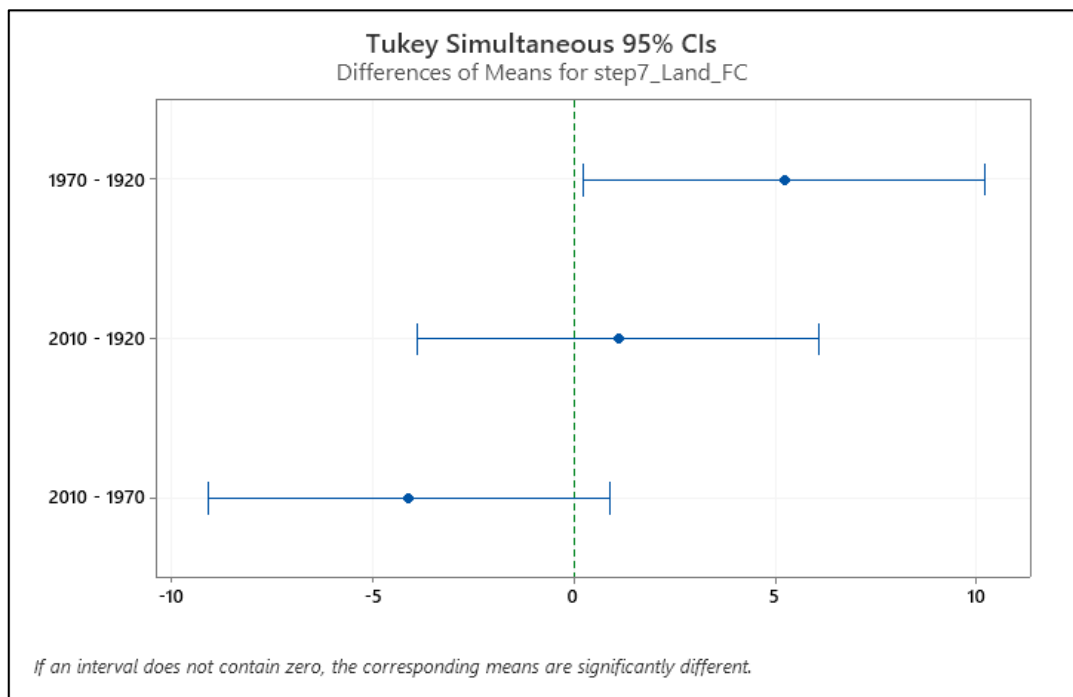


Figure 5.8 Confidence interval (CI) for the three different houses' foot clearance, the confidence intervals for the (1970-1920) house pairs of means range does not include zero, which indicates that the difference is statistically significant.

Below Table 5.1 describes more about individual steps foot clearance in three different houses. Even though there were slight differences in the foot clearance between different houses, these differences were not statistically significant except for step7.

Table 5.1 Foot clearance Mean for all three houses (ascending)

Foot clearance	Step 1	Step 2	Step 3	Step 4	Step 5	Step 6	Step 7	Step 8	Step 9	Step 10	Step 11
1920	26.72	27.94	26.26	27.94	27.68	28.34	25.01	29.37	25.44	30.50	27.89
Mean±	±	±	±	±	±	±	±	±	±	±	±
Standard deviation	13.50	17.52	11.44	13.27	14.47	14.39	11.12	14.56	11.76	12.50	13.89
1970	29.08	26.44	26.84	28.85	27.44	26.72	30.22	27.42	26.37	27.01	27.92
Mean±	±	±	±	±	±	±	±	±	±	±	±
Standard deviation	14.12	13.50	12.25	13.36	12.56	12.56	14.13	12.68	11.58	12.38	13.78
2010	26.84	26.17	28.24	27.76	29.14	26.93	26.12	29.22	28.38	27.89	30.13
Mean±	±	±	±	±	±	±	±	±	±	±	±
Standard deviation	13.47	13.17	14.45	14.45	14.01	11.76	13.31	14.61	12.81	13.16	14.52

Older adults' percentage of foot contact length decreased in the 2010's staircase due to less going on the stair dimension. There was a main effect of different staircase dimension on percentage of foot contact length over step3 ($F(2,222)=83.127, p=0.0000$) and step4 ($F(2,222)=80.8540, p=0.0000$). Post-hoc comparisons revealed that decreased percentage of foot contact length (Figure 5.9 and Figure 5.10) in 2010's staircase at step3 and step4 ($M=59.29\%$ at step3, $M=59.29\%$ at step4) compared to 1920's ($M=74.90\%$ at step3, $M=73.78\%$ at step4) and 1970's ($M=83.36\%$ at step3, $M=79.61\%$ at step4). Due to the winder staircase in 2010's house, older adults' percentage of foot contact length significantly reduced, which may initiate the slip-induced fall. Due to the straight staircase in the 1920s and 1970's house, the percentage of foot contact length were not significantly different, except the step3 and step4. However, the percentage of foot contact length is significantly different for the 2010's staircase and the other two staircases for the remaining steps.

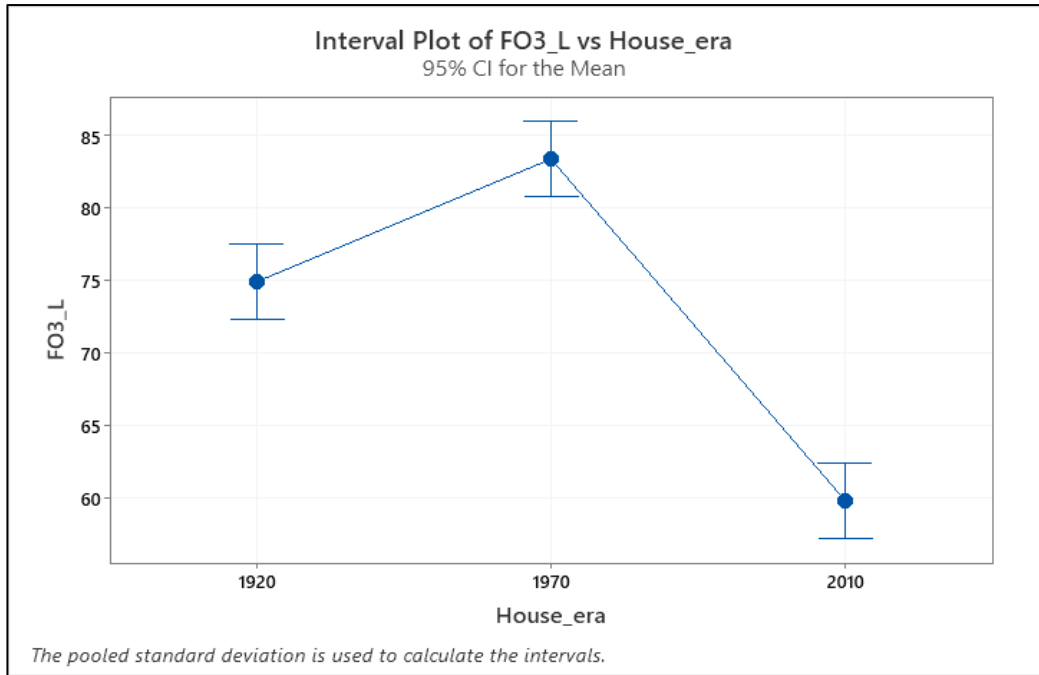


Figure 5.9 Interval plot for the difference of mean in foot contact length ratio for three houses, it displays that in step3 older people have more foot contact length ratio in 1970s and 1920s house compared to other houses foot contact length ratio

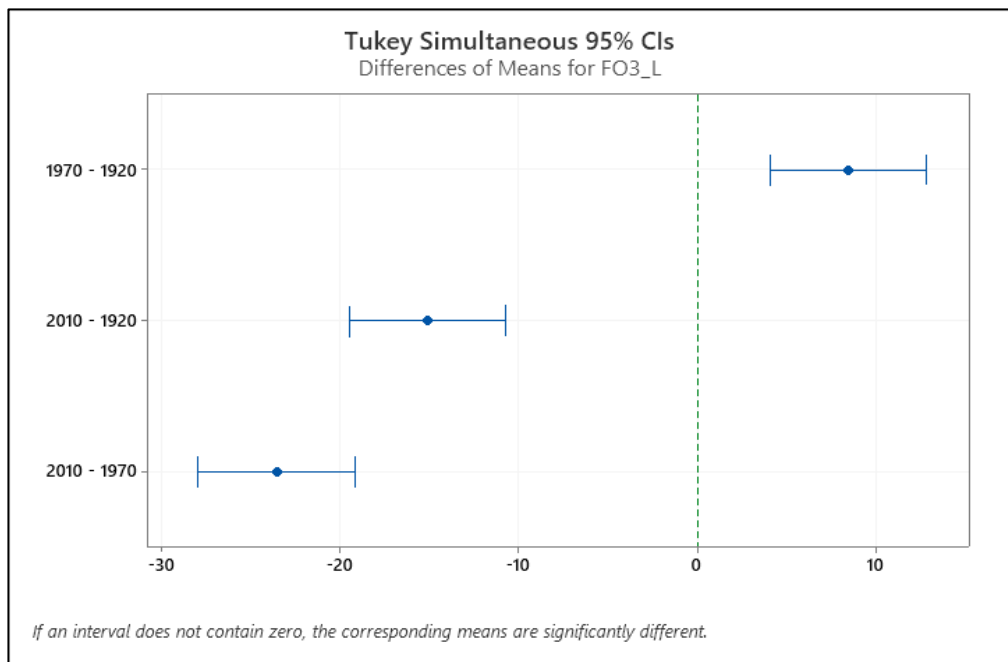


Figure 5.10 Confidence interval (CI) for the three different houses' foot contact length. The confidence intervals for all three house pairs of means range do not include zero, which indicates that the difference is statistically significant for all three houses.

Below Table 5.2 shows the significant percentage of foot contact length among three houses for all steps.

Table 5.2 Post hoc result for foot contact length (FCL) ratio for each step in all three houses (ascending)

Post hoc result for Foot contact length ratio N=75	2010	1970	1920	Sig.	Degree of freedom Df (2,222)	Significant difference
Subset for alpha = 0.05	Mean	Mean	Mean		F	1=2010, 2=1970&192, 3=1920
FCL1	67.0133	78.3467	79.2000	0.000	35.7710	1,2
FCL2	62.0133	75.9867	79.3600	0.000	64.2140	1,2
FCL3	59.8000	74.9067	83.3600	0.000	83.1270	1,2,3
FCL4	59.2933	73.7867	79.6133	0.001	80.8540	1,2,3
FCL5	61.3067	74.4533	75.1600	0.000	32.4600	1,2
FCL6	59.8533	73.3067	74.2400	0.000	51.2870	1,2
FCL7	62.1867	74.5467	74.5467	0.000	26.5450	1,2
FCL8	59.4133	72.9200	73.7067	0.000	52.5330	1,2
FCL9	62.6933	74.3733	76.8933	0.000	31.8210	1,2
FCL10	60.4267	73.0533	74.5600	0.000	46.3970	1,2
FCL11	65.3867	79.7200	82.0933	0.000	61.6030	1,2

5.7.2. Differences between Laboratory and Houses during stairs ascent

The second ANOVA test was conducted to compare the difference between laboratory and houses (independent of follow up fall details). There were seven steps in the laboratory; foot clearance was calculated for all seven steps in the laboratory. Only the first, fourth, fifth, sixth, seventh, eighth, and last steps foot clearance average were considered for houses to compare with laboratory data. For the laboratory, foot contact length was calculated for the first four steps placed on force plates. Only the first four-foot contact lengths from the house were considered to compare with a laboratory (Table 5.3).

Older adults' cadence decreased in the house staircase compared to the laboratory. For example, different environments' main effect on foot cadence $F(1,98) = 8.17, p = .005$. Post-hoc comparisons revealed decreased cadence in the house (Mean=0.910seconds)

compared to the laboratory (Mean=1.07seconds) staircase. However, ascending results showed no significant difference in cadence variability between houses and laboratories.

Older adults' entry steps' foot clearance decreased in the house staircase compared to the laboratory. For example, the main effect was on foot clearance in different environments over step1 $F(1,98) = 5.54, p = 0.021$. Post-hoc comparisons revealed decreased foot clearance in the house (Mean=26.24mm) compared to the laboratory (M=31.24 mm) staircase. There was no significant difference in foot clearance variability between houses and laboratories during the first step in different environments.

Older adults' middle steps' foot clearance increased in house staircase compared to a laboratory. For example, the main effect was on foot clearance in different environments over step2 $F(1,98) = 14.83, p = 0.000$. Post-hoc comparisons revealed increased foot clearance in the house (Mean=27.66 mm) compared to the laboratory (M=20.25mm) staircase. Older adults' middle steps' foot clearance variability increased in house staircase compared to a laboratory. For example, different environments' main effect on foot clearance variability over step2 $F(1,98) = 6.72, p = 0.011$. Post-hoc comparisons revealed increased foot clearance variability in the house (Mean=8.57mm) compared to the laboratory (M=5.2 mm) staircase.

There were no changes in foot clearance during the exit step in different environments. However, older adults' end steps' foot clearance variability increased in house staircase compared to a laboratory. For example, different environments' main effect on foot clearance variability over step7 $F(1,98) = 4.77, p = 0.030$. Post-hoc comparisons revealed increased foot clearance variability in the house (Mean=10.35 mm) compared to the laboratory (M=6.6mm) staircase.

Ascending results showed no significant differences in foot contact length between houses and laboratory's first step, second step and third step. Older adults' fourth steps' foot contact length decreased in the house staircase compared to the laboratory. For example, there was a main effect on different environments foot contact length over step4 $F(1,98) = 5.59, p = 0.020$. Post-hoc comparisons revealed decreased foot contact length in the house (Mean=70.90%) compared to the laboratory (M=77.45) staircase. There were

changes in foot contact length variability during the first, second, third and fourth steps in different environments.

Table 5.3 Difference between Laboratory and House ascend ANOVA results

Variables -Ascent	Alpha <0.05	House (1)	Laboratory (2)
Cadence	Y, F (1,98) =8.17, p=.005	0.910±0.22	1.07±0.25
Cadence variability	N		
FC start	Y, F (1,98) =5.54, p=0.021	26.24±9.46	31.24±8.37
FC middle (2)	Y, F (1,98) =14.83, p=0.000	27.66±9.10	20.25±5.24
FC middle (3)	N		
FC middle (4)	Y, F (1,98) =9.90, p=0.002	27.56±8.93	21.12±8.66
FC middle (5)	Y, F (1,98) =7.18, p=0.009	26.04±6.90	21.51±8.56
FC middle (6)	Y, F (1,98) =18.48, p=0.000	28.40±9.11	19.60±8.07
FC end	N		
FC start var	N		
FC middle_var2	Y, F (1,98) =6.72, p=0.011	8.57±6.11	5.2±2.9
FC middle_var3	N		
FC middle_var4	N		
FC middle_var5	Y, F (1,98) =8.10, p=0.005	9.23±7.4	4.90±2.1
FC middle_var6	Y, F (1,98) =4.30, p=0.041	8.46±6.56	5.6±3.2
FC end var	Y, F (1,98) =4.77, p=0.030	10.35±7.8	6.6±4.8
FCL start	N		
FCL second	N		
FCL third	N		
FCL fourth	Y, F (1,98) =5.59, p=0.020	70.90±11.92	77.45±12.28
FCL start var	Y, F (1,98) =51.15, p=0.000	0.11±0.10	3.80±4.34
FCL second	Y, F (1,98) =58.00, p=0.000	0.15±0.17	3.52±3.86
FCL third	Y, F (1,98) =36.29, p=0.000	0.097±0.08	2.35±3.27
FCL fourth	Y, F (1,98) =51.53, p=0.000	0.09±0.08	3.0±3.6

5.7.3. Difference between fallers and non-fallers during stairs ascent

The third ANOVA test was conducted to compare within the different environments (laboratory and houses) between the fallers group and the non-fallers group. The follow-up-fall variable contains two groups: the fallers and the non-fallers groups. Fallers group is considered a high risk of falling due to the previous fall history. On the other hand, the

Non-fallers group has a low risk of falling due to no previous fall history. These groups were created based on the six months of follow-up-fall information.

The environment contains four different staircases (the 1920s, 1970s, 2010s and laboratory). However, two of the staircase dimensions were the same (the 1920s and 1970s), so only one of the staircases (1920) was selected along with the 2010s house and laboratory. This selection was because the 1920s staircase contained consistent steps (21cm rise, 23cm going), and the 2010s staircase had inconsistent (winder staircase) steps. The Laboratory staircase was constant but different dimensions (rise 19.5cm and going 23.5cm).

The mixed-model ANOVA test was performed to calculate the difference between fallers and non-fallers groups within the different environments (three different staircase dimensions) and the interaction between the fallers and non-fallers group x different environments. The mixed-model ANOVA results showed that the fallers and non-fallers group x different environments interaction was not significant for cadence, foot clearance, foot contact length ratio (FCL) and its variability for ascending. Table 5.4 shows the difference between fallers and non-fallers results in ascending.

Table 5.4 difference between fallers and non-fallers in ascent

Risk-Parameters	Alpha $p < 0.05$	Fallers	Non-Fallers
Entry steps Foot clearance	$F(1,23) = 6.795, p = .016$	24.77 mm	30.45 mm
Middle steps Foot clearance	$F(1,23) = 10.613, p = .003$	22.02 mm	28.09 mm
Exit steps Foot clearance	Not significant	No	No
Entry steps Foot clearance variability	$F(1,23) = 10.613, p = .003$	7.4 mm	9.9 mm
Foot contact length and variability	Not significant	No	No

A mixed-model ANOVA revealed that the main effect of fallers and non-fallers group in cadence and its variability were not significant ($p > .05$). The main effect of fallers and non-fallers group in entry-foot clearance was significant $F(1,23) = 6.795, p = .016$; post hoc results showed that the fallers group had less foot clearance (mean=24.77mm) than the non-fallers group (mean=30.45). The main effect of fallers and non-fallers group in

middle-foot clearance was significant $F(1,23) = 10.613, p=.003$, post hoc results showed that fallers group have less foot clearance (mean=22.02mm) than non-fallers group (mean=28.09mm). Finally, the main effect of the fallers and non-fallers group in exit-foot clearance was not significant.

The main effect of fallers and non-fallers group in entry steps foot clearance variability was significant $F(1,23) = 10.613, p=.003$, post hoc results showed that non-fallers had increased entry foot clearance variability (mean=9.9mm) than fallers (mean=7.4mm). On the other hand, the main effect of fallers and non-fallers group in middle and exit-foot clearance variability was not significant.

The main effect of fallers and non-fallers group foot contact length was insignificant. In addition, the main effect of the fallers and non-fallers group in the entry and middle foot contact length variability was not significant.

Table 5.5 Difference between fallers and non-fallers in different environments during ascent

Variables -Ascent	Alpha <0.05	Laboratory	1920	2010
Cadence	Y, $F(2,23) = 5.67, p=.000$	0.069 s	.806 s	.860 s
Cadence variability	Not significant			
Foot clearances entry steps	Y, $F(2,23) = 4.750, p=0.40$	31 mm	25 mm	26 mm
Foot clearance middle steps	Y, $F(2,23) = 7.663, p=0.011$	20 mm	27 mm	27 mm
Foot clearances exit steps	Not significant			
Foot clearance variability	Not significant			
Foot contact length ratio in entry steps	Y, $F(2,23) = 22.559, p=0.000$	77%	79%	67%
Foot contact length ratio in Middle steps	Y, $F(2,23) = 55.123, p=0.000$	77%	74%	59%
Foot contact length ratio in exit steps	Not significant			
Foot contact length ratio variability in entry steps	Y, $F(2,23) = 11.945, p=0.002$	3.8%	1%	1%
Foot contact length ratio variability in middle steps	Y, $F(2,23) = 17.603, p=0.000$	2.3%	1%	1%
Foot contact length ratio variability in exit steps	Not significant			

Table 5.5 shows the results of the difference between fallers and non-fallers in different environments during ascent. The main effect of cadence in different environments was significant $F(2,23) = 5.67, p = .000$, so the mean cadence for the laboratory was significantly higher (1.069) than houses (1920=.806seconds, 2010=.860seconds). There was no significant difference in cadence variability in different environments.

The main effect of different environments in entry steps foot clearance was significant $F(2,23) = 4.750, p = 0.040$, post hoc results showed that older adults had less entry foot clearance in the houses (the 1920s = 25mm, 2010s = 26mm) than the laboratory (mean=31mm). The main effect of different environments (location) in middle-foot clearance was significant $F(2,23) = 7.663, p = 0.011$, post hoc results showed that older adults had less entry foot clearance in the laboratory (mean=20mm) than the houses (mean 1920s=27mm and 2010=27mm). And there was no significant difference between the environments for exit-foot clearance. And there was no significant difference between the environments for entry, middle and exit-foot clearance variability.

The main effect of different environments in entry steps foot contact length (FCL) was significant $F(2,23) = 22.559, p = 0.000$, so the entry mean foot contact length for houses particularly 2010s was significantly lower (67%) than the 1920s (mean=79%) house and laboratory (mean=77%). Similarly, the main effect of different environments in intermediate steps foot contact length (FCL) was significant $F(2,23) = 55.123, p = 0.000$, particularly in the 2010s, was significantly lower (59%) than in the 1920s (mean=74%) house and laboratory (mean=77%).

The main effect of different environments in entry foot contact length (FCL) variability was significant $F(2,23) = 11.945, p = 0.002$, so the entry mean foot contact length variability for laboratory (mean=3.8%) was higher than the houses (mean=1%). Similarly, the main effect of different environments (location) in middle foot contact length (FCL) variability was significant $F(2,23) = 17.603, p = 0.000$, so the entry mean foot contact length variability for laboratory (mean=2.3%) was higher than the houses (mean=1%).

5.7.4. Differences between three houses during stair descent

The first ANOVA test for descending results showed a significant cadence difference between house stairs ($F(2,224) = 8.249, p = .00$). Similar cadence was used in the 1920 and 2010's house stairs ($M=1.0s, M=1.03s$); in contrast, older adults took more time to climb 1970's stairs ($M=1.2$). These results showed that older adults were not more cautious while using difficult (winder) stairs; going fast will lead to stair fall.

Older adults' foot clearance increased in the 1970's staircase. For example, there was a main effect of different staircase dimension on foot clearance over step10 ($F(2,224) = 3.413, p = .035$). Post-hoc comparisons revealed increased foot clearance in the 1970s ($M=34.02mm$) compared to the 1920's and 2010s ($M=32.01mm, M=29.12mm$) staircase. These 1920's and 2010's reduced foot clearance might lead to an increase in the chances of falling. There were no changes in foot clearance during the entry and exit steps in different houses' staircases.

Older adults' percentage of foot contact length (foot overhang) decreased in 2010's staircase. There was a main effect of different staircase dimension on percentage of foot contact length from step2 ($F(2,222) = 171.447, p=0.0000$) to step11 ($F(2,222) = 390.811, p=0.0000$). Post-hoc comparisons revealed that decreased percentage of foot contact length in 2010's house step2 to step11 ($M=65.82%$ at step2, $M=69.54%$ at step11) compared to 1970's ($M=84.52%$ at step2, $M=89.05%$ at step11) and 1920's ($M=84.52%$ at step2, $M=84.80%$ at step11). Due to the winder staircase in 2010's house, older adults' percentage of foot contact length significantly reduced, which may initiate the slip-induced fall. Due to the straight staircase in the 1920s and 1970's house, the percentage of foot contact length were not significantly different. Below Table 5.6 shows the significant percentage of foot contact length among three houses for all steps.

Table 5.6 Post hoc result for foot contact length ratio for each step in all three houses (descending)

Post Hoc result for Foot contact length ratio in descending	2010	1970	1920	Sig.	Df (2,222)
N=75	Mean	Mean	Mean	alpha = 0.05	F
Foot Contact length step1	70.3733	84.5200	84.2533	0.0000	334.156
Foot Contact length step2	65.8267	84.5200	81.4267	0.0000	171.447
Foot Contact length step3	69.9200	89.3467	76.5067	0.0000	247.767
Foot Contact length step4	65.6000	86.1200	81.2267	0.0010	174.200
Foot Contact length step5	68.9733	89.6000	84.4633	0.0000	464.929
Foot Contact length step6	64.9067	84.4533	82.0000	0.0000	177.450
Foot Contact length step7	69.0533	89.1467	84.7600	0.0000	436.971
Foot Contact length step8	65.1233	86.3467	81.7733	0.0000	188.358
Foot Contact length step9	68.9333	89.0400	84.7867	0.0000	450.253
Foot Contact length step10	65.5733	85.8133	81.4667	0.0000	178.279
Foot Contact length step11	69.5467	89.0533	84.8000	0.0000	390.811

5.7.5. Differences between laboratory and houses during stairs descent

The second ANOVA test was conducted to compare the difference between laboratory and houses (independent of follow up fall details). Descending results (Table 5.7) showed no significant differences in cadence and cadence variability between houses and laboratories.

Older adults' entry steps' foot clearance increased in the house staircase compared to the laboratory. For example, the main effect was on foot clearance in different environments over step1 $F(1,98) = 22.08, p = 0.0000$. Post-hoc comparisons revealed increased foot clearance in the house (Mean=28.13 mm) compared to the laboratory (M=19.30mm) staircase. Older adults' entry steps' foot clearance variability increased in the house staircase compared to the laboratory. For example, different environments' main effect on foot clearance variability over step1 $F(1,98) = 15.33, p = 0.0000$. Post-hoc comparisons revealed increased foot clearance variability in the house (Mean=7.6 mm) compared to the laboratory (M=3.6 mm) staircase.

Older adults' middle steps' foot clearance increased in the house staircase compared to the laboratory. For example, the main effect was on foot clearance in different environments over step2 $F(1,98) = 14.22, p = 0.0000$. Post-hoc comparisons revealed

increased foot clearance in the house (Mean=30.70mm) compared to the laboratory (M=24.35mm) staircase. Older adults' middle steps' foot clearance variability increased in the house staircase compared to the laboratory. For example, different environments' main effect on foot clearance variability over step2 $F(1,98) = 8.17, p = 0.005$. Post-hoc comparisons revealed increased foot clearance variability in the house (Mean=10.82 mm) compared to the laboratory (M=7.3 mm) staircase.

Older adults' end steps' foot clearance increased in the house staircase compared to the laboratory. For example, the main effect was on foot clearance in different environments over step7 $F(1,98) = 6.28, p = 0.014$. Post-hoc comparisons revealed increased foot clearance in the house (Mean=31.71mm) compared to the laboratory (M=27.48mm) staircase. There was no change in foot clearance variability during the exit step in different environments.

Table 5.7 Difference between Laboratory and House descend ANOVA results

Variables Descend	Alpha <0.05	House	Lab
Cadence	N		
Cadence variability	N		
FC start	Y, $F(1,98) = 22.08, p = 0.0000$	28.13±9.24	19.30±2.58
FC middle (2)	Y, $F(1,98) = 14.22, p = 0.0000$	30.70±7.62	24.35±6.21
FC middle (3)	N		
FC middle (4)	Y, $F(1,98) = 9.93, p = 0.002$	34.42±8.51	28.33±7.89
FC middle (5)	Y, $F(1,98) = 5.87, p = 0.017$	31.32±6.94	27.55±6.12
FC middle (6)	N		
FC end	Y, $F(1,98) = 6.28, p = 0.014$	31.71±7.9	27.48±5.05
FC start var	Y, $F(1,98) = 15.33, p = 0.000$	7.6±4.7	3.6±3.05
FC middle_var2	Y, $F(1,98) = 8.17, p = 0.005$	10.82±5.3	7.3±5.14
FC middle_var3	Y, $F(1,98) = 7.52, p = 0.007$	11.21±5.6	7.76±4.8
FC middle_var4	Y, $F(1,98) = 6.14, p = 0.015$	11.91±5.5	8.8±4.9
FC middle_var5	Y, $F(1,98) = 4, p = 0.048$	12.32±6.0	9.54±5.91
FC middle_var6	N		
FC end var	N		
FCL start	N		
FCL middle2	Y, $F(1,98) = 11.28, p = 0.001$	89.36±3.52	85.71±7.25

FCL middle3	N		
FCL end	Y, F (1,98) =14.03, p=0.000	89.42±3.86	85.20±7.15
FCL start var	N		
FCL middle_var2	N		
FCL middle_var3	N		
FCL end var	N		

Descending results showed no significant differences in foot contact length and its variability between houses and the laboratory's first step. Older adults' middle steps' foot contact length increased in the house staircase compared to the laboratory. For example, different environments' main effect on foot contact length over step2 $F(1,98) = 11.28$, $p = 0.001$. Post-hoc comparisons revealed increased foot contact length in the house (Mean=89.36%) compared to the laboratory (M=85.71%) staircase. There was no change in foot contact length variability during the second step in different environments. Also, there were no changes in foot contact length and its variability during the third step in different environments.

Older adults' fourth steps' foot contact length increased in the house staircase compared to the laboratory. For example, different environments' main effect on foot contact length over step4 $F(1,98) = 14.03$, $p = 0.000$. Post-hoc comparisons revealed increased foot contact length in the house (Mean=89.42%) compared to the laboratory (M=85.20%) staircase. There were no changes in foot contact length variability during the fourth step in different environments.

5.7.6. Differences between fallers and non-fallers during stair descent

The third ANOVA test was conducted to compare within the laboratory and houses between fallers and non-fallers group in descending. The mixed-model ANOVA test was performed to calculate the difference between fallers and non-fallers groups within the different environments and the interaction between the fall risk groups x different environments in descending.

The mixed-model ANOVA results showed that the fallers and non-fallers group x different environments interaction was not significant for cadence, foot clearance, foot contact length (FCL) and its variability for descending.

Table 5.8 Difference between fallers and non-fallers in descending

Risk-Parameters for Stair Descent	Alpha $p < 0.05$	Fallers	Non-Fallers
Cadence and its variability	Not significant	No	No
Foot clearance and its variability	Not significant	No	No
Foot contact length and variability	Not significant	No	No

The mixed-mode ANOVA test revealed that the main effect of cadence and its variability in the fallers and non-fallers group was insignificant. The main effect of fallers and non-fallers group in entry, middle, exit foot clearance and its variability were not significant. The main effect of the fallers and non-fallers group in the foot contact length and its variability were not significant. Table 5.8 shows the results of the difference between fallers and non-fallers in descending.

Table 5.9 Difference between fallers and non-fallers in different environments in descending

Variables -Descent	Alpha < 0.05	Laboratory	1920	2010
Cadence	Y, F (2,23) =6.788, $p = .016$	0.941 s	.941 s	1.035 s
Cadence variability	Not significant			
Foot clearances entry steps	F (2,23) =15.098, $p = .001$	18 mm	28 mm	27 mm
Foot clearance middle steps	Not significant			
Foot clearances exit steps	Not significant			
Foot clearance variability in entry steps	F (2,23) =8.094, $p = .009$	3 mm	7 mm	7 mm
Foot clearance variability in middle steps	F (2,23) =8.638, $p = .007$	9 mm	14 mm	14 mm
Foot contact length ratio and its variability	Not significant			
Foot contact length ratio in exit steps	Not significant			

Table 5.9 shows the results of the difference between fallers and non-fallers in different environments in descending. The main effect of cadence in different environments was significant $F(2,23) = 6.788, p = .016$, so the mean cadence for 2010s house was significantly higher (1.03seconds) than the mean cadence time for 1920s houses (mean=.941seconds) and laboratory (mean=0.941seconds). There was no significant difference in cadence variability in different environments.

The main effect of entry-foot clearance in different environments was significant $F(2,23) = 15.098, p = .001$; post hoc results showed that older adults had less entry foot clearance in the laboratory (mean=18mm) than the houses (1920=28mm, 2010=27mm). The main effect of environments in entry foot clearance variability was significant $F(2,23) = 8.094, p = .009$, post hoc results showed that older adults had increased variability in the houses (7mm) than the laboratory (mean=3mm).

There was no significant difference between the environments for middle-foot clearance. The main effect of environments in middle foot clearance variability was significant $F(2,23) = 8.638, p = .007$, post hoc results showed that older adults had increased intermediate steps foot clearance variability in the houses (14mm) than the laboratory (mean=9mm). There was no significant difference between the environments for exit-foot clearance and its variability.

The main effect of different environments (location) in foot contact length (FCL) and its variability were insignificant.

5.8 Discussion

The safety of stair negotiation depends on the interactions between the behaviour of humans and their staircase environment. All older adults used the step-over-step method to negotiate the different staircases during the data collection in the houses and laboratory. This step-over-step method requires alternation between limbs by which each limb should contribute to single-limb support. This method is most demanding even though it is the fastest and most efficient (King, Underdown et al. 2018)

5.8.1. First Hypothesis

The first ANOVA test compared the houses' cadence, foot clearance, and foot contact length ratio. One-way ANOVA test results support the first hypothesis: significant differences in foot clearance, foot contact length ratio, and cadence between different houses.

Older adults were tested in three houses' staircases; two staircases were straight, and the exact dimensions were used. The third staircase dimension and structure differed from the other two houses' staircases. The reason for the testing at three houses and data comparison was that people encounter a wide variety of staircases in real life to discover how older adults negotiate different staircase dimensions and similar staircase dimensions. This study helps to find which staircase is dangerous for older people. Also, when older adults encounter different staircase dimensions, they might need to change their walking trajectory to cope with that particular staircase; they are at risk if they do not change. In similar staircase (the 1920s and 1970s) contains similar dimensions; will older adults negotiate a similar staircase in the same manner (consistent walking trajectory)? If so, they have more balance control and are safe on the stairs; if older adults use a different manner (inconsistent walking trajectory), the risk for fall in the future. The results showed that older adults' feet followed a similar trajectory for entry, exit and except a few steps in the middle stairs. For example, in both ascending and descending, in similar staircases (the 1920s and 1970s), older adults showed no significant statistical difference in foot contact length ratio (FCL), so their feet followed a similar trajectory for both similar staircases. Also, for similar staircases, older adults used similar cadence for ascending and different cadence for descending. There was no significant difference for entry and exit foot clearance in a similar staircase for both ascent and descent. However, in ascending, there was a significant difference over step7 foot clearance in a similar staircase and in descending, there was a significant difference over step10.

In ascending, older adults spent less time climbing consistent (the 1920s and 1970s) straight stairs. This research (Templer 1995) found that straight flights of stairs without landings accounted for 52% of all accidents. This straight might be the case because the path of straight flights is often clear and uninterrupted, so stair users are reassured into a false sense of security and reduced attention. Straight flights may also result in more

severe injuries because there is no place where the fall may be broken on the stairway. In ascending, older adults spent more time climbing uneven stairs (the 2010s); in contrast, in descending, older adults spent less time negotiating uneven stairs. Older adults negotiated stairs considerably faster, which is considered riskier.

The foot contact length ratio was less (mean= 67%) for inconsistent (the 2010s) stairs for both ascending and descending. It shows that the risk of overstepping increases on narrower stairs (the 2010s) due to lack of space to place the foot safely (Roys and Wright 2005). The foot contact length ratio is more crucial for descending than ascending for safe stair negotiation (Roys, 2013). For example, older adults who usually have less foot contact length ratio might experience a fall (Roys and Wright 2005). If less than 70% of the foot contact length regularly, there is an increased risk of a slip over the step-edge (Roys 2013), but the British Standards Institution (BSI) indicate that less than 50% of foot contact length ratio would most likely lead to a fall (BSI 2010).

For both ascending and descending, older adults foot clearances over the intermediate steps were reduced for the 2010s staircase, increasing the risk of toe-catching due to less foot clearance, the chances of tripping increase (Hamel, Okita et al. 2005).

5.8.2. Second Hypothesis

The second ANOVA test was conducted for stair fall risk factors such as cadence, foot clearance and foot contact length ratio to compare the difference between laboratory and houses. Again, one-way ANOVA test results support the second hypothesis: significant differences in foot clearance, foot contact length ratio, and cadence between houses (uncontrolled environment) and laboratory (controlled environment).

In ascending, older adults walked slowly in the lab than the house. The measurements of this study were conducted on an experimental staircase using a safety harness in a laboratory environment, which differs from house staircases, and this might have had psychological effects on the stair performance of the older adults' cadence. The home staircase did not use a safety harness.

Older adults showed a safe strategy for ascending in the lab; for example, older adults had increased foot clearance in the start and middle steps and also showed less foot

clearance variability. In addition, older adults foot contact length increased in the laboratory's exit steps. However, older adults foot contact length variability was higher for the laboratory than houses.

In contrast, older adults showed a risky strategy while descending laboratory stairs; for example, starting, middle and end foot clearance reduced in the lab than in the houses. In addition, the intermediate step's foot contact length was less in the lab. Older adults used only one safe technique; it was less variability in the foot clearance in the laboratory's entry and intermediate steps.

Older adults showed a risky strategy for ascending in the houses; for example, older adults had decreased foot clearance in the start and middle steps and also showed more foot clearance variability. In addition, older adults foot contact length decreased in the houses' exit steps. However, older adults foot contact length variability was less for houses.

In contrast, older adults showed a safe strategy while descending houses' stairs; for example, starting, middle and end foot clearance increased. Also, the intermediate step's foot contact length increased in the houses. However, older adults showed more variability in the foot clearance in the houses' entry and intermediate steps.

5.8.3. Third Hypothesis

The third ANOVA test compared differences in the stair fall risk factors within laboratory and houses (different environments) between the fallers and non-fallers groups. The 2(fall/non-fall) x 3(environment) mixed-model ANOVA test revealed three different results. The first results were significant differences in cadence, foot clearance, foot contact length and their variability due to the main effect of fallers and non-fallers groups. The second results were substantial differences in cadence, foot clearance, foot contact length and their variability due to the main impact of different environments (laboratory and two different houses staircase). Finally, the third results were significant differences in cadence, foot clearance, foot contact length and their variability due to the main effect of risk group x different environments interaction. In summary, there was a significant change only due to the risk group and different environments. There was no significant difference between the fallers and non-fallers group x different environments interaction, so only part of Hypothesis 3 was accepted.

The mixed-model ANOVA results showed that the risk group x different environments interaction was not significant for cadence, foot clearance, foot contact length (FCL) and its variability for descending. Differences in behaviour observed between the fallers and non-fallers group, the effect of the different environments were similar for the fallers and non-fallers group older adults (risk group x different environment interactions were not detected). Therefore, it is expected that both groups would be at an increased fall risk by the same mechanisms on different environments' staircases. However, the consequences will likely be more severe for the fallers group (Foster, Maganaris et al. 2019) as they do not have the adequate strength reserves to recover when they lose balance (Reeves, Spanjaard et al. 2008).

The significant differences due to the main effect of fallers and non-fallers group were obtained. For example, in ascending high risk, older adults had less foot clearance at the entry and middle steps; they had more foot clearance variability in the entry steps. This result suggests that the fallers group in this present study did not adopt more conservative stepping strategies during stair ascent compared to low-risk older adults. Showing less foot clearance and more variability in foot clearance would increase the risk for a trip (Roys 2001).

The significant differences due to the different environments are as below: cadence results showed that older adults ascended the laboratory staircase slowly than the houses staircases; this is because the safety harness was used in the laboratory, which might affect older adults' cadence. Also, results showed that older adults descended the 2010s(winder) staircase slowly (more time) and spent less time negotiating consistent staircases such as 1920s and the laboratory. Even though the winder staircase was narrow steeper, older adults took more care when walking on the winder staircase (uneven staircase), and this showed that older people were more cautious in the winder staircase.

In ascending, older adults had less entry foot clearance in the house staircases such as the 2010s and 1920s. Also, during descending older adults showed more variability in the foot clearance for entry steps and less entry foot clearance in the laboratory. The reason for this less foot clearance and its variability in the entry steps were already demonstrated that a disproportionate amount of stairway accidents occurs on the top or bottom stairs (Templer, Archea et al. 1985). At these locations, the older adult might be

looking around for the next part of the journey or the route to be taken, so their attention might not be entirely focussed on the stairway (Templer 1995).

In ascending, older adults showed that foot contact length ratio reduced for the 2010s(winder) staircase, and foot contact length variability increased in the laboratory. This reduced foot contact length ratio increases the risk of slipping. The reason for this, older adults get their best support when they place most of their foot on the tread, but this is not always possible because the going of the winder staircase was less (below 250mm) than the older adults foot length. To safely negotiate this small going, older adults need to turn their feet to the side of each step.

5.8.4. Other fall risk parameters

The Berg Balance Scale (BBS) (Berg et al., 1989) (Appendix E) was used to measure older people's balance. The Berg balance scale contains fourteen assessment tasks such as standing with eyes closed, turning around, and standing on one leg. This Berg balance scale task assessment is subjective and qualitative, typically using threshold assessment scores to categorise people as low fall risk, moderate fall risk and high fall risk. Possible scores are 0 to 56, and the maximum score of 41 to 56 signifies no balance impairment (low risk), 0-20 score implies a high risk of fall and, from 21 to 40 indicates a medium risk of fall. The BBS is highly sensitive and specific to identify older adults at higher risk of falling (Shumway-Cook, Baldwin et al. 1997). In this study, there were 25 participants assessed based on the Berg balance scale; only one participant had high fall risk, 6 participants had moderate fall risk, and 18 participants had low fall risk. In descending, Berg balance-high risk older adults had increased cadence (Mean=1.37s) compared to low and moderate risk older adults (Mean=.810s for low risk and mean=.900s for medium risk).

After data collection, participants were followed up for six months to measure fall occurrences via email and phone calls by the researcher. Older adults were classified into two groups (fallers and non-fallers) based on the fall event. Among 25 participants, 13 people had at least one fall or trip or slip in the last six months, so they were assigned into the Fallers group; 12 people did not experience any fall in the last six months, so they

were in a non-Fallers group. These risk groups were used in chapter 6 to create a machine-learning algorithm to predict future fall risk on stairs.

Fear of falling and previous fall history was assessed by oral interview. The risk of a fall was higher in older adults who experienced a previous fall. Among 25 participants, eight people had a fear of falling, and 17 people did not have a fear of falling. Among these 8 (fear of falling) older adults, five of them already had a fall in the six months follow-up time.

The risk of a fall is higher in older adults who experienced a previous fall (Hamel, Okita et al. 2005). The older adults who had a previous fall showed high variability in foot clearance compared to the older adults who had not had any previous fall (in ascending, previous faller: Standard Deviation (SD)=8mm vs previous non-faller older adults: SD=5mm foot clearance variability). In addition to foot clearance variability, older adults who had experienced a previous fall showed more percentage of foot contact length variability compared to older adults who had not had any previous fall (in ascending, previous faller: SD=3.10% vs the previous non-faller: SD=1.10% foot contact length variability).

Fear of falling was known as a risk factor for a trip on stairs. Older adults who had a fear of falling showed increased cadence variability than older adults who did not have a fear of falling. Cadence variability implies the older adult's stability. This reduced stability may lead to future falls.

5.9 Conclusion

There was a significant difference in selected stair fall biomechanical factors among the houses and laboratory. Even though the 1920s and 1970s staircases have similar dimensions, older adults negotiated middle steps differently, and there were no changes in stair negotiation for the entry and exit steps. Although it has been generally considered that winders stairs are more dangerous than standard stair designs because of the non-uniform tread width or the wedge shape of the winder tread, recent studies concerning stair accidents reveal that this is not true (Wells 1977). Older adults used increased cadence and more foot clearance than other houses to support this. In contrast, the percentage of foot contact length decreased compared to other houses. This is because the

walking portion of the tread is less than the other two houses. Older adults showed a safe strategy for ascending in the laboratory, descending in the houses.

In contrast, older adults showed a riskier strategy for descending in the laboratory, ascending in the houses. The risk group comparisons suggest that high-risk fallers implemented a biomechanically risky strategy that could increase overall falling risk. However, only selected stair fall risk parameters were compared in this study. In the future, more stair fall parameter comparisons would be helpful to predict stair fall risk by finding people who are all at the risk of falling; by giving intervention, the future fall will be controlled.

CHAPTER 6: Identify Fall Risk using Novel sensor and Machine learning algorithm

6.1 Abstract

Stair falls continue to be a prominent cause of unintentional injury in older people. It can result in a significant loss of mobility and independence, which significantly affects the quality of life, and in some cases, it can be fatal. The causes of stair fall risk identification were limited to the controlled environment (laboratory). Laboratory-based measurements help identify the factors of older people's stair fall risk. Some of the stair fall risk parameters were foot clearance, variability in foot clearance, foot contact length ratio, variability in foot contact length ratio, cycle time, stance time, and swing time. However, no systems can directly calculate all those stairs fall risk parameters in an uncontrolled environment (houses). So, this work aimed to design a sensor shoe system to calculate all those parameters directly and test in the actual houses' staircase. Twenty-five older adults were tested using the sensor shoe system in LJMU's exemplar houses staircase. The Berg Balance scale was measured to evaluate older adults' balance and lower limb strength. Also, previous fall risk information was collected. After the data collection, participants were followed up for six months to measure the occurrence of falls.

Based on the fall occurrence, older adults are divided into fallers and non-fallers. After collecting the follow-up information about falls, a stair fall risk classification system was developed using a machine learning algorithm. The stair fall risk classification system helps identify fall risk factors to estimate the probability of a real-time fall occurrence (Hemmatpour, Ferrero et al. 2019). Three classifier algorithms were trained to classify fallers and non-fallers class with high precision, specificity, and f-measure. F-measure for Support vector machine (SVM) was 90%, the ensemble was 89% and, k-Nearest Neighbors (k-NN) was 84% using feature set selected by chi-square feature selection method. The trained algorithm can be used in the future for new data set to predict fall risk for older people with high precision.

6.2 Introduction

Currently, 11.6 million individuals are aged 65 or over in the UK (Mid 2015). More than one-third of those individuals experience at least one fall each year, and 10-15% of these falls occur on stairs (van Schooten, Pijnappels et al. 2015). Falls are the second leading cause of accidental or unintentional injury deaths worldwide. These falls lead to significant loss of mobility and independence for older people, significantly affecting

their quality of life (Alexander, Rivara et al. 1992). Furthermore, these stair falls often result in early death or secondary complications during hospitalization, usually the following surgery to repair a fracture. Moreover, injuries cause an expensive bill to National Health Services: the UK's annual cost of fall injuries is more than £2.3 billion per year (Age-UK, 2010).

In laboratory settings, various stairs fall risk-related studies used photo-electronic systems and force plates; using this laboratory setting, a lot of research has demonstrated older people's fall risk factors and causes. Trip and slip were the two main underlying mechanisms for stair fall. A trip's risk has been linked to reduced foot clearance (Kesler, Horn et al. 2016). The risk of trip increases when the variability of foot clearances increases (Roys 2001). The risk for a slip increases when the percentage of the foot contact length is reduced (Roys and Wright 2005). Also, the foot contact length ratio variability indicates older adults' inability to place the foot safely on the step continually. The other crucial personal stair fall factors are fear of falling (Jacobs 2016) and low muscle strength (Reeves, Spanjaard et al. 2008). In addition to individual factors, the other important factor related to stair fall is the environmental factor. Environmental factors contain stair geometry linked with stair falls (Reeves, Spanjaard et al. 2008). Stair geometry, for example, each staircase step dimensions varies, staircases are more difficult to negotiate when the steps height (rise) increased or steps run (going) reduced (Roys and Wright 2005). However, stair fall risk factors identification was limited to the controlled environment (laboratory).

Measurements in a controlled and standardised environment like a laboratory are the first necessary step, but on their own, they are unlikely to lead to a translational outcome. Furthermore, this type of stair fall risk measurement may not represent real-life-based measurements in natural settings such as homes or public places (Wahab, Bakar et al. 2014). Despite the prevalence and devastating consequences of stair falls for older people, systems that can be used in a home environment for timely identification of people at a high risk of a fall are currently lacking.

So, there is a need for a real-time testing system to predict stair fall risk parameters at home environment stairs. Over the past decade, there has been a great deal of research on

developing methods to detect falls based on wearable sensors (Li, Ho et al. 2012, Wang, Wu et al. 2016) and distance sensors (Selvaraj, Baltzopoulos et al. 2018).

IMU sensor was used to calculate foot clearance in level walking. MIT Media Laboratory has developed an electric field sensing technique and proved this technique is used to calculate foot clearance on level walking (Wahab 2009). The downside of this system is that it can only measure up to 5cm (Wahab 2009). An ultrasonic sensor has been used to calculate foot clearance (Hamel and Cavanagh 2004); the problem with this system is that this sensor is too big to fit in the shoe, which might affect participants' walking. The shoe-integrated direct foot clearance measurement system is the most unexplored topic in stair gait analysis.

There is no sensor shoe available to calculate foot overhanging on the stairs; some force sensors-based insoles exist, which are used to calculate foot distribution while level walking. The main commercially available in-shoe measurement systems are F-Scan and Pedar systems, but they are very expensive application-oriented devices.

All the above custom made or instrumented sensors did not focus on all stair fall risk parameters. So, this project's motivation was to design and develop a low cost, reliable, and portable sensor shoe system to detect stair fall risk factors in a typical living environment. An instrumented shoe system was investigated and designed. Developed sensor shoe system enabled to perform the stair gait analysis in a less expensive and non-traditional motion laboratory environment. Sensor shoe system contains a custom-made insole that can find foot contact length ratio and distance sensors fitted in the shoe to calculate foot clearance and inertia measurement unit (IMU) sensor to find motion parameters.

Although the sensor shoes could reliably measure body movement, identification of specific movement patterns and their fall risk prediction could not be achieved without using advanced machine learning algorithms. Therefore, three different machine learning classifier algorithms, such as support vector machine (SVM), K-Nearest neighbors (KNN) and ensemble, were used to train stair fall risk classification system.

6.3 *Methods*

6.3.1. Sensor Shoe Design

Detailed information about instrumented sensor shoe development, data collection method, sensor calibration, static and dynamic testing can be found in chapter3.

6.3.2. Participants

Twenty-five older adults participated in this study (female: 20; male: 5; age: $70.72\pm 4.0Y$; body mass: $70.18\pm 10.0kg$; body height: $1.62\pm 0.06m$; mean and standard deviation). All the participants were recruited from the local community of Wirral and Liverpool, UK. All these participants lived independently, able to climb stairs without help. This study was approved by the Liverpool John Moores University ethics committee in the UK (REF: 18/SPS/024). After the explained procedure, informed written consent was obtained from all participants.

6.3.3. Data collection location

Initially, sensor-based data and VICON data were collected on a custom-made staircase located in the biomechanics laboratory. Sensor data was filtered and processed in Matlab. Laboratory-based motion data (VICON) was filtered and processed in visual 3D and Matlab. Stair fall risk parameters such as foot clearance, foot contact length ratio and cadence were derived for VICON and sensor data and validated.

After the validation, older adult data were collected using instrumented sensor shoes in the LJMU's Exemplar houses. Liverpool John Moores University (LJMU) has a branch of the BRE (Building Research Establishment) Innovation Park on the LJMU's Campus, which was opened in September 2016. The Innovation Park consists of three Exemplar houses that LJMU and BRE use to provide test facilities. These three houses have been constructed using designs, technologies, and materials from the 1920s, 1970s and 2000s. Detailed information about the staircase dimension details can be found in chapter5.

6.3.4. Data collection procedure

After the successful validation against the VICON system, data collection took place in the three LJMU experimental houses. Data collection took place in a single day with two sections (laboratory and houses) lasting approximately two hours. Following informed

consent, participants completed a berg balance scale assessment and acknowledged any previous falls.

Participants were familiarised with all three exemplar houses staircase before the data collection. Participants wore comfortable clothes with sensor shoes, and the LabVIEW user interface in computer was used to collect data in the houses. No markers and cameras were used in the houses. Sensor shoe's data collection procedure was explained in chapter3. All participants performed three ascending and descending trials for each house (3 houses ×3ascending ×3descending) in a total of eighteen trials. The participants navigated the stairs step-over-step and were permitted to use the handrails if they wished. The sensor data was stored in the shoe's SD (storage) card and transferred to a computer for further processing. When all trials had been completed, the sensor shoe was removed from the participant's foot, and participants changed back into their shoes. Factors such as foot clearance, foot contact length ratio on the step, speed of movement and motion data were collected in the university's houses using instrumented sensor shoes. There were 450 trials used for further analysis (Table 6.1).

Table 6.1 Data collection location and trial details

Data collection Location		Number of trials	Total Participants	Total participants
1920's house	Ascending	3trials	25	75
	Descending	3trials	25	75
1970's house	Ascending	3trials	25	75
	Descending	3trials	25	75
2010's house	Ascending	3trials	25	75
	Descending	3trials	25	75
	Total trials			450 trials

6.4 Data Analysis and features extraction

A Machine learning algorithm from Matlab was used to design a fall risk classification system. A complete machine learning process is composed of three steps: data pre-processing, feature extraction and dimension reduction, and system modelling. Data pre-processing contains noise filtering and data normalization.

The second step was feature extraction. The goal was to extract parameters that represent discriminative information about risk fall identification. Matlab was used to extract all the bio-mechanical fall risk factors from LMU's experimental houses' collected sensor data. After successful parameter extraction, an algorithm was designed using extracted features and six months of follow-up fall data from participants' actual living houses.

The last step was establishing a system model for classification. Once a feature set was obtained for each sensor type, the next step was finding the appropriate classifiers. Three classifier algorithms, such as Support Vector Machines (SVM), Ensemble, and K Nearest Neighbour (KNN) algorithm, were used to design a stair fall risk classification system.

6.4.1. Pre-processing

IMU sensor data can contain unwanted noise mixed in with the acceleration data. This noise, referred to as artefacts, can originate from various sources such as the subject, equipment, or environment.

Artefacts distort data and can disrupt the detection of high-risk fallers. Therefore, removing as many artefacts as possible from the acceleration data before feature extraction is crucial. Certain artefacts reside at specific frequencies and can be removed by filtering the signal, and this is usually done by removing frequencies from the acceleration data using some cut-off frequencies. Many researchers used between 0.1 and 0.5 Hz frequency as a cut off frequency (Mathie, Coster et al. 2004). Acceleration data was filtered with a fifth-order Butterworth high pass filter with a cut-off frequency of 0.36Hz.

6.4.2. Features extraction

Five different sets of features were extracted from the dataset: time-domain features, frequency domain features, biomechanical features, strength test features and personal features. Below Table 6.2 shows the extracted features.

Table 6.2 Extracted Features details

Features				
Time Domain Features	Frequency Domain Features	Biomechanical features from sensors	Strength Test features	Personal features
Mean_Acc_X	PeakmagX	Totaltime	Berg balance test	Height
Mean_Acc_X_R	peakfreqX	Cycletime	Fear of falling (FOF)	Mass
Mean_Acc_Y	peakmagY	Stancetime	6month Follow-up	Age
Mean_Acc_Y_R	peakfrqY	Swingtime		
Mean_Acc_Z	peakfeqZ	FC_Entry		
Mean_Acc_Z_R	peakmagZ	FC_Middle		
SD_Acc_X	accx_kurtosis	FC_exit		
SD_Acc_X_R	accx_skewness	FC_SD		
SD_Acc_Y	accx_entropy	FO_entry		
SD_Acc_Y_R	accy_kurtosis	FO_Middle		
SD_Acc_Z	accy_skewness	FO_Exit		
SD_Acc_Z_R	accy_entropy	FO_SD		
VarAccX	accz_kurtosis	AccMax_entry		
VarAccX_R	accz_skewness	AccMax_middle		
VarAccY	accz_entropy	AccMax_exit		
VarAccY_R	PeakmagX_R	Pitch_entry		
VarAccZ	peakfreqX_R	Pitch_middle		
VarAccZ_R	peakmagY_R	Pitch_exit		
RmsAccX	peakfrqY_R	Vel_entry		
RmsAccX_R	peakfeqZ_R	Vel_middle		
RmsAcc_Y	peakmagZ_R	Vel_exit		
RmsAccY_R	accx_kurtosis_R			
RmsAcc_Z	accx_skewness_R			
RmsAccZ_R	accx_entropy_R			
	accy_kurtosis_R			
	accy_skewness_R			
	accy_entropy_R			

	accz_kurtosis_R			
	accz_skewness_R			
	accz_entropy_R			
Total=24	Total=30	Total=21	Total=3	Total=3
Total features =81				

Time-domain and frequency-domain Features

The motion data was collected in the time domain, and it was transformed into the frequency domain so that frequency-based features could be extracted. Features from both the time and frequency domains can be incorporated into a feature vector that increases classification accuracy.

Time-domain features were responsible for the most frequent variations in the acceleration signal. Time-domain features were derived directly from accelerometer sensor data and were typically statistical measures. Example time-domain features used in many activity monitoring include the mean, standard deviation (SD), variability, root mean square (RMS), skewness, entropy, kurtosis (Preece, Goulermas et al. 2009, Ejupi, Lord et al. 2014). Linear acceleration was calculated to measure participants' physical movements by removing a gravitational component. Time-domain features of mean, standard deviation (SD), variability, root mean square (RMS), skewness, entropy, and kurtosis were calculated for all three directions.

Kurtosis of signal amplitude describes the extent to which the distribution of amplitudes was concentrated; kurtosis high values suggest that distribution was more peaked, with occasional severe variations.

Entropy rate computes the signal regularity; entropy values range from 0-1, 0 denotes the maximum randomness among consecutive data points, and 1 denotes the complete regularity.

Skewness rate computed asymmetry of signal distribution, skewness value either zero or positive or negative. A positive value representing the distribution was right-skewed, the negative one representing the distribution was left-skewed, and zero representing the normal distribution.

Measurement of postural sway was used to measure older adults balance and falls risk (Mathie, Coster et al. 2004). Both amplitude and frequency were significant in the postural sway assessment, with large sway amplitudes and higher frequencies being indicative of postural instability (Mathie, Coster et al. 2004). Therefore, frequency domain features were calculated to measure amplitude and frequency. Accelerometer sensor data was converted into the frequency domain using a 'Fast Fourier transform' (FFT) to derive frequency domain features. The output of an FFT typically gives a set of basic coefficients representing the amplitudes of the signal's frequency components and the distribution of the signal energy (Preece, Goulermas et al. 2009). The maximum spectral power was the peak frequency. Using FFT, peak frequency and peak magnitude were calculated for each step, and then chose only the maximum frequency and magnitude for each trial in three directions for further analysis.

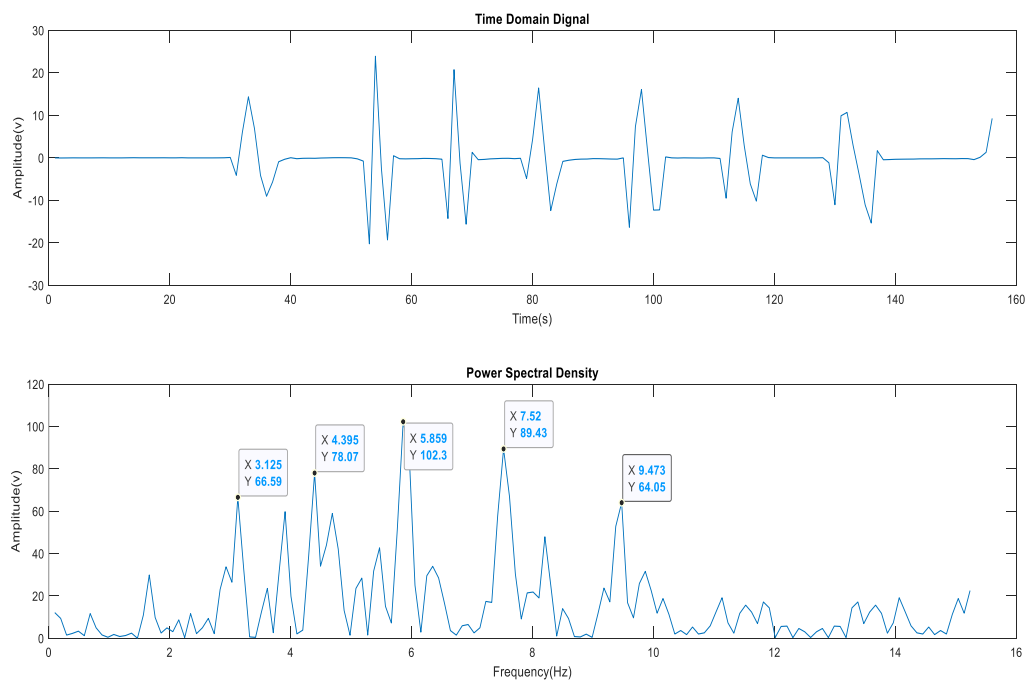


Figure 6.1 Acceleration up data for time domain to frequency domain conversion, x is frequency and y is amplitude

The above example of going up trial data had shown in Figure 6.1; it had a larger magnitude at 3.1 Hz, 4.3 Hz, 5.8 Hz and 7.5 Hz. The higher magnitude was in the middle at 5.8 Hz.

Biomechanical features

It was crucial to extract the relevant and appropriate information from the datasets. The literature review showed that minimum foot clearance, variability in foot clearance, foot contact length ratio, variability in foot contact length are fall risk parameters, so all those factors were extracted. The minimum foot clearance indicates a fall risk for a trip; a more significant fall risk was associated with smaller foot clearance. In this work, vertical foot clearance was calculated. All these instrumented sensor shoes fall risk parameters' calculation procedure was explained in chapter 4.

During the swing phase, foot clearance was calculated for descending, when the sensor shoe's back distance sensor of the leading limb (Chapter 4's Figure 4.6) passed the step edge's vertical position (1). For ascending, during the swing phase, foot clearance was calculated when the sensor shoe's front distance sensor of the leading limb passed the vertical position of the second step edge (2) before placing the foot on the stairs. The minimal foot clearance was calculated for steps 1-12 in all three trials, and the twelve-step foot clearance was divided into three parts, entry (first step), exit (last step), middle (combined all remaining steps) for each trial. The measured twelve-step foot clearance was used to calculate the foot clearance variability using the standard deviation for each house's trials.

Foot contact length ratio indicates fall risk for slip; a more significant fall risk was associated with reduced foot contact length ratio relative to the step edge. Chapter 4's Figure 4.7 shows the foot contact length ratio calculation. For example, if all the sensors have the forces, 100% of the foot is placed on the stairs. If only the last sensor does not have any force ($100\% - 11\% = 89\%$), 89% of the foot is placed on the stairs. Suppose the last two sensors do not have forces, which means ($100\% - 22\% = 78\%$) 78% of the foot placed on the stairs. Similarly, remaining sensor forces were checked to measure the foot contact length ratio.

Foot contact length ratio was calculated for all twelve steps. The 12 steps foot contact length ratio was divided into three parts, entry Foot Contact length ratio (FCLR) (first step), exit FCLR (last step), middle FCLR (combined all remaining steps). The measured twelve-step foot contact length ratio was used to calculate the foot contact length ratio

variability using the standard deviation for each houses' trial. Higher variability indicates an inability to place the foot safely on the step continually.

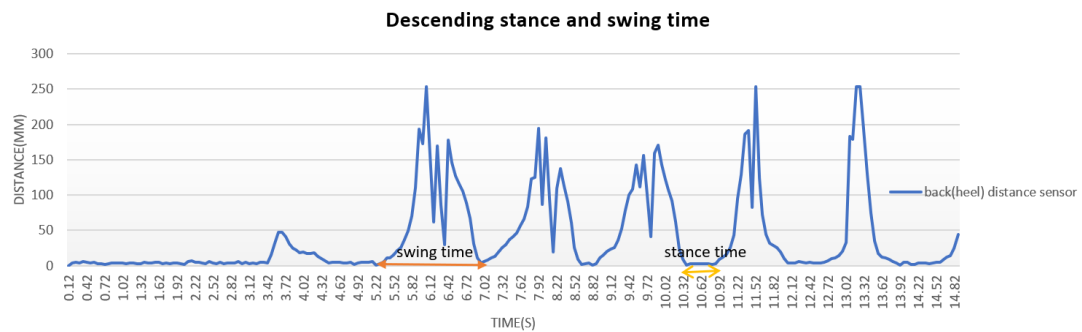


Figure 6.2 Stance time Swing time graphical representation, stance time was calculated as the duration of the foot contact on the step, swing time was calculated as the duration of the foot off the step

Going down fast on the stairs may increase the fall risk. The duration of one gait cycle was measured for the left and right limbs. Fallers walk with greater stance and swing time variability than non-fallers(Mathie, Coster et al. 2004). Stance and swing time was measured using a distance sensor (Figure 6.2). Stance time was calculated as the duration of the foot contact on the step, and swing time was calculated as the duration of the foot off the step. Stance time, swing time, cycle time and total time were calculated for all the twelve steps. The 12steps measurements were divided into three parts, entry swing, stance, cycle, and total time (first step), exit swing, stance, cycle, and total time (last step), middle swing, stance, cycle, and total time (combined all the remaining steps).

A fall event can be predicted by processing the acceleration signal because changing body movement in a pre-fall state causes alternation in the acceleration. For example, older people, who have an increased fall risk, manage to walk slowly(Tong, Song et al. 2013); this fall risk can be measured using velocity. The velocity was obtained from single integration to the acceleration component corresponding to the foot's forward motion.

Acceleration, velocity, and foot angle were calculated for all twelve steps. The 12steps measurements were divided into three parts, entry acceleration, velocity, and foot angle(first step), exit acceleration, velocity, and foot angle (last step), middle acceleration, velocity, and foot angle (combined all remaining steps).

After calculating all the biomechanical risk factors, to determine any fall risk parameters related to fallers and non-fallers, ANOVA was used to calculate the mean and standard deviation for each factor in two different categories of fallers and non-fallers. Table 6.3 shows the results.

Table 6.3 Biomechanical features for fallers and non-fallers (Mean \pm SD)

Variable	Fallers	Non-Fallers
Totaltime	11.45 \pm 3.0	12.3 \pm 3.2
Cycletime	1.04 \pm 0.31	1.00 \pm 0.30
Stancetime	7.96 \pm 2.4	8.6 \pm 2.5
Swingtime	3.49 \pm 1.54	3.67 \pm 1.86
FootClearance_Entry	25.19 \pm 11	29.33 \pm 13.13
FootClearance_Middle	28.84 \pm 6.23	29.81 \pm 4.94
FootClearance_exit	30.23 \pm 14.00	30.69 \pm 13.97
FootClearance_SD	9.5 \pm 18.4	10.35 \pm 4.2
FootContactLength_entry	76.74 \pm 10.0	77.8 \pm 9.8
FootcontactLength_Middle	74.81 \pm 10.4	74.6 \pm 10.7
FootContactLength_Exit	77.31 \pm 12.01	78 \pm 10.48
FootContactLength_SD	6.2 \pm 3.6	6.04 \pm 3.4
AccMax_entry	11.1 \pm 4.5	12.27 \pm 4.95
AccMax_middle	15.26 \pm 4.0	15.20 \pm 3.5
AccMax_exit	13.96 \pm 6.6	12.74 \pm 5.9
Pitch_entry	17.30 \pm 10.65	10.23 \pm 11.59
Pitch_middle	11.85 \pm 18.92	11.70 \pm 19.71
Pitch exit	12.56 \pm 12.57	12.87 \pm 14.53
Vel_entry	0.51 \pm 0.32	0.57 \pm 0.35
Vel_middle	0.71 \pm 0.30	0.68 \pm 0.21
Vel_exit	0.74 \pm 0.49	0.64 \pm 0.33

Fallers took less total time, swing time and stance time than non-fallers, and there were no significant changes in the cycle time. Fallers had less foot clearance for entry and intermediate steps compared to non-fallers. Similarly, fallers have a slightly less foot

contact length ratio for entry and exit steps. Fallers had more pitch at the entry than non-fallers. Fallers' velocity was high for the middle and exit phase.

Personal Features

Personal features such as age, height, and mass were extracted from the dataset. According to Table 6.4, fallers' age was slightly less (70.4 ± 4.05) than the non-fallers (71 ± 3.9). In contrast, fallers' height and mass were higher than the non-fallers.

Table 6.4 Personal Features for fallers and non-fallers(Mean \pm SD)

Variable	Fallers	Non-Fallers
Age	70.4 ± 4.05	71 ± 3.9
Height	165.11 ± 5.6	160 ± 6.4
Mass	71.65 ± 11.7	68.58 ± 7.53

Strength Test features

Postural transition duration specifies the duration of a transition from one posture to another one. Balance control and stability of the body during postural transitions were key factors for avoiding falls. Postural transition duration can be an indicator of fall because it was significantly correlated with the fall risk(Guimarães, Ribeiro et al. 2013). Higher transition duration means lower muscle strength which might lead to a fall. This postural transition (berg balance scale assessment) duration was measured using a stopwatch.

Table 6.5 Berg Balance results

Berg balance				
	Frequency	Percent	Valid Percent	Cumulative Percent
1.00, High Risk	1	4.0	4.0	4.0
2.00, Moderate Risk	6	24.0	24.0	28.0
3.00, Low Risk	18	72.0	72.0	100.0
Total	25	100.0	100.0	

Functional assessments such as the berg balance scale were subjective and qualitative and typically used threshold assessment scores to categorise people as low fall risk, moderate fall risk and high fall risk. There were 25 participants (Table 6.5), based on the berg balance scale; only one participant had high fall risk, 6 participants had moderate fall risk, and 18 participants had low fall risk.

Fear of falling

The risk of a fall was higher in older adults who experienced a previous fall.

Table 6.6 Fear of Falling results

FOF (Fear of Falling)				
	Frequency	Percent	Valid Percent	Cumulative Percent
1, Yes for Fear of Falling	8	32.0	32.0	32.0
2, No for Fear of Falling	17	68.0	68.0	100.0
Total	25	100.0	100.0	

Among 25 participants (Table 6.6), eight people had a fear of falling, and 17 people did not have a fear of falling. Among these 8 (fear of falling) older adults, five of them already had a fall in the six months follow-up time.

Follow-ups fall

After data collection, participants were followed up for six months to measure fall occurrences; based on the fall occurrence, older adults were classified into fallers and non-fallers.

Table 6.7 Follow-up fall risk results

Fall risk				
	Frequency	Percent	Valid Percent	Cumulative Percent
Fallers	13	52.0	52.0	52.0
Non-Fallers	12	48.0	48.0	100.0
Total	25	100.0	100.0	

Among 25 participants (Table 6.7), 13 people had at least one fall or trip or slip in the last six months, so they were in the Fallers group. Twelve people did not experience any fall in the six months, so they were in a non-Fallers group.

6.5 Features Selection

After extracting features from the data collection, the next challenge was classifying the features. Totally 81 features were extracted. If all features are used to train the classifier algorithm (81 features = 80 dependent features + 1 response feature), then the possibility of getting biased results is very high. The feature selection method was used to avoid the above problem; this feature selection method reduces features with the same information as others and features that do not relate to the class (fallers/non-fallers).

6.5.1. Feature selection using F-test

The performance of a classification algorithm directly depends on the size of the feature set. The features should be minimized, and dimensionality should be reduced to improve the performance of the fall risk classifiers. One way to reduce dimensionality would be to apply feature selection algorithms. Feature selection was used to determine which features are informative and can significantly differentiate between fallers and non-fallers. A rank-based system was implemented to determine which features to select from the extracted features. A rank-based system was implemented, which computes the F-test and p-value on each feature, which helps determine which features to use. The “fsrftest” Matlab function was used to get the p-values (Vallabh, Malekian et al. 2016). An empirical cumulative distribution function (CDF) of the p-values, as shown in Figure 6.3, shows the difference in feature values between the fallers and non-fallers.

About 15% (15% of 80 = 12) of features had p -values smaller than 0.05, meaning there were 12 features among the original 80 features that have strong discrimination power. Features were sorted based on their p -values (or the absolute values of the F -statistic). Features selected for classification mainly use a p -value range of [0.0005, 0.055] (Vallabh, Malekian et al. 2016).

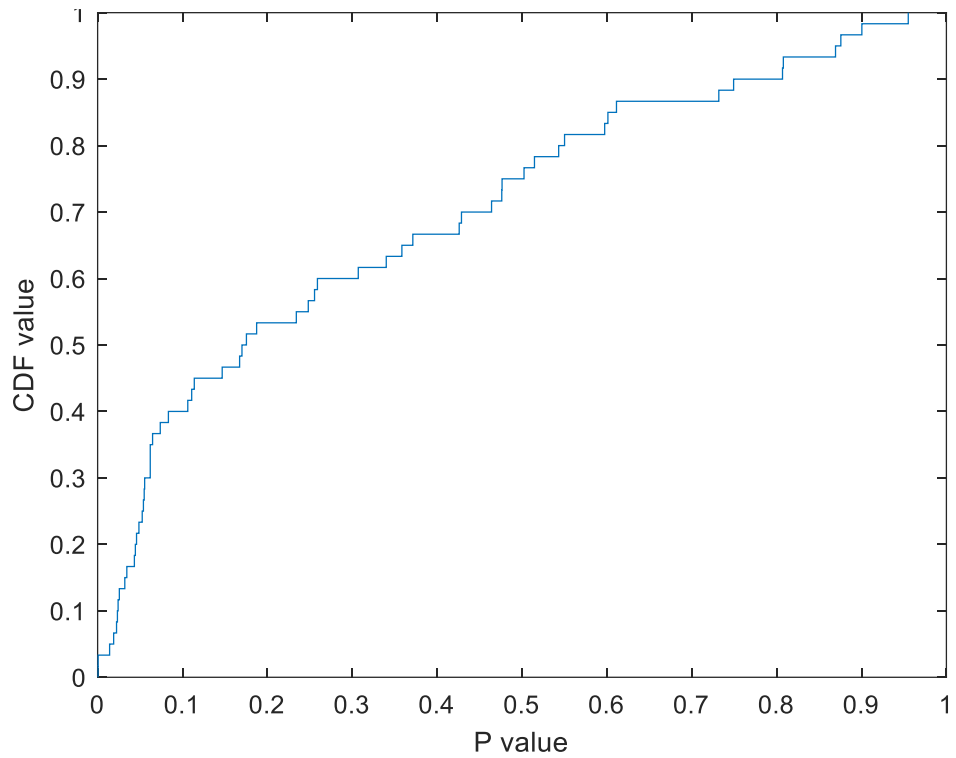


Figure 6.3 Features selection using a Filter method (F-Test), CDF means Cumulative distribution function, p values smaller than 0.05 has more discrimination features between fallers and non-fallers, so those features were selected to create a machine learning algorithm

Table 6.8 P-value for selected Features

Feature Number	P-value	Features name
1	0.000502	Mean_Acc_Z_R
2	0.00058	vel_exit
3	0.014115	vel_middle
4	0.018885	accxmax_exit
5	0.02229	stancetime
6	0.023324	Mean_Acc_Z
7	0.024122	peakfeqZ
8	0.025587	FO_exit
9	0.032013	totaltime
10	0.034406	RmsAccZ_R
11	0.043307	peakfreqX

12	0.04446	cycletime
13	0.045848	accy_skewness
14	0.048657	VarAccZ_R
15	0.052541	accxmax_entry
16	0.053947	accy_entropy
17	0.05488	SD_Acc_Z_R
18	0.055399	Mean_Acc_Y

The P-value of mean acceleration and velocity was very small; a small p-value of the statistic indicates that the corresponding predictor was significant. Features that had low p-value are shown in Table 6.8. The eighteen features were selected, along with these features, some other features were included, which were biomechanically important to predict fall risk (7 other features). The seven features were berg balance, fear of falling, foot clearance variability, foot contact length ratio variability, foot clearance entry and exit and foot contact length ratio entry. So, in total, 25 features were used to train the classifier algorithm.

6.5.2. Feature selection using rank features (chi-square test)

Another rank-based system was implemented to determine which features to select from the extracted features. A filter approach rank-based system was implemented, which computes the chi-square test on each feature. The “fscchi2” Matlab function was used; this is a non-parametric test and computes **Pearson’s chi-square test of association**. The Chi-square test checks whether the fall risk factors (80 features) and response class (fallers/non-fallers) are dependent. By calculating the chi-square scores for all the features, features can be ranked by the chi-square scores, the top-ranked features were selected to train the classifiers.

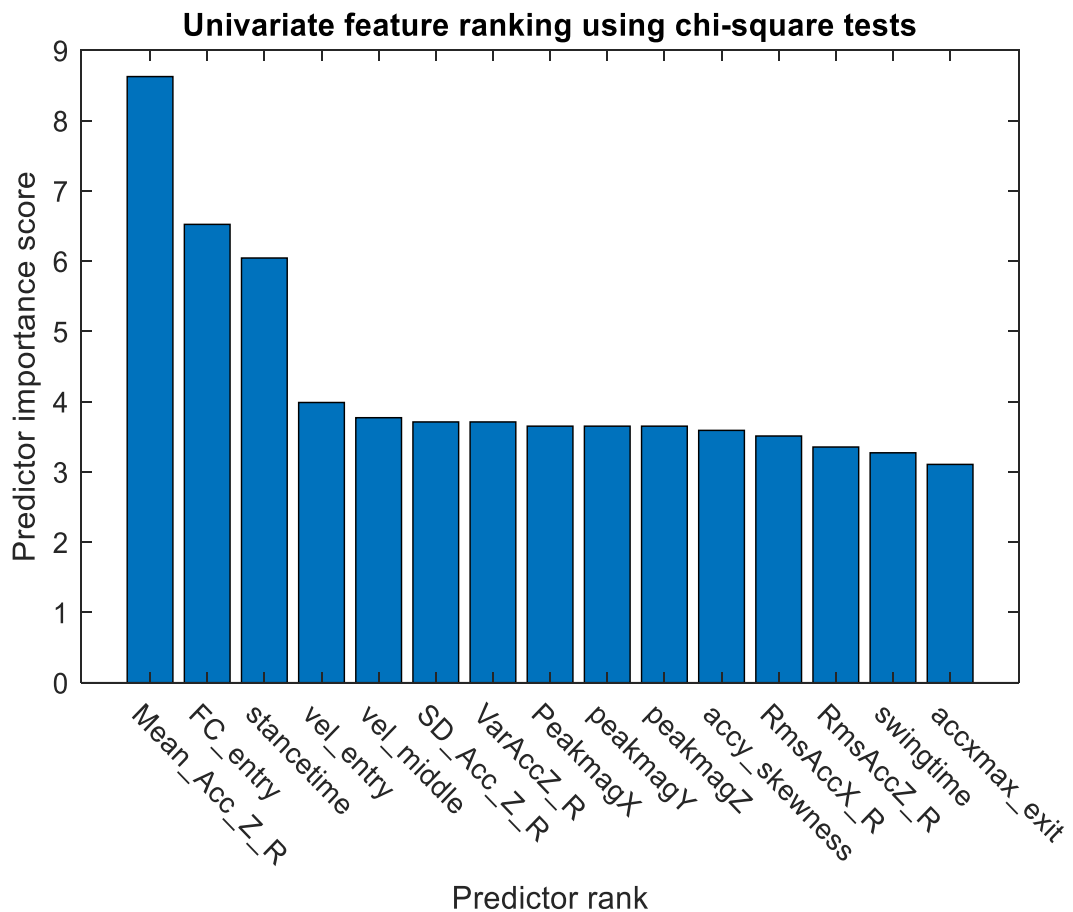


Figure 6.4 Feature selection using the Chi-square test, the features selected by predictor rank has more discrimination features between fallers and non-fallers, so those features were selected to create a machine learning algorithm

The mean acceleration for z-direction (Figure 6.4) was the most crucial response class predictor (fallers/non-fallers). The other most essential predictors were foot clearance, stance time, velocity, acceleration's standard deviation, acceleration variance, frequency domain features such as peak frequency, magnitude, and some of the time domain features acceleration skewness, acceleration root mean square. The fifteen features were selected, along with these features, some other features were included, which were biomechanically important to predict fall risk (7 other features). The seven features were berg balance, fear of falling, foot clearance variability, foot contact length ratio variability, foot clearance exit and foot contact length ratio entry and exit. So, 22 features were used to train the classifier algorithm in total.

6.6 Training Classification Algorithms

Supervised machine learning algorithms or classifiers were used to categorise an observation based on trained observations. The observations were fed into the classifier in the training phase, and the classifier learns the patterns that differentiate between the categories (fallers/non-fallers), the observations in this study were the features mentioned in the previous section.

In most cases, fall risk classification was a binary classification problem in that there were two categories, fallers and non-fallers. Therefore, the classifier used the features in the training phase to learn the differences between these two categories. This section explores the classifiers, specifically looking at each classifier's results; this can be used to compare this study's results.

6.6.1. Classification Evaluation Metrics

There were two different methods (statistical and visualization) were used to compare the performance evaluation results:

- i. **Statistical Analysis:** This method was used to compare the evaluation results by mathematical formulas such as classification accuracy (Confusion Matrix), Precision, Recall, Sensitivity, Specificity and F-Measure.
- ii. **Visualization:** representing the possible outcome of true and false values of a classifier in the form of graphs, AUC and ROC curves.

Confusion Matrix

The confusion matrix was used to measure the classification algorithm's performance (or the classifiers) on the test data. The confusion matrix was quite simple to understand. The confusion matrix used the binary classification test to measure the predictive abilities of the classifier.

Classifiers were usually evaluated by using four metrics:

- True Positive (TP)- fallers that were correctly classified as fallers
- False Positive (FP)- non-fallers incorrectly classified as fallers (false alarm)
- True Negative (TN)-non-fallers that were correctly classified as non-fallers
- False Negative (FN)-fallers incorrectly classified as non-fallers (miss)

Table 6.9 Confusion matrix with advanced classification metrics (Matrix 2019)

		Predicted Class	
		Positive	Negative
Actual Class	Positive	True Positive (TP)	False Negative (FN) Type2 Error
	Negative	False Positive (FP) Type1 Error	True Negative (TN)

Using the binary classification test (Table 6.9) confusion matrix produces true positives and true negative results; these results were divided by the total number of entries that gives the accuracy.

$$\text{Confusion Matrix(accuracy)} = \frac{TP + TN}{TP + FP + TN + FN}$$

Precision: It was a function of true positive and the misclassified objects as positive, for example, false positive.

$$\text{Precision} = \frac{TP}{TP + FP}$$

Recall/Sensitivity and Specificity: Sensitivity determines how accurately the true positives have been predicted. For example, true positive (correctly classifying as fallers) and the objects that were classified incorrectly (false negative) and was defined as

$$\text{Recall/sensitivity} = \frac{TP}{TP + FN}$$

Specificity determines how accurately the true negatives (non-fallers) have been predicted, for example, correctly classifying as non-fallers, defined as:

$$Specificity = \frac{TN}{TN + FP}$$

F-Measure was another standard evaluation metric combining precision and recall into a single value. The formula is as:

$$F\ Measure(F1\ score) = 2 \times \frac{Recall \times Precision}{Recall + Precision}$$

AUC-ROC The ‘Receiver Operating Characteristic curve’ (ROC) was a standard technique used to summarise classifier performance based on trade-offs between true positive and true negative error rates. ROC Type1 error (False Positive-false alarm) and Type2 error (False Negative-missed positive).

$$Type1\ Error = \frac{FN}{TP + FN}$$

$$Type2\ Error = \frac{FP}{TN + FP}$$

AUC (Area Under the Curve) - ROC curve was used to measure the classification problem's performance. ROC was a probability curve, and AUC represents the degree of separability. It describes how much the model could distinguish between classes. The higher the AUC values better the model at distinguishing between fallers and non-fallers.

6.6.2. Classification Algorithms

Supervised machine learning classification is the automatic assignment of a class (fallers/non-fallers) to the feature vector that had been previously extracted from the collected data. The algorithms used for this classification are known as “classifiers”. A classifier is a program built by a learner. The learner takes the input from the dataset and produces the classifier. Classifiers learn how to identify the class of a feature vector from the training dataset. The training set comprised the feature vectors and class labels.

Many classifiers are available to get better results, and we need to try different classifiers because almost every dataset comes with different specifications. This project used some of the most common classification algorithms. However, only some classification

algorithms like Support Vector Machine (SVM), k-nearest neighbors algorithm and Ensemble (AdaBoost) performed well.

The Support Vector Machine (SVM) Classifier: The SVM classifier calculates the best smoothing parameter (hyperplane) using a linear decision boundary to separate two different classes (fallers and non-fallers) in the database. The best property of SVM is that it concurrently reduces the classification error and increases the geometric margin. A linear hyperplane that entirely separates between two classes. In real-world examples, it may not be possible to sufficiently split the two classes using a linear hyperplane.

Instead of using a non-linear separator (high-order polynomial), SVM uses a method to convert the feature space such that the classes do become linearly separable. This method is called the kernel trick, and it alters the feature space, separating the classes with a linear hyperplane. The radial basis function (RBF) is a standard method for kernel transformation in high-dimensional space is the radial basis function (RBF). Training sets are mapped with a higher dimensional space using the radial basis function (RBF) in the SVM classification. Four basic kernels are available in SVM: linear, radial, polynomial, and sigmoid.

Ensemble methods Ensemble models are a useful, practical tool for different predictive tasks, as they could consistently provide higher accuracy results than conventional single strong machine learning models. However, ensemble classifications require more computation than any other single model. The common types of ensembles are Bayes optimal classifier and boosting.

Bayes optimal classifier is a simple method to construct a machine learning classifier. A Bayes optimal classifier considered each input feature are assumed to be independent of each other. For example, some fruits are maybe orange fruit, orange colour, round, and about 10 cm in diameter. There are three features created for orange fruit classification: colour, shape, and size. A Bayes optimal classifier considers each of these features to contribute independently to the probability that this fruit is an orange, regardless of any possible correlation between the colour, shape, and size features. Bayes optimal classifier can be trained efficiently for probability models in supervised machine learning. Also, Bayes optimal classifier uses a maximum likelihood method for parameter estimation.

AdaBoost is the most common boosting algorithm's implementation. In AdaBoost algorithms, the learning procedure consecutively fitted new models to provide a more accurate estimate of the response variable. This algorithm's principal idea is to construct the new base-learners to be maximally correlated with the negative gradient of the loss function associated with the whole ensemble.

k-nearest neighbors algorithm (k-NN) k-NN is a simple classification algorithm based on calculating the distance (usually the Euclidean distance) between the new element to be classified and the elements in the training set. k-NN is also called instance-based learning, where all computations are postponed until the end of classification. Classification of the object is based on the neighbours' selection, which was correctly classified at the time of training, and that neighbour's class is assigned to the object. k-NN accuracy can be improved by normalizing the training data. A useful technique is to allocate weights to the neighbors so that the closer neighbors can contribute more to the average than the more distant ones.

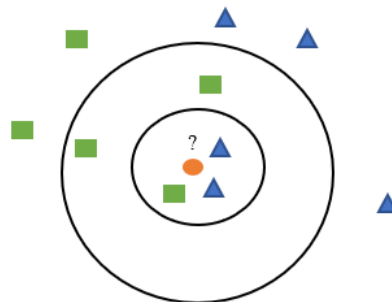


Figure 6.5 Example for k-NN (Wikipedia)

For example (Figure 6.5), the test sample (orange dot) should be classified as either green squares or blue triangles. If $k = 3$ (the inner circle), it was assigned to the blue triangles because there were two triangles and only one square inside the inner circle. If $k = 5$ (outer circle), it was assigned to the green squares (three squares vs two triangles inside the outer circle).

6.6.3. Validation Methods

The dataset data set was divided into two parts; one part was for training, and the second part was for validation. K fold cross-validation technique was used for validation. The k-fold technique partitions data into k fold; for example, if k=5, the feature set would be divided into five equal sizes. One subset was used for validation, and the remaining subsets were used for training. This process was repeated k times, such that each subset was used exactly once for validation. Finally, the k-fold cross-validation technique was used to estimate the accuracy of the classifiers. In this project, the results obtained for k-fold cross validation uses five folds.

6.7 Results

A total of 450 trials were used to create a dataset. All five sets of features such as time domain, frequency domain features, biomechanical features, strength features, and person features were extracted for all 450 trials. This feature set referred to a feature vector, follow up fall information listed as a class in the dataset, can either be fallers or non-fallers. In this dataset, 234 trials were identified as fallers, and 216 trials were identified as non-fallers.

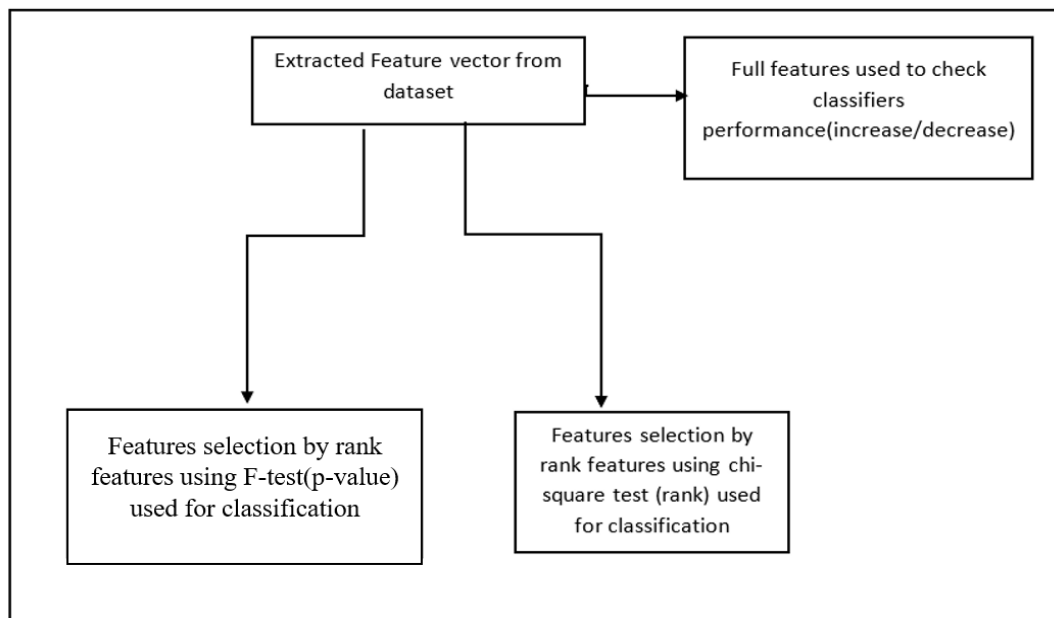


Figure 6.6 Selected three feature set for classification training

In this work, three feature sets (Figure 6.6) were used for classification; the first feature set contained all the features, the second feature set contained features selected by f-test (18features+7biomechancial features=25features), and the feature set contained features selected by chi-square test (15feature+7biomechanical features=22features). All the features were standardised before classifier training.

6.7.1. Full Feature set results

Full features were used to train the classifier. Many classifiers were tested, but three classifiers (SVM, k-NN and Ensemble) performed better than other classifiers. Cubic kernel function was used by the SVM classifier. Ensemble classifier used boosted trees, the method was AdaBoost, and learner type was decision tree. Fine k-NN was used by k-NN, the number of neighbors was 1, Euclidean distance Metrix was used, and distance weight was equal.

For full features (Table 6.10), three classifiers had given comparatively better results: SVM, k-NN and ensemble with 80.2%, 79.6%, and 77.6% accuracy, respectively. k-NN classifier had more sensitivity (81%) than the other two classifiers (79% SVM and 78% ensemble). SVM classifier (81.5%) had better specificity than other classifiers (78.2% k-NN, 77.3% ensemble). SVM had better precision (82.2%) than the other two classifiers (80.1% k-NN, 78.8% ensemble). The F-Measure result had been used to compare classifier performance; SVM (80.57%) and k-NN (80.55%) were performed better than ensemble (78.45%)

Table 6.10 Full Feature set classification results

Classifier	SVM (cubic SVM)	KNN (fine KNN)	Ensemble
Confusion Matrix Accuracy	80.2%	79.6%	77.6%
Precision	82.2%	80.1%	78.8%
Recall/Sensitivity	79%	81%	78%
Specificity	81.5%	78.2%	77.3%
F-Measure	80.57%	80.55%	78.45%
Type1 Error	19%	22%	23%

Type2 Error	20.9%	20.4%	22.2%
Error rate	19.80%	20.40%	22.40%
AUC	0.87	0.80	0.85

Type1 Error (false alarm) represented the “False Positive” values. In contrast, Type2 Error (missed positive case) presents the “False Negative” Type2 Error-values that show the system’s failure to predict any fallers and label them non-fallers. SVM classifier had less type1 error (0.19%) rate compared to other classifier (0.22% k-NN and 0.23% ensemble). The K-NN classifier had a lower type2 error rate of 20.4 % than other classifiers (20.9% SVM, 22.2% ensemble).

The ROC curve (Figure 6.7) was plotted with TPR against the FPR, where TPR was on the y-axis and FPR was on the x-axis. The AUC gave a single value which explains the probability that each algorithm would correctly classify a random sample. All models performed very well in this complete feature set, but the SVM algorithm showed the best performance, with AUC = .87 compared to the k-NN (AUC = .80) and the ensemble (AUC = .85).

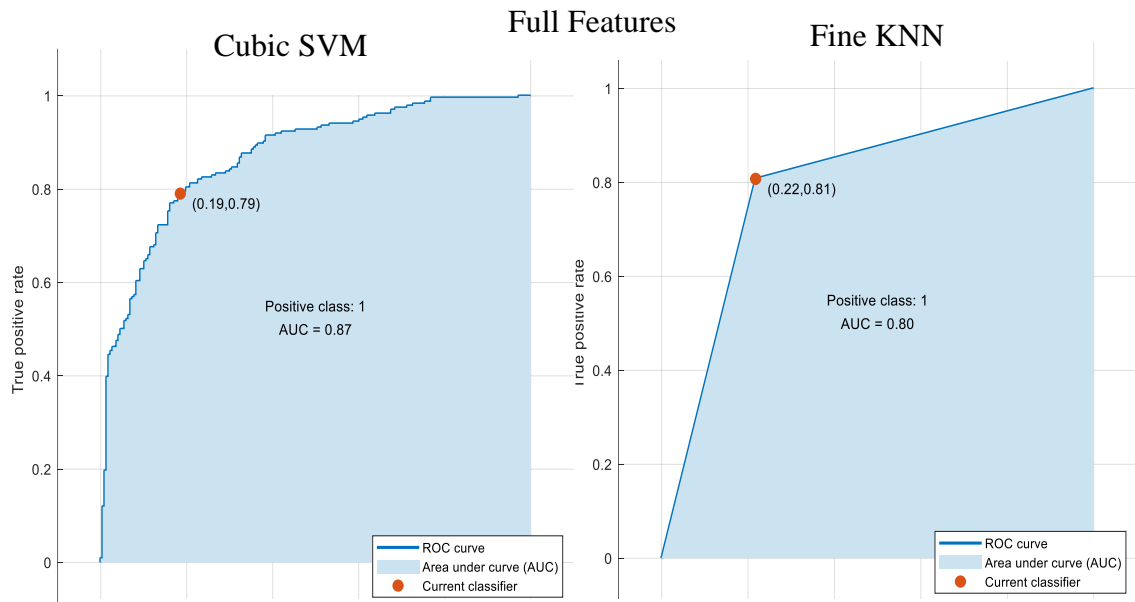


Figure 6.7 Area Under the Curve (AUC) results for best two classifiers using Full feature set, cubic SVM algorithm produced 87% AUC and the Fine KNN produced 80% AUC

6.7.2. Chi-square Feature set results

Twenty-two features were used to train the classifier. Again, many classifiers were tested, but again same three classifiers (SVM, k-NN and ensemble) performed better than other classifiers. The SVM classifier used the cubic kernel function. Ensemble classifier used boosted trees, the method was AdaBoost, and learner type was decision tree. Fine k-NN was used by k-NN, the number of neighbors was 1, Euclidean distance Metrix was used, and distance weight was equal.

The results (Figure 6.8) reveal that some of the classifiers had shown a comparatively lower error rate, especially the SVM, which had classified 209/234 fallers and 192/234 non-fallers correctly.

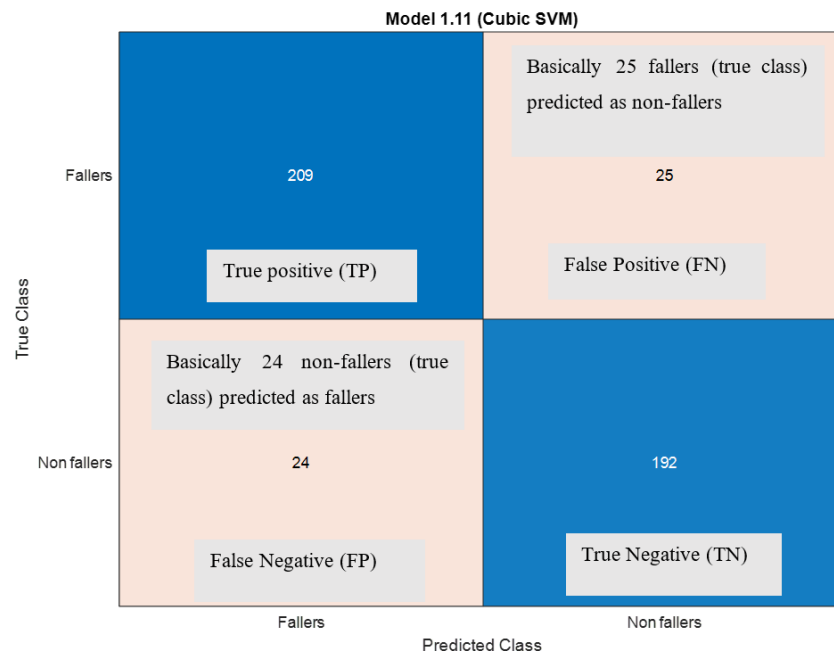


Figure 6.8 Confusion matrix for SVM

Table 6.11 shows the chi-square feature set classification results for best-performing three classifiers for the chi-square feature set. The three classifiers with comparatively better results were SVM, ensemble, and k-NN with 89.3%, 89.1%, and 83.6% accuracy. SVM classifier had more sensitivity (88.9%) than the other two classifiers (88.0% ensemble and 82.1% k-NN). Ensemble classifiers had better specificity (90.3%) than other classifiers (88.9% SVM, 85.2% k-NN). Ensemble had better precision (90.7%) than the

other two classifiers (90.4% SVM, 85.7% k-NN). The F-Measure result had been used to compare classifier performance; SVM (90%) and ensemble (89%) were performed better than k-NN (84%).

Table 6.11 Classification results for the chi-square feature set

Chi-square features set classification results /Classifier	SVM Cubic	Ensemble Boosted Trees	KNN Fine KNN
Confusion Matrix Accuracy	89.3%	89.1%	83.6%
Precision	90.4%	90.7%	85.7%
Recall/Sensitivity	88.9%	88.0%	82.1%
Specificity	89.8%	90.3%	85.2%
F-Measure	90%	89%	84%
Type1 Error	11.1%	12%	17.9%
Type2 Error	10.2%	9.7%	14.8%
Error rate	10.70%	10.90%	16.40%
AUC	0.93	0.95	0.84

SVM classifier had less type1 error (11.1%) rate than other classifiers (12% ensemble and 17.9% k-NN). Ensemble classifiers had a lower type2 error rate of 9.7% than other classifiers (10.2 % SVM, 14.8% k-NN).

The AUC gave (Figure 6.9) a single value which explains the probability that each algorithm would correctly classify a random sample. All models perform very well in this chi-square feature set, but the Ensemble algorithm showed the best performance, with AUC = 0.95 compared to the k-NN (AUC = 0.84) and the SVM (AUC = 0.93).

Chi-square feature selection

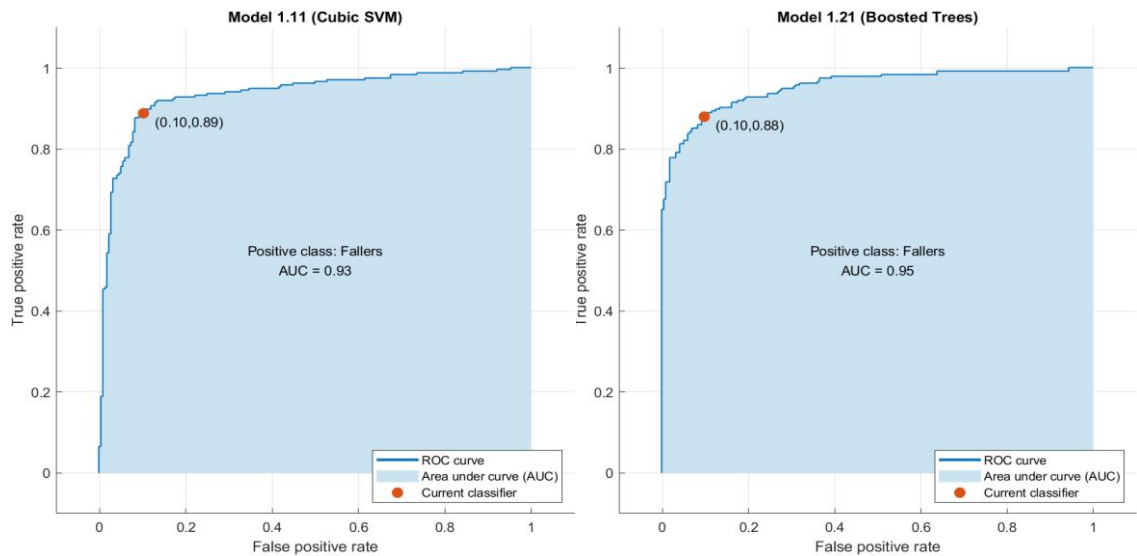


Figure 6.9 Area Under the Curve (AUC) results for best two classifiers using chi-square feature set, cubic SVM algorithm produced 93% AUC and the Boosted trees produced 95% AUC

6.7.3. F-Test Feature set results

Twenty-five features were used to train the classifier. Again, many classifiers were tested, but again same three classifiers (SVM, k-NN and ensemble) performed better than other classifiers.

The SVM classifier used the cubic kernel function. Ensemble classifier used boosted trees, the method was AdaBoost, and learner type was decision tree. Fine k-NN was used by k-NN, the number of neighbors was 1, Euclidean distance Metrix was used, and distance weight was equal.

For F-test features, Table 6.12 shows the result, three classifiers with comparatively better results were SVM, ensemble and k-NN with 89.1%, 86.2%, and 83.6% accurate results, respectively. SVM classifier had more sensitivity (89.3%) than the other two classifiers (82.1% ensemble and 83.3% k-NN). Ensemble classifiers had better specificity (90.7%) than other classifiers (88.9% SVM, 83.3% k-NN). Ensemble had better precision (90.6%) than the other two classifiers (89.7% SVM, 84.8% k-NN). The F-Measure result had been used to compare classifier performance; SVM (89%) and ensemble (86%) were performed better than k-NN (84%). SVM classifier had less type1 error (10.7%) rate

compared to other classifier (17.9% ensemble and 16.7% k-NN). Ensemble classifiers had less type2 error rate of 9.3% than other classifiers (11.1 % SVM, 16.2% k-NN)

Table 6.12 Classification results for F-Test feature set

Classifiers for F-test	SVM (Cubic SVM)	Ensemble (Boosted Trees)	KNN (Fine KNN)
Confusion Matrix Accuracy	89.1%	86.2%	83.6%
Precision	89.7%	90.6%	84.8%
Recall/Sensitivity	89.3%	82.1%	83.3%
Specificity	88.9%	90.7%	83.3%
AUC	0.94	0.94	0.84
F-Measure	0.89	0.86	0.84
Type1 Error	10.7%	17.9%	16.7%
Type2 Error	11.1%	9.3%	16.2%
Error rate	10.90%	13.80%	16.40%

In this F-Test feature set, all models performed very well, but the Ensemble and SVM classifiers showed the best performance (Figure 6.10), with AUC = 0.94 for both compared to the k-NN (AUC = 0.84).

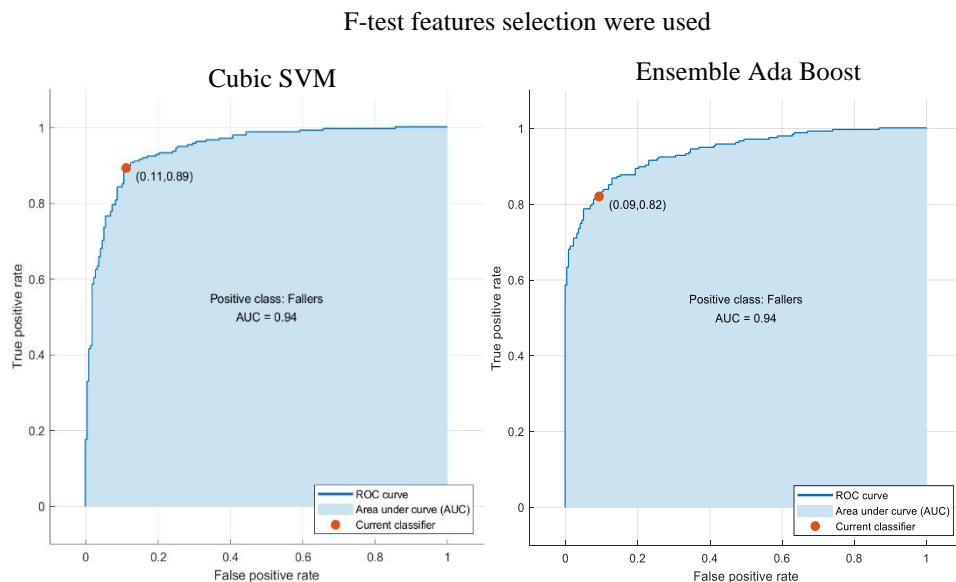


Figure 6.10 Area Under the Curve (AUC) results for best two classifiers using F-Test feature set, cubic SVM algorithm produced 94% AUC and the Ensemble Ada Boost produced 94% AUC

6.8 *Discussion*

This study aimed to design the stair fall risk classification system using supervised machine learning algorithms. The input data sample represents the older participants trials (450 trials). Each sample in the dataset represents an older adult who belongs to one of the two classes (fallers or non-fallers). The input dimension depends on the features (81) associated with older adults' trials. The classifiers' outputs were binary values; for example, 1 represents the fallers group, and 0 represents the non-fallers group. There were 52% of sample data fallers and 48% non-fallers.

This work explored two filter type features-selection algorithms to reduce the feature set's size and improve classification accuracy. Those two algorithms were the chi-square test and F-test. The chi-square feature selection algorithm's advantage was that it returned rank for each feature (risk factor), based on the discriminative power between fallers and non-fallers. F-test returns a p-value for each feature, which had less than 0.05 p-values indicating that the corresponding predictor was significant for classification. By selecting these features, the classification accuracy was improved. Both algorithms showed that mean acceleration, foot clearance, and velocity were the top three features with strong discrimination power between fallers and non-fallers. This is because fallers' foot clearance was less than that of non-fallers, and acceleration and velocity were higher for fallers than non-fallers (table 6.3).

Three different feature sets were trained, one with full features (A), chi-square feature set (B) and F-test feature set (C). The feature set that contained all the features (A) did not perform well, so it was not compared with other results. The other two feature sets (B and C) performed well, so the feature sets B and C results are compared below.

After selecting feature sets, many algorithms were trained to classify fallers and non-fallers. However, only three algorithms were performed well: Support Vector Machine (SVM), k-nearest neighbors algorithm, and Ensemble (AdaBoost). Results showed that all three selected algorithms could perform with high accuracy, sensitivity, and specificity despite substantial differences in how the algorithms work.

Table 6.13 Chi-square and F-Test classification results in comparison, green colour indicates that the first-best results for that evaluation metrics, the red colour shows the second-best results for that evaluation metrics

Evaluation metrics	Precision		Recall/sensitivity		Accuracy		F-Measure	
	Feature set(B)	Feature set(C)	Feature set(B)	Feature set(C)	Feature set(B)	Feature set(C)	Feature set(B)	Feature set(C)
SVM	90.4%	89.7%	88.9%	89.3%	89.3%	89.1%	90%	89%
Ensemble	90.7%	90.6%	88.0%	82.1%	89.1%	86.2%	89%	86%
k-NN	85.7%	84.8%	82.1%	83.3%	83.6%	83.6%	84%	84%

The above Table 6.13 shows the precision, recall and F-measure for all three trained algorithms from two different feature sets (B and C). Green colour indicates the first-best results for that evaluation metrics; the red colour shows the second-best results for that evaluation metrics.

Accuracy is the percentage of the total number of correct predictions. The 89.3% of fallers were correctly classified by the SVM classifier (feature set B). The Ensemble classifier correctly classified 89.1% of fallers.

Precision calculates the ratio of correctly classified instances among those classified as positive. For example, precision represents the ratio between the number of fallers correctly predicted and the total number of predicted fallers correctly and incorrectly; the 90.7% of older adults who were classified as fallers were actually fallers. The ensemble classifier had better precision (90.7(B), 90.6(C)) than the other two classifiers in both feature sets.

Sensitivity is the ability of a test to correctly identify fallers (true positive rate); for example, Recall(sensitivity) is the ratio between the number of fallers that are correctly predicted and the total number of actual fallers in the dataset. SVM algorithm had better sensitivity for both feature sets (89.3 % (C), 88.9 % (B)) than the other classifiers. So, the SVM algorithm can classify 89.3% of fallers among all fallers in the dataset.

The weighted average of the sensitivity and precision is called the F1 score. F-Measure provides a single score that balances both the concerns of precision and recall in one number, and it helps to distinguish the model's performance. Based on the F1 score, the overall feature set(B)'s classifier performed well; for example for SVM algorithm had better F-measure of 90% for feature set (B) and the ensemble algorithm had second better results for F-measure 89% for feature set(B).

Support Vector Machine classifier gives significant prediction results, shown in Table 6.13, as they have their own predictive power in computing. Also, SVM gives significant results in terms of ROC value and lower error rate for fallers misclassification, which was much better than the other classifiers.

Overall, the support vector machine classification model was more effective than other models for predicting fallers (Fallers).

6.8.1. The prediction of stair fall risk in future

A classification model had been trained to classify fall information (Appendix G). Fall risk prediction can be made in the future based on the instrumented sensor shoe and our trained classification algorithms if applied to large groups of older people.

In future, instrumented sensor shoes can be tested in a home environment. The raw data from instrumented sensor shoes in the houses are not directly applicable to our trained classification model. Before using our trained algorithm, we need to extract the same features (features set (B)) used in this project. Follow up fall information (fallers/non-fallers) is not required in the future to use our trained classification algorithm. Because our trained algorithm learned the patterns from the database used in this project. After successful features extraction, our trained classification model can be applied to new extracted features (without a class label).

The trained classification model can then predict either fallers (high risk of falling) or non-fallers (low risk of falling). Figure 6.11 shows how these data are represented and processed by the trained model in the future. In Figure 6.11, (A) represents classification training, (B) represents Validation, and (C) represents new data testing using the trained

algorithm. Note that all algorithms that return predictions that suggest a near-certainty that this trial is a high risk of falling/low risk of falling.

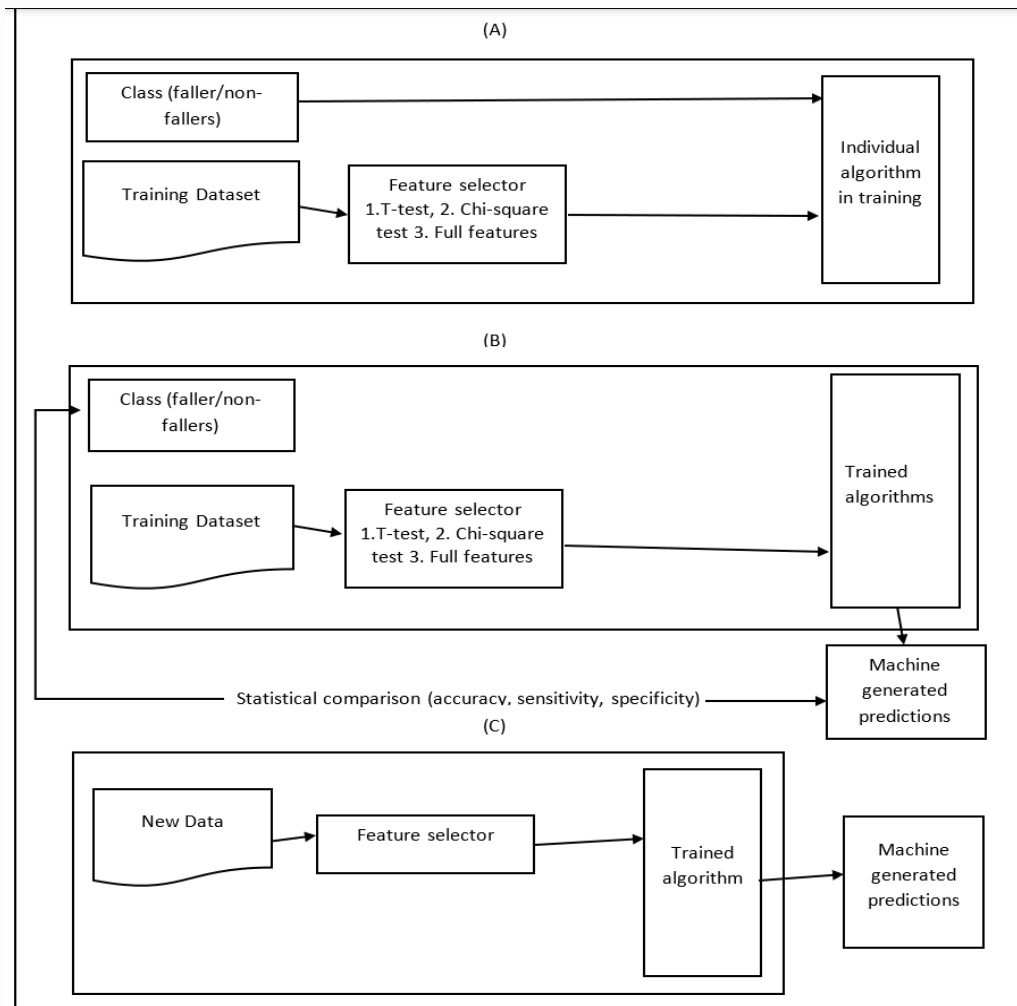


Figure 6.11 (A)Training (B)Validation (C)Trained algorithm for future testing

Simulating all the external conditions is technically challenging and may modify the older adult's stair negotiation performance. The realistic approach could test the stair fall risk parameter in real-life staircases. The developed instrumented sensor shoe allows recording various stair fall risk parameters to identify the stair fall risk. Using stair-specific biomechanical parameters measured in real-life conditions together with a higher sample size in real life stair negotiation conditions could improve the predictive power of our trained machine learning algorithm.

6.9 Conclusion

In this study, instrumented sensor shoe was successfully designed, validated, tested in the houses. Also, a stair fall classification system was created using supervised machine learning algorithms. SVM, ensemble and k-NN algorithm gave better precision, sensitivity, and F-measure. Data need to be collected from their own living environment using sensor shoes for future fall risk prediction. These collected data need to be analysed to compute the appropriate feature set. Then, the risk of a possible fall can be evaluated through our trained classification algorithms. Once the trained algorithm provides output about the subjects at high risk of falling, those older people will be informed about their high risk of falling. They will be recommended for a fall prevention exercise program run by NHS to improve their balance on the stairs.

CHAPTER 7: General Discussion

7.1 Purpose

The overall purpose of this thesis was to develop an instrumented shoe with a novel combination of sensors that can identify older adults risk parameters for a fall on stairs at the community level and in their natural home environment. Identified fall risk parameters were used in the machine learning algorithm to classify older adults at risk of falling. Identified high risk older adults can then be referred to fall prevention and exercise programs to improve their strength and balance to avoid future falls.

7.2 Summary of experimental findings

Chapter 3 Sensor Shoe Development

Stair fall risk parameters have been identified using extensive study on stairs in the laboratory. However, laboratory-based fall risk parameters require expensive, cumbersome equipment and instrumentation. Also, laboratory-based equipment is not able to test at real houses. On the other hand, most stair falls occur at home, so a simple solution would be helpful to predict fall risk at home. So, a simple prototype wearable sensor shoe was developed to fill the gap between the laboratory measurements and stair fall risk assessment in actual houses.

An instrumented shoe was developed to detect stair fall risk parameters at the community level and not only in the laboratory. Three low-cost sensors were used to create the instrumented shoe: a vl6180x distance sensor, a BNO055 IMU and an FSR force sensor and each sensor shoe cost £200 to produce, so a total cost of £400 for both instrumented shoes. Participants walked with this instrumented shoe outside the houses during the data collection in different homes. The sensors were not damaged due to the sensor cases, so this showed the durability of the instrumented shoe.

Fitting many sensors all over the body might affect a participant's daily activity. In contrast, if the sensors are incorporated in the shoe, many people will happily wear them at home to collect data for longer. That was the main reason for focusing on only instrumented shoes. Even though few risk parameters were implemented, we can predict the fall risk in the future using this set of powerful parameters. The sensor shoe has the potential to add more sensors in future. Older people can use this sensor shoe at home

without any assistance (just required to press a button on the shoe). Data is stored in the Storage (SD) card and are processed later to predict stair fall risk. This system won't affect their gait, is less expensive, and can collect data for longer.

Chapter 4 Sensor Shoe's stair fall risk parameters validation

The instrumented shoe's extracted stair fall risk parameters were validated against fall risk parameters collected through a Vicon system in a biomechanics laboratory. Different approaches are available to track human motion: Optical motion systems (such as Vicon or Optotrak) and commercial IMU sensors such as MTw(Xsens). However, the most widely used and accepted system to track stair climbing motion is the optical motion system because it has high accuracy when operating in controlled environments. This Vicon optical motion system was used in our lab, so it was decided to compare the sensor results with the Vicon system.

Instrumented shoes' fall risk parameters such as foot clearance, foot contact length, and cycle time were validated against the parameters measured with the Vicon system. There were two different methods, correlation and Bland Altman plot(B&A), used to compare the results. The correlation coefficient describes the relationship between two methods (sensor and vicon); sensor shoe's foot clearance, foot contact length ratio and cycle time had a high positive linear correlation with the vicon system. But this correlation does not describe their agreement (Bland and Altman 1986). A high correlation does not mean a good agreement between the two methods. So, the Bland-Altman plot was used to measure the agreement between two methods by constructing limits of agreement.

The maximum acceptable difference for foot clearance was 5 mm, and this was set by the researcher. The B&A plot results showed that the sensor shoe's foot clearance measurements were 0.05 mm(bias), and the limits of agreements results were from 4.7 mm to -4.6 mm. This limit comes within the acceptable difference, so this method of calculating foot clearance can be used in the future.

The maximum acceptable difference for foot contact length was 15%; this was set by the researcher. The B&A plot results showed that the sensor shoe's foot contact length measurements were -2%(bias), and the limits of agreements results were from 10% to -

13.9%. This limit comes within the acceptable difference, so this method of calculating foot contact length can be used in the future.

The maximum acceptable difference for cycle time was 0.5 seconds; this was set by the researcher. The B&A plot results showed that the sensor shoe's cycle time measurements were 0.2 seconds (bias), and the limits of agreement results were from 0.5 seconds to -0.14 seconds. This limit comes within the acceptable difference, so this method of calculating cycle time can be used in the future.

These 95% limits of agreement were small enough to be confident that the new method (sensor shoe) can calculate foot clearance, foot contact length ratio and cycle time in place of the VICON method.

Chapter 5 Stair fall risk parameters comparison between a controlled environment and uncontrolled environment

This chapter investigated whether older adults maintained their stair-negotiating behaviour when negotiating different staircase dimensions. It was found that most of the older adults did maintain their stair-negotiating behaviour, for both ascent and descent in similar staircases, altered their stair behaviour for different stair dimensions of 2010, 1920 and 1970's houses.

In ascending, older adults spent less time (faster) to climb consistent (the 1920s and 1970s) straight stairs. This research (Templer 1995) found that straight flights of stairs without landings accounted for 52% of all accidents. The straight staircase might be the case because the path of straight flights is often clear and uninterrupted, so stair users are reassured into a false sense of security and reduced attention. However, straight flights may also result in more severe injuries because there is no place where the fall may be broken on the stairway.

The ascending and descending foot contact length ratio was less (mean= 67%) for inconsistent (the 2010s) stairs. It shows that the risk of overstepping increases on narrower stairs (the 2010s) due to lack of space to place the foot safely (Roys and Wright 2005). Descending foot contact length ratio is more critical for safe stair negotiation (Roys, 2013); for example, older adults who usually have less foot contact length ratio

might experience a fall (Roys and Wright 2005). If less than 70% of the foot contact length regularly, there is an increased risk of a slip over the step-edge (Roys 2013), but the British Standards Institution (BSI) indicate that less than 50% of foot contact length ratio would most likely lead to a fall (BSI 2010).

Winder stairs are more dangerous than standard stair designs because of the non-uniform tread width; recent studies concerning stair accidents reveal that this is not true (Wells 1977). Older adults used increased cadence and increased entry and exit foot clearance compared to other houses to support this. In contrast, the foot contact length ratio decreased compared to other houses due to the walking portion of the tread being less than the other two houses. The 2010s staircase (winder staircase) contains 210 mm rise and from 185 mm to 230 mm going configuration; if the feet are placed forward, the ball of the lead foot is placed outside the edge of the step, which can reduce the balance and result in a fall. Older adults find it challenging to negotiate staircases with high step-rises or short step-goings, and this configuration challenges muscle strength and postural stability. The reason for this, older adults get their best support when they place most of their foot on the tread, but this is not always possible because the going of the winder staircase was less than the older adults foot length. Therefore, to safely negotiate this small going, they need to turn their feet to the side of each step. Otherwise, more of the feet will overhang. In addition, older adults foot clearances over the middle steps were less for the 2010s staircase for both ascending and descending; this would increase the risk of a toe-catch, and the chances of tripping increase when individuals have less foot clearance (Hamel, Okita et al. 2005).

Older adults showed a safe strategy for ascending in the laboratory and descending in the houses. In contrast, older adults showed a riskier strategy for descending in the laboratory and ascending in the houses. Older adults had less foot clearance in the entry steps and more variability in the foot clearance in the houses than in the lab. It is already demonstrated that many stairway accidents occur on the top or bottom stairs (Templer 1985) as an older adult might be looking around for the next part of their movement, so their attention might not be entirely focused on the stairway (Templer 1995). It is possible to conclude that house staircases are not safer because there was more variability in the foot clearance, leading to trip. In the laboratory staircase, due to less rise and more going,

starting foot clearance and ending foot contact length was high compared to houses with less variability. Therefore, it shows that the laboratory staircase is safer than the exemplar houses.

There was no interaction between the follow-up group (faller/non-fallers) and different environments, so both fallers and non-fallers group would be at an increased fall risk by the exact mechanism on different environments. However, the consequences will likely be more severe for the fallers group because they do not have the adequate strength reserves to recover when they lose balance (Foster, Maganaris et al 2019)

Older adults who had a previous fall showed more variability in foot clearance and more variability in foot contact length than others. Older adults afraid of falling showed increased cadence variability; this showed less stability and led to a fall. High risk older adults from the berg balance scale had normal cadence (1.37 s) compared to low and moderate risk older adults (high cadence); this shows that high risk older adults take some cautious strategies to stay safe in the stairs.

With only current statistical results, it is hard to state who is at risk of falling in the future, so the machine learning method was used to find future fall risk prediction. Despite many similarities between the statistical and machine learning methods, the Machine Learning algorithm is differentiated from statistical inference by predicting real-life outcomes from new data.

Chapter 6: Identify Fall risk using Novel sensors and Machine learning algorithm

This study aimed to design the stair fall-risk detection system using supervised machine learning algorithms. The input data sample represents the older participants trials (450 trials) in this study. Each sample in the dataset represents an older adult who belongs to one of the two classes (fallers or non-fallers). The input dimension depends on the features (81 features) associated with older adults' trials. The classifiers' outputs were binary values; for example, 1 represents the fallers group, and 0 represents the non-fallers group. There were 52% of sample data contained fallers, and 48% of sample data had non-fallers.

There were 81 features (risk parameters) extracted from the data set; feature selection methods were applied to select appropriate features. Feature selection methods showed

that mean acceleration, foot clearance, and velocity were the top three features with strong discrimination power between fallers and non-fallers. Fallers' foot clearance was less than the non-fallers group, and acceleration and velocity were higher for fallers than non-fallers.

After selecting feature sets, many algorithms were trained to classify fallers and non-fallers. However, only three algorithms were performed well: Support Vector Machine (SVM), k-nearest neighbors algorithm, and Ensemble (AdaBoost).

The ensemble classifier had better precision than the other two classifiers. On the other hand, the SVM algorithm had better sensitivity than the other classifiers. So, the SVM algorithm can classify 89.3% of fallers among all fallers in the dataset. Based on the F1 score, the overall SVM algorithm had better F-measure of 90%, and the ensemble algorithm had second better results for F-measure 89%.

Support Vector Machine classifier gives significant prediction results, as they have their own predictive power in computing. Also, SVM provides substantial results in ROC value and lower error rate for fallers misclassification, which was much better than the other classifiers. Overall, the support vector machine (SVM) classification model was more effective than other machine learning models for predicting fallers. A successfully developed machine learning algorithm can test future fall risks of older people.

Simulating all the external conditions that may modify the older adult's stair negotiation, and also it is technically challenging. So the realistic approach could be to test the stair fall risk parameter in real-life staircases. Advancements in wearable sensors, such as our developed instrumented sensor shoe, allow recording various input parameters to identify the stair fall risk. Using biomechanical parameters measured in real-life conditions could improve the machine learning algorithm's predictive power. In addition, older people can use this sensor shoe at home without any assistance (just pressing the button in the shoe). Data will be stored in the storage (SD) card. Those data will be processed to predict stair falls. The collected raw data from sensor shoes in the houses are not directly applicable for our trained classification model. Before using our trained algorithm, we need to extract the same features used in this project. Follow up fall information (fallers/non-fallers) is not required in the future to use our trained classification algorithm. Because our trained

algorithm learned the patterns from the database used in this project, after successful features extraction, our trained classification model can be applied to the new extracted features (without a class label).

The trained classification model can then predict fallers (high risk of falling) and non-fallers (low risk of falling). In the future, all algorithms return predictions that suggest a near-certainty that this trial is a high risk of falling(fallers)/low risk of falling(non-fallers). Once the trained algorithm provides output about who are at high risk of falling, those older people will be informed about their high risk of falling and recommended for the fall prevention exercise programs run by NHS to improve their balance on the stairs.

The developed instrumented shoe in large-scale populations without a dedicated gait laboratory opens new possibilities for stair fall risk detection and prevention at the community level. The instrumented shoe was successfully developed, validated, and tested in actual houses. In addition, a classification algorithm was developed to differentiate fallers and non-fallers, which could detect stair fall risk in the future. Despite many similarities, the Machine Learning algorithm is distinguished from statistical inference by predicting real-life outcomes from new data. First, data must be collected from sensors at home and analysed to compute the appropriate feature set to predict fall risk. Then, the risk of a possible fall will be evaluated through classification algorithms. Finally, some specialised exercise programs will prevent future falls by improving the gait and mobility of high risk older adults.

7.3 Stair falls

Many studies focus on falls in general, but only a few studies focus on stair falls. Two different stair falls study paradigms are available, the one in the laboratory to examine stair fall risk parameters with specialist and expensive biomechanical analysis equipment. The other research paradigm focuses on detecting falls (actual fall- when it is happening) using sensors at home. This project fills the gap between these two domains by using an instrumented shoe with special sensors to detect fall risk using the parameters that have been found to constitute a fall risk in the laboratory. Twenty-five people were tested, and 13 people had a slip, trip, and fall in the following six months (Appendix F). Although one of the participants had two falls in the six-month follow-up, that participant slowly negotiated the laboratory staircase. Even though that participant was cautious, she did not

pay attention to the environment (things on the stair), which caused her a fall, and she needed surgery after a fall. Another participant showed less foot contact length ratio in the laboratory, and he had two trips at his home staircase, but they did not cause a significant fall. Another participant had a trip, but she managed to retain her balance, so no fall was recorded, based on the sensor data, and she did not show any risky behaviour for falls. The remaining participants who had a fall or slip did not show any risky behaviour for fall at the lab and houses data.

7.4 Limitations

Improvement in printed circuit board size (sensor shoe), making it even smaller, keep it in a small, enclosed box would be ideal. Data were collected from only 25 participants; more participants would be better, along with a new, improved circuit board. This project only focuses on different stair dimensions of how older people perform. It would be better to include various risk factors such as light, carpet, and so on. In addition, the current circuit could only measure vertical clearance, not horizontal clearance. The horizontal clearance is essential to find a risk for slip while descending stairs. This project's printed circuit board can add a few more distance sensors. With this ability, we can fit the distance sensor at the back of the shoe to find out horizontal foot clearance while descending stairs. We tried to fit the distance sensor at the shoe's back (heel counter), but the data collection frequency decreased. In addition, it was hard to fit the back (heel counter) of the shoe; when the shoe's outer layer was thinner, the sensor went inside the shoe and was not comfortable to walk, so we didn't use this back distance sensor(horizontal) for data collection.

People would not wear shoes at home in real life, but they wear slippers. It was hard to fit all the sensors in the slipper, so we decided to use the shoe to include the required sensors, which was practical. Instead of bringing older people to the lab to test whether they have a risk of falling in the future, we can test them at home with this sensor shoe. They need to wear them only when they use stairs. Instead of collecting in a controlled environment, we will get realistic data that cause falls. Older adults need to wear them for a few days, and then by analysing (machine learning algorithm) their data, future fall risk can be predicted.

7.5 Future recommendations

In the future, we need to extract more fall risk parameters within the user environment as this would be more beneficial for predicting stair falls. Also, we need to test the instrumented shoe in different staircase dimensions in the broader general living environment of various user groups. Testing more people on real stairs will improve the prediction of the stair fall risk.

Future research should implement the machine learning method in real-life stair negotiation conditions, avoiding the constraints necessary to conduct biomechanical research in the lab. A way to achieve this is to collect relevant data using instrumented sensor shoes. Furthermore, it has been found that horizontal clearance of the foot to the step edge, which indicates trip risk during descending, can be obtained using a distance sensor by attaching the sensor at the shoe's back (heel counter). Therefore, the instrumented sensor shoe with additional sensors for horizontal foot clearance will be useful to detect stair fall risk. Furthermore, these biomechanical parameters could be used as input to the machine learning algorithm, thus allowing the identification of risky stepping strategies which causes the future fall in real-life situations.

The present research work involves the potential study that has monitored falls on stairs specifically and tested older adults in different house stairs. The current machine learning was created with fall and no-fall as an output. This prediction system could be improved by grouping the hazardous events based on the underlying mechanism that caused the event (e.g., trip, slip or loss of balance) and linking these as an output to the machine learning algorithm to predict future risk of fall.

One other important factor that could facilitate the prevention of falls in older adults is increasing the awareness of the consequences of stair falls. Attention must be given to people in their own homes, where they might falsely feel safer compared to less familiar environments. When individuals feel more confident and safer, they are more likely to take more risks, which increases the potential for a fall. Increasing awareness of stair fall and the fundamental dangers of stairs might be an effective fall reduction intervention, and future studies should consider experimentally testing this.

The NHS is providing muscle strengthening and balance training for older people who are all at risk of falls by recommending people who are at risk of falling, and this will help them avoid future falls.

7.6 Implications of this project

This project's approach testing at different houses' staircases has policy implications. It may lead to revisions of the current building regulations relating to stair design; older adults can negotiate standard stair configurations, although they adopt different strategies. However, these strategies become more common and exaggerated as the staircase configuration becomes challenging. In stair design, step-rise imposes the highest demand on older individuals. Therefore, optimising step-rise and step-going may reduce lower-limb muscle strength demands and potentially lower fall risk.

We have explored stair dimensions, specifically the step-rise and step-going, since older people may lack the strength to cope with high steps and have difficulty landing safely on narrow steps. The Chapter 5 results showed that most older adults maintained their stepping behaviour when negotiating a similar staircase and altered stepping behaviour for the different staircase. Furthermore, these findings indicate that the underlying mechanism of a stair fall may remain stair dimensions that contain less going and more rise. Thus, the stepping behaviour of an individual at risk for a stair fall can be improved through changing staircase dimensions.

Stairs should be designed so that everybody using the stair can do so comfortably and safely while exerting the least energy. To ensure comfortable use and adequate proportioning, rise and going should be considered together. If the rise is small, the going should be proportionately greater to ensure that the stair is comfortable to use.

7.7 Conclusion

Applying the developed instrumented shoe in large-scale populations without a dedicated gait laboratory opens new possibilities for the community's stair fall risk detection and prevention. The prototype instrumented shoe was successfully developed, validated, and tested in actual exemplar houses. In addition, a classification algorithm was developed to differentiate fallers and non-fallers, which could detect stair fall risk in the future. Future

research should implement the ubiquitous measurement of more fall risk parameters in more people in real-life stair negotiation conditions to improve stair fall risk prediction.

Appendices

Appendix A:

Instrumented sensor shoe's PCB (Printed Circuit Board) from Eagle software: Figure A.1 and Figure A.2 show the designed right shoe's PCB design. Figure A.3 and Figure A.4 show the designed left shoe's PCB design.

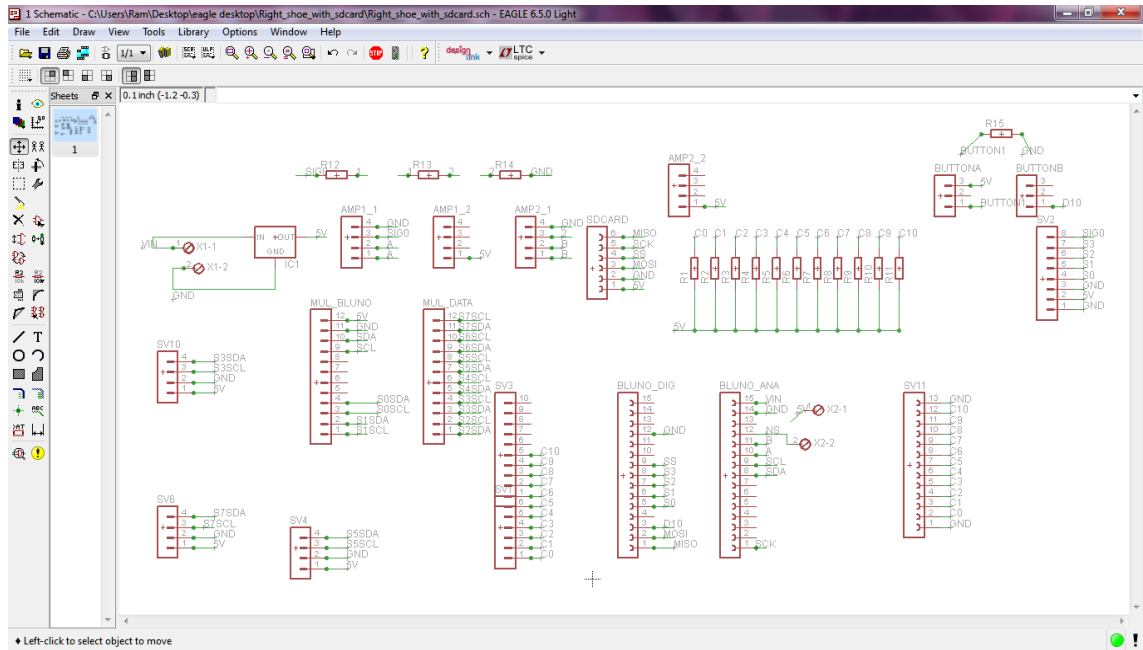


Figure A.1 Right Shoe's PCB schematic design Eagle software

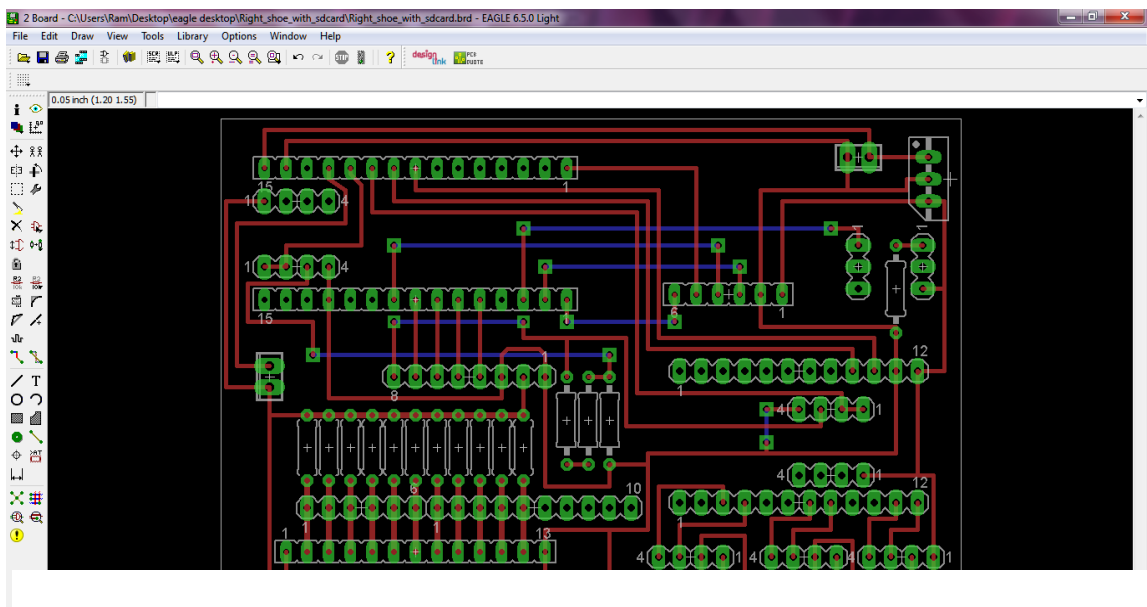


Figure A.2 Right Shoe's PCB board design from Eagle software

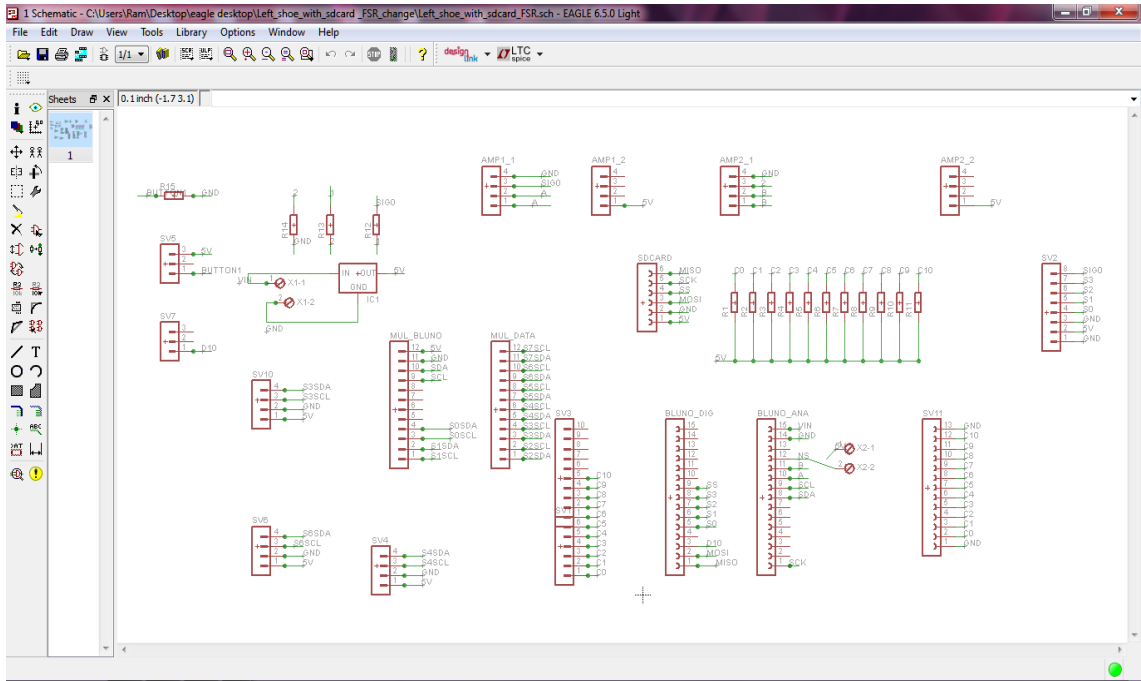


Figure A.3 Left Shoe's PCB board design from Eagle software

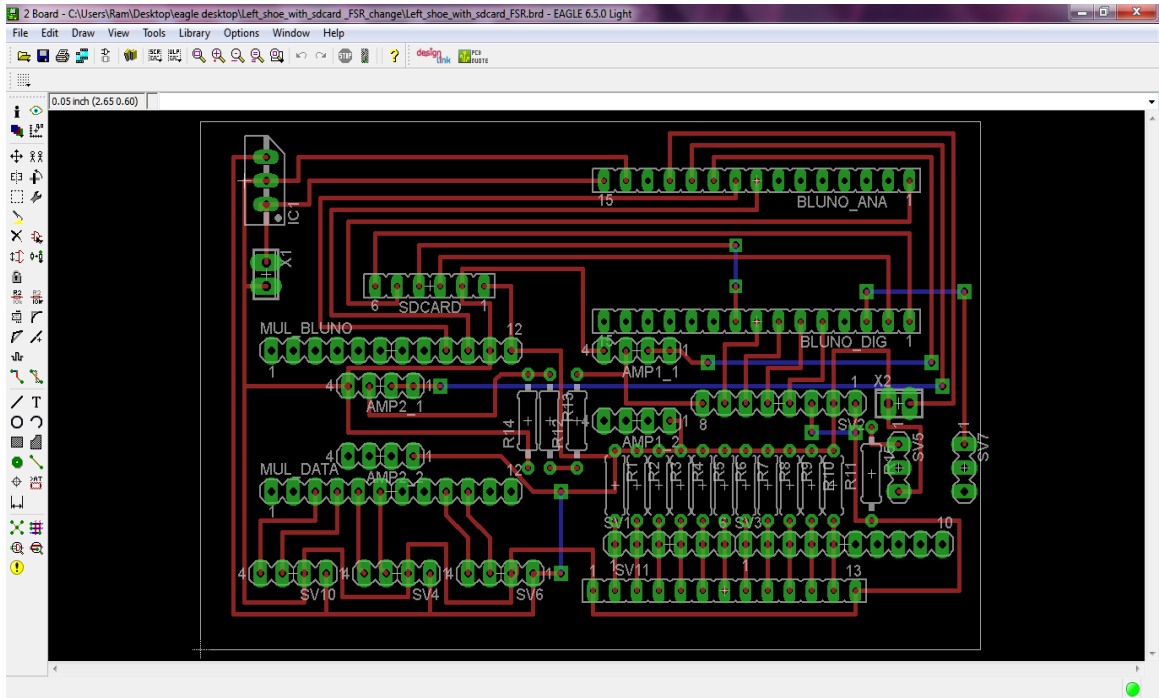


Figure A.4 Left Shoe's PCB board design from Eagle software

Right Shoe's insole design:

Figure A.5 shows the designed insole PCB design.

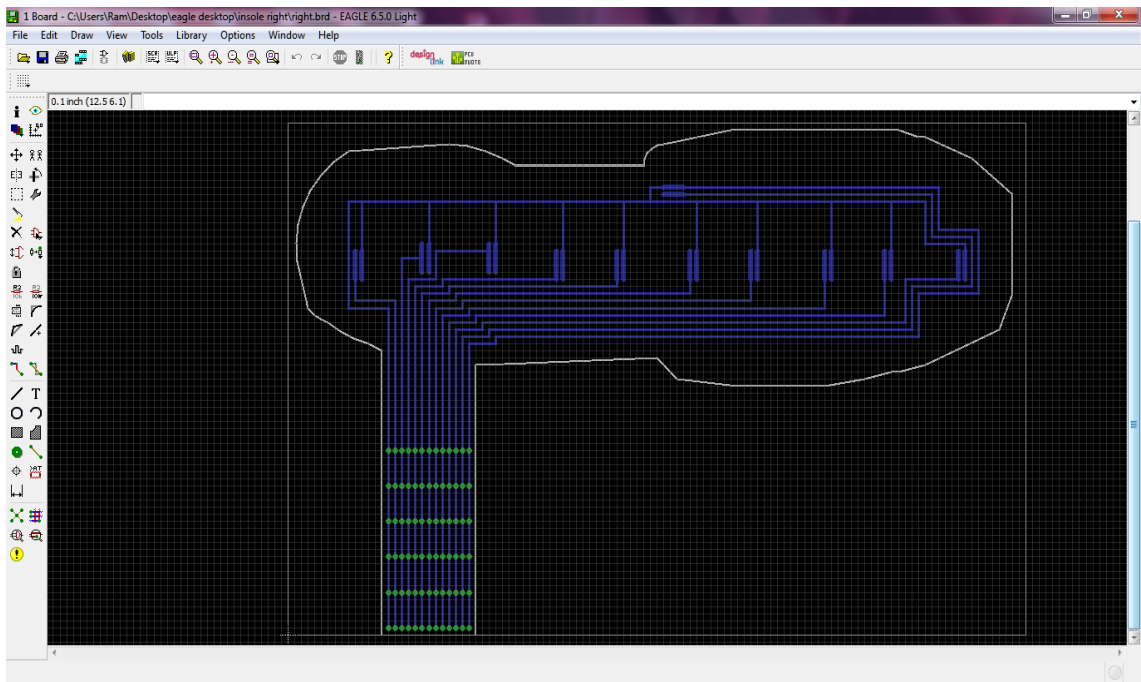


Figure A.5 Insole's design from Eagle software

Appendix B: LabVIEW User Interface Design:

Figure A.6 shows the LabVIEW user interface design.

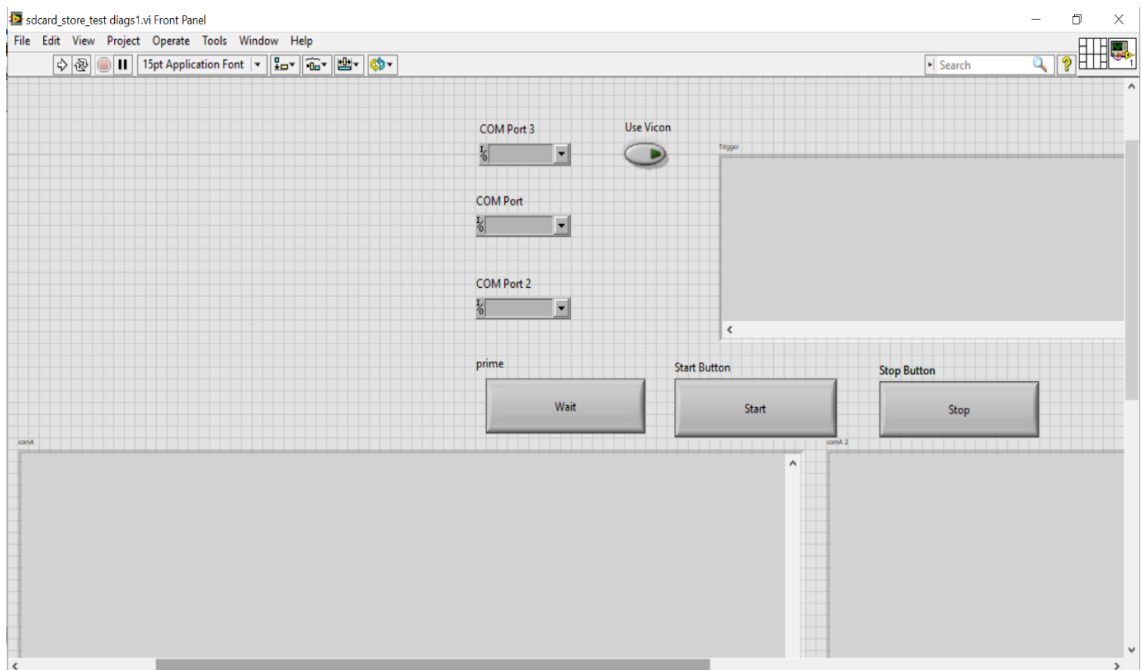


Figure A.6 User Interface designed using LABVIEW software

LabVIEW Block Diagram for the user interface:

There were three COM ports (Figure A.7), one for a left shoe (COM port), one for a right shoe (COM port2), and one for Arduino, which was connected with the Vicon system for synchronising (COM port3).

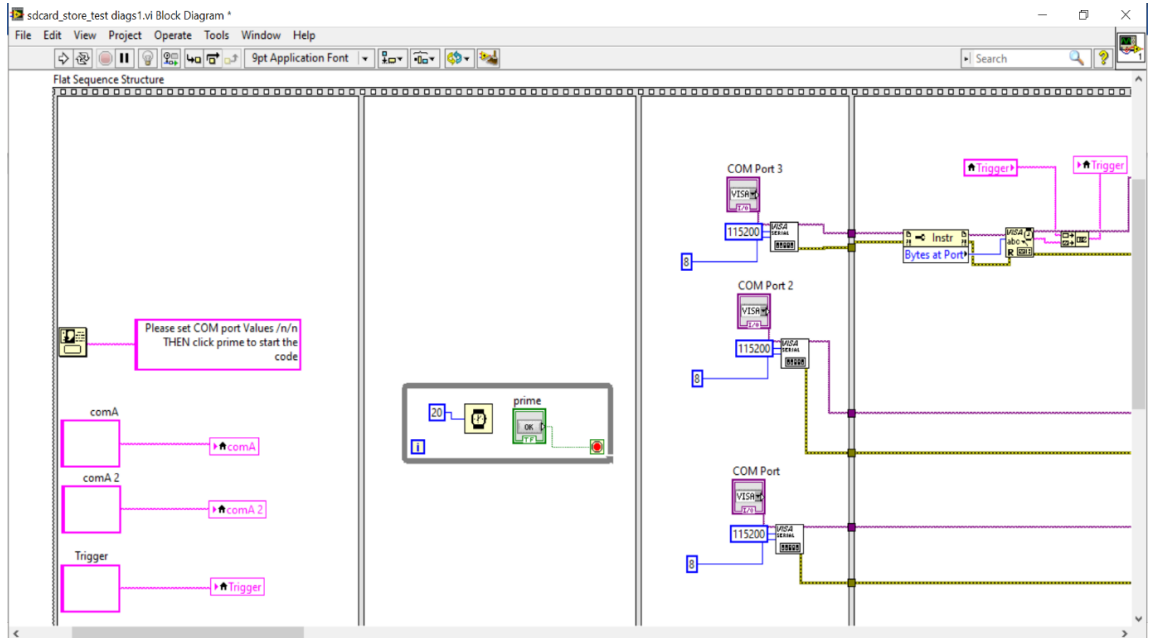


Figure A.7 COM ports and Trigger process

When the vicon system starts collecting data, Vicon's synchronise port sends a 'high voltage signal' to Arduino. Arduino constantly checks these voltages; when the voltage reaches 'greater than 3v', this sends an 'H' signal to LabVIEW (Figure A.8).

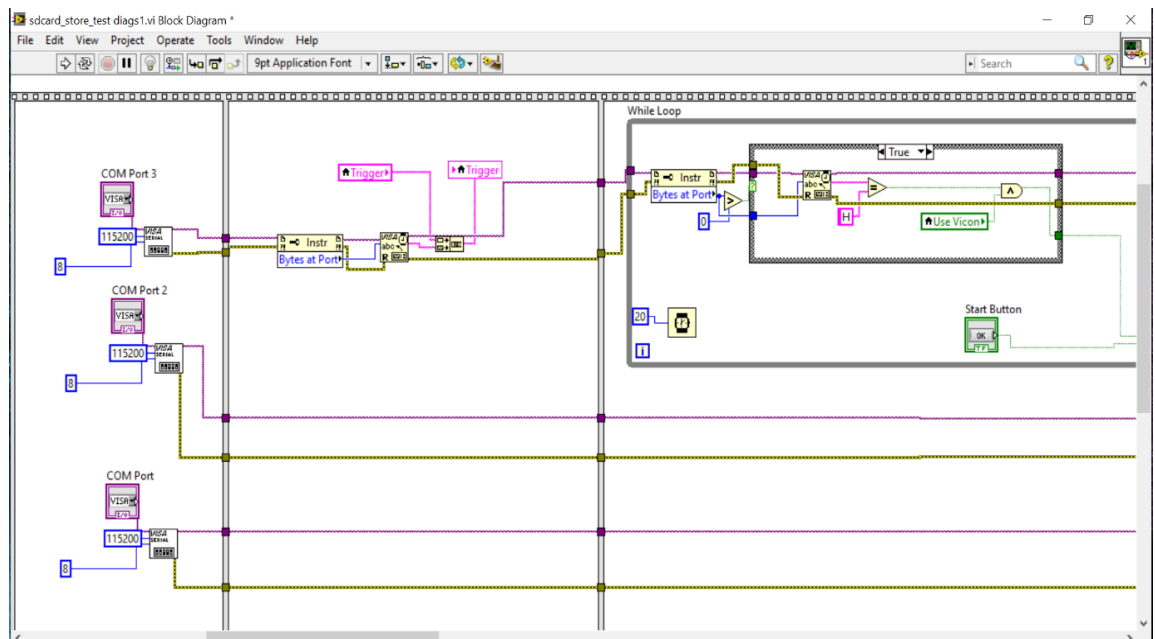


Figure A.8 Trigger to start data collection from Vicon

LabVIEW constantly checks the 'Arduino trigger port'; when LabVIEW receives an 'H' signal, then LabVIEW sends a 'start signal (S)' to both the shoes via a dedicated Bluetooth system to start data collection from the shoes (Figure A.9).

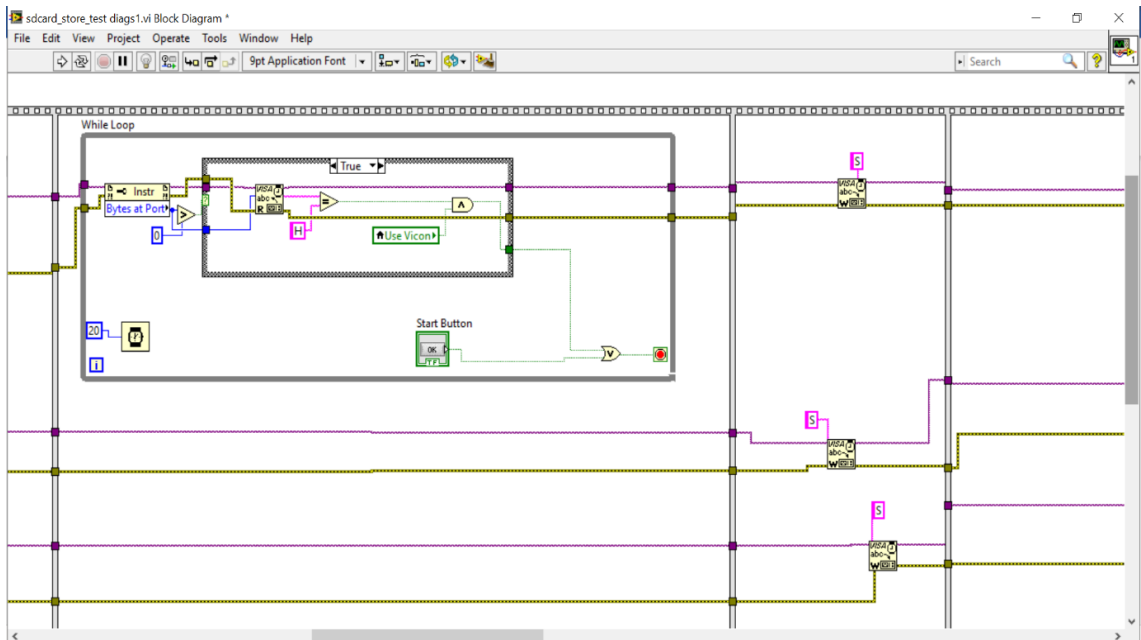


Figure A.9 After receiving start trigger, start signal send to shoes PCB board

As soon as the 'Vicon system' stops collecting data, the 'Vicon's synchronise port' sends a low voltage signal to Arduino. On receiving this low voltage signal of 'less than 3v', the Arduino sends an 'L' signal to the LabVIEW (Figure A.10).

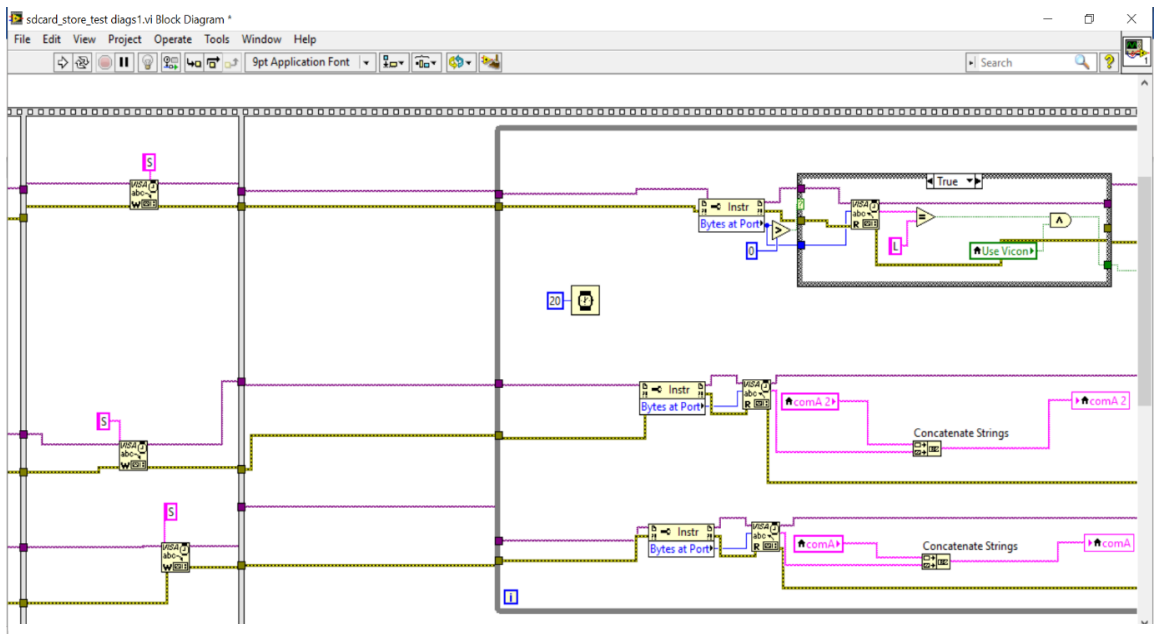


Figure A.10 Trigger to stop data collection from Vicon

When LabVIEW receives the ‘L’ signal then, LabVIEW sends a ‘stop signal (N)’ in the above manner to stop data collection by the shoes (Figure A.11).

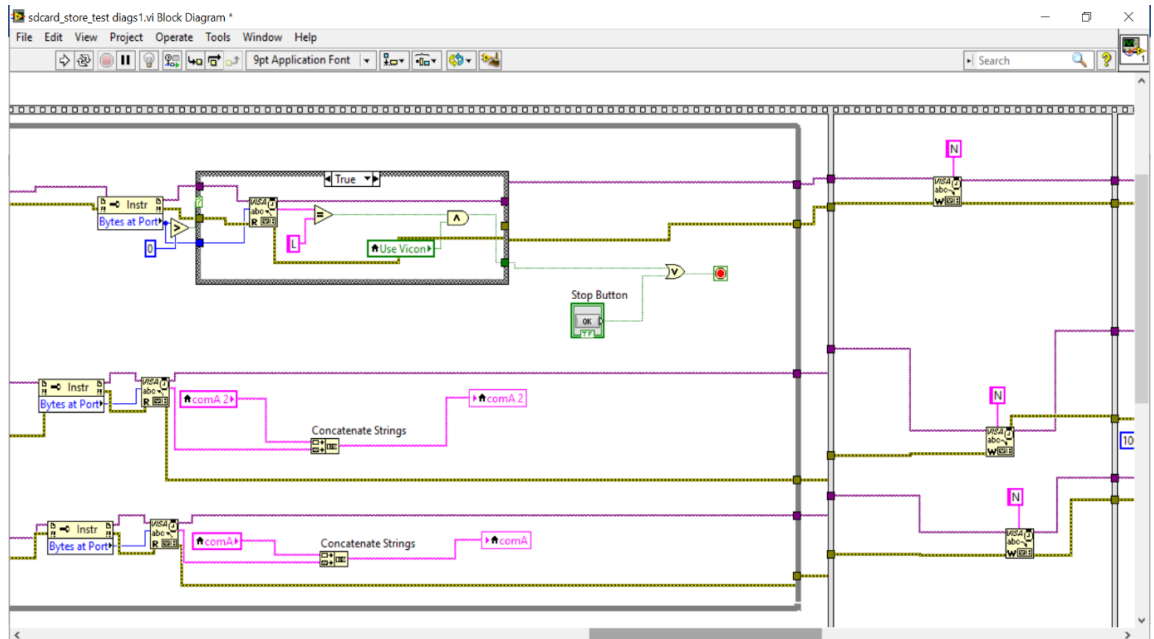


Figure A.11 After receiving stop trigger, start stop send to shoes PCB board

Once the data collection is started, LabVIEW reads the data sent by the shoes and writes them into an ‘SD storage card’ with a ‘Unique/itemised file name’ for each data. This Unique file is closed when the LabVIEW receives the ‘L’ signal by sending a ‘stop signal (N)’ to the shoes (Figure A.12).

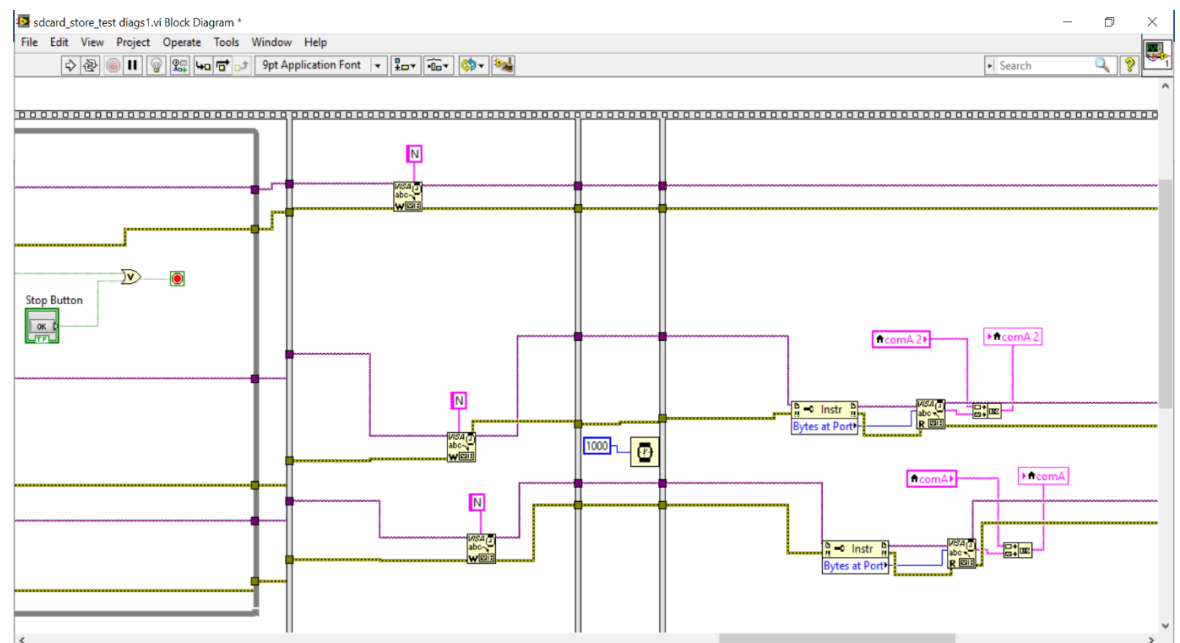


Figure A.12 Writing data in the SD (Secure Digital) card

In this process, if anything goes wrong, then an error message will be displayed.

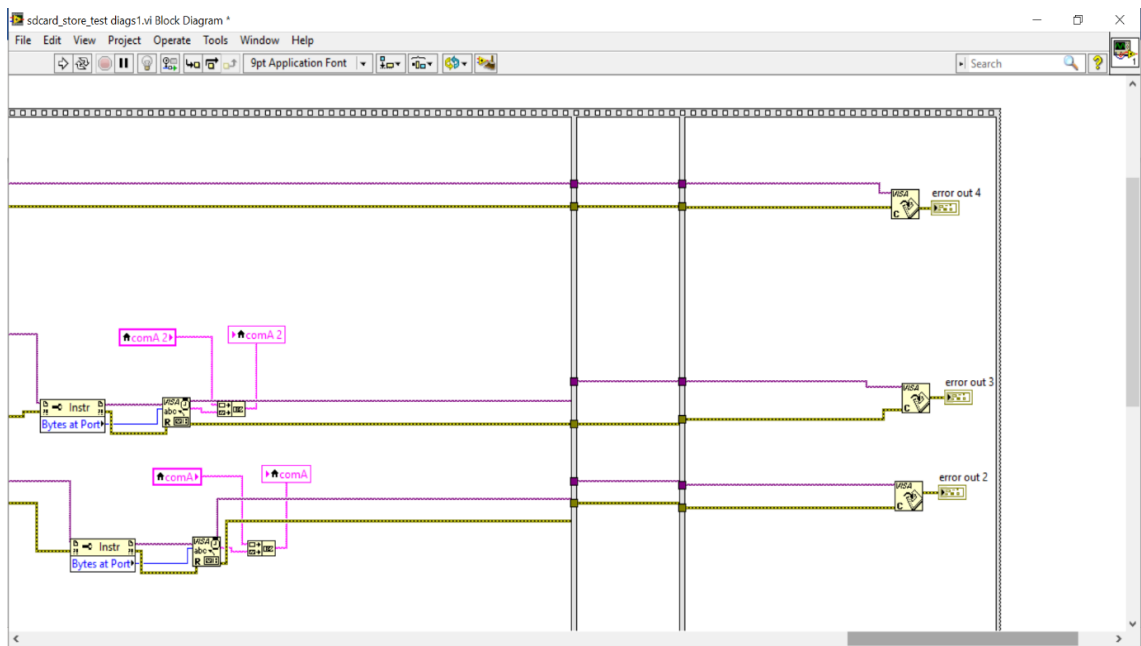







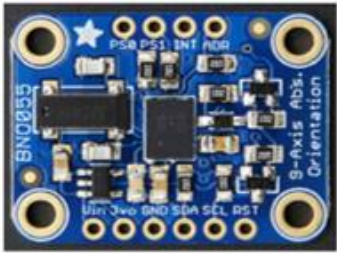
Figure A.13 Error message generation

Appendix C: FSR testing with Material testing Machine used for FSR calibration



Figure A.14 FSR testing with Material Testing Machine

Appendix D: Sensors used to develop sensor shoe

Sensors used to develop instrumented sensor shoe and insole	
<p>Bluno Nano Microcontroller (DFROBOT 2015)</p> 	<p>Micro SD card breakout board (Ada 2020)</p> 
<p>I2c Multiplexer (Instruments, 2015)</p> 	<p>VL6180X distance Sensor (STMicroelectronics 2010)</p> 
<p>Analog Multiplexer (Sparkfun 2005)</p> 	<p>BNO055 IMU sensor (Townsend 2018)</p> 

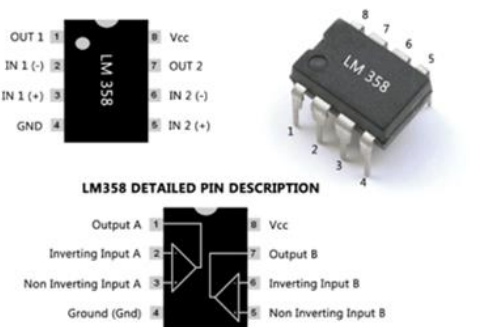

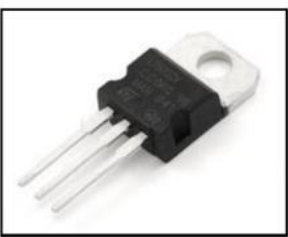

<p style="text-align: center;">LM358 Amplifier (Sparkfun 2005)</p>  <p>The image shows two views of the LM358 amplifier: a top-down view of the chip and a perspective view of the component. To the left is a pinout diagram with labels: OUT 1 (1), IN 1 (-) (2), IN 1 (+) (3), GND (4), Vcc (8), OUT 2 (7), IN 2 (-) (6), and IN 2 (+) (5). Below this is a schematic diagram titled "LM358 DETAILED PIN DESCRIPTION" showing two operational amplifiers. The labels for the schematic are: Output A (1), Inverting Input A (2), Non Inverting Input A (3), Ground (Gnd) (4), Vcc (8), Output B (7), Inverting Input B (6), and Non Inverting Input B (5).</p>	<p style="text-align: center;">Force Sensitive Resistor</p>  <p>The image shows a circular Force Sensitive Resistor (FSR) component with a grid of conductive traces on its surface and two gold-colored leads extending from one side. The text "IEEFSR.COM" is visible on the top edge of the component.</p>
<p style="text-align: center;">LM7805 5V Voltage regulator (STMicroelectronics 2018)</p>  <p>The image shows an LM7805 voltage regulator component, which is a black integrated circuit with a white plastic tab on top and three pins extending from the bottom.</p>	<p style="text-align: center;">Rechargeable battery 7.4v 500mAh (UUMART 2016)</p>  <p>The image shows a rectangular rechargeable battery with a yellow and black casing. It has two wires (red and black) connected to a black connector. The text on the battery reads: "DS 602540-2S", "7.4V 500mAh", and "+ 150621".</p>

Figure A.15 Sensors used to develop sensor shoe

Appendix E: Berg Balance Scale

Category	Component	Score
Sitting balance	Sitting unsupported	0-4
Standing balance	Standing unsupported	0-4
	Standing with eyes closed	0-4
	Standing with feet together	0-4
	Standing on one foot	0-4
	Turning to look behind	0-4
	Retrieving object from floor	0-4
	Tandem standing	0-4
	Reaching forward with an outstretched arm	0-4
	Dynamic balance	Sitting to standing
Standing to sitting		0-4
Transfer		0-4
Turning 360 degrees		0-4
Stool stepping		0-4
Total		0-56

Figure A.16 Berg Balance Scale

Appendix F: Follow-up-fall information

Table A.1 Six months follow up fall information

Participant ID	Gender	Age	Height	Weight	Previous Fall History	Berg Balance Scale	Causes of Fall
J01_OA	F	68	161	80	N	Low risk	uneven pavement trip
M03_OA	F	68	160	84.2	Yes	Moderate risk	Slip on stairs
M04_OA	M	65	174.7	89.9	yes	High risk	fall on stairs
E09_OA	F	70	168.5	77.4	N	Low risk	trip
A10_OA	M	70	172	63.75	N	Low risk	trip
J11_OA	M	65	175	109	N	Low risk	slip on stairs
T14_OA	M	70	180	87	N	Low risk	uneven pavement trip
S15_OA	F	74	160	51.45	Yes	Moderate risk	tripped twice
L17_OA	F	66	162	61	No	Low risk	missed step
A24_OA	F	74	160	63	Yes	Low risk	trip
D25_OA	M	68	177	90	No	Moderate risk	missed step
K26_OA	M	72	150	78	Yes	Low risk	tripped twice
B29_OA	F	74	161.3	58.4	No	Low risk	trip

Appendix G: Coding

Trigger code for VICON Synchronization:

```
void setup()
{
  // initialize the serial communication:
  Serial.begin(115200);
}
void loop()
{
  //read voltage input
  int Val = analogRead(A1);
  //convert analog reading to digital
  float voltage = Val * (5.0 / 1023.0);
  Serial.println(voltage);
  if (voltage < 3.0 )
  {
    Serial.write('L');
  }
  else
  {
    Serial.write('H');
  }
  delay(1000);
}
```

//Left_shoe_arduino(Microcontroller code for left shoe's Printed Circuit Board from Arduino)

```
#include <Wire.h>
```

```

#include <VL6180X.h>
#include <TimeLib.h>
#include <Adafruit_Sensor.h>
#include <Adafruit_BNO055.h>
#include <utility/imumaths.h>
#include <SPI.h>
#include <SD.h>

// Base name must be six characters or less for short file names.
#define FILE_BASE_NAME "Data"
const uint8_t CS_PIN = 4;
File file;
//to store upto999
char filename[12] = "DATA001.csv";
char numb[4];
String str;
//File mFile;
byte logflag;
byte endflag;
// sd card log
char inbyte=0;
int currenttime;
//declaring dataString to store data
String dataString="";
int h1,m1,s11;

// *****Multiplexer *****
#define TCAADDR 0x70
void tcselect(uint8_t i) {
  if (i > 7) return;
  Wire.beginTransmission(TCAADDR);
  Wire.write(1 << i);
  Wire.endTransmission();

```

```

}
//Range sensors
VL6180X sensor;
VL6180X sensor1;
/* Set the delay between fresh samples */
#define BNO055_SAMPLERATE_DELAY_MS (5)
Adafruit_BNO055 bno = Adafruit_BNO055();
//Force Sensor
int s0 = 8;
int s1 = 7;
int s2 = 6;
int s3 = 5;
//Mux in "SIG" pin
int SIG_pin = A6;
int SIG_pin1 = A7;
int val;
int val1;
void setup()
{
Serial.begin(115200);
//force sensors declare
analogReference(INTERNAL);
pinMode(s0, OUTPUT);
pinMode(s1, OUTPUT);
pinMode(s2, OUTPUT);
pinMode(s3, OUTPUT);
digitalWrite(s0, LOW);
digitalWrite(s1, LOW);
digitalWrite(s2, LOW);
digitalWrite(s3, LOW);
logflag=false;
if (!SD.begin(CS_PIN)) {
Serial.println(F("begin failed"));
}
}

```

```
return;  
}
```

```
Wire.begin();  
/*****Singleshot range sensor*****/  
tcselect(3);  
sensor.init();  
sensor.configureDefault();  
sensor.setTimeout(500);  
tcselect(6);  
sensor1.init();  
sensor1.configureDefault();  
sensor1.setTimeout(500);  
  
/* Initialise imu the sensor */  
tcselect(4);  
if(!bno.begin())  
{  
  /* problem in detecting the BNO055 ... check your connections */  
  Serial.print("Ooops, no BNO055 detected ... Check your wiring or I2C  
ADDR!");  
  while(1);  
}  
}  
  
void loop()  
{  
  endflag=0;  
  //filename goes here  
  filename[4] = '0';  
  filename[5] = '0';  
  filename[6] = '1';  
  for (int m = 1; m < 999; m++) { //Maximum 999 Files.
```



```

str = String(m);
str.toCharArray(num, 4);
if (m < 10) {
    filename[6] = num[0];
}
else if (m < 100) {
    filename[6] = num[1];
    filename[5] = num[0];
}
else {
    filename[4] = num[0];
    filename[5] = num[1];
    filename[6] = num[2];
}
if (!SD.exists(filename)) {
    break;
}
}
Serial.print(F("opened: "));
Serial.println(filename);
file.close();

```

//filename finishes

```

while(endflag==0){
if(Serial.available())
{
inbyte=(Serial.read());
if(inbyte=='S')
{
Serial.println("S");
logflag=true;
}
}
}

```

```

if(inbyte=='N')
{
  Serial.println("N");
  logflag=false;
  endflag=1;
}
}

unsigned long runMillis=millis();
unsigned long allSeconds=millis()/1000;
int runHours=allSeconds/3600;
int secRemaining=allSeconds%3600;
int runMinutes=secRemaining/60;
int runSeconds=secRemaining%60;
char buf[21];

//sprintf(buf,"Runtime%02d:%02d:%02d",runHours,runMinutes,runSeconds);
  sprintf(buf,"%02d,%02d,%02d",runHours,runMinutes,runSeconds);
  dataString =buf;
  dataString+=",";

//Range sensor
tcselect(3);
int range_sensor=sensor.readRangeSingleMillimeters();
dataString+=range_sensor;
dataString+=",";
tcselect(6);
int range_sensor1=sensor1.readRangeSingleMillimeters();
dataString+=range_sensor1;
dataString+=",";

  tcselect(4);
// Possible vector values can be:

```

```

// - VECTOR_ACCELEROMETER - m/s^2
// - VECTOR_MAGNETOMETER - ut
// - VECTOR_GYROSCOPE - rad/s
// - VECTOR_EULER - degrees
// - VECTOR_LINEARACCEL - m/s^2
// - VECTOR_GRAVITY - m/s^2

//imu::Vector<3>accel=bno.getVector(Adafruit_BNO055::VECTOR_ACCELE
ROMETER);

// Display the floating point data
// Quaternion data*/
imu::Quaternion quat = bno.getQuat();
/* Create Rotation Matrix rm from Quaternion */
/*double rm[3][3];
rm[1][1] =quat.w()*quat.w()+quat.x()*quat.x()-quat.y()*quat.y() -
quat.z()*quat.z());
rm[1][2] = 2*quat.x()*quat.y() - 2*quat.w()*quat.z());
rm[1][3] = 2*quat.x()*quat.z() + 2*quat.w()*quat.y());
rm[2][1] = 2*quat.x()*quat.y() + 2*quat.w()*quat.z());
rm[2][2] =quat.w()*quat.w()-quat.x()*quat.x()+quat.y()*quat.y() -
quat.z()*quat.z());
rm[2][3] = 2*quat.y()*quat.z() - 2*quat.w()*quat.x());
rm[3][1] = 2*quat.x()*quat.z() - 2*quat.w()*quat.y());
rm[3][2] = 2*quat.y()*quat.z() + 2*quat.w()*quat.x());
rm[3][3] =quat.w()*quat.w()-quat.x()*quat.x()-quat.y()*quat.y() +
quat.z()*quat.z());

/* Display Rotation Matrix
Serial.print(rm[1][1],5);Serial.print(" \t");
Serial.print(rm[1][2],5);Serial.print(" \t");
Serial.println(rm[1][3],5);
Serial.print(rm[2][1],5);Serial.print(" \t");
Serial.print(rm[2][2],5);Serial.print(" \t");

```

```

Serial.println(rm[2][3],5);
Serial.print(rm[3][1],5);Serial.print(" \t");
Serial.print(rm[3][2],5);Serial.print(" \t");
Serial.println(rm[3][3],5);*/

/* Create Roll Pitch Yaw Angles from Quaternions */
double yy = quat.y() * quat.y(); // 2 Uses below
double      roll      =atan2(2*(quat.w()*quat.x()+quat.y()*quat.z()),1-
2*(quat.x()*quat.x() + yy));
double pitch = asin(2 * quat.w() * quat.y() - quat.x() * quat.z());
double yaw = atan2(2 * (quat.w() * quat.z() + quat.x() * quat.y()), 1 -
2*(yy+quat.z() * quat.z()));

/* Convert Radians to Degrees */
float rollDeg = 57.2958 * roll;
float pitchDeg = 57.2958 * pitch;
float yawDeg = 57.2958 * yaw;
float rollDeg1 = rollDeg*2;
float pitchDeg1= pitchDeg*2;
float yawDeg1 = yawDeg*2;

//Linear accerleration
imu::Vector<3>
linearaccel=bno.getVector(Adafruit_BNO055::VECTOR_LINEARACCEL);
//Vector gyroscope radions per second
imu::Vector<3>
lineargyro=bno.getVector(Adafruit_BNO055::VECTOR_GYROSCOPE);
dataString+=rollDeg;
dataString+=",";
dataString+=pitchDeg;
dataString+=",";
dataString+=yawDeg;
dataString+=",";

```

```

dataString+=linearaccel.x();
dataString+=",";
dataString+=linearaccel.y();
dataString+=",";
dataString+=linearaccel.z();
dataString+=",";
dataString+=lineargyro.x();
dataString+=",";
dataString+=lineargyro.y();
dataString+=",";
dataString+=lineargyro.z();
dataString+=",";
//force sensor data
for(int i = 1; i < 11; i ++)
{
  readMux(i);
  dataString+=(val);
  dataString+=",";
  dataString+=(val1);
  dataString+=",";
}
if(logflag==true)
{
  //Serial.println("L");
  File mfile = SD.open(filename, FILE_WRITE);

  if(mfile)
  {
    mfile.println(dataString);
    //print to the serial port too:
    Serial.println(dataString);
    dataString="";
    mfile.close();
  }
}

```

```

    }
}
delay(BNO055_SAMPLERATE_DELAY_MS);
}
}
//Force sensor function
void readMux(int channel)
{
int controlPin[] = {s0, s1, s2, s3};
int muxChannel[16][4]={
    {1,1,1,1}, //14
    {0,1,1,1}, //13
    {0,0,1,1}, //12
    {1,1,0,1}, //11
    {0,1,0,1}, //10
    {1,0,0,1}, //9
    {0,0,0,1}, //8
    {1,1,1,0}, //7
    {0,1,1,0}, //6
    {1,1,1,1}, //5
    {0,0,1,0}, //4
    {1,1,0,0}, //3
    {0,1,0,0}, //2
    {1,0,0,0}, //1
    {0,0,0,0} //channel 0
};
//loop through the 4 sig
for(int i = 0; i < 4; i ++)
{
    digitalWrite(controlPin[i], muxChannel[channel][i]);

}
//read the value at the SIG pin

```

```

    val = analogRead(SIG_pin);
    val1 = analogRead(SIG_pin1);
}

```

Matlab code for foot clearance and foot overhanging:

```

%%%%%%%%%% Setting variables to all files %%%%%%%%%%%
clear all
clc
%data1=datastore("C:\Users\ramst\Desktop\houses\up\P31\left\u319.csv");
data1=datastore("C:\Users\ramst\Desktop\lab\down\all_lab_down_right\down318.csv");
                tablename='down318_R.csv';
preprocds = transform(data1,@scale)
data1=read(preprocds);
%path=('C:\Users\ramst\Desktop\lab\up\all_lab_up_right\');
path=('C:\Users\ramst\Desktop\lab\down\all_lab_down_right\');
warning('off','MATLAB:xlswrite')

writetable(data1,[path tablename]);
function data = scale(data)
Var_Names=["time","front","back","roll","pitch","yaw","accx","accy","accz","gyrox",""
gyroy","gyroz","foot","p_id","age","height","weight","fall"];
data=table(data.time,data.front,data.back,data.roll,data.pitch,data.yaw,data.accx,data.acc
y,data.accz,data.gyrox,data.gyroy,data.gyroz,data.foot,data.p_id,data.age,data.height,d
a.weight,data.fall,'VariableNames',Var_Names);
end
%%%%%%%%%%Joining           multiple           files           together
%%%%%%%%%%

pathName = 'C:\Users\ramst\Desktop\results_Senosr\lab\ascending';
fileList = dir(fullfile(pathName, '*.csv'));
out1     = fopen(fullfile(pathName, 'Joined_result_houses_up.csv'), 'w');

```

```

for k = 1:numel(fileList)
s = fileread(fullfile(pathName, fileList(k).name));
fwrite(out1, s, 'int');
end
fclose(out1);
%%%%%%%%%% All Combined down features extraction
%%%%%%%%%%

clear all;

clc

data1=datastore("C:\Users\ramst\Desktop\lab\down\P31\left");
featds=transform(data1,@extract)
fsrds=transform(preprocds,@force_calculation)
datas=readall(featds)
datas1=readall(fsrds)

path=('C:\Users\ramst\Desktop\lab\down\P31\left\');
warning('off','MATLAB:xlswrite')
features_list1= datas;
tablename='lab_down_31_1.csv';
writetable(features_list1,[path tablename]);
fsrs=table(datas1);
tablename1='fsr_down_lab_31_1.csv';
writetable(fsrs,[path tablename1]);

function feat = extract(data)
% Aspect ratio
% aratio = range(data.acy)/range(data.accx);

%% removing offset from distance sensor
going = data.back;%going down back sensor
mini=min(going); %minimum of going to get offset

```



```

going1=(going-mini); %removing offset

%% swingtime calculation
stance=(going1<10);
time1=data.time
time1(stance)=0;
A=time1';
%A = [0 0 1 2 3 0 0 0 0 0 2 3 4 0 0 0 0 0 4 5 6 7 0 0 0 0 1 1 1 0 0 0];
ne0 = find(A~=0); % Nonzero Elements
ix0 = unique([ne0(1) ne0(diff([0 ne0])>1)]); % Non-Zero Segment Start Indices
eq0 = find(A==0); % Zero Elements
ix1 = unique([eq0(1) eq0(diff([0 eq0])>1)]); % Zero Segment Start Indices
ixv = sort([ix0 ix1 length(A)]); % Consecutive Indices Vector
for k1 = 1:length(ixv)-1
    section{k1} = A(ixv(k1):ixv(k1+1)-1);
end
%because we made stance into zero, all the swing will be one, for each
%'1'cell array we calculate minimum and maximum to get swing time.
for i=1:(length(section)-1)
result1=min(section{i});
result2=max(section{i});
swingresult(i)=result2-result1; % for each cell swing time
sr=(swingresult>0);
finalswingresult=swingresult(sr);
end
total_swing_time=sum(finalswingresult);
total_no_swing=nnz(finalswingresult);
step1_swing_time=finalswingresult(1);
step3_swing_time=finalswingresult(2);
step5_swing_time=finalswingresult(3);
step7_swing_time=finalswingresult(4);

time2=data.time

```

```

total_time=time2(end);
stance_time=total_time-total_swing_time;

%step1_swing_time,step3_swing_time,step5_swing_time,step7_swing_time,step9_swi
ng_time,step11_swing_time,step13_swing_time
%"step1_swing_time","step3_swing_time","step5_swing_time","step7_swing_time","st
ep9_swing_time","step11_swing_time","step13_swing_time"

%% Landing Foot Clearance for descending is calculated immediately from
%stance to swing phase or push off and swing phase
%foot_clearance_down
descending = data.back;% going down back sensor
m=min(descending); %minimum of going to get offset
descending1=(descending-m); %removing offset

% we need only more than 10 and less than 45mm
zeross=((descending1<10)); %it means foot is landed already
oneee=(descending1>=45);% foot is in swing position
descending1(zeross)=0; %applying 0 to landed position
descending1(oneee)=0; % applying 0 to swing position, so we will only starting swing
and end of swing, before landing position value

% splitting zeros and ones
AA=descending1';

%A = [0 0 1 2 3 0 0 0 0 0 2 3 4 0 0 0 0 0 4 5 6 7 0 0 0 0 1 1 1 0 0 0];
nne0 = find(AA~=0); % Nonzero Elements
iix0 = unique([nne0(1) nne0(diff([0 nne0])>1)]); % Non-Zero Segment Start Indices
eeq0 = find(AA==0); % Zero Elements
iix1 = unique([eeq0(1) eeq0(diff([0 eeq0])>1)]); % Zero Segment Start Indices
iixv = sort([iix0 iix1 length(AA)]); % Consecutive Indices Vector
for I1 = 1:length(iixv)-1

```

```

    section2{I1} = AA(iixv(I1):iixv(I1+1)-1); % this will more than 14mm and less than
45mm, and this will splitted into cell array
end
for i=1:(length(section2)-1)
result3(i)=min(section2{i});
finall=result3';
finall1=(finall>0);
finalfinall=finall(finall1);
foot_clearance = finalfinall(1:2:end,:)% before crossing the foot on the stair edge we
calculate foot clearance
end
step1_Land_FC=foot_clearance(1);
step3_Land_FC=foot_clearance(2);
step5_Land_FC=foot_clearance(3);
step7_Land_FC=foot_clearance(4);

% numpitchmax = nnz(foot_clearance);
%"step1_Land_FC","step3_Land_FC","step5_Land_FC","step7_Land_FC","step9_Lan
d_FC","step11_Land_FC","step13_Land_FC"
%step1_Land_FC,step3_Land_FC,step5_Land_FC,step7_Land_FC,step9_Land_FC,ste
p11_Land_FC,step13_Land_FC
%% Passing Foot Clearance for Down(Descending)

des = data.back;%going down back sensor
m=min(des); %minimum of going to get offset
descending2=(des-m); %removing offset

% we only need more 45mm and > than 200
zeros1=((descending2>=1) &(descending2<45)); %it means foot starting from landing
to swing
onee1=(descending2>=150);% foot is in swing position maximum
descending2(zeros1)=0; %applying 0 to landed position

```

descending2(onee1)=0; % applying 0 to swing positon, so we will only starting swing and end of swing, before landing positon value

```

% splitting zeros and ones
X2=descending2';
%A = [0 0 1 2 3 0 0 0 0 0 2 3 4 0 0 0 0 0 4 5 6 7 0 0 0 0 1 1 1 0 0 0];
nne02 = find(X2~=0); % Nonzero Elements
iix02 = unique([nne02(1) nne02(diff([0 nne02])>1)]); % Non-Zero Segment Start
Indices
eeq02 = find(X2==0); % Zero Elements
iix12 = unique([eeq02(1) eeq02(diff([0 eeq02])>1)]); % Zero Segment Start Indices
iixv2 = sort([iix02 iix12 length(X2)]); % Consecutive Indices Vector
for I2 = 1:length(iixv2)-1
    section3{I2} = X2(iixv2(I2):iixv2(I2+1)-1); % this will more than 14mm and less than
45mm, and this will splited into cell array
end
for LL=1:(length(section3)-1)
result4(LL)=min(section3{LL});
finals=result4'
finals1=(finals>0);
finals2=finals(finals1);
Passing_foot_clearance =finals2(1:1:end,:);% while crossing the foot on the stair edge we
calculate foot clearance
end
step1_Passing_FC=Passing_foot_clearance(1);
step3_Passing_FC=Passing_foot_clearance(2);
step5_Passing_FC=Passing_foot_clearance(3);
step7_Passing_FC=Passing_foot_clearance(4);

% numpitchmax = nnz(foot_clearance);
%"step1_Passing_FC","step3_Passing_FC","step5_Passing_FC","step7_Passing_FC","
step9_Passing_FC","step11_Passing_FC","step13_Passing_FC"

```

```

%step1_Passing_FC,step3_Passing_FC,step5_Passing_FC,step7_Passing_FC,step9_Pas
sing_FC,step11_Passing_FC,step13_Passing_FC

% %%right
% idxmax1 = islocalmin(data.pitch,"MinProminence",0.1);
% results2=data.pitch(idxmax1);
% results3=results2<-10;
% finalresults1=results2(results3);

% % % % % Local max/min of pitch
idxmax1 = islocalmax(data.pitch,"MinProminence",0.1);
results2=data.pitch(idxmax1);
results3=results2>15;
finalresults1=results2(results3);

step1_pitch_max=finalresults1(1);
step3_pitch_max=finalresults1(2);
step5_pitch_max=finalresults1(3);
step7_pitch_max=finalresults1(4);

numpitchmax = nnz(finalresults1);
%step1_pitch_min,step3_pitch_min,step5_pitch_min,step7_pitch_min,step9_pitch_min,
step11_pitch_min,step13_pitch_min,
%"step1_pitch_min","step3_pitch_min","step5_pitch_min","step7_pitch_min","step9_p
itch_min","step11_pitch_min","step13_pitch_min",

%Mean,SD,Variance of Pitch
Mean_Pitch=mean(data.pitch);
SD_Pitch=std(data.pitch);
Variance_Pitch=var(data.pitch);
Rms_Pitch=rms(data.pitch);
%pitch_statistics=[Mean_Pitch, SD_Pitch, Variance_Pitch];

```

```

%pitch_statistics="Mean_Pitch", "SD_Pitch", "Variance_Pitch"

% Local max/min of accelerometer
idxmin = islocalmin(data.accx,"MinProminence",0.1);
results=data.accx(idxmin);
results1=results<-5;
finalresults=results(results1);
step1_accx_min=finalresults(1);
step3_accx_min=finalresults(2);
step5_accx_min=finalresults(3);
step7_accx_min=finalresults(4);

numXmin = nnz(finalresults);

%local max of acceleometer
idxmax= islocalmax(data.accx,"MinProminence",1);
result=data.accx(idxmax);
result1=result>4;
finalresult=result(result1);
step1_accx_max=finalresult(1);
step3_accx_max=finalresult(2);
step5_accx_max=finalresult(3);
step7_accx_max=finalresult(4);

numXmax = nnz(finalresult);

%acc mean,sd,var
Mean_Acc_X=mean(data.accx);
Mean_Acc_Y=mean(data.accy);
Mean_Acc_Z=mean(data.accz);
SD_Acc_X=std(data.accx);
SD_Acc_Y=std(data.accy);
SD_Acc_Z=std(data.accz);

```

```

Variance_Acc_X=var(data.accx);
Variance_Acc_Y=var(data.acy);
Variance_Acc_Z=var(data.accz);
Rms_Acc_X=rms(data.accx);
Rms_Acc_Y=rms(data.acy);
Rms_Acc_Z=rms(data.accz);

%ACC_statistics=[Mean_Acc_X,      Mean_Acc_Y,Mean_Acc_Z,      SD_Acc_X
,SD_Acc_Y, SD_Acc_Z, Variance_Acc_X, Variance_Acc_Y, Variance_Acc_Z];
%ACC_statistics=["Mean_Acc_X",  "Mean_Acc_Y","Mean_Acc_Z",  "SD_Acc_X"
,"SD_Acc_Y",      "SD_Acc_Z",      "Variance_Acc_X",      "Variance_Acc_Y",
"Variance_Acc_Z"];

% Velocity
velx=0;
vely=0;
velz=0;
velocity_x = velx+ cumtrapz(data.time,data.accx);
velocity_y = vely+ cumtrapz(data.time,data.acy);
velocity_z = velz+ cumtrapz(data.time,data.accz);
vel_x= diff(velocity_x);
vel_y= diff(velocity_y);
vel_z= diff(velocity_z);

Mean_vel_X=mean(vel_x);
Mean_vel_Y=mean(vel_y);
Mean_vel_Z=mean(vel_z);
SD_vel_X=std(vel_x);
SD_vel_Y=std(vel_y);
SD_vel_Z=std(vel_z);
Variance_vel_X=var(vel_x);
Variance_vel_Y=var(vel_y);
Variance_vel_Z=var(vel_z);

```

```

Rms_vel_X=rms(vel_x);
Rms_vel_Y=rms(vel_y);
Rms_vel_Z=rms(vel_z);

% Vell_statistics=[Mean_vel_X, Mean_vel_Y ,Mean_vel_Z, SD_vel_X, SD_vel_Y
,SD_vel_Z ,Variance_vel_X, Variance_vel_Y, Variance_vel_Z];
%"Mean_vel_X"," Mean_vel_Y"," Mean_vel_Z", "SD_vel_X", "SD_vel_Y",
"SD_vel_Z", "Variance_vel_X", "Variance_vel_Y", "Variance_vel_Z"
[pks,locs] = findpeaks(vel_x,'MinPeakDistance',10);
pks1=pks>0.1;
vel_pks2=pks(pks1);
step1_velx_max=vel_pks2(1);
step3_velx_max=vel_pks2(2);
step5_velx_max=vel_pks2(3);
step7_velx_max=vel_pks2(4);

%"step1_velx_max", "step3_velx_max", "step5_velx_max", "step7_velx_max",
"step9_velx_max", "step11_velx_max", "step13_velx_max"
%step1_velx_max,step3_velx_max,step5_velx_max,step7_velx_max,step9_velx_max,s
tep11_velx_max,step13_velx_max
angular_velcocity_x=data.gyrox;
angular_velcocity_y=data.gyroY;
angular_velcocity_z=data.gyroz;
Mean_ang_vel_X=mean(angular_velcocity_x);
Mean_ang_vel_Y=mean(angular_velcocity_y);
Mean_ang_vel_Z=mean(angular_velcocity_z);
SD_ang_vel_X=std(angular_velcocity_x);
SD_ang_vel_Y=std(angular_velcocity_y);
SD_ang_vel_Z=std(angular_velcocity_z);
Variance_ang_vel_X=var(angular_velcocity_x);
Variance_ang_vel_Y=var(angular_velcocity_y);
Variance_ang_vel_Z=var(angular_velcocity_z);

```



```

Rms_ang_vel_X=rms(angular_velcocity_x);
Rms_ang_vel_Y=rms(angular_velcocity_y);
Rms_ang_vel_Z=rms(angular_velcocity_z);

%Mean_ang_vel_X,Mean_ang_vel_Y,Mean_ang_vel_Z,SD_ang_vel_X,SD_ang_vel_
Y,SD_ang_vel_Z,Variance_ang_vel_X,Variance_ang_vel_Y,Variance_ang_vel_Z
%"Mean_ang_vel_X","Mean_ang_vel_Y","Mean_ang_vel_Z","SD_ang_vel_X","SD_a
ng_vel_Y","SD_ang_vel_Z","Variance_ang_vel_X","Variance_ang_vel_Y","Variance_
ang_vel_Z"

gyroy=data.gyroy;
[gyroypks,locs] = findpeaks(gyroy,'MinPeakDistance',10);
gyroypks1=gyroypks>80;
gyroypks2=gyroypks(gyroypks1);
step1_ang_vely_max=gyroypks2(1);
step3_ang_vely_max=gyroypks2(2);
step5_ang_vely_max=gyroypks2(3);
step7_ang_vely_max=gyroypks2(4);

%step1_ang_vely_max,step3_ang_vely_max,step5_ang_vely_max,step7_ang_vely_ma
x,step9_ang_vely_max,step11_ang_vely_max,step13_ang_vely_max
%"step1_ang_vely_max","step3_ang_vely_max","step5_ang_vely_max","step7_ang_ve
ly_max","step9_ang_vely_max","step11_ang_vely_max","step13_ang_vely_max"

%{'foot','p_id','age','height','weight','gender','fall'}
foot=data.foot(1);
p_id=data.p_id(1);
age=data.age(1);
height=data.height(1);
weight=data.weight(1);
gender="F";
fall=data.fall(1);

```

% Put it all together into a table

```
featurenames =  
["total_time","stance_time","total_no_swing","total_swing_time","step1_swing_time","  
step3_swing_time","step5_swing_time","step7_swing_time","step1_Land_FC","step3_  
Land_FC","step5_Land_FC","step7_Land_FC","step1_Passing_FC","step3_Passing_F  
C","step5_Passing_FC","step7_Passing_FC","NumMinX","step1_accx_min","step3_ac  
cx_min","step5_accx_min","step7_accx_min","numXmax","step1_accx_max","step3_a  
ccx_max","step5_accx_max","step7_accx_max","Mean_Acc_X","Mean_Acc_Y","Mea  
n_Acc_Z",          "SD_Acc_X",          "SD_Acc_Y",          "SD_Acc_Z",  
"Variance_Acc_X","Variance_Acc_Y",  
"Variance_Acc_Z","Rms_Acc_X","Rms_Acc_Y","Rms_Acc_Z","Mean_Pitch","SD_Pi  
tch","Variance_Pitch","Rms_Pitch","numpitchmin","step1_pitch_max","step3_pitch_m  
ax","step5_pitch_max","step7_pitch_max","Mean_vel_X","          Mean_vel_Y", "  
Mean_vel_Z",          "SD_vel_X",          "SD_vel_Y",          "SD_vel_Z",  
"Variance_vel_X","Variance_vel_Y","Variance_vel_Z","Rms_vel_X","Rms_vel_Y", "  
Rms_vel_Z","step1_velx_max",          "step3_velx_max",          "step5_velx_max",  
"step7_velx_max","Mean_ang_vel_X","Mean_ang_vel_Y","Mean_ang_vel_Z","SD_an  
g_vel_X","SD_ang_vel_Y","SD_ang_vel_Z","Variance_ang_vel_X","Variance_ang_ve  
l_Y","Variance_ang_vel_Z","Rms_ang_vel_X","Rms_ang_vel_Y","Rms_ang_vel_Z", "  
step1_ang_vely_max","step3_ang_vely_max","step5_ang_vely_max","step7_ang_vely  
_max","foot","p_id","age","height","weight","gender","fall"];  
feat =  
table(total_time,stance_time,total_no_swing,total_swing_time,step1_swing_time,step3_  
swing_time,step5_swing_time,step7_swing_time,step1_Land_FC,step3_Land_FC,step5_  
_Land_FC,step7_Land_FC,step1_Passing_FC,step3_Passing_FC,step5_Passing_FC,ste  
p7_Passing_FC,numXmin,step1_accx_min,step3_accx_min,step5_accx_min,step7_acc  
x_min,numXmax,step1_accx_max,step3_accx_max,step5_accx_max,step7_accx_max,  
Mean_Acc_X,Mean_Acc_Y,Mean_Acc_Z, SD_Acc_X ,SD_Acc_Y, SD_Acc_Z,  
Variance_Acc_X,          Variance_Acc_Y,  
Variance_Acc_Z,Rms_Acc_X,Rms_Acc_Y,Rms_Acc_Z,Mean_Pitch,SD_Pitch,Varian  
ce_Pitch,Rms_Pitch,numpitchmax,step1_pitch_max,step3_pitch_max,step5_pitch_max,  
step7_pitch_max,Mean_vel_X, Mean_vel_Y ,Mean_vel_Z, SD_vel_X, SD_vel_Y
```

```

,SD_vel_Z
,Variance_vel_X,Variance_vel_Y,Variance_vel_Z,Rms_vel_X,Rms_vel_Y,Rms_vel_Z
,step1_velx_max,step3_velx_max,step5_velx_max,step7_velx_max,Mean_ang_vel_X,
Mean_ang_vel_Y,Mean_ang_vel_Z,SD_ang_vel_X,SD_ang_vel_Y,SD_ang_vel_Z,Var
iance_ang_vel_X,Variance_ang_vel_Y,Variance_ang_vel_Z,Rms_ang_vel_X,Rms_ang
_vel_Y,Rms_ang_vel_Z,step1_ang_vely_max,step3_ang_vely_max,step5_ang_vely_m
ax,step7_ang_vely_max,foot,p_id,age,height,weight,gender,fall,'VariableNames',feature
names);
end

```

```

function FSR_sum_result1 = force_calculation(data)
% y=-0.0955x + 101.33
big13=-0.0955*(data.b1) + 101.33;
big15=-0.0955*(data.b2) + 101.33;
big17=-0.0955*(data.b3) + 101.33;
big19=-0.0955*(data.b4) + 101.33;
big21=-0.0955*(data.b5) + 101.33;
big23=-0.0955*(data.b6) + 101.33;
big25=-0.0955*(data.b7)+ 101.33;
%big_result=big13+big15+big17+big19+big21+big23+big25;
big27=-0.0955*(data.b8) + 101.33;
%big_result=big13+big15+big17+big19+big21+big23+big25+big27;
big29=-0.0955*(data.b9)+ 101.33;
big_result=big13+big15+big17+big19+big21+big23+big25+big27+big29;
%big31=-0.0955*(data.b10) + 101.33;
%big_result=big13+big15+big17+big19+big21+big23+big25+big27+big29+big31;
big_result=big_result-min(big_result);

% y = -11ln(x) + 68.178
small14 = -11*log(data.s1) + 68.178;
small16 = -11*log(data.s2) + 68.178;
small18 = -11*log(data.s3) + 68.178;
small20 = -11*log(data.s4) + 68.178;

```

```

small22 = -11*log(data.s5) + 68.178;
small24 = -11*log(data.s6) + 68.178;
small26 = -11*log(data.s7) + 68.178;
%small_result=small14+small16+small18+small20+small22+small24+small26;
small28 = -11*log(data.s8) + 68.178;
%small_result=small14+small16+small18+small20+small22+small24+small26+small28;
small30 = -11*log(data.s9)+ 68.178;

small_result=small14+small16+small18+small20+small22+small24+small26+small28+
small30;
% %small32 = -11*log(data.s10) + 68.178;
%small_result=small14+small16+small18+small20+small22+small24+small26+small28+small30+small32;
small_result=small_result-min(small_result);

body_weight=64;
ttt=data.time;

FSR_result=big_result+small_result;
FSR_sum_result=[big_result small_result FSR_result];
FSR_percentage_result=((FSR_sum_result/8)/body_weight)*100;
FSR_sum_result1=[ttt FSR_sum_result FSR_percentage_result];
end

%%%%%%%%%% Features fft %%%%%%%%%%%

clear all
clc

```

```

data1=datastore("C:\Users\ramst\Desktop\all_data_features\houses\down\all_house_down_left");
featds=transform(data1,@extract)
datas=readall(featds)
path=('C:\Users\ramst\Desktop\all_data_features\houses\down\all_house_down_left\');
warning('off','MATLAB:xlswrite')
features_list1= datas;
tablename='frequency_features_left.csv';
writetable(features_list1,[path tablename]);

function feat = extract(data)
L=length(data.accx);
fs=1/L;
time=0:1/(L-1):1;
subplot(3,1,1)
plot(time,data.accx)
title('Time Domain Dignal');
xlabel('Time(s)');
ylabel('Amplitude(v)');
accx_fft=fft(data.accx,L)/L;
x_amplitude=2*abs(accx_fft(1:L/2+1));
x_freq=fs/2*linspace(0,1,L/2+1);
subplot(3,1,2)
plot(x_freq,x_amplitude);

[pks1,locs1] = findpeaks((x_amplitude),'MinPeakHeight',0.5);
subplot(3,1,3)
plot(x_freq(locs1),pks1,'or');
hold on;
plot(x_freq,x_amplitude)
ff=x_freq(locs1)
peak_magnitude=[ff,pks1];
accx_peak_freq_mag_one=peak_magnitude(1,:)

```

```

accx_peak_freq_mag_three=peak_magnitude(2,:)
accx_peak_freq_mag_five=peak_magnitude(3,:)
accx_peak_freq_mag_seven=peak_magnitude(4,:)
accx_peak_freq_mag_nine=peak_magnitude(5,:)
accx_peak_freq_mag_eleven=peak_magnitude(6,:)

featurenames =
["accx_peak_freq_mag_one","accx_peak_freq_mag_three","accx_peak_freq_mag_five"
,"accx_peak_freq_mag_seven","accx_peak_freq_mag_nine","accx_peak_freq_mag_ele
ven"];
feat =
table(accx_peak_freq_mag_one,accx_peak_freq_mag_three,accx_peak_freq_mag_five,
accx_peak_freq_mag_seven,accx_peak_freq_mag_nine,accx_peak_freq_mag_eleven,'V
ariableNames',featurenames);
end
%%%%%%%%%%%%%%%%%%%%%%%%%%%%%%%%%%%%%%%%%%%%%%%%%%%%%%%%%%%%%%%%%%%%%%%%%%%%%% Feature Selection
%%%%%%%%%%%%%%%%%%%%%%%%%%%%%%%%%%%%%%%%%%%%%%%%%%%%%%%%%%%%%%%%%%%%%%%%%%%%%%
house_data4= house_data3(:,3:end);
house_data4=table2array(house_data4 (:,1:end-1));
response_data= house_data4 (:,end);

[idx,scores] = fscchi2(house_data4,response_data) %Univariate feature ranking for
classification using chi-square tests
figure
bar(scores(idx(1:15)))
xlabel('Predictor rank')
ylabel('Predictor importance score')
xticklabels(strrep(house_data4.Properties.VariableNames(idx),'_','\_''))
xtickangle(-45)
title('Univariate feature ranking using chi-square tests')

[idx2 scores2] = fsrftest(house_data4,response_data)
figure

```

```

bar(scores2(idx2(1:15)))
xlabel('Predictor rank')
ylabel('Predictor importance score')
xticklabels(strrep(house_data3.Properties.VariableNames(idx2),'_','\_''))
xtickangle(-50)
title('Univariate feature ranking for regression using F-Test')
chiresult=[scores ; idx]
chiresult_var=house_data.Properties.VariableNames(idx)
ftestresult=[scores2 ; idx2]
p_value_ftest=1./(-log(scores2))
ftestresult_var=house_data.Properties.VariableNames(idx2)
% % holdoutCVP = cvpartition(house_data4,'holdout',150)
a=(house_data4((response_data==1),:));
b=(house_data4((response_data==2),:));
a1=a(1:150,:);
b1=b(1:150,:);
[h,p,ci,stats] = ttest(a1,b1)
figure
ecdf(p);
xlabel('P value');
ylabel('CDF value')
title('Features selection Using a Simple Filter Approach-ttest');

%%%%%%%%%%%%%%%%%%%%%%%%%%%%%%%%%%%%%%%%%%%%%%%%%%%%%%%%%%%%%%%%%%%%%%%%%% Classifier results %%%%%%%%%%%
function [trainedClassifier, validationAccuracy] = trainClassifier(trainingData)
% [trainedClassifier, validationAccuracy] = trainClassifier(trainingData)
% Returns a trained classifier and its accuracy. This code recreates the
% classification model trained in Classification Learner app. Use the
% generated code to automate training the same model with new data
%
% Input:
% trainingData: A table containing the same predictor and response

```

```

% columns as those imported into the app.
%
% Output:
% trainedClassifier: A struct containing the trained classifier. The
% struct contains various fields with information about the trained
% classifier.
%
% trainedClassifier.predictFcn: A function to make predictions on new
% data.
%
% validationAccuracy: A double containing the accuracy in percent. In
% the app, the History list displays this overall accuracy score for
% each model.
%
% Use the code to train the model with new data. To retrain your
% classifier, call the function from the command line with your original
% data or new data as the input argument trainingData.
%
% For example, to retrain a classifier trained with the original data set
% T, enter:
% [trainedClassifier, validationAccuracy] = trainClassifier(T)
% To make predictions with the returned 'trainedClassifier' on new data T2,
% use
% yfit = trainedClassifier.predictFcn(T2)
%
% T2 must be a table containing at least the same predictor columns as used
% during training. For details, enter:
% trainedClassifier.HowToPredict

% Auto-generated by MATLAB on 08-Dec-2020 12:18:37

% Extract predictors and response

```



```

% This code processes the data into the right shape for training the
% model.
inputTable = trainingData;
predictorNames = {'stancetime', 'swingtime', 'FC_entry', 'FC_exit', 'FC_sd', 'FO_entry',
'FO_exit', 'FO_sd', 'accxmax_exit', 'Mean_AccZ_R', 'SD_AccZ_R', 'VarAccY_R',
'RmsAccX_R', 'RmsAccZ_R', 'vel_entry', 'vel_middle', 'PeakmagX', 'peakmagY',
'peakmagZ', 'accy_skewness'};
predictors = inputTable(:, predictorNames);
response = inputTable.Follow_up_fall;
isCategoricalPredictor = [false, false, false, false, false, false, false, false, false, false,
false, false, false, false, false, false, false, false, false];

% Train a classifier
% This code specifies all the classifier options and trains the classifier.
classificationSVM = fitsvm(...
    predictors, ...
    response, ...
    'KernelFunction', 'polynomial', ...
    'PolynomialOrder', 3, ...
    'KernelScale', 'auto', ...
    'BoxConstraint', 1, ...
    'Standardize', true, ...
    'ClassNames', categorical({'Fallers'; 'Non fallers'}));

% Create the result struct with predict function
predictorExtractionFcn = @(t) t(:, predictorNames);
svmPredictFcn = @(x) predict(classificationSVM, x);
trainedClassifier.predictFcn = @(x) svmPredictFcn(predictorExtractionFcn(x));

% Add additional fields to the result struct
trainedClassifier.RequiredVariables = {'FC_entry', 'FC_exit', 'FC_sd', 'FO_entry',
'FO_exit', 'FO_sd', 'Mean_AccZ_R', 'PeakmagX', 'RmsAccX_R', 'RmsAccZ_R',

```

```

'SD_AccZ_R', 'VarAccY_R', 'accxmax_exit', 'accy_skewness', 'peakmagY', 'peakmagZ',
'stancetime', 'swingtime', 'vel_entry', 'vel_middle'};
trainedClassifier.ClassificationSVM = classificationSVM;
trainedClassifier.About = 'This struct is a trained model exported from Classification
Learner R2020a.';

% Extract predictors and response
% This code processes the data into the right shape for training the
% model.
inputTable = trainingData;
predictorNames = {'stancetime', 'swingtime', 'FC_entry', 'FC_exit', 'FC_sd', 'FO_entry',
'FO_exit', 'FO_sd', 'accxmax_exit', 'Mean_AccZ_R', 'SD_AccZ_R', 'VarAccY_R',
'RmsAccX_R', 'RmsAccZ_R', 'vel_entry', 'vel_middle', 'PeakmagX', 'peakmagY',
'peakmagZ', 'accy_skewness'};
predictors = inputTable(:, predictorNames);
response = inputTable.Follow_up_fall;
isCategoricalPredictor = [false, false, false, false, false, false, false, false, false, false,
false, false, false, false, false, false, false, false, false];

% Perform cross-validation
partitionedModel = crossval(trainedClassifier.ClassificationSVM, 'Kfold', 5);

% Compute validation predictions
[validationPredictions, validationScores] = kfoldPredict(partitionedModel);

% Compute validation accuracy
validationAccuracy = 1 - kfoldLoss(partitionedModel, 'LossFun', 'ClassifError');

```

References

- Age, U. (2010). "Stop Falling: start saving lives and money." Age UK.
- Alexander, B. H., et al. (1992). "The cost and frequency of hospitalization for fall-related injuries in older adults." American journal of public health **82**(7): 1020-1023.
- Aminian, K. and B. Najafi (2004). "Capturing human motion using body-fixed sensors: outdoor measurement and clinical applications." Computer animation and virtual worlds **15**(2): 79-94.
- Applebey, L. (2016, June 9, 2016). "Stair Safety Factsheet." from https://www.shponline.co.uk/resources/stair-safety-day-25-facts-about-stair-safety/#_ftn3.
- Arens, B., et al. (1999). "Binocular function after bilateral implantation of monofocal and refractive multifocal intraocular lenses." Journal of Cataract & Refractive Surgery **25**(3): 399-404.
- Bamberg, S. J. M., et al. (2008). "Gait analysis using a shoe-integrated wireless sensor system." IEEE transactions on information technology in biomedicine **12**(4): 413-423.
- Benbasat, A. Y., et al. (2003). A wireless modular sensor architecture and its application in on-shoe gait analysis. SENSORS, 2003 IEEE, IEEE.
- Benbasat, A. Y. and J. A. Paradiso (2005). A compact modular wireless sensor platform. IPSN 2005. Fourth International Symposium on Information Processing in Sensor Networks, 2005., IEEE.
- Bertuccio, M. and P. Cesari (2009). "Dimensional analysis and ground reaction forces for stair climbing: effects of age and task difficulty." Gait & Posture **29**(2): 326-331.
- Bertuletti, S., et al. (2016). Measurement of the inter-foot distance using a Time-of-Flight proximity sensor: Preliminary evaluation during leg oscillation exercises. Proceedings of the GNB Conference, Naples, Italy.
- Bland, J. M. and D. Altman (1986). "Statistical methods for assessing agreement between two methods of clinical measurement." The lancet **327**(8476): 307-310.
- Cavanagh, P. R., et al. (1997). "How do the elderly negotiate stairs?" Muscle & Nerve. Supplement **5**: S52-55.
- Chabikuli, B., et al. (2017). "Design and Implementation of an Exercise Monitoring System Using 3-Dimensional Skeleton Tracking."
- Cumming, R. G., et al. (2000). "Prospective study of the impact of fear of falling on activities of daily living, SF-36 scores, and nursing home admission." The Journals of Gerontology Series A: Biological Sciences and Medical Sciences **55**(5): M299-M305.

Dempster, W. T. (1955). Space requirements of the seated operator, geometrical, kinematic, and mechanical aspects of the body with special reference to the limbs, Michigan State Univ East Lansing.

DFROBOT (2015). "Bluno Nano." from https://wiki.dfrobot.com/Bluno_Nano_SKU_DFR0296#target_0.

Di Giulio, I., et al. (2020). "Stair gait in older adults worsens with smaller step treads and when transitioning between level and stair walking." Frontiers in sports and active living **2**: 63.

Dias, R. C., et al. (2011). "Characteristics associated with activity restriction induced by fear of falling in community-dwelling elderly." Brazilian Journal of Physical Therapy **15**(5): 406-413.

Ejupi, A., et al. (2014). "New methods for fall risk prediction." Current Opinion in Clinical Nutrition & Metabolic Care **17**(5): 407-411.

Electronics, I. (2010). "Force Sensing Resistor." from <https://www.sparkfun.com/datasheets/Sensors/Pressure/fsrguide.pdf>.

Electronics, S. (2010). "SD library for Arduino." from <https://github.com/arduino-libraries/SD>.

Foster, R. J., et al. (2019). "Centre of mass control is reduced in older people when descending stairs at an increased riser height." Gait & Posture **73**: 305-314.

Frenzel, L. (2012). "What's The Difference Between Bit Rate And Baud Rate?". from <https://www.electronicdesign.com/technologies/communications/article/21802272/whats-the-difference-between-bit-rate-and-baud-rate>.

Giavarina, D. (2015). "Understanding bland altman analysis." Biochemia medica: Biochemia medica **25**(2): 141-151.

GmbH, B. S. (2020). "BNO055." from <https://www.bosch-sensortec.com/products/smart-sensors/bno055.html#documents>.

Grandez, K., et al. (2009). Wearable wireless sensor for the gait monitorization of parkinsonian patients. 2009 16th IEEE International Conference on Electronics, Circuits and Systems-(ICECS 2009), IEEE.

Guimarães, V., et al. (2013). A smartphone-based fall risk assessment tool: measuring one leg standing, sit to stand and falls efficacy scale. 2013 IEEE 15th International Conference on e-Health Networking, Applications and Services (Healthcom 2013), IEEE.

Hamel, K. A. and P. R. Cavanagh (2004). "Stair performance in people aged 75 and older." Journal of the American Geriatrics Society **52**(4): 563-567.

Hamel, K. A., et al. (2005). "Foot clearance during stair descent: effects of age and illumination." Gait & Posture **21**(2): 135-140.

Hanavan Jr, E. P. (1964). A mathematical model of the human body, Air Force Aerospace Medical Research Lab Wright-Patterson AFB OH.

Hausdorff, J., et al. (1999). "Maturation of gait dynamics: stride-to-stride variability and its temporal organization in children." Journal of applied physiology **86**(3): 1040-1047.

Hemmatpour, M., et al. (2019). "A review on fall prediction and prevention system for personal devices: evaluation and experimental results." Advances in Human-Computer Interaction **2019**.

Instruments, T. (2015). "Adafruit TCA9548A." from <https://cdn-shop.adafruit.com/datasheets/tca9548a.pdf>.

Jacobs, J. V. (2016). "A review of stairway falls and stair negotiation: Lessons learned and future needs to reduce injury." Gait & Posture **49**: 159-167.

Jagos, H., et al. (2010). "A multimodal approach for insole motion measurement and analysis." Procedia Engineering **2**(2): 3103-3108.

Kesler, R. M., et al. (2016). "Analysis of foot clearance in firefighters during ascent and descent of stairs." Applied ergonomics **52**: 18-23.

King, S. L., et al. (2018). "Alternate stair descent strategies for reducing joint moment demands in older individuals." Journal of biomechanics **78**: 126-133.

Lai, D. T., et al. (2008). Measuring toe clearance using a wireless inertial sensing device. 2008 International Conference on Intelligent Sensors, Sensor Networks and Information Processing, IEEE.

Lamb, S. E., et al. (2005). "Development of a common outcome data set for fall injury prevention trials: the Prevention of Falls Network Europe consensus." Journal of the American Geriatrics Society **53**(9): 1618-1622.

Li, Y., et al. (2012). "A microphone array system for automatic fall detection." IEEE Transactions on Biomedical Engineering **59**(5): 1291-1301.

Lord, S. R., et al. (1993). "An epidemiological study of falls in older community-dwelling women: the Randwick falls and fractures study." Australian journal of public health **17**(3): 240-245.

Mathie, M. J., et al. (2004). "Accelerometry: providing an integrated, practical method for long-term, ambulatory monitoring of human movement." Physiological measurement **25**(2): R1.

Matrix, C. (2019). "What is Confusion Matrix and Advanced Classification Metrics?". from <https://manisha-sirsat.blogspot.com/2019/04/confusion-matrix.html>.

Mid (2015). Population Estimates UK Office for National Statistics, 2016.

Mikhailchuk, D. (2017). "Motion Capture: What Is It?". from <https://teslasuit.io/blog/motion-capture-what-it-is/>.

Morris, S. J. (2004). A shoe-integrated sensor system for wireless gait analysis and real-time therapeutic feedback, Massachusetts Institute of Technology.

- Murphy, J. and B. Isaacs (1982). "The post-fall syndrome." *Gerontology* **28**(4): 265-270.
- Nagata, H. (1991). "Occupational accidents while walking on stairways." *Safety science* **14**(3-4): 199-211.
- NHS (2018, 24 April 2018). "Falls." from <https://www.nhs.uk/conditions/falls/>.
- Pauls, J. L. (1985). "Review of stair-safety research with an emphasis on Canadian studies." *Ergonomics* **28**(7): 999-1010.
- Preece, S. J., et al. (2009). "Activity identification using body-mounted sensors—a review of classification techniques." *Physiological measurement* **30**(4): R1.
- Reeves, N. D., et al. (2008). "The demands of stair descent relative to maximum capacities in elderly and young adults." *Journal of Electromyography and Kinesiology* **18**(2): 218-227.
- Regulations, B. (2000). Part M: 'Access to and Use of Buildings', HMSO, London.
- Roys, M. (2013). *Refurbishing Stairs in Dwellings to Reduce the Risk of Falls and Injuries*, IHS BRE Press.
- Roys, M. and M. Wright (2005). "Minor variations in gait and their effect on stair safety." *Contemporary Ergonomics*: 427.
- Roys, M. S. (2001). "Serious stair injuries can be prevented by improved stair design." *Applied ergonomics* **32**(2): 135-139.
- Samuel, D., et al. (2011). "The biomechanical functional demand placed on knee and hip muscles of older adults during stair ascent and descent." *Gait & Posture* **34**(2): 239-244.
- Scott, A. (2005). "Falls on stairways." *Harpur Hill*.
- Scott, G., et al. (2007). "Age-related differences in foot structure and function." *Gait & Posture* **26**(1): 68-75.
- Selvaraj, M., et al. (2018). *Stair Fall Risk Detection Using Wearable Sensors*. 2018 11th International Conference on Developments in eSystems Engineering (DeSE), IEEE.
- Shumway-Cook, A., et al. (1997). "Predicting the probability for falls in community-dwelling older adults." *Physical therapy* **77**(8): 812-819.
- Simoneau, G. G., et al. (1991). "The influence of visual factors on fall-related kinematic variables during stair descent by older women." *Journal of gerontology* **46**(6): M188-M195.
- Sparkfun (2005). "LM258-Dual Operational Amplifier IC." from <https://www.sparkfun.com/datasheets/Components/General/LM358.pdf>.
- Startzell, J. K., et al. (2000). "Stair negotiation in older people: a review." *Journal of the American Geriatrics Society* **48**(5): 567-580.

STMicroelectronics (2010). "vl6180X." from https://www.st.com/resource/en/user_manual/dm00247018-vl6180x-proximity-gesture-and-ambient-light-sensing-als-module-stmicroelectronics.pdf.

STMicroelectronics (2018). "Voltage Regulator ".

Templer, J. (1995). The staircase: history and theories, Mit Press.

Templer, J. (1995). The staircase: studies of hazards, falls, and safer design, MIT press.

Templer, J., et al. (1985). "Study of factors associated with risk of work-related stairway falls." Journal of Safety Research **16**(4): 183-196.

Tiedemann, A. C., et al. (2007). "Physical and psychological factors associated with stair negotiation performance in older people." The Journals of Gerontology Series A: Biological Sciences and Medical Sciences **62**(11): 1259-1265.

Tinetti, M. E., et al. (1995). "The contribution of predisposing and situational risk factors to serious fall injuries." Journal of the American Geriatrics Society **43**(11): 1207-1213.

Tong, L., et al. (2013). "HMM-based human fall detection and prediction method using tri-axial accelerometer." IEEE Sensors Journal **13**(5): 1849-1856.

Townsend, K. (2018). "Adafruit BNO055 Absolute Orientation Sensor." from <http://descargas.cetronic.es/BNO055.pdf>.

Vallabh, P., et al. (2016). Fall detection using machine learning algorithms. 2016 24th International Conference on Software, Telecommunications and Computer Networks (SoftCOM), IEEE.

van Schooten, K. S., et al. (2015). "Ambulatory fall-risk assessment: amount and quality of daily-life gait predict falls in older adults." Journals of Gerontology Series A: Biomedical Sciences and Medical Sciences **70**(5): 608-615.

Wahab, Y. (2009). Design and implementation of MEMS biomechanical sensors for real-life measurements of gait parameters, Victoria University.

Wahab, Y., et al. (2014). "Development of Shoe Attachment Unit for Rehabilitation Monitoring." Procedia Computer Science **42**: 46-53.

Wang, Y., et al. (2016). "Wifall: Device-free fall detection by wireless networks." IEEE Transactions on Mobile Computing **16**(2): 581-594.

Wells, H. L. (1977). "Safe stairs--landings, platforms, porches & winders."

Wijlhuizen, G. J., et al. (2007). "Older persons afraid of falling reduce physical activity to prevent outdoor falls." Preventive medicine **44**(3): 260-264.

Woodman, O. J. (2007). An introduction to inertial navigation, University of Cambridge, Computer Laboratory.

Yang, C.-M., et al. (2009). A wireless gait analysis system by digital textile sensors. 2009 Annual International Conference of the IEEE Engineering in Medicine and Biology Society, IEEE.

Zietz, D. and M. Hollands (2009). "Gaze behavior of young and older adults during stair walking." Journal of motor behavior **41**(4): 357-366.

Zietz, D., et al. (2011). "Stepping characteristics and Centre of Mass control during stair descent: Effects of age, fall risk and visual factors." Gait & Posture **34**(2): 279-284.